ISSN 0021-9673

VOL. 351 NO. 1 JANUARY 3, 1986

JOURNAL OF CHROMATOGRAPHY

INTERNATIONAL JOURNAL ON CHROMATOGRAPHY, ELECTROPHORESIS AND RELATED METHODS

ELSEVIER

JOURNAL OF CHROMATOGRAPHY

Scope. The *Journal of Chromatography* publishes papers on all aspects of chromatography, electrophoresis and related methods. Contributions consist mainly of research papers dealing with chromatographic theory, instrumental development and their applications. The section *Biomedical Applications,* which is under separate editorship, deals with the following aspects: developments in and applications of chromatographic and electrophoretic techniques related to clinical diagnosis (including the publication of normal values); screening and profiling procedures with special reference to metabolic disorders; results from basic medical research with direct consequences in clinical practice; combinations of chromatographic and electrophoretic methods with other physicochemical techniques such as mass spectrometry. In *Chromatographic Reviews,* reviews on all aspects of chromatography, electrophoresis and related methods are published.

Submission of Papers. Papers in English, French and German may be submitted, in three copies. Manuscripts should be submitted to: The Editor of *Journal of Chromatography,* P.O. Box 681, 1000 AR Amsterdam, The Netherlands, or to: The Editor of *Journal of Chromatography, Biomedical Applications,* P.O. Box 681, 1000 AR Amsterdam, The Netherlands. Review articles are invited or proposed by letter to the Editors and will appear in *Chromatographic Reviews* or *Biomedical Applications.* An outline of the proposed review should first be forwarded to the Editors for preliminary discussion prior to preparation. Submission of an article is understood to imply that the article is original and unpublished and is not being considered for publication elsewhere. For copyright regulations, see below.

Subscription Orders. Subscription orders should be sent to: Elsevier Science Publishers B.V., P.O. Box 211, 1000 AE Amsterdam, The Netherlands. The *Journal of Chromatography* and the *Biomedical Applications* section can be subscribed to separately.

Publication. The *Journal of Chromatography* (incl. *Biomedical Applications, Chromatographic Reviews* and *Cumulative Author and Subject Indexes, Vols. 326–350*) has 38 volumes in 1986. The subscription prices for 1986 are:

J. Chromatogr. (incl. *Chromatogr. Rev.* and *Cum. Indexes, Vols. 326–350*) + *Biomed. Appl.* (Vols. 346–383): Dfl. 6080.00 plus Dfl. 912.00 (postage) (total *ca.* US$ 2411.00)

J. Chromatogr. (incl. *Chromatogr. Rev.* and *Cum. Indexes, Vols. 326–350*) only (Vols. 346–373): Dfl. 5040.00 plus Dfl. 672.00 (postage) (total *ca.* US$ 1969.75)

Biomed. Appl. only (Vols. 374–383): Dfl. 1850.00 plus Dfl. 240.00 (postage) (total *ca.* US$ 720.75).

Journals are automatically sent by airmail at no extra costs to Argentina, Australia, Brasil, Canada, China, Hong Kong, India, Israel, Japan, Malaysia, Mexico, New Zealand, Pakistan, Singapore, South Africa, South Korea, Taiwan, Thailand and the U.S.A. Back volumes of the *Journal of Chromatography* (Vols. 1 through 345) are available at Dfl. 219.00 (plus postage). Claims for issues not received should be made within three months of publication of the issue. If not, they cannot be honoured free of charge. Customers in the U.S.A. and Canada wishing information on this and other Elsevier journals, please contact Journal Information Center, Elsevier Science Publishing Co. Inc., 52 Vanderbilt Avenue, New York, NY 10017. Tel. (212) 916-1250.

Abstracts/Contents Lists published in Analytical Abstracts, Biochemical Abstracts, Biological Abstracts, Chemical Abstracts, Chemical Titles, Current Contents/Physical, Chemical & Earth Sciences, Current Contents/Life Sciences, Deep-Sea Research/Part B: Oceanographic Literature Review, Index Medicus, Mass Spectrometry Bulletin, PASCAL-CNRS, Referativnyi Zhurnal and Science Citation Index.

See page 3 of cover for Publication Schedule, Information for Authors and information on Advertisements.

0021-9673/86/$03.50

Printed in The Netherlands

CONTENTS

(Abstracts/Contents Lists published in Analytical Abstracts, Biochemical Abstracts, Biological Abstracts, Chemical Abstracts, Chemical Titles, Current Contents/Physical, Chemical & Earth Sciences, Current Contents/Life Sciences, Deep-Sea Research/Part B: Oceanographic Literature Review, Index Medicus, Mass Spectrometry Bulletin, PASCAL-CNRS, Referativnyi Zhurnal and Science Citation Index)

(Continued overleaf)

JOURNAL OF CHROMATOGRAPHY

VOL. 351 (1986)

JOURNAL *of* CHROMATOGRAPHY

INTERNATIONAL JOURNAL ON CHROMATOGRAPHY,
ELECTROPHORESIS AND RELATED METHODS

ELSEVIER
AMSTERDAM — OXFORD — NEW YORK — TOKYO

0021-9673/86/$03.50

Printed in The Netherlands

Journal of Chromatography, 351 (1986) 1–16
Elsevier Science Publishers B.V., Amsterdam — Printed in The Netherlands

CHROM. 18 172

A GENERAL MODEL OF LIQUID–SOLID CHROMATOGRAPHY WITH MIXED MOBILE PHASES INVOLVING CONCURRENT ADSORPTION AND PARTITION EFFECTS

M. JARONIEC* and D. E. MARTIRE*
Department of Chemistry, Georgetown University, Washington, DC 20057 (U.S.A.)
(First received March 21st, 1985; revised manuscript received September 5th, 1985)

SUMMARY

Liquid–solid chromatography (LSC) with mixed mobile phases is discussed in terms of classical thermodynamics. It is shown that a rigorous consideration of solute and solvent competitive adsorption in systems with a non-ideal mobile (bulk) phase and a surface-influenced non-ideal stationary phase leads to a new general equation for the distribution coefficient of a solute involving concurrent adsorption and partition effects. For special sets of parameters this equation reduces to familiar limiting expressions describing either adsorption or partition effects. A detailed discussion is presented for LSC systems with binary phases, in which bulk and surface solutions are assumed to be regular ones.

INTRODUCTION

Two limiting models are usually employed to describe the experimental data of liquid–solid chromatography (LSC) with mixed mobile phases. One of them, widely known in the chromatographic literature as the displacement model, was proposed in the 1960's by Snyder[1]. According to this model a solute is distributed between a surface phase, usually assumed to be monolayer, and a mobile phase as a result of a competitive solute and solvent adsorption. In adsorption from solutions on solids and similarly in LSC with mixed mobile phases this competitive adsorption is represented by suitable phase-exchange reactions[1–7]. Experimental and theoretical studies of many authors have shown that solute and solvent competitive adsorption plays an important role in the process of solute distribution between the two phases, especially in LSC systems in the normal-phase mode[4–10]. There is a great number of theoretical papers starting with the original displacement model and incorporating additional details such as surface heterogeneity[11,12], non-specific interactions in both phases[13–15], solvation and solvent association in both phases[16–18] and other factors[19,20].

* Permanent address: Institute of Chemistry, M. Curie-Sklodowska University, 20031 Lublin, Poland.

0021-9673/86/$03.50

The second limiting model of the LSC process is that assuming distribution of a solute between two phases as a consequence of classical partitioning[21–24]. Equations describing partitioning of a solute between a surface-influenced stationary phase and mobile phase are quite analogous to those used in gas–liquid and liquid–liquid chromatography. Ościk[25] was the first to derive an equation for LSC with mixed mobile phases, which, as our recent studies have shown[26,27], reflects partition effects in the chromatographic process. These effects are dominant in the typical reversed-phase chromatographic systems with chemically bonded phases[21–23]. If the models involving classical partitioning give a good representation of the LSC process in many of the systems in question, there is a great number of systems, in which adsorption and partition phenomena give comparable contributions to the total solute retention. In contrast to the simple approaches describing the above-mentioned limiting models[6,7,21,24,27], there is no simple model involving concurrent adsorption and partition effects. Although the unified stastistico-thermodynamical description of LSC with mixed mobile phases due to Martire and Boehn[24,28,29] automatically incorporates the competitive character of solute and solvent adsorption and all contributions from solution nonideality, the final expressions resulting from this description are quite complicated and frequently inconvenient for practical applications. Therefore, in this paper a simple model involving concurrent adsorption and partition effects is proposed and formulated in terms of classical thermodynamics. This formulation makes possible a clear and rigorous definition of adsorption and partition phenomena in LSC with mixed mobile phases and leads to a new general equation describing dependence of the distribution coefficient of a solute upon mobile phase composition. All familiar limiting equations, having rigorous thermodynamical foundations, may be deduced from this general expression.

ADSORPTION FROM MULTICOMPONENT SOLUTIONS ON SOLID SURFACES

This section is devoted to adsorption from multicomponent liquid mixtures on solid surfaces, which is a natural basis to formulate a theory of LSC with mixed mobile phases. Let us consider a $(n + 1)$-component liquid mixture contacting with a homogeneous solid surface. The liquid mixture contains only nonelectrolytes and its deviation from ideality is described in terms of the activity coefficients. In general, a $(n + 1)$-component solution contains molecules of different sizes; this means that a molecule of the i-th component contains r_i segments. The adsorption occurs as a consequence of an exchange of the different molecules between two phases, bulk phase and surface phase. The latter phase is assumed to be an autonomous phase, in which molecules lie parallel to the solid surface. The adsorption process may be represented by a series of the following phase-exchange reactions[3]:

$$r_i\,(n+1)^l + r_{n+1}\,(i)^\sigma \rightleftarrows r_i\,(n+1)^\sigma + r_{n+1}\,(i)^l \quad \text{for } i = 1,2,\ldots,n \tag{1}$$

where $(i)^\rho$ denotes a molecule of the i-th component in the ρ-th phase and $\rho = l$ (bulk phase) and σ (surface phase). Although the phase-exchange reaction given by eqn. 1 suggests a monolayer character of adsorption, the recent statistico-thermodynamical studies of Dabrowski *et al.*[30] showed that the above reaction may be used to represent the adsorption process for surface phases of greater thickness than the monolayer thickness but showing a special ordering of adsorbed molecules.

The equilibrium constant $K^*_{n+1,i}$ relating to the reaction given by eqn. 1 is defined as follows:

$$K^*_{n+1,i} = (a^\sigma_{n+1}/a^l_{n+1})^{r_i}(a^l_i/a^\sigma_i)^{r_{n+1}} \quad \text{for } i = 1,2,\ldots,n \tag{2}$$

where

$$K^*_{n+1,i} = \alpha_{n+1,i} \exp[(r_i\varepsilon_{n+1} - r_{n+1}\varepsilon_i)/(k_BT)] \quad \text{for } i = 1,2,\ldots,n \tag{3}$$

In the above, a^ρ_i is the activity of the i-th component in the ρ-th phase, ε_i is the adsorption energy of the i-th component and $\alpha_{n+1,i}$ is the factor connected with partition functions of isolated molecules of the i-th and $(n+1)$-th components in both phases[3]. The activity a^ρ_i is defined in a standard way, *i.e.*,

$$a^\rho_i = \varphi^\rho_i\gamma^\rho_i \quad \text{for } i = 1,2,\ldots,n+1 \text{ and } \rho = l, \sigma \tag{4}$$

where φ^ρ_i and γ^ρ_i denote the volume fraction and activity coefficient of the i-th component in the ρ-th phase, respectively, where $\gamma^\rho_i \to 1$ as $\varphi^\rho_i \to 1$. According to the theory of regular solutions the activity coefficient γ^ρ_i is expressed as follows:

$$\ln \gamma^\rho_i = \sum_{j=1}^{n+1} (1 - r_i/r_j)\varphi^\rho_j + r_i \sum_{\substack{j=1 \\ j\neq i}}^{n+1} \chi^\rho_{ji}\varphi^\rho_j(1-\varphi^\rho_i) - r_i \sum_{\substack{j,k=1 \\ j,k\neq i \\ k>j}}^{n+1} \chi^\rho_{jk}\varphi^\rho_j\varphi^\rho_k \tag{5}$$

for $i = 1,2,\ldots,n+1$ and $\rho = l, \sigma$. In the above, the interaction parameter χ^ρ_{ij} is defined by the following equation:

$$\chi^\rho_{ij} = [z^\rho/(k_BT)]\,[\omega^\rho_{ij} - 0.5(\omega^\rho_{ii} + \omega^\rho_{jj})] \tag{6}$$

$$\text{for } i,j = 1,2,\ldots,n+1,\ i \neq j,\ \rho = l, \sigma \text{ and } \chi^\rho_{ij} = \chi^\rho_{ji}$$

The symbol ω^ρ_{ij} denotes the interaction energy between two segments of the i-th and j-th molecules in the ρ-th phase, z^ρ is the lattice coordination number in the ρ-th phase. Distinguishing the parameters ω^l_{ij} and ω^σ_{ij}, we assume that the interaction energies in the surface solution are perturbed by the potential field of the adsorbent and as a consequence of this, they differ from those in the bulk solution.

Eqns. 2, 4 and 5 make possible calculation of the volume fractions of all components in the surface phase for a given composition of the bulk phase. In other words, these equations describe adsorption from $(n+1)$-component regular solutions on a homogeneous solid surface in the whole concentration region.

The equilibrium constant $K^*_{n+1,i}$ may be rewritten in a slightly different form:

$$K_{n+1,i} = (K^*_{n+1,i})^{1/r_i} = (\alpha_{n+1,i})^{1/r_i}\exp[(\varepsilon_{n+1} - r_{n+1}\varepsilon_i/r_i)/(k_BT)] \tag{7}$$

for $i = 1,2,\ldots,n$. Then, eqn. 2 becomes

$$K_{n+1,i} = [(\varphi^{\sigma}_{n+1}\gamma^{\sigma}_{n+1})/(\varphi^{l}_{n+1}\gamma^{l}_{n+1})][(\varphi^{l}_{i}\gamma^{l}_{i})/(\varphi^{\sigma}_{i}\gamma^{\sigma}_{i})]^{r_{n+1}/r_i} \quad \text{for } i = 1,2,\ldots,n \quad (8)$$

Eqn. 8 is more convenient to formulate equations describing LSC with mixed mobile phases.

FUNDAMENTAL EQUATIONS DESCRIBING LSC WITH MIXED MOBILE PHASES

Let us consider an adsorption system described by eqns. 5 and 8 but at infinitely low concentration of the $(n + 1)$-th component (solute), *i.e.*,

$$\varphi^{\rho}_{s} \to 0 \text{ for } s = n + 1 \text{ and } \rho = l, \sigma. \quad (9)$$

The subscript "s" denotes the $(n + 1)$-th component at infinitely low concentration in the mobile (bulk) phase, and then its concentration in the surface phase is also infinitely low. The volume fractions of the remaining components (solvents) $1,2,\ldots,n$ fulfill the following condition:

$$\sum_{i=1}^{n} \varphi^{\rho}_{i} = 1 \quad \text{for } \rho = l, \sigma \quad (10)$$

The components $1,2,\ldots,n$ are treated as the solvents. The expression defining the activity coefficient of the s-th solute in the ρ-th phase may be obtained from eqn. 5 replacing in it the volume fraction $\varphi^{\rho}_{n+1} = \varphi^{\rho}_{s}$ by zero; finally we have

$$\ln \tilde{\gamma}^{\rho}_{s} = \sum_{i=1}^{n} (1 - r_s/r_i)\varphi^{\rho}_{i} + r_s \sum_{i=1}^{n} \chi^{\rho}_{is}\varphi^{\rho}_{i} - r_s \sum_{\substack{i,j=1 \\ j>i}}^{n} \chi^{\rho}_{ij}\varphi^{\rho}_{i}\varphi^{\rho}_{j} \quad \text{for } \rho = l, \sigma \quad (11)$$

where

$$\tilde{\gamma}^{\rho}_{s} = \lim_{\varphi^{\rho}_{s}\to 0} \gamma^{\rho}_{s} \quad \text{for } \rho = l, \sigma \quad (12)$$

It is convenient to express the activity coefficient $\tilde{\gamma}^{\rho}_{s}$ by means of the activity coefficients $\tilde{\gamma}^{\rho}_{s(i)}$ for $i = 1,2,\ldots,n$. The symbol $\tilde{\gamma}^{\rho}_{s(i)}$ denotes the activity coefficient of the s-th solute in the i-th pure solvent, *i.e.*,

$$\tilde{\gamma}^{\rho}_{s(i)} = \lim_{\varphi^{\rho}_{i}\to 1} \gamma^{\rho}_{s} = \lim_{\varphi^{\rho}_{i}\to 1} \tilde{\gamma}^{\rho}_{s} \quad \text{for } i = 1,2,\ldots,n \text{ and } \rho = l, \sigma \quad (13)$$

Eqn. 11 gives the following expression for $\ln \tilde{\gamma}^{\rho}_{s(i)}$:

$$\ln \tilde{\gamma}^{\rho}_{s(i)} = (1 - r_s/r_i) + r_s \chi^{\rho}_{is} \quad \text{for } i = 1,2,\ldots,n \text{ and } \rho = l, \sigma \tag{14}$$

Combination of eqns. 11 and 14 gives

$$\ln \tilde{\gamma}^{\rho}_{s} = \sum_{i=1}^{n} \varphi^{\rho}_{i} \ln \tilde{\gamma}^{\rho}_{s(i)} - r_s \sum_{\substack{i,j=1 \\ j>i}}^{n} \chi^{\rho}_{ij} \varphi^{\rho}_{i} \varphi^{\rho}_{j} \quad \text{for } \rho = l, \sigma \tag{15}$$

The activity coefficients $\tilde{\gamma}^{\rho}_{i}$ for $i = 1,2,\ldots,n$ at $\varphi^{\rho}_{s} \to 0$ are expressed as follows:

$$\ln \tilde{\gamma}^{\rho}_{i} = \lim_{\varphi^{\rho}_{s} \to 0} \ln \gamma^{\rho}_{i} = \sum_{j=1}^{n} (1 - r_i/r_j) \varphi^{\rho}_{j} + r_i \sum_{j=1}^{n} \chi^{\rho}_{ji} \varphi^{\rho}_{j} (1 - \varphi^{\rho}_{i}) - r_i \sum_{\substack{j,k=1 \\ j,k \neq i \\ k>j}}^{n} \chi^{\rho}_{jk} \varphi^{\rho}_{j} \varphi^{\rho}_{k} \tag{16}$$

for $i = 1,2,\ldots,n$ and $\rho = l, \sigma$. For $\varphi^{\rho}_{i} \to 1$ eqn. 16 gives

$$\lim_{\varphi^{\rho}_{i} \to 1} \gamma^{\rho}_{i} = \lim_{\varphi^{\rho}_{i} \to 1} \tilde{\gamma}^{\rho}_{i} = 1 \text{ for } \rho = l, \sigma \tag{17}$$

The distribution coefficients of the s-th solute in a n-component eluent and the i-th pure solvent are defined as follows:

$$k_s = \lim_{\varphi^{l}_{s} \to 0} (\varphi^{\sigma}_{s}/\varphi^{l}_{s}) \tag{18}$$

$$k_{s(i)} = \lim_{\varphi^{l}_{i} \to 1} (\varphi^{\sigma}_{s}/\varphi^{l}_{s}) \text{ for } i = 1,2,\ldots,n \tag{19}$$

Taking into account eqns. 18, 19 in eqn. 8 we obtain

$$\ln k_s = \ln K_{si} + (r_s/r_i) \ln[(\varphi^{\sigma}_{i} \tilde{\gamma}^{\sigma}_{i})/(\varphi^{l}_{i} \tilde{\gamma}^{l}_{i})] + \ln(\tilde{\gamma}^{l}_{s}/\tilde{\gamma}^{\sigma}_{s}) \tag{20}$$

$$\ln k_{s(i)} = \ln K_{si} + \ln(\tilde{\gamma}^{l}_{s(i)}/\tilde{\gamma}^{\sigma}_{s(i)}) \quad \text{for } i = 1,2,\ldots,n \text{ and } s = n+1 \tag{21}$$

Combining eqns. 14, 15, 16 and 20 we obtain the general expression defining the dependence of $\ln k_s$ upon mobile phase composition:

$$\ln k_s = \ln K_{si} + (r_s/r_i) \ln(\varphi^{\sigma}_{i}/\varphi^{l}_{i}) + r_s \sum_{j=1}^{n} (\chi^{l}_{js} - \chi^{\sigma}_{js}) \varphi^{l}_{j} + r_s \sum_{j=1}^{n-1} (\chi^{\sigma}_{ns} - \chi^{\sigma}_{js}) (\varphi^{\sigma}_{j} - \varphi^{l}_{j}) - r_s \sum_{\substack{j=1 \\ j \neq i}}^{n} \chi^{l}_{ji} \varphi^{l}_{j} + r_s \sum_{\substack{j=1 \\ j \neq i}}^{n} \chi^{\sigma}_{ji} \varphi^{\sigma}_{j} \tag{22}$$

This expression may be rewritten in terms of the distribution coefficients of the s-th solute in the pure solvents forming the mixed eluent. For this purpose we express the term $\ln(\tilde{\gamma}_s^l/\tilde{\gamma}_s^\sigma)$ appearing in eqn. 20 by means of $\ln k_{s(i)}$ for $i = 1,2,\ldots,n$; it is

$$\ln(\tilde{\gamma}_s^l/\tilde{\gamma}_s^\sigma) = \sum_{j=1}^{n} \varphi_j^l \ln k_{s(j)} - \sum_{j=1}^{n} \varphi_j^l \ln K_{sj} - \sum_{j=1}^{n} (\varphi_j^\sigma - \varphi_j^l) \ln \tilde{\gamma}_{s(j)}^\sigma + \\ + r_s \sum_{\substack{j,k=1 \\ k>j}}^{n} \chi_{jk}^\sigma \varphi_j^\sigma \varphi_k^\sigma - r_s \sum_{\substack{j,k=1 \\ k>j}}^{n} \chi_{jk}^l \varphi_j^l \varphi_k^l \qquad (23)$$

Substitution of eqns. 23 and 16 into eqn. 20 gives the general expression for the distribution coefficient of the s-th solute in term the distribution coefficients of this solute in the pure solvents; it is

$$\ln k_s = \sum_{\substack{j=1 \\ j\neq i}}^{n} (r_s/r_j)\, \varphi_j^l \ln K_{ji} + (r_s/r_i) \ln (\varphi_i^\sigma/\varphi_i^l) + \sum_{j=1}^{n} \varphi_j^l \ln k_{s(j)} + \\ + \sum_{j=1}^{n-1} r_s (\chi_{ns}^\sigma - \chi_{js}^\sigma)(\varphi_j^\sigma - \varphi_j^l) + r_s \sum_{\substack{j=1 \\ j\neq i}}^{n} \chi_{ji}^\sigma \varphi_j^\sigma - r_s \sum_{\substack{j=1 \\ j\neq i}}^{n} \chi_{ji}^l \varphi_j^l \qquad (24)$$

where $K_{ii} = 1$ and $\chi_{ji}^\rho = \chi_{ij}^\rho$. At this point it is worth noting that eqns. 22 and 24 defining the distribution coefficient of the s-th solute in a n-component eluent are equivalent; the first of them is written in terms of the molecular parameters characterizing regular bulk and surface solutions, whereas the second equation is written in terms of the distribution coefficients of the s-th solute in pure solvents forming the mixed eluent. These equations have been obtained from eqn. 20 by replacing the activity coefficients of the s-th solute and the i-th solvent in both phases by analytical expressions resulting from the model of regular solutions. Thus, eqn. 20 is a fundamental relationship in LSC with mixed eluents.

With special assumptions eqns. 20, 22 and 24 yield equations having rigorous thermodynamical foundations, which have been used up to date in LSC with mixed mobile phases. Before discussing this question we consider definitions of adsorption and partition phenomena in LSC.

ADSORPTION AND PARTITION PHENOMENA IN LSC

Let us return to eqn. 21 defining the distribution coefficient of the s-th solute in the i-th pure solvent. Rewriting this equation in a slightly different form we obtain:

$$k_{s(i)} = K_{si}\, (\tilde{\gamma}_{s(i)}^l/\tilde{\gamma}_{s(i)}^\sigma) \quad \text{for } i = 1,2,\ldots,n \qquad (25)$$

A simple analysis of eqn. 25 shows that distribution of the s-th solute between stationary (surface) and mobile (bulk) phases consisting of the i-th pure solvent is determined by two terms: K_{si} (equilibrium constant describing phase-exchange of solute and solvent molecules) and $(\tilde{\gamma}^{l}_{s(i)}/\tilde{\gamma}^{\sigma}_{s(i)})$ (ratio of the activity coefficients of the s-th solute in the bulk and surface phases). The equilibrium constant K_{si} (eqn. 7) contains the pre-exponential entropy factor involving the difference in partition functions of isolated molecules of the s-th solute and i-th solvent in the bulk solution and surface layer, and an exponential factor containing the difference in adsorption energies of the s-th solute and i-th solvent. This exponential term gives the greatest contribution to the constant K_{si}. For the same entropy factor, adsorption of the s-th solute increases with an increasing difference in adsorption energies of the s-th solute and i-th solvent. This difference of energies mainly determines the distribution of the s-th solute between the two one-component phases occuring as a result of the competitive solute and solvent adsorption process, which is represented by the phase-exchange reaction (eqn. 1). Such a mechanism of distribution of the s-th solute between one-component bulk and surface-influenced stationary phases has been described earlier in terms of the displacement model[1,4–9].

The second factor determining the distribution of the s-th solute between surface and bulk phases consisting of the i-th pure solvent is the ratio of the activity coefficients $\tilde{\gamma}^{l}_{s(i)}/\tilde{\gamma}^{\sigma}_{s(i)}$. This ratio is different from unity for $\chi^{l}_{is} \neq \chi^{\sigma}_{is}$, *i.e.*, when we assume different values of the interchange energies of the s-th solute in the i-th solvent forming the bulk and surface-influenced stationary phases. Thus, differences in the interchange energies characterizing solute–solvent interactions in surface and bulk dilute solutions (s,i) may also affect distribution to the s-th solute between the two phases. Such a mechanism of distribution of the s-th solute between the surface and mobile phases consisting of the i-th solvent is quite analogous to that appearing in gas–liquid and liquid–liquid chromatographic systems and has been already described in terms of the so-called partition model[24–27].

The above discussion enables us to distinguish three main models of the LSC process. In the case of LSC with a one-component eluent, equations defining these models may be obtained on the basis of eqn. 25. They are:

$$k_{s(i)} = K_{si} = (\alpha_{si})^{1/r_i}\exp[(\varepsilon_s - r_s\varepsilon_i/r_i)/(k_B T)] \tag{26}$$

with the condition

$$\tilde{\gamma}^{l}_{s(i)}/\tilde{\gamma}^{\sigma}_{s(i)} = 1;\ i = 1,2,\ldots,n \tag{27}$$

for the displacement model (DM), and

$$k_{s(i)} = \tilde{\gamma}^{l}_{s(i)}/\tilde{\gamma}^{\sigma}_{s(i)} = \exp[r_s(\chi^{l}_{is} - \chi^{\sigma}_{is})] \tag{28}$$

with the condition

$$K_{si} = 1 \text{ for } i = 1,2,\ldots,n \tag{29}$$

for the partition model (PM), and

$$K_{si} \neq 1;\ \gamma^l_{s(i)}/\tilde{\gamma}^\sigma_{s(i)} \neq 1 \text{ for } i = 1,2,\ldots,n \tag{30}$$

for the mixed model (MM).

Similar equations to eqns. 26–29 may be written for the displacement and partition models of LSC with multicomponent eluents. In this case eqn. 20 gives:

$$\ln k_s = \ln K_{si} + (r_s/r_i) \ln (\varphi^\sigma_i/\varphi^l_i) \tag{31}$$

with the condition

$$\ln[(\tilde{\gamma}^l_s/\tilde{\gamma}^\sigma_s)(\tilde{\gamma}^\sigma_i/\tilde{\gamma}^l_i)^{r_s/r_i}] = 0 \text{ for } i = 1,2,\ldots,n \tag{32}$$

for the displacement model, and

$$\ln k_s = \ln (\tilde{\gamma}^l_s/\tilde{\gamma}^\sigma_s) \tag{33}$$

with the condition

$$K_{ij} = 1 \text{ for } i,j = 1,2,\ldots,n,s \tag{34}$$

for the partition model. Eqns. 31 and 33 defining the distribution coefficient of the s-solute between two multicomponent phases by assuming displacement and partition models, respectively, are well known in the chromatographic literature[4–8,24–27]. These equations have been obtained from eqn. 20 by assuming special conditions given by eqns. 32 and 34. Discussion of these conditions in terms of our treatment is both interesting and pertinent because it can reveal the physical limitations of the above models.

Let us consider the condition given by eqn. 32. On the basis of eqns. 14–16 we can write:

$$(r_s/r_i)\ln(\tilde{\gamma}^\sigma_i/\tilde{\gamma}^l_i) = \sum_{j=1}^{n-1} (r_s/r_n - r_s/r_j)(\varphi^\sigma_j - \varphi^l_j) + r_s \sum_{j=1}^{n} [\chi^\sigma_{ji}(\varphi^\sigma_j)^2 - \chi^l_{ji}(\varphi^l_j)^2] +$$

$$+ r_s \sum_{\substack{j,k=1 \\ j,k\neq i \\ k>j}}^{n} (\chi^\sigma_{ji} + \chi^\sigma_{ki} - \chi^\sigma_{jk})\varphi^\sigma_j\varphi^\sigma_k - r_s \sum_{\substack{j,k=1 \\ j,k\neq i \\ k>j}}^{n} (\chi^l_{ji} + \chi^l_{ki} - \chi^l_{jk})\varphi^l_j\varphi^l_k \tag{35}$$

and

$$\ln(\tilde{\gamma}^l_s/\tilde{\gamma}^\sigma_s) = -\sum_{j=1}^{n} (r_s/r_n - r_s/r_j)(\varphi^\sigma_j - \varphi^l_j) + r_s \sum_{j=1}^{n} (\chi^l_{js} - \chi^\sigma_{js})\varphi^l_j +$$

$$+ r_s \sum_{j=1}^{n-1} (\chi^\sigma_{ns} - \chi^\sigma_{js})(\varphi^\sigma_j - \varphi^l_j) + r_s \sum_{\substack{j,k=1 \\ k>j}}^{n} \chi^\sigma_{jk}\varphi^\sigma_j\varphi^\sigma_k - r_s \sum_{\substack{j,k=1 \\ k>j}}^{n} \chi^l_{jk}\varphi^l_j\varphi^l_k \tag{36}$$

Comparing eqns. 35 and 36 according to the condition given by eqn. 32 we can see that terms containing $(r_s/r_n - r_s/r_j)$ cancel out. Thus, eqn. 32 is fulfilled if the parameters χ_{ij}^{ρ} are equal zero, *i.e.*,

$$\chi_{ij}^{\rho} = 0 \text{ for } i,j = 1,2,\ldots,n,s,\ i \neq j \text{ and } \rho = l,\ \sigma \tag{37}$$

Eqn. 37 defines LSC systems with ideal surface and mobile phases.

Now, we consider eqn. 33 describing dependence of ln k_s upon mobile phase composition according to the partition model of LSC with mixed eluents. This equation is valid when eqn. 34 is fulfilled. The equilibrium constant K_{ij} describing the phase-exchange reaction for molecules of the i-th and j-th components contained in an infinitely dilute solution with respect to the s-th solute, may be expressed as follows:

$$K_{ij} = [(\varphi_i^{\sigma}\gamma_i^{\sigma})/(\varphi_i^{l}\gamma_i^{l})][(\varphi_j^{l}\tilde{\gamma}_j^{l})/(\varphi_j^{\sigma}\tilde{\gamma}_j^{\sigma})]^{r_i/r_j} \quad \text{for } i,j = 1,2,\ldots,n,s \tag{38}$$

Since, for the partition model (eqn. 34) the constants $K_{ij} = 1$ for $i,j = 1,2,\ldots,n$, (no displacement process between solute and solvent molecules), eqn. 38 gives

$$(\varphi_i^{\sigma}\tilde{\gamma}_i^{\sigma})/(\varphi_i^{l}\tilde{\gamma}_i^{l}) = [(\varphi_j^{\sigma}\tilde{\gamma}_j^{\sigma})/(\varphi_j^{l}\tilde{\gamma}_j^{l})]^{r_i/r_j} \quad \text{for } i,j = 1,2,\ldots,n,s \tag{39}$$

For different values of r_i eqn. 39 is fulfilled when[31]

$$(\varphi_i^{\sigma}\tilde{\gamma}_i^{\sigma})/(\varphi_i^{l}\tilde{\gamma}_i^{l}) = 1 \text{ for } i = 1,2,\ldots,n,s \tag{40}$$

It is easy to see that eqn. 40 for $i = s$ associated with the definition of k_s (see eqn. 18) gives eqn. 33. Moreover, eqn. 20 becomes eqn. 33 when $K_{si} = 1$ and eqn. 40 is fulfilled.

Eqns. 31, 32 and 33, 34 define the so-called pure displacement and partition models, respectively. The pure displacement model of LSC assumes identical interactions between solute and solvent molecules (see eqn. 37). Then distribution of solute and solvent molecules between two phases occurs only as a result of the competitive adsorption. However, the pure partition model of LSC assumes no competitive solute and solvent adsorption. In this case the distribution of a solute between the two phases is a result of differences in its activity coefficients in the mobile and surface-influenced stationary phases. Besides the above "pure" models of LSC, eqn. 20 can describe different mixed models involving concurrent adsorption and partition effects, *e.g.*, models assuming competitive adsorption for solute and one solvent or only competitive solvent adsorption, etc. One of the main advantages of eqn. 20 is its general character; this equation coupled with the expressions defining solute and solvent activity coefficients (eqns. 15 and 16) can also generate the most popular equations derived up to date for displacement and partition models of LSC[6,7,24,29].

PURE DISPLACEMENT MODEL OF LSC

Eqn. 37 defines the physical condition where only solute and solvent competitive adsorption determines the LSC process. Under this condition the dependence of the distribution coefficient of the s-th solute upon mobile phase composition is given by eqn. 31. This equation may be rewritten in a slightly different form:

$$\ln k_s = \ln k_{s(i)} + v_i \ln (\varphi_i^\sigma/\varphi_i^l) \quad \text{for } v_i = r_s/r_i \text{ and } i = 1,2,\ldots,n \tag{41}$$

In many chromatographic models the eluent is assumed to be a mixture consisting of molecules of identical sizes, then $r_1 = r_2 = \ldots = r_n = r$. Hence, the volume fractions of solvents are equivalent to the mole fractions. Taking this into account in eqn. 41, we have

$$\ln k_s = \ln k_{s(i)} + v \ln(x_i^\sigma/x_i^l) \quad \text{for } v = r_s/r \text{ and } i = 1,2,\ldots,n \tag{42}$$

where x_i^ϱ denotes the mole fraction of the i-th solvent in the ϱ-th phase. Eqn. 42 has been derived by Jaroniec *et al.*[13]. As $x_i^\sigma \to 1$ this equation becomes the well-known Snyder–Soczewiński relationship[4,9]:

$$\ln k_s = \ln k_{s(i)} - v \ln x_i^l \tag{43}$$

A similar relationship to that expressed by eqn. 43 may be obtained from eqn. 41 by assuming $\varphi_i^\sigma \to 1$:

$$\ln k_s = \ln k_{s(i)} - v \ln \varphi_i^l \tag{44}$$

Eqn. 44 may be used to describe chromatographic data measured for mixed eluents consisting of molecules of different molecular sizes.

An interesting expression may be obtained from eqn. 42 by assuming Everett's equation for x_i^σ (refs. 2 and 3):

$$x_i^\sigma = K_{in} x_i^l \Big/ \left(x_n^l + \sum_{j=1}^{n-1} K_{jn} x_j^l \right) \quad \text{for } i = 1,2,\ldots,n \tag{45}$$

Eqns. 45 and 42 give

$$k_s = \left\{ \sum_{j=1}^{n} [x_j^l/(k_{s(j)})^{1/v}] \right\}^{-v} \tag{46}$$

where

$$K_{jn} = [k_{s(n)}/k_{s(j)}]^{1/v} \quad \text{for } j = 1,2,\ldots,n-1 \tag{47}$$

Eqn. 46 has been recently obtained by Borówko[32]. For $r_s = r$ (identical molecular

sizes of solute and solvent molecules) eqn. 46 becomes the well-known relationship[28,29,33]:

$$k_s = \left[\sum_{j=1}^{n} (x_j^l / k_{s(j)})\right]^{-1} \tag{48}$$

Jaroniec *et al.*[33] showed that eqn. 48 is equivalent to Snyder's fundamental relationship[1]:

$$k_s = \sum_{j=1}^{n} x_j^\sigma \, k_{s(j)} \tag{49}$$

This problem was also discussed in terms of statistical thermodynamics[28,29,34]. The equations considered in this section, referring to the pure displacement model, have been discussed in detail in two reviews[6,7].

PURE PARTITION MODEL OF LSC

Eqns. 33 and 34 defining the distribution coefficient of the s-th solute in terms of the pure partition model, combined with eqn. 23 give:

$$\ln k_s = \sum_{i=1}^{n} \varphi_i^l \ln k_{s(i)} + \sum_{i=1}^{n-1} [(r_s/r_i - r_s/r_n) + r_s(\chi_{ns}^\sigma - \chi_{is}^\sigma)](\varphi_i^\sigma - \varphi_i^l) + \\ + r_s \sum_{\substack{i,j=1 \\ j>i}}^{n} \chi_{ij}^\sigma \varphi_i^\sigma \varphi_j^\sigma - r_s \sum_{\substack{i,j=1 \\ j>i}}^{n} \chi_{ij}^l \varphi_i^l \varphi_j^l \tag{50}$$

This equation has been recently derived by Martire and Jaroniec[27]. Two important special cases may be deduced from this equation. The first case refers to chromatographic systems with nearly ideal eluents containing solvents strongly interacting with solute molecules. Under these assumptions eqn. 50 reduces to Ościk's relationship[6,25]:

$$\ln k_s = \sum_{i=1}^{n} \varphi_i^l \ln k_{s(i)} + \sum_{i=1}^{n-1} (\varphi_i^\sigma - \varphi_i^l) \ln \kappa_{s(in)}^\sigma \tag{51}$$

where

$$\ln \kappa_{s(in)}^\sigma = (r_s/r_i - r_s/r_n) + r_s (\chi_{ns}^\sigma - \chi_{is}^\sigma) \tag{52}$$

For chromatographic systems showing ideal behaviour the term containing $\ln \kappa_{s(in)}^\sigma$ becomes zero and then eqn. 51 reduces to the well-known relationship[7,27]

$$\ln k_s = \sum_{i=1}^{n} \varphi_i^l \ln k_{s(i)} \tag{53}$$

Eqn. 53 is, besides the Snyder–Soczewiński eqn. 43, one of the most popular relationships used for describing LSC data. This equation represents the linear dependence of the logarithm of the distribution coefficient upon the volume fractions of solvents forming a mixed eluent. Eqn. 53 and other equations presented in this section describe distribution of the s-th solute between the bulk and surface-influenced stationary phases. In other words, these equations describe partition effects in LSC with mixed mobile phases.

LSC WITH BINARY ELUENTS

In this section we present a short discussion of equations describing LSC with binary eluents. A general equation for binary eluents may be obtained from eqn. 24 for $n = 2$; it is

$$\ln k_s = (r_s/r_2)\varphi_2^l \ln K_{21} + (r_s/r_1) \ln (\varphi_1^\sigma/\varphi_1^l) + \varphi_1^l \ln k_{s(1)} + \varphi_2^l \ln k_{s(2)} + \\ + r_s(\chi_{2s}^\sigma - \chi_{1s}^\sigma)(\varphi_1^\sigma - \varphi_1^l) + r_s \chi_{12}^\sigma \varphi_2^\sigma - r_s \chi_{12}^l \varphi_2^l \quad (54)$$

Eqn. 54 may be also obtained from eqn. 20, in which the subscript "i" is replaced by "1" and γ_s^ρ and γ_1^ρ ($\rho = l, \sigma$) are replaced by suitable equations defining activity coefficients of the s-th solute and 1-st solvent in an infinitely dilute regular solution (s,1,2) with respect to the s-th solute. It is difficult to obtain special cases of eqn. 54 relating to the pure displacement and partition models because some terms appearing in the expressions $\ln (\tilde{\gamma}_s^l/\tilde{\gamma}_s^\sigma)$ and $\ln (\tilde{\gamma}_1^\sigma/\tilde{\gamma}_1^l)$ have cancelled out. However, these equations may be easily obtained from eqns. 46 and 50 when $n = 2$. In the case of the displacement model we have:

$$k_s = [x_1^l/(k_{s(1)})^{1/\nu} + x_2^l/(k_{s(2)})^{1/\nu}]^{-\nu} \quad (55)$$

The Snyder–Soczewiński relationship is valid for chromatographic systems with binary eluents, which contain solvents showing a great difference in elution strengths, then $k_{s(2)} \gg k_{s(1)}$ where the subscript "1" denotes the more efficient eluting solvent[6,7]. Under this condition eqn. 55 becomes the Snyder–Soczewiński relationship:

$$\ln k_s = \ln k_{s(1)} - \nu \ln x_1^l \quad (56)$$

In the case of the partition model, eqn. 50 for $n = 2$ gives an extended form of Ościk's equation[27]:

$$\ln k_s = \varphi_1^l \ln k_{s(1)} + \varphi_2^l \ln k_{s(2)} + (\varphi_1^\sigma - \varphi_1^l) \ln \kappa_{s(12)}^\sigma - \\ r_s \chi_{12}^l \varphi_1^l \varphi_2^l + r_s \chi_{12}^\sigma \varphi_1^\sigma \varphi_2^\sigma \quad (57)$$

Let us return to the general eqn. 54. It is interesting to consider this equation for ideal binary eluents ($\chi_{12}^\sigma = \chi_{12}^l = 0$ and $r_1 = r_2 = r$). If, in addition, the solute

molecules have comparable interactions with molecules of the 1-st and 2-nd solvents and they are not perturbed by the solid surface, then

$$\chi^{\sigma}_{1s} = \chi^{l}_{1s} = \chi^{\sigma}_{2s} = \chi^{l}_{2s} \tag{58}$$

Under these conditions eqn. 54 gives eqn. 55, which has been derived for the pure displacement model. This indicates that Ościk's equation should contain terms referring to solvent–solvent interactions in both phases because for systems with strong solvent–solvent interactions partition effects should be dominant and this enables us to neglect the effects connected with the displacement process.

CONCLUDING REMARKS

Eqn. 20 contains activity coefficients of the solute and a reference solvent. These activity coefficients may be expressed in an analytical form when we assume a definite molecular model for the bulk and surface solutions. This paper presents equations for the distribution coefficient by taking the model of regular solutions for the mobile and surface-influenced stationary phases, where the surface layer has been formed on an energetically homogeneous solid. This model is based on random mixing and, hence, involves primarily dispersive interactions between the molecules. However, according to Dubinin *et al.*[35] it is possible to express the total activity coefficient of the j-th component in the mobile and surface phases as follows:

$$\tilde{\gamma}^{\sigma}_{j} = \tilde{\gamma}^{\sigma}_{j,d}\tilde{\gamma}^{\sigma}_{j,s}\tilde{\gamma}^{\sigma}_{j,h} \tag{59}$$

and

$$\tilde{\gamma}^{l}_{j} = \tilde{\gamma}^{l}_{j,d}\tilde{\gamma}^{l}_{j,s} \quad \text{for } j = 1,2,\ldots,n,s \tag{60}$$

In the above, $\tilde{\gamma}^{\rho}_{j,d}$ and $\tilde{\gamma}^{\rho}_{j,s}$ denote the activity coefficients of the j-th component in the ρ-th phase reflecting nonideality of the solution due to dispersive (d) and specific (s) interactions, whereas, $\tilde{\gamma}^{\sigma}_{j,h}$ denotes the activity coefficient of the j-th component in the surface phase reflecting nonideality of the surface solution due to adsorbent heterogeneity (h). Expressing activity coefficients of the solute and solvent in eqn. 20 by expressions of the type eqn. 59 it should be possible to derive equations for LSC involving adsorbent heterogeneity and association effects.

There is also the possibility of describing LC systems containing different numbers of components in both phases, *e.g.*, systems containing liquid components in the stationary phase, which are immiscible with the mobile phase and vice versa. Such a situation may appear in liquid–liquid chromatography with mixed phases and LC with chemically bonded phases. The activity coefficients for such systems may be expressed by eqn. 15, in which terms containing the volume fractions of components not appearing in the ρ-th phase are neglected.

As an example we present equations for LC containing one component in the stationary phase immiscible with the binary mobile phase, *e.g.*, LC with a homogeneous chemically bonded phase. Then the activity coefficient $\tilde{\gamma}^{\sigma}_{s}$ may be expressed as follows:

$$\ln \tilde{\gamma}_s^\sigma = \varphi_1^\sigma \ln \gamma_{s(1)}^\sigma + \varphi_2^\sigma \ln \tilde{\gamma}_{s(2)}^\sigma + \varphi_c^\sigma \ln \tilde{\gamma}_{s(c)}^\sigma - r_s\chi_{12}^\sigma\varphi_1^\sigma\varphi_2^\sigma - r_s\chi_{1c}^\sigma\varphi_1^\sigma\varphi_c^\sigma - r_s\chi_{2c}^\sigma\varphi_2^\sigma\varphi_c^\sigma \quad (61)$$

where φ_c^σ and $\tilde{\gamma}_{s(c)}^\sigma$ denote the volume fraction of the c-th immiscible component in the stationary phase and the activity coefficient of the s-th solute in the c-th pure component, respectively. The activity coefficient $\tilde{\gamma}_{s(c)}^\sigma$ in the c-th component bonded to the solid surface may be defined analogously to eqn. 14:

$$\ln \tilde{\gamma}_{s(c)}^\sigma = (1 - r_s/r_c) + r_s\chi_{sc}^\sigma + \Delta_{sc} \quad (62)$$

where Δ_{sc} is a correction term. A simple correction of the form shown is strictly valid when the chemically bonded phase is "collapsed" or nearly so, implying little uptake of solvent components 1 and 2 by the stationary phase, *i.e.*, φ_1^σ and φ_2^σ are small[24]. In this collapsed-chain limit Δ_{sc} depends only on the surface coverage and intrinsic flexibility of the chemically bonded chains, and on the nature of the solute. However, the activity coefficient $\tilde{\gamma}_s^l$ is given by eqn. 15 for $n = 2$. Combination of eqn. 33 defining the distribution coefficient of the s-th solute for the partition model with eqn. 61 and eqn. 15 for $n = 2$ gives:

$$\ln k_s = \varphi_1^l \ln k_{s(1/12c)} + \varphi_2^l \ln k_{s(2/12c)} - r_s\chi_{12}^l\varphi_1^l\varphi_2^l \quad (63)$$

where

$$\ln k_{s(i/12c)} = \ln (\tilde{\gamma}_{s(i)}^l/\tilde{\gamma}_s^\sigma) \quad \text{for } i = 1,2 \quad (64)$$

The symbol $k_{s(i/12c)}$ denotes a hypothetical distribution coefficient for the s-th solute between the i-th bulk solvent and surface-influenced stationary phase $(1+2+c)$ having an equilibrium composition. Let us consider a case when the solvents are excluded from the stationary phase; then the distribution coefficient $k_{s(i/12c)}$ becomes a physically attainable quantity and represents partition of the s-th solute between the i-th pure solvent and a stationary phase containing only a component immiscible with this solvent. Under this condition we have

$$k_{s(i/12c)} = k_{s(i/c)} \quad \text{for } \varphi_1^\sigma = \varphi_2^\sigma = 0 \text{ and } i = 1,2 \quad (65)$$

and eqn. 63 becomes

$$\ln k_s = \varphi_1^l \ln k_{s(1/c)} + \varphi_2^l \ln k_{s(2/c)} - r_s\chi_{12}^l\varphi_1^l\varphi_2^l \quad (66)$$

Eqn. 66 has been derived by Martire and Boehm[24] for LSC with chemically bonded phases in terms of statistical thermodynamics. This short derivation shows the great utility of the above description to derive equations involving adsorption and partition effects in liquid chromatographic systems with an arbitrary number of components in both phases.

Therefore, it has been demonstrated that various well-known retention–solvent composition relationships can be readily derived from the basic general equation under certain simplifying assumptions. These familiar relationships have been applied

extensively to the interpretation of liquid chromatographic data. Their limitations and range of applicability are a matter of record. It is clear that none of these simple relationships is completely adequate.

Indeed, as has also been recognized and studied by others[36–39], retention behavior in liquid chromatographic systems is generally complex, especially with mixed mobile phases, and usually cannot be fully described through a single, simple mechanism. However, the problem of practical application of our general equation to a wide range of normal and reversed phase systems, although it is an important (and difficult) one, is beyond the scope of the present paper. It will be the subject of our future studies.

The aim of the present paper was to develop a comprehensive theoretical framework for liquid–solid chromatography. The resulting general equation has been phrased in terms of interaction parameters and activity coefficients, which would need to be evaluated or estimated in actual applications. It should be noted that, as a starting point, approximate methods[35,40] exist for treating these thermodynamic quantities.

ADDED NOTE

As should be evident from the equations and text in the section titled "Adsorption and Partition Phenomena in LSC", by the term "partition" we refer to that contribution arising from the distribution of solute between a surface-influenced (stationary) liquid layer and a bulk-liquid mobile phase. Even though this effect is similar to liquid–liquid equilibria, we regarded such alternative terms as "solvation", "solution" or "liquid–liquid partition" to be misleading because the stationary layer is by no means a bulk liquid.

However, the Editor has pointed out that, strictly, the term "partition" has a broader connotation and should not be solely reserved to describe liquid–liquid equilibria (or, by extension, a process akin to it), despite its common usage in that regard. This point is well taken. We do not wish it to be inferred that we support or encourage propagation of this historical distortion. Simply, given the nature of the stationary layer and the role of the underlying solid surface in determining its existence and composition, the term "partition" was favored in the present instance by its very broadness.

ACKNOWLEDGEMENT

This material is based upon work supported by the National Science Foundation under Grant CHE-8305045.

REFERENCES

1 L. R. Snyder, *Principles of Adsorption Chromatography*, Marcel Dekker, New York, 1968.
2 M. Jaroniec, *Advan.-Colloid Interface Sci.*, 18 (1983) 149.
3 M. Borówko and M. Jaroniec, *Advan. Colloid Interface Sci.*, 19 (1983) 137.
4 L. R. Snyder and H. Poppe, *J. Chromatogr.*, 184 (1980) 363.
5 L. R. Snyder, *High Performance Liquid Chromatography*, Vol. 3, Academic Press, New York, 1983, p. 157.

6 M. Jaroniec and J. Ościk, *J. High Resolut. Chromatogr. Chromatogr. Commun.*, 5 (1982) 3.
7 M. Jaroniec, D. E. Martire and M. Borówko, *Advan. Colloid Interface Sci.*, 22 (1985) 177.
8 E. Soczewiński, *Anal. Chem.*, 41 (1969) 179.
9 E. Soczewiński, *J. Chromatogr.*, 130 (1977) 23.
10 M. Jaroniec and J. A. Jaroniec, *J. Liquid Chromatogr.*, 7 (1984) 393.
11 M. Jaroniec, J. K. Różyło and W. Gółkiewicz, *J. Chromatogr.*, 178 (1979) 27.
12 M. Borówko and M. Jaroniec, *Chromatographia*, 12 (1979) 672.
13 M. Jaroniec, J. K. Różyło and B. Ościk-Mendyk, *J. Chromatogr.*, 179 (1979) 237.
14 M. Jaroniec and A. Patrykiejew, *J. Chem. Soc. Faraday I*, 76 (1980) 2468.
15 M. Jaroniec and B. Ościk-Mendyk, *J. Chem. Soc. Faraday I*, 77 (1981) 1277.
16 M. Jaroniec and J. Piotrowska, *J. High Resolut. Chromatogr. Chromatogr. Commun.*, 3 (1980) 257.
17 M. Jaroniec and J. A. Jaroniec, *J. Liquid Chromatogr.*, 4 (1981) 2121.
18 M. Jaroniec and J. A. Jaroniec, *J. Chromatogr.*, 295 (1984) 377.
19 L. R. Snyder, J. L. Glajch and J. J. Kirkland, *J. Chromatogr.*, 218 (1981) 299.
20 L. R. Snyder and J. L. Glajch, *J. Chromatogr.*, 214 (1981) 1.
21 W. R. Melander and Cs. Horváth, *Chromatographia*, 18 (1984) 353.
22 W. R. Melander and Cs. Horváth, *High Performance Liquid Chromatography*, Vol. 2, Academic Press, New York, 1980, p. 113.
23 R. E. Majors, *High Performance Liquid Chromatography*, Vol. 1, Academic Press, New York, 1980, p. 75.
24 D. E. Martire and R. E. Boehm, *J. Phys. Chem.*, 87 (1983) 1045.
25 J. Ościk, *Przem. Chem.*, 44 (1965) 129.
26 M. Jaroniec, A. Dawidowicz and J. A. Jaroniec, *J. Liquid Chromatogr.*, 8 (1985) 441.
27 D. E. Martire and M. Jaroniec, *J. Liquid Chromatogr.*, 8 (1985) 1363.
28 D. E. Martire and R. E. Boehm, *J. Liquid Chromatogr.*, 3 (1980) 753.
29 R. E. Boehm and D. E. Martire, *J. Phys. Chem.*, 84 (1980) 3620.
30 A. Dabrowski, M. Jaroniec and J. K. Garbacz, *Thin Solid Films*, 103 (1983) 399.
31 E. H. Slaats, J. C. Kraak, W. J. T. Brugman and H. Poppe, *J. Chromatogr.*, 149 (1978) 255.
32 M. Borówko, *J. High Resolut. Chromatogr. Chromatogr. Commun.*, in press.
33 M. Jaroniec, J. Narkiewicz and M. Borówko, *Chromatographia*, 11 (1978) 581.
34 M. Borówko, *J. Colloid Interface Sci.*, 102 (1984) 519.
35 M. M. Dubinin, T. S. Jakubov, M. Jaroniec and V. V. Serpinsky, *Polish J. Chem.*, 54 (1980) 1721.
36 R. P. W. Scott and P. Kucera, *J. Chromatogr.*, 142 (1977) 213.
37 R. P. W. Scott and C. F. Simpson, *Faraday Symp. Chem. Soc.*, 15 (1980) 69.
38 R. P. W. Scott in C. F. Simpson (Editor), *Techniques of Liquid Chromatography*, Wiley, Chichester and New York, 1982, p. 141.
39 E. H. Slaats, W. Markovski, J. Fekete and H. Poppe, *J. Chromatogr.*, 207 (1981) 299.
40 B. L. Karger, L. R. Snyder and C. Eon, *Anal. Chem.*, 50 (1978) 2126.

Journal of Chromatography, 351 (1986) 17–29
Elsevier Science Publishers B.V., Amsterdam — Printed in The Netherlands

CHROM. 18 179

EXPERIMENTAL AND THEORETICAL DYNAMICS OF ISOELECTRIC FOCUSING

ELUCIDATION OF A GENERAL SEPARATION MECHANISM

W. THORMANN, R. A. MOSHER* and M. BIER
Center for Separation Science, University of Arizona, Tucson, AZ 85721 (U.S.A.)
(First received June 24th, 1985; revised manuscript received September 16th, 1985)

SUMMARY

The transient states in isoelectric focusing were monitored using a potential gradient array detector. Electric field profiles are presented which show the formation of transient moving boundaries, as well as the approach of the steady state distribution, during the focusing of two and three component systems. The experimental results are completely consistent with corresponding computer simulation data. The focusing process is comprised of two sequential phases, a relatively rapid separation phase and a much slower stabilizing phase. A phenomenological separation mechanism is presented for the two and three component systems, based on distinct, transient moving boundaries, which describes the first phase. This mechanism is discussed with respect to n component idealized systems. The second phase provides insight into a primary cause of pH gradient instability. It was found that the time necessary for the adjustment to the steady state, the second phase, can be as much as twenty times longer than the time needed for the separation of the constituents.

INTRODUCTION

A knowledge of the dynamics in isoelectric focusing (IEF) is essential for the characterization of this electrophoretic mode. Various procedures for the determination of transient states have been developed. Repetitive scanning of the focusing column with an optical detector[1], a pH sensor[2] or a radiometric detector[2] has been employed. The measuring of schlieren patterns or shadowgrams[3], the visual inspection or photographic registration of fluorescing carrier and/or test components as well as of colored proteins represent alternate methods. Another approach consists of segmentation of gels or paper strips after various times of current flow, followed by pH, conductance, absorbance, radioactivity or other measurements, such as bioassays, on the segments[4]. Comparable procedures include the freezing and segmentation of a plastic tube containing the medium to be tested[5] and the evaluation of fractions collected from density stabilized columns[6]. None of these methodologies provide complete insight into the evolution of the entire IEF pattern, but do permit monitoring the kinetics of specific constituents.

0021-9673/86/$03.50

The electric field is the most general physical property in electrophoresis. Its distribution along an isoelectric focusing column is important for both theoretical and practical purposes. Without accurate measurement of the local potential gradient it is particularly difficult to give a physicochemical description of the separation mechanism or of a focused zone. The local electric field strength further determines the migration rate of components and the generation of heat. The potential gradient across IEF gel slabs is commonly measured by inserting one or two electrodes into evenly spaced holes in the top of a slab apparatus[7], with sliding contacts or by conductivity measurements on segmental fractions referred to above[4–6]. Jackiw *et al.*[8] constructed a device for measuring the voltage gradient along tube gels. Their detector consists of 11 platinum sensors sealed into the wall of a Pyrex tube (6 mm I.D.) at 1-cm intervals.

We incorporated an array detector as one wall of the separation trough, which enables us to make almost simultaneous measurements of the potential gradient at 100 (or 255) equidistant positions along a 10-cm column[9]. The construction of the apparatus is based on the principle described by Thormann *et al.*[10] for the detection of transient and steady state zone structures in electrophoresis. Monitoring the electric field with this array detector permits following the dynamics in a continuous fashion, under full computer control. The apparatus allows focusing in free solution. Resolution is far better than that of Jackiw *et al.*[8], thus permitting a detailed monitoring of the focusing process. Data showing the focusing dynamics of systems comprising two and three buffer components are given which illustrate the mechanism of separation.

There have been many theoretical treatments of the focusing of components in an equilibrium gradient[11–22]. Most of these have utilized simplified models. Descriptions of the equilibrium distribution of sample components[12–14] and of the resolution in IEF[15,16] are based on several restrictive assumptions, including constant conductivity and linear pH gradients. Steady state concentration, pH and conductivity profiles have been calculated with simplified mathematical models[17,18] and by sophisticated computational analysis[19]. Theoretical discussions of transient states are confined to systems where the focusing of an ampholyte is described in a preestablished, linear pH gradient[20]. Computer modeling is the only methodology at hand for the prediction of concentration, pH and conductivity profiles as functions of time[21,22]. The general model of Bier *et al.*[22] predicts the salient features of all the classically recognized methods in electrophoresis, including IEF. It is based upon equations describing the component's chemical equilibria, electroneutrality as well as conservation of mass and charge, and computes the net mass transport of each component due to electromigration and diffusion. This model, in contrast to that of Svendsen *et al.*[21], is not restricted to electromigration only and incorporates the proper boundary conditions for IEF. In this paper computer simulation data are employed, in conjunction with experimental data, to describe the mechanism of focusing of two and three component mixtures. This mechanism is then generalized to specialized systems to elucidate a general focusing mechanism of n components.

MATERIALS AND METHODS

Potential gradient measurements

Our apparatus comprises a rectangular separation trough (about 0.4 × 1 mm)

with an ordered array of 100 electrodes over the total length of 10 cm[9]. Gold electrodes are produced by silk screening of formulated metallo-organics on a Pyrex glass plate, followed by heat decomposition of the organic matrix. The electrodes have a width of about 0.025 cm, a height of about 0.2 μm and are 0.076 cm apart. The rectangular focusing trough is defined by a silicone rubber gasket between the glass plate and a block of plexiglass. This block contains the electrode assemblies. The electrode array is enlarged at the outer edge of the detector plate to allow mechanical scanning[9]. The potential gradient between adjacent electrodes is monitored and the data are processed and stored in the computer. A complete scan consists of 99 data points and requires 14 min in the present configuration.

All presented experiments were performed in free solution and at ambient temperature. The current was a constant 10 μA unless otherwise indicated. Electrode assemblies included dialysis membranes for the isolation of the focusing column from the electrode compartments. The anolyte and catholyte solutions were 0.1 *M* phosphoric acid and 0.1 *M* sodium hydroxide, respectively. The solution with carrier components was uniformly distributed throughout the column before application of the constant driving current. Analytical grade chemicals were used as available.

Computer simulations

Our computer model is one dimensional and assumes the absence of convective flows or thermal gradients. No *ad hoc* stipulations are made concerning pH or voltage gradients, rather these profiles are computed as a part of the solution. The focusing column is overlaid with a set of grid points for discretization of the spatial derivatives. Central differences are used wherever possible, with forward and backward differences used at the boundaries. The resulting ordinary differential equations with time as the independent variable are integrated using software developed on the basis of DARE-P language[23,24]. The inputs required to perform a simulation include the dissociation constants of the compounds, mobility coefficients of the positive, negative and neutral species, initial concentration of the components in the column, cross sectional area and length of the column and the current. The amount of electrophoresis time is also specified. The values used for the presented example are summarized in Table I. The boundary conditions are given by the assumption that the current across the ends of the column is carried by hydrogen and hydroxyl ions only[22]. The outputs from a simulation are the concentration of each component at each grid point across the column, and the pH and conductivity profiles. The maximum relative local truncation error for these simulations, as computed by the order difference method, is $1.0 \cdot 10^{-4}$.

RESULTS AND DISCUSSION

Experimental investigation

The focusing of three different 3 component systems and one 2 component system has been monitored. The data obtained from all systems are consistent with a general mechanism of isoelectric focusing which is represented schematically in Fig. 1. The physical properties of the three components were chosen such that constituent A is the most basic, C the most acidic and B has an intermediate isoelectric point. Focusing is divided into two phases, a separation phase and a stabilizing phase. The

TABLE I

CONDITIONS FOR COMPUTER SIMULATION

General values			
Column length	1 cm		
Segmentation	100 segments/cm		
Current density	0.001 A/cm^2		
pK_a and mobility values			
Component	*pK_{a_1}*	*pK_{a_2}*	*Mobility $\times 10^4$ [cm^2/Vs]**
Glutamic acid	2.16	4.29	2.97
Histidine	6.02	9.17	2.85
Arginine	9.04	12.48	2.26
H_3O^+			36.27
OH^-			19.87

* It was assumed that all species of a component have equal mobility coefficients. Note that this is not required by our model.

separation phase comprises two clearly distinguishable classes of transient stages. The initial stage (a) and stage (c) represent distinct time points whereas the transient stages (b) and (d) are characteristic time intervals during which five-zone structures are present. Fig. 1e shows complete separation of the 3 constituents and marks the start of the stabilizing phase.

Fig. 1a depicts the initial state prior to voltage application with all components evenly distributed. Transient stage (b) is characterized by the formation of two transient moving boundaries from each electrode. α_1 is the boundary between the zone of pure component A at the cathode, and a mixed zone composed of A and the intermediate component B. The boundary α_2 is the demarcation between a zone of pure component C at the anode and a mixed zone of B and C. The more rapidly migrating β boundaries separate the initial mixture and the transient mixed zones A–B and B–C. They represent the trailing boundaries of the faster components; β_2 for A on the anodic side and β_1 for C on the cathodic side. This is indicated by the letters below the vectors. Both the transient stages (b) and (d) are five-zone structures whereas the time point (c) comprises four zones only. When the faster β boundaries meet, the pure zone of constituent B starts to evolve. This corresponds to the time point depicted in Fig. 1c. Two new boundaries appear, γ_1 and γ_2, which migrate in opposite directions. These are the evolving fronts of the pure zone of component B [transient stage (d)]. Each merges with a corresponding α boundary approaching from the column end to produce the boundaries δ_1 and δ_2. This configuration, presented as Fig. 1e, is the end of the separation phase. δ_1 and δ_2 slowly migrate toward their proximal electrodes. The approach to the steady state distribution (Fig. 1f) denotes the end of the stabilizing phase. The separation scheme presented assumes that the two δ boundaries are formed simultaneously. This is, of course, a somewhat idealized situation. In reality, transient stage (d) is first reduced to a four-zone struc-

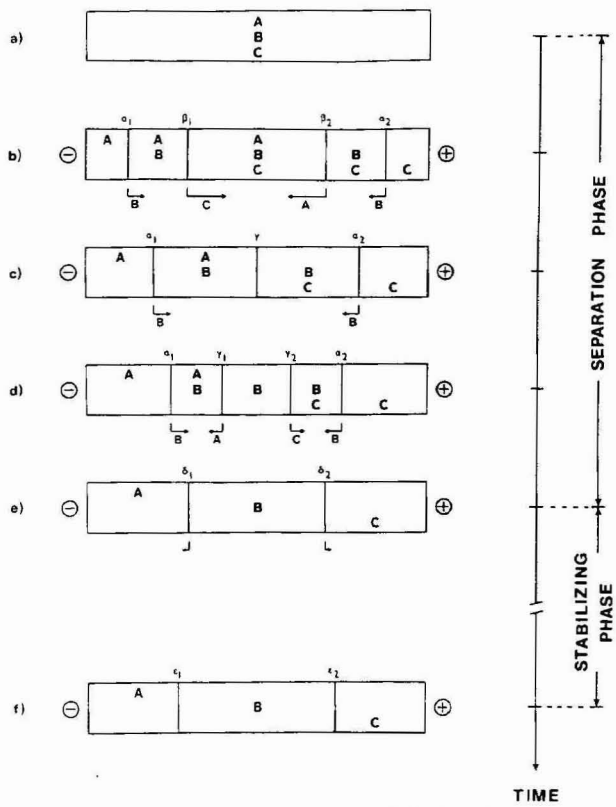

Fig. 1. Idealized schematic presentation of the focusing stages with three buffer components. Component A is the most basic, C the most acidic and B has an intermediate isoelectric point. The boundaries between zones are depicted by vertical solid lines and denoted by greek letters. The vectors indicate the direction and the relative velocity of the migrating boundaries. The letters below the vectors denote the component responsible for the boundary. Stages (a) to (e) depict the separation phase. Between stages (e) and (f) the system stabilizes and attains steady state. To simplify matters it is assumed that the two δ boundaries are formed simultaneously and that the three components have similar concentration in the initial mixture.

ture with one δ boundary before the three-zone configuration of Fig. 1e is established. It is also assumed that the three components have similar concentration in the initial mixture.

Fig. 2 shows the dynamics of the electric field during the focusing of a mixture of 3 amino acids, arginine, histidine and glutamic acid, which correspond to components A, B and C respectively, of Fig. 1. The boundaries α_1, β_1 and α_2 are present by scan 3. The field change across the β_2 boundary was insufficient to be detected in this system. The spike in the center of scan 8 indicates the onset of transient stage (d), the beginning of the evolution of the pure histidine zone. The γ boundaries are fully established by scan 9 and the two δ transitions are detected by scan 11. Scan 10 illustrates that the two δ boundaries are not formed simultaneously, the δ_2 transition being established first. Each experimental electric field profile in this and other figures has been corrected for irregularities in the cross sectional area of the column[25].

The transient behavior of the voltage gradient during the focusing of a mixture

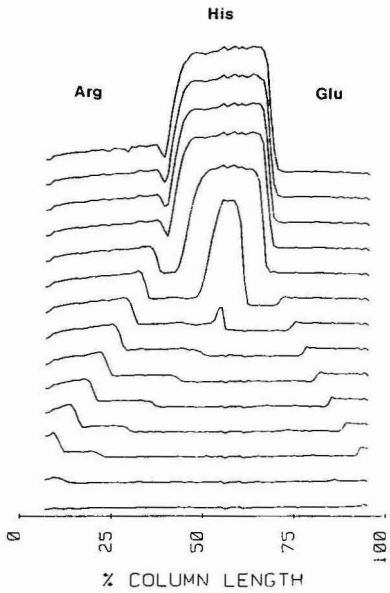

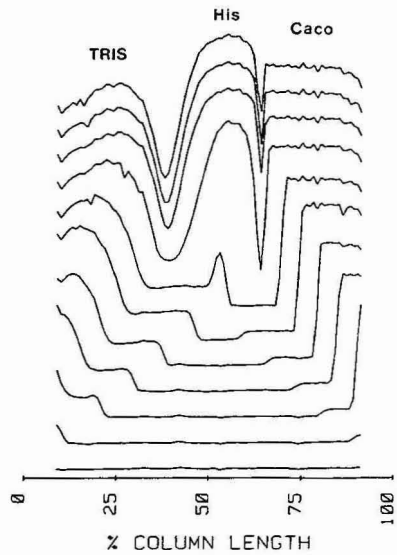

Fig. 2. Dynamics of the potential gradient monitored during the focusing of a mixture of arginine (Arg), histidine (His) and glutamic acid (Glu). Initial concentrations were 10 m*M* each. The pH of the mixture was 7.47 and the conductivity 0.469 mS/cm. The bottom scan is the uniform profile obtained just after application of the current. The scan interval was 21 min with each successive scan offset from the previous one by 0.5 V. The final focusing voltage across the whole cell was about 150 V. The anode is to the right.

Fig. 3. Dynamics of the electric field monitored during the focusing of Tris, histidine (His) and cacodylic acid (Caco). The initial concentrations were 8.27, 7.05 and 8.76 m*M* respectively. The pH of the mixture was 7.36 and the conductivity 0.438 mS/cm. The final focusing voltage was about 300 V. Other conditions as in Fig. 2.

of the base Tris [tris(hydroxymethyl)aminomethane], the amino acid histidine and cacodylic acid is depicted in Fig. 3. These correspond to components A, B and C respectively, of Fig. 1. All four boundaries, the two α and the two β, of the separation phase are present by scan 3. The evolution of the pure histidine zone has begun by scan 7. The δ boundary between Tris and histidine is much more broad than that between histidine and cacodylic acid. This is consistent with the computer predicted profile reported in ref. 22. The two presented systems clearly reveal that the more rapidly migrating β boundaries are characterized by a substantially smaller field change than are α boundaries. This is because the α boundaries border zones of pure compounds which are less conductive. The γ and δ boundaries represent substantial field changes.

Two amino acids and a dipeptide comprise the mixture used to obtain the data in Fig. 4. Arginine and *p*-aminobenzoic acid correspond to components A and C respectively, and L-lysyl-1-aspartic acid represents the intermediate constituent B, of Fig. 1. Both α and β boundaries are visible by scan 2. The beginning of transient stage (d) is marked by a substantial increase in the voltage gradient in the center of the column. The detected signal even becomes too large for the data aquisition system as shown by the recorder going off scale in scan 7 of Fig. 4a. The pure zone of the dipeptide has a very low conductivity. To obtain the complete profile of Fig. 4b, the

current was decreased from 10 μA to 2.5 μA. The α_2 boundary in this system is unusual because the electric field increases across the boundary in the direction of migration, whereas all other experimentally detected boundaries exhibit a field decrease in the direction of migration. A field decrease across an electrophoretic boundary in the direction of migration produces a steady state shape[26]. All detected boundaries which fit this criterion appear to exhibit a steady state. It is difficult to determine from the data however, whether the α_2 boundary of Fig. 4a is becoming broader as it migrates.

The registration of the focusing current under constant voltage is an alternate way of characterizing the focusing process. Fig. 5 presents the temporal behavior of the current for the system of Fig. 4. The applied voltage was a constant 100 V. The current decreases substantially as focusing progresses. The distinct inflection point in this graph (shown by the arrow) was found to mark the time point of transient stage (c) of Fig. 1, *i.e.* the start of the evolution of the pure middle zone with high resistance [transient stage (d)]. This point is also present in the current-time plots of the systems shown in Figs. 2 and 3 (data not shown) although it is less pronounced because of the higher relative conductivity of their central zones.

Fig. 6 depicts the experimentally determined transient and steady state electric field profiles during the focusing of glutamic acid and histidine. This experiment

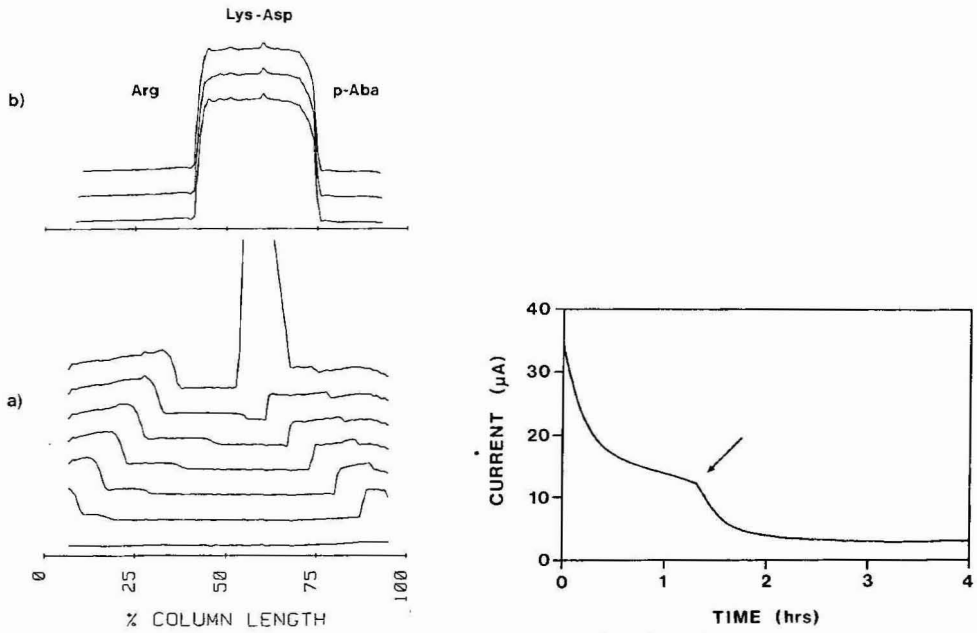

Fig. 4. Dynamics of the potential gradient monitored during the focusing of arginine (Arg), lysyl–aspartic acid (Lys–Asp) and *p*-aminobenzoic acid (*p*-Aba). Initial concentrations were 8, 10 and 6 m*M* respectively. The pH of the mixture was 7.29 and the conductivity 0.406 mS/cm. Scans 1–7 were monitored with a constant current of 10 μA (a) and scans 13–15 were registered at a constant current of 2.5 μA (b). The focusing voltage at this stage was about 400 V. Other conditions as in Fig. 2.

Fig. 5. Variation of current during focusing under a constant 100 V of the system shown in Fig. 4. The arrow indicates the time point of transient state (c) of Fig. 1.

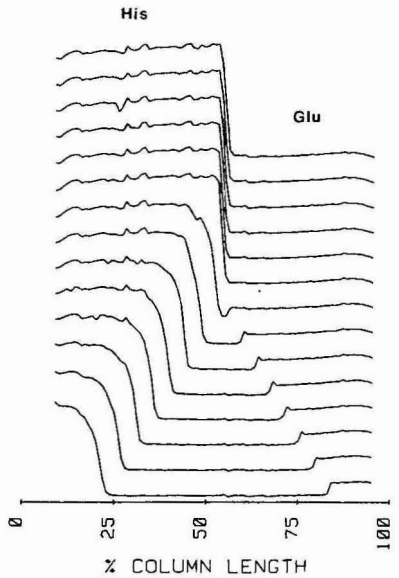

Fig. 6. Dynamics of the potential gradient monitored during the focusing of histidine (His) and glutamic acid (Glu). Initial concentrations were 15 m*M* each. The pH of the mixture was 5.23 and the conductivity 0.645 mS/cm. The final focusing voltage across the whole cell was about 180 V. The anode is to the right. Other conditions as in Fig. 2.

clearly illustrates the formation of two transient moving boundaries; one arising from the anode, the other from the cathodic column end. They are interfaces between the evolving zones of pure amino acids and the initial mixture. The boundary arising from the cathodic end is the trailing boundary of glutamic acid and corresponds to α_1 of Fig. 1. The trailing boundary of histidine originates at the anode and is equivalent to α_2 of Fig. 1. Both are migrating toward the center of the column, where a stationary boundary is formed. The two migrating boundaries have a steady state shape across which the electric field increases opposite to the direction of migration. They also represent pH gradients.

Theoretical investigation

Fig. 7 depicts the computer predicted concentration, pH and conductivity profiles for the system of Fig. 2. The simulation conditions are summarized in Table I. The conductivity profiles are nicely consistent with the experimentally detected evolution of the electric field. Not only the number of transient boundaries representing electric field changes matches those experimentally monitored, but also their relative velocities, such as the earlier establishment of boundary δ_2 compared to δ_1, agree nicely. The corresponding concentration profiles illustrate the composition of the zones defined by the transient boundaries. The excellent correlation between the theoretical predictions and experimental data confirm the mechanism of IEF presented schematically in Fig. 1. Other simulations with three buffer components[22,23] and the predictions for two component systems (not displayed) have produced similar results. Although the array detector provides outstanding resolution, it is not capable of discerning all of the fine structure predicted within a boundary. The conductivity

spike present in the histidine-arginine boundary in Fig. 7 is mirrored in the experimental data of Fig. 2, but the corresponding spike in the histidine–glutamic acid boundary was not monitored. The experimental current density was about twice that used for the computer simulation, and the spike in the latter boundary is apparently either too sharp to be observed or even absent due to convective disturbances caused by the temperature gradient across the boundary. The effects of temperature gradients are not included in our mathematical model. The relative conductivities of the focused zones of pure components are different in the experimental and simulation data. This is due to the actual mobility of histidine being different from the value used in the simulation and due to the neglection of temperature gradients.

The boundaries present after full separation of the three components (*cf.* scans 11–14 in Fig. 2) were found to slowly migrate towards either column end. This effect is best illustrated by Fig. 8 in which the scan interval was increased to about one hour. The observation time of approximately 15 h is much longer than needed for complete separation of the three amino acids. Fig. 9 displays the potential gradient distribution of the same system after 4 h (solid line) and a scan taken after 18 h of current flow (broken line). The arginine–histidine boundary in the cathodic half of the column was found to migrate about twice as fast as the anodic boundary and the two profiles exhibit a field increase in the middle zone as electrophoresis progresses. Both effects are in good agreement with our simulation analysis. The computed profiles presented in Fig. 7 illustrate a similar displacement of the two final boundaries (δ boundaries of Fig. 1) between 25 and 150 min. The histidine–glutamic acid boundary is predicted to migrate a bit away from the anode between 150 and 400 min of current flow. This and related effects may be attributable to the concentration slope of the histidine zone at 150 min which must revert to being flat. Further data after

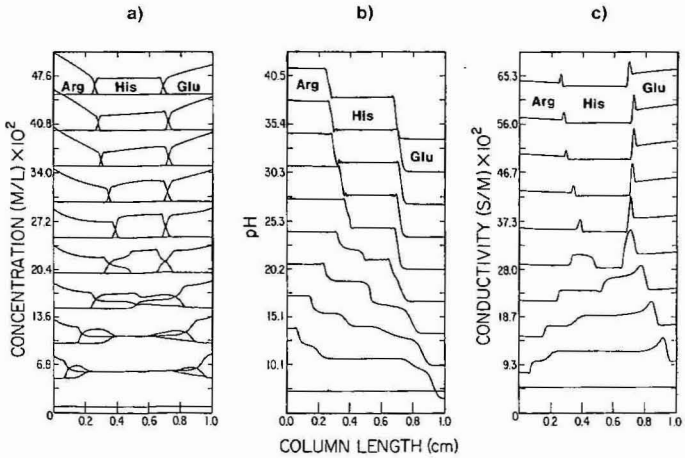

Fig. 7. Computer predicted concentration (a), pH (b) and conductivity (c) profiles for the simulated mixture of arginine (Arg), histidine (His) and glutamic acid (Glu). The time points plotted, from bottom to top, are 0, 5, 10, 15, 20, 25, 50, 100, 150 and 400 min of current flow. Each successive set of concentration profiles is offset from the previous set by 50 m*M*. The offsets for the conductivity and pH profiles are 0.07 S/m and 3.4 pH units respectively. Initial concentrations were 10 m*M* each. See Table I for additional data. The damped sinusoidal oscillations are numerical in nature and do not represent true fluctuations in the concentrations. The anode is to the right.

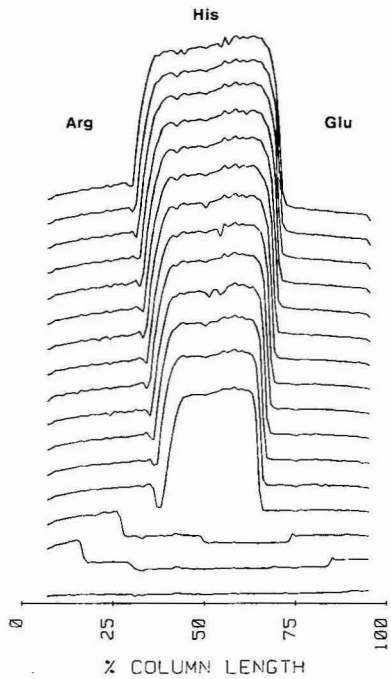

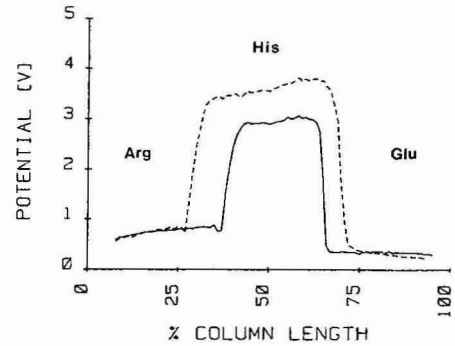

Fig. 8. Dynamics of the electric field during the extended focusing of arginine (Arg), histidine (His) and glutamic acid (Glu), the same system depicted in Fig. 2. The scan interval was 1 h. All other conditions as in Fig. 2.

Fig. 9. A comparison of the potential profiles detected after 4 h (solid line), and after 18 h (broken line) of focusing of the system presented in Figs. 2 and 8.

500, 600, 700 and 800 min and the prediction of our steady state IEF program[19] were found to be equivalent to the profiles obtained after 400 min of current flow. With the 2 component system presented in Fig. 6 a small displacement of the final boundary towards the anode was both experimentally observed and theoretically computer predicted. This indicates the existence of two phases during the focusing of two and three components; first the constituents separate according to the principle shown for three components in Fig. 1a–e, which we call the separation phase. This is followed by a stabilizing phase which results in the attainment of the true steady state. The mechanistic description presented in the separation phase is in complete accord with the concepts of Svendsen and Schafer-Nielsen[21].

The drifting boundaries in the stabilizing phase are a manifestation of pH gradient instability, a phenomenon which has been thoroughly studied (for a review see ref. 4, pp. 299–303). The data presented provide an explanation for the observation of the formation of a pH plateau in the neutral region with a decrease in the number of stainable ampholyte species there and an increase in the stainable ampholyte species at the ends of the gradient[28]. The details of the mechanism causing this instability are currently under investigation[29]. Our simulation data indicate that the stabilizing phase for the system depicted in Figs. 2, 7 and 8 is roughly fifteen times as long as the separation phase. It is harder to determine the relative lengths

of these two phases from experimental data. This is because there are several factors which contribute to pH gradient instability. Our experiments utilized dialysis membranes to separate the focusing capillary from the electrode compartments[9]. These are not perfect boundary conditions for IEF because of the permeability of the membranes to the ampholytes and electrode solutions. The experimental systems described herein were found to degrade after about 20 h of current flow.

CONCLUSIONS

A detector array of the type utilized in these experiments is capable of providing valuable information concerning the dynamics of IEF. Both transient and steady state zone distributions can be monitored. The experimental data represent the first visualization of the moving boundaries present during the transient stages of IEF. Jackiw *et al.*[2,8] failed in this respect because of the limited resolution of their apparatus. These results and those presented in refs. 10, 22 and 27 clearly indicate that moving boundaries, at least as transient phenomena, are ubiquitous in all modes of electrophoresis.

The combination of computer modelling and appropriate experimental data provides a powerful tool for the analysis of electrophoretic systems. The excellent agreement between these approaches has allowed an unambiguous definition of the composition of the zones on either side of each transient moving boundary present in the laboratory data. This made it possible to construct a theory describing the dynamics of three component IEF systems which is applicable to systems containing ampholytes as well as weak acids and bases. In the configurations studied focusing proceeds in two phases, a relatively rapid separation phase and a much slower stabilizing phase. The latter is an adjustment to the theoretical steady state, and can be as much as twenty times as long as the former at constant current. It is present when the pH gradient encompasses regions significantly far from neutrality. This phase occurs because the zones of pure acidic and basic ampholytes do not have flat concentration profiles at the steady state[12]. After the initial, rapid condensation of these components into pure zones (separation phase), the concentration profiles slowly acquire a slope, increasing in the direction of the cathode in the case of basic ampholytes, and in the direction of the anode with acidic ampholytes. This is attributable to the inequality in the concentration of the positively and negatively charged species. The presence of hydrogen ions in a zone of pure acidic ampholyte requires, as a consequence of electroneutrality, that the concentration of the negatively charged ampholyte species is greater than that of positively charged species by an amount equal to the hydrogen ion concentration. Similar relationships apply for the basic column end with hydroxyl ions and positively charged ampholyte species respectively. Thus, even condensed zones of ampholytes at their isoelectric points have a net charge and therefore a tendency to migrate electrophoretically. The slope of the final concentration profile simply reflects the equal and opposite mass transports due to diffusion and electromigration which characterizes the IEF steady state. The stabilizing phase provides insight into one of the contributing factors to pH gradient instability. This is currently being analyzed in depth in our laboratory and will be reported in due course[29].

The mechanism by which two and three buffer components focus is clearly

defined by the amalgam of experimental and simulation data. The elucidated mechanism holds for systems comprising amino acids, small peptides and weak monovalent acids and bases. The acids and bases must be the most acidic or basic components respectively in the mixture, however, for the mechanism to apply. A system composed of glutamic acid, cacodylic acid and histidine, for example, would be unlikely to focus according to the mechanism described because of the relative acidities of the glutamic and cacodylic acids and, of course, the non amphoteric nature of cacodylic acid.

During the separation phase described for two ($n = 2$) and three ($n = 3$) components, two classes of transient stages are distinguishable if it is assumed that the two δ boundaries are formed simultaneously (Fig. 1): (i) $n - 1$ transient stages representing time intervals during which a $2n - 1$ zone structure is present; and (ii) n intermediate transient time points, the first being the initial stage (one zone configuration), the second representing the stage when the first two boundaries meet (two-zone structure for $n = 2$; four-zone structure for $n = 3$) and when $n = 3$, the third being the stage when the final three-zone configuration is formed. A transient moving boundary is attributable to a single component, as is indicated by the letters below the vectors in Fig. 1. Whenever $n > 2$, the separation phase will contain time points when two boundaries, travelling in opposite direction, meet and two new boundaries migrate away from the meeting point. That the boundaries which leave this meeting point are attributable to the same components as were the boundaries which met could lead to the erroneous impression that this is simply two boundaries crossing. In electrophoretic theory, however, boundaries are usually defined by the composition of the zones on either side. It is therefore clear from the simulation data that new boundaries form at these time points.

The focusing process of n ampholytes ($n > 3$) becomes very complex. Essentially such a system is producing distinct transient states with moving boundaries which consist of more than $n - 1$ characteristic time intervals referred to above. The focusing mechanism presented in Fig. 1 can be generalized to describe the focusing of n ampholytes, if it is assumed that these components have evenly spaced isoelectric points, nearly equivalent ionic mobilities and ΔpK_a values and have similar concentrations in the initial mixture. Such a system will produce $n - 1$ transient time intervals, each characterized by distinct $2n - 1$ zones and punctuated by stages representing points in time when boundaries meet. A total of n such time points are present which mark the disappearance of certain zones and the appearance of new zones. The first is the initial stage (one-zone configuration). The subsequent $n - 1$ time points are characterized by a stepwise decrease in their zone number from $2n - 2$ to n. This general description of the focusing process for n ampholytes was verified by computer simulation. While the mechanism applies only to restricted situations, we believe that it is a valuable aid to the understanding of IEF. It does not describe systems containing a variety of weak acids and bases, but such components are allowed to be the most acidic and the most basic constituents respectively. The summation of the number of transient stages representing time intervals and the number of time points for an idealized situation, $2n - 1$, represents the minimum theoretical number of transient states produced during the separation phase of n components.

Complex mixtures of real ampholytes, such as mixtures of synthetic carrier

ampholytes, will be unlikely to follow precisely the mechanism presented and will produce more than $2n - 1$ transient states during the separation phase. This is due to an unequal distribution of their isoelectric points, unequal net mobilities due to both unequal ionic mobilities and unequal ΔpK_a values, and differences in the initial concentrations in the mixture. However, the existence of the two phases during focusing was verified experimentally using synthetic carrier ampholyte mixtures in our capillary device[30].

ACKNOWLEDGEMENTS

The authors would like to acknowledge valuable discussions with Dr. N. B. Egen, the experimental assistance of L. Zawadsky and the careful presentation of computer generated data by J. Walker. This work was partly supported by NASA grant NSG-7333, NSF grant CPE-8311125 and by a grant from the Swiss National Science Foundation.

REFERENCES

1 N. Catsimpoolas, in P. G. Righetti (Editor), *Progress in Isoelectric Focusing and Isotachophoresis*, North Holland, Amsterdam, 1974, pp. 77–92.
2 B. A. Jackiw and A. Chrambach, *Electrophoresis*, 1 (1980) 150.
3 E. Fries, *Anal. Biochem.*, 70 (1976) 124.
4 P. G. Righetti, *Isoelectric Focusing: Theory, Methodology and Applications*, Elsevier, Amsterdam, 1983.
5 W. J. Gelsema, C. J. de Ligny and N. G. van der Veen, *J. Chromatogr.*, 173 (1979) 33.
6 S. Fredriksson, *J. Chromatogr.*, 135 (1977) 441.
7 A. Murel, S. Vilde, A. Kongas and O. Kirret, *Electrophoresis*, 5 (1984) 139.
8 B. A. Jackiw, B. E. Chidakel, A. Chrambach and R. K. Brown, *Electrophoresis*, 1 (1980) 102.
9 W. Thormann, G. Twitty, A. Tsai and M. Bier, in V. Neuhoff (Editor), *Electrophoresis '84*, Verlag Chemie, 1984, Weinheim, pp. 114–117.
10 W. Thormann, D. Arn and E. Schumacher, *Electrophoresis*, 5 (1984) 323.
11 A. Kolin, *Proc. Natl. Acad. Sci. U.S.A.*, 41 (1955) 101.
12 H. Svensson, *Acta Chem. Scand.*, 15 (1961) 325.
13 E. Schumacher, *Helv. Chim. Acta*, 40 (1957) 2322.
14 W. G. Kauman, *Classe des Sciences de l'Academie Royale de Belgique*, 43 (1957) 854.
15 J. C. Giddings and K. Dahlgren, *Sep. Sci.*, 6 (1971) 345.
16 H. Rilbe, *Ann. N.Y. Acad. Sci.*, 209 (1973) 11.
17 M. Almgren, *Chemica Scripta*, 1 (1971) 69.
18 K. Shimao, *Seibutsu Butsuri Kagaku*, 24 (1981) 59.
19 M. Bier, R. A. Mosher and O. A. Palusinski, *J. Chromatogr.*, 211 (1981) 313.
20 G. H. Weiss, N. Catsimpoolas and D. Rodbard, *Arch. Biochem. Biophys.*, 163 (1974) 106.
21 P. J. Svendsen and C. Schafer-Nielsen, in D. Stathahkos (Editor), *Electrophoresis '82*, Walter de Gruyter, Berlin, 1983, pp. 83–89.
22 M. Bier, O. A. Palusinski, R. A. Mosher and D. A. Saville, *Science*, 219 (1983) 1281.
23 G. A. Korn and J. V. Wait, *Digital Continuous System Simulation*, Prentice-Hall, Englewood Cliffs, N.J., 1978.
24 A. Graham, O. A. Palusinski, R. A. Mosher, M. Bier and D. A. Saville, *Proceedings of the 10th IMACS World Congress on System Simulation and Scientific Computations*, Vol. 4, International Association for Mathematics and Computers in Simulation, Montreal, 1982, pp. 92–94.
25 E. Schumacher, D. Arn and W. Thormann, *Electrophoresis*, 4 (1983) 390.
26 R. A. Mosher, W. Thormann and M. Bier, *J. Chromatogr.*, 320 (1985) 23.
27 W. Thormann, R. A. Mosher and M. Bier, in V. Neuhoff (Editor), *Electrophoresis '84*, Verlag Chemie, Weinheim, 1984, pp. 118–121.
28 R. Frater, *Anal. Biochem.*, 38 (1970) 536.
29 R. A. Mosher, W. Thormann and M. Bier, *J. Chromatogr.*, 351 (1986) 31–38.
30 W. Thormann, N. B. Egen, R. A. Mosher and M. Bier, *J. Biochem. Biophys. Methods.*, 11 (1985) 287.

Journal of Chromatography, 351 (1986) 31–38
Elsevier Science Publishers B.V., Amsterdam — Printed in The Netherlands

CHROM. 18 216

AN EXPLANATION FOR THE PLATEAU PHENOMENON IN ISOELECTRIC FOCUSING

RICHARD A. MOSHER*, WOLFGANG THORMANN and MILAN BIER
Center for Separation Science, Room 156, Building 20, University of Arizona, Tucson, AZ 85721 (U.S.A.)
(First received August 10th, 1985; revised manuscript received September 26th, 1985)

SUMMARY

Isoelectric focusing of mixtures of simple ampholytes occurs in two phases, an initial rapid separation phase and a second relatively slow stabilizing phase. Transient and steady-state computer simulation data are shown to predict the development of pH plateaus around neutrality during the stabilizing phase of the focusing of such mixtures. This occurs because a non-zero electrophoretic flux is present in a pure zone of focused ampholyte, which is a function of both its isoelectric point (pI) and its ΔpK value. For an ampholyte with a pI $>$ 9 or $<$ 5 this flux causes the development of a significant concentration gradient within its focused zone which is accompanied by a contraction of this zone along the focusing axis. Acidic and basic ampholytes are thereby displaced toward the anode and cathode respectively, creating a pH plateau in the neutral region. Thus, there will be regions of the focusing column, closer to the electrodes and containing more acidic or basic pH values, within which the resolution of samples will reach a maximum and then decrease.

INTRODUCTION

Isoelectric focusing (IEF) is an exceptionally valuable technique for the fractionation of complex mixtures of proteins. Its widespread popularity was achieved with the introduction of synthetic carrier ampholyte mixtures[1] which produce reasonably linear pH gradients that are stable for several hours. In extended experiments, however, these gradients exhibit a progressive flattening around neutrality which has been referred to as the "plateau phenomenon"[2]. This behavior is characterized by a progressive loss of stainable ampholyte species near the center of the gel and a concomitant increase in such species closer to its ends[3]. Similar results have been observed when the pH gradient is formed with mixtures of simple ampholytes[4]. Several characteristics associated with the plateau phenomenon have been described by Miles *et al.*[5]. These include: (a) displacement of protein bands away from the center with no change in pI; (b) the rate of change of pH along the neutral region decreases with time; (c) the rate of plateau formation is proportional to the applied field; (d) plateau formation does not require loss of ampholytes; (e) there is a decrease in conductivity in the neutral region and an increase in conductivity in the acidic and

0021-9673/86/$03.50

basic regions; (f) increasing viscosity and ionic strength decrease the rate of plateau development.

In a previous paper[6] we have presented experimental and computer simulation data describing the dynamics of the potential gradient during the IEF of mixtures of simple buffers including amino acids, dipeptides and monovalent acids and bases. These data show focusing to occur in two phases, an initial rapid separation phase and a second relatively slow stabilizing phase which is most evident when the pH gradient encompasses regions significantly removed from neutrality, *i.e.* above pH 9 and below pH 5. The first phase involves the condensation of each buffer into a pure zone. The second phase is much longer and constitutes the approach to the final steady-state distribution. During this phase the boundaries between the buffer zones drift toward the electrodes; those below pH 7 toward the anode and those above pH 7 toward the cathode. This behavior appears to provide an explanation for the events which occur during the formation of the pH plateaus referred to above. We have used our computer models for the steady state in IEF[7,8] and for transient electrophoretic processes[9–12] to examine this phenomenon. We show the plateau phenomenon to be an integral aspect of the focusing process.

MATHEMATICAL MODELLING

Our mathematical models have been described in detail elsewhere[7–12]. The inputs required for a simulation of the steady state in IEF include the concentrations of each component (ampholytes or monovalent weak buffers) at one end of the focusing column, pK and mobility values for each component, the current and column length. The outputs include the concentration profile of each component along the column length and a variety of data which can be derived therefrom including the pH, conductivity and buffer capacity profiles. The inputs required for a transient simulation include the pK values and mobilities of each component, current, column length, the initial distribution of each component within the electrophoretic column and the amount of electrophoresis time to be simulated. The outputs include the data mentioned for the steady-state program at specified time points. All simulations were performed with a column length of 0.01 m with the solution computed at 101 evenly spaced grid points.

RESULTS

The drift which occurs after focusing ampholytes have condensed into pure zones but before the steady-state distribution has been reached is most clearly shown by conductivity profiles. Fig. 1A presents four conductivity profiles from the computer simulation of the focusing of three hypothetical ampholytes. Each was uniformly distributed throughout the column at a concentration of 10 mM prior to applying a current of 10 A/m^2. The time points shown are after 25, 50, 100 and 150 min of current flow. This system is very similar to the glutamic acid, histidine and arginine system presented previously[6], the pI values being 3, 7 and 11. The boundary shapes change very little during this time span but their positions clearly shift towards the electrodes. The boundary between the basic ampholyte and the neutral component shifts somewhat more than does the acidic boundary. Fig. 1B and C present the

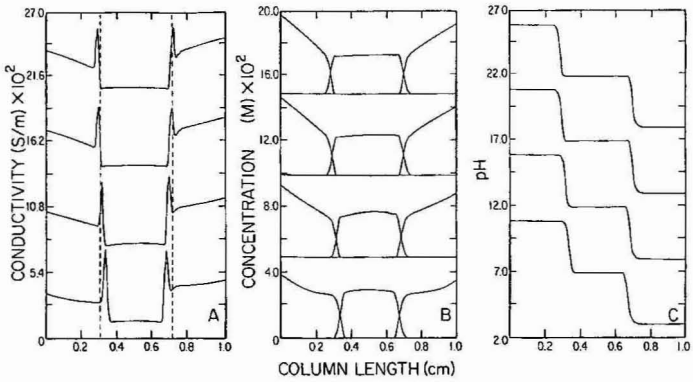

Fig. 1. Data derived from a simulation of the focusing of three hypothetical ampholytes with pI values of 3, 7 and 11. All ΔpK values are 2 and all ionic mobilities $3.0 \cdot 10^{-8}$ m²/Vs. The anode is to the right. The time points displayed are after 25 (bottom), 50, 100 and 150 (top) min of current flow. In panel A each successive conductivity profile is offset from the previous one by $6.5 \cdot 10^{-2}$ S/m for purposes of presentation. The cathodic boundary clearly drifts more than the anodic one. Panel B displays the corresponding concentration profiles plotted with an offset of $5.0 \cdot 10^{-2}$ M and panel C the corresponding pH profiles plotted with an offset of 5 pH units.

corresponding concentration and pH profiles. The 150-min time point is very close but not identical to the steady-state distribution. The experimental data for the glutamic acid, histidine and arginine system have been presented elsewhere[6].

This drift occurs because the zones of pure ampholytes which have formed during the separation phase have not yet reached the steady state. Those ampholytes with pI values other than 7 are not isoelectric, in the sense that the concentrations of the positively and negatively charged species are equal. A pure zone of acidic ampholyte has an excess of negatively charged ampholyte species, equal to the concentration of hydrogen ion present, to satisfy the requirement of electroneutrality. Thus, even after an acidic ampholyte has condensed into an "isoelectric zone" it retains an electrophoretic flux toward the anode. Similar statements apply to basic ampholytes which show a flux toward the cathode. The slow boundary drift occurs as the concentration profile across a zone of acidic or basic ampholyte acquires a slope. This generates a diffusional flux in a direction opposite to the electrophoretic flux and establishes the steady state[13]. The stabilizing phase is much longer than the separation phase[6] because the net mobilities of the focusing components are much smaller when in pure zones than when mixed with other buffers.

Systems of ampholytes with pI values closer to neutrality display a smaller drift. The pH dependence of this boundary migration is shown in Fig. 2. These conductivity data are derived from a simulation of the focusing of a hypothetical system of five ampholytes with pI values of 5, 6, 7, 8 and 9. Each was initially uniformly distributed throughout the column at a concentration of 10 mM. The applied current was 10 A/m². The times shown are 50, 100, 150 and 200 min after current application. These boundaries do not appreciably drift. The zones of the focused ampholytes display flat concentration profiles (data not shown) because the difference in the concentrations of the oppositely charged species of each is quite small. Therefore

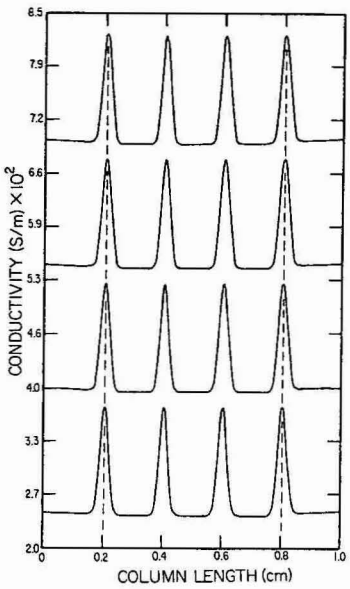

Fig. 2. Conductivity data derived from a simulation of the focusing of five hypothetical ampholytes with pI values of 5, 6, 7, 8 and 9. All ΔpK values were 2 and all ionic mobilities $3.0 \cdot 10^{-8}$. The anode is to the right and the current density was 10 A/m^2. Each successive time point is offset from the previous one by $1.5 \cdot 10^{-2}$ S/m. The time points shown are after 50, 100, 150 and 200 min of current flow.

there is a very low net electrophoretic flux of these components and no significant concentration gradient is required to establish the steady state.

The concentration gradient across a zone of focused ampholyte is a function of the pI of the ampholyte. This is shown in Fig. 3 which presents the steady-state concentration profiles of three different ampholyte mixtures. These systems are identical with respect to molar amounts of each ampholyte present, component mobilities and current. The only difference lies in the isoelectric points. The three components displayed in Fig. 3A have pI values of 3, 7 and 11. This profile is the steady-state distribution for the system presented in Fig. 1. The central component is the same in each panel and has a pI of 7. The other components have pI values of 4 and 10 in Fig. 3B and 5 and 9 in Fig. 3C. It is clear that the slopes of the zones increase as the isoelectric point recedes from pH 7. With an acidic and a basic ampholyte which have pI values equidistant from neutrality, the basic ampholyte zone has a greater slope than the acidic one. This is due to the greater electrophoretic mobility of the hydrogen ion as compared to the hydroxyl ion. The zones of focused basic ampholytes thus possess lower conductivities and greater voltage gradients than do zones of equivalent acidic ampholytes. Equivalent in this case means equal ionic mobilities and equal differences between the pK values which bracket the isoelectric point (ΔpK), as well as isoelectric points equidistant from neutrality. Given equal initial amounts, an ampholyte zone with a greater concentration slope will occupy less distance along the focusing axis. It is this contraction of the ampholyte zones along the focusing axis which causes the movement of the boundaries and the creation of

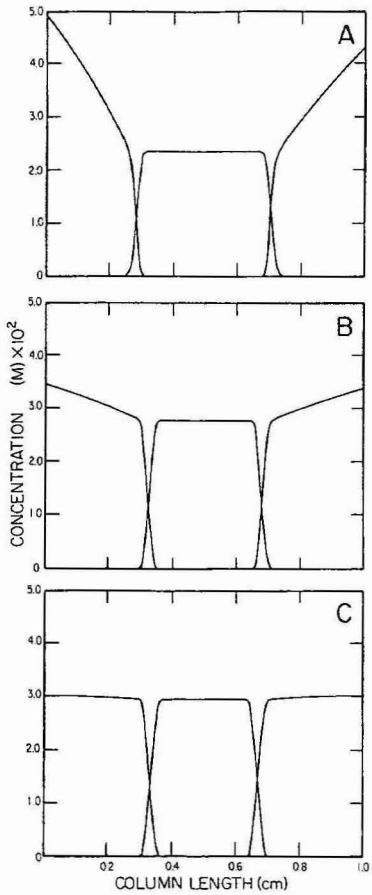

Fig. 3. Steady-state IEF profiles for three different three-component systems. The same molar amount of each ampholyte is present in all cases. The current density in each simulation was 10 A/m². The ΔpK value for each component is 2; all ionic mobilities are $3.0 \cdot 10^{-8}$. The cathode is to the left in each case. The only differences between the simulations are the pI values of the components involved. Panel A shows the profiles with pI values 3, 7 and 11; panel B with pI values of 4, 7 and 10; panel C with pI values of 5, 7 and 9. The concentration gradient across a zone of focused ampholyte is dependent upon its pI. A basic ampholyte displays a greater concentration gradient than an acidic ampholyte which has a pI equidistant from neutrality.

the pH plateau. The position of each boundary and the net electrophoretic flux of each acidic and basic component in Fig. 3 is shown in Table I.

The ΔpK value of an ampholyte also has an effect on the steady-state concentration profile. The amount of the ampholyte present in charged form in a focused zone decreases logarithmically as the ΔpK increases[14]. Thus, the conductivity of the zone decreases and the voltage gradient increases as does the slope of the steady-state concentration profile. The system shown in Fig. 4 is the same as that presented in Fig. 3A except that the ΔpK values are 3 instead of 2. The slopes of the focused zones of acidic and basic ampholytes become greater as ΔpK increases. The electrophoretic fluxes and boundary positions are shown in Table I.

TABLE I

STEADY-STATE ELECTROPHORETIC FLUX AND BOUNDARY POSITIONS AS FUNCTIONS OF ISOELECTRIC POINT AND ΔpK

pI	*ΔpK*	*Flux**	*Boundary position**
3	2	5.38	70
3**	3	6.75	71
4	2	1.55	68
5	2	0.200	67
9	2	0.202	33
10	2	1.67	32
11	2	7.24	28
11**	3	10.2	26

* Flux is the net electrophoretic flux of the given component from the simulations in Figs. 3 and 4 (mol/m² s × 10^6). Calculated for components with p*I* values 3, 4 and 5 at segment 90; for components with p*I* values 9, 10 and 11 at segment 10. The position of the center of the boundary between the component listed and the one focused adjacent to it (p*I* = 7) is given as the segment number (% column length). All simulations were performed with 101 grid points (100 segments) defining the column. The mobility of all ampholyte species was $3.0 \cdot 10^{-8}$ m²/Vs.

** From Fig. 4.

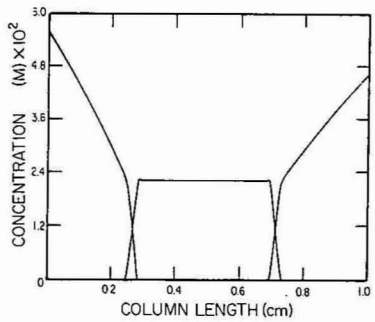

Fig. 4. The effect of ΔpK on the steady-state concentration gradients within zones of focused ampholytes can be seen by comparing this figure to Fig. 3A. The p*I* values of the components are identical in both figures (3, 7, 11). These profiles were computed using $\Delta pK = 3$ for each ampholyte. In Fig. 3A the ΔpK values are 2. All other parameters are identical.

DISCUSSION

Mixtures of ampholytes focus in two phases[6]. In the first of these, which has been termed the separation phase, individual ampholytes condense into pure zones. During the second, stabilizing phase of focusing those ampholytes with isoelectric points above 9 or below 5 will develop significant concentration gradients across their zones. This creates a diffusional mass flux to balance the non-zero electrophoretic flux and produces the steady state. The acquisition of this slope causes the ampholyte zone to contract along the focusing axis. This compaction of the acidic and of the basic ampholytes results in a depletion of the neutral region and the formation of the pH plateau.

The non-zero electrophoretic flux is a function of both the pI and the ΔpK of the ampholyte. The pH in the zone of focused ampholyte controls the imbalance in the concentrations of the positively and negatively charged species due to the requirements of electroneutrality. The more removed the pI from neutrality the greater the electrophoretic flux of the ampholyte and the greater the concentration gradient across the focused zone. Under equivalent conditions, which include equal ΔpK values, ionic mobilities, molar amount present and current density, the steady-state length of an ampholyte zone along the focusing axis is a function of its pI. Therefore, the extent of the plateau phenomenon is a function of the extremes of pH encompassed by the gradient.

The concentration of charged species in a zone of focused ampholyte has a direct influence on the voltage gradient within the zone, and thus on the electrophoretic flux. The ΔpK of the ampholyte affects the concentration gradient across the focused domain as a result of its influence on the amount of charged species present at the isoelectric point[14]. As the ΔpK increases, the amount of the ampholyte possessing a net charge decreases, and the voltage gradient increases as does the concentration gradient at the steady state.

Basic ampholytes tend to have a greater slope at the steady state than do acidic ampholytes due to the greater mobility of the hydrogen ion as compared to the hydroxyl ion. While this means that the drift in basic systems is greater than that in acidic systems it is unlikely that this provides a complete explanation for cathodic drift[15]. This also does not explain the frequent observations of the progressive acidification of the anodic end of the gradient. Righetti (see ref. 15, p. 300) has suggested that the plateau phenomenon and cathodic drift are different terms for the same instability. However it appears likely that these are different phenomena. This is supported by the observation of Chrambach *et al.*[16] that a pH gradient spanning the range 3–6 drifted toward the cathode. The mechanism presented here would predict that this gradient would drift toward the anode. It is difficult to apply this interpretation of the plateau phenomenon to synthetic mixtures of carrier ampholytes with any precision because they are so poorly characterized. There is little information pertaining to ionic mobilities, ΔpK values and the relative amounts of acidic, basic and neutral ampholyte species present. That these mixtures exhibit the plateau phenomenon is qualitatively explained by the stabilizing phase of IEF, during which there is a progressive loss of ampholytes from the neutral pH region. However, the often observed cathodic shift of the position of lowest conductivity in extended experiments[17] is apparently not based solely on this mechanism. Other factors, such as the design of the electrode assemblies and electroosmosis, can contribute to pH gradient instability.

Svendsen and Schafer-Nielsen[18] have proposed that the imbalance in the concentration of the positively and negatively charged species of a focused ampholyte is the cause of pH gradient decay. In their computer modelling system the ends of the focusing column were open to the ampholytes and the decay of the pH gradient proceeded by an isotachophoretic mechanism with the components migrating out of the ends of the column. In most IEF experiments, however, the ends of the column are defined by small volumes of relatively high concentrations of strongly acidic and basic electrolytes. Ampholytes will not migrate isotachophoretically into these solutions. Our results show that the plateau phenomenon can occur without the loss

of any ampholyte. This has been confirmed experimentally by others[5]. The type of decay reported here proceeds by an IEF mechanism, not an isotachophoretic one. This means that natural pH gradients, formed with ampholytes and spanning neutrality, will always exhibit the plateau phenomenon. Thus, there will be regions of the focusing column, closer to the electrodes and containing more acidic or basic pH values, within which the resolution of samples will reach a maximum and then decrease.

ACKNOWLEDGEMENTS

This work was supported by NSF grant CBT-8311125-01 and by NASA grants NSG-7333 and NAGW-693.

REFERENCES

1 O. Vesterberg, *Acta Chem. Scand.*, 23 (1969) 2653.
2 G. R. Finlayson and A. Chrambach, *Anal. Biochem.*, 40 (1971) 292.
3 R. Frater, *Anal. Biochem.*, 38 (1970) 536.
4 N. Y. Nguyen and A. Chrambach, *Anal. Biochem.*, 74 (1976) 145.
5 L. E. M. Miles, J. E. Simmons and A. Chrambach, *Anal. Biochem.*, 49 (1972) 109.
6 W. Thormann, R. A. Mosher and M. Bier, *J. Chromatogr.*, 351 (1986) 17.
7 O. A. Palusinski, T. T. Allgyer, R. A. Mosher, M. Bier and D. A. Saville, *Biophys. Chem.*, 13 (1981) 193.
8 M. Bier, R. A. Mosher and O. A. Palusinski, *J. Chromatogr.*, 211 (1981) 313.
9 M. Bier, O. A. Palusinski, R. A. Mosher and D. A. Saville, *Science*, 219 (1983) 1281.
10 O. A. Palusinski, M. Bier and D. A. Saville, *Biophys. Chem.*, 14 (1981) 389.
11 D. A. Saville and O. A. Palusinski, *AIChE J.*, in press.
12 O. A. Palusinski, A. Graham, R. A. Mosher, M. Bier and D. A. Saville, *AIChE J.*, in press.
13 H. Svensson, *Acta Chem. Scand.*, 15 (1961) 325.
14 H. Rilbe, *Ann. NY Acad. Sci.*, 209 (1973) 11.
15 P. G. Righetti, in T. S. Work and E. Work (Editors), *Isoelectric Focusing: Theory, Methodology and Applications, Laboratory Techniques in Biochemistry and Molecular Biology, Series, Vol. 11*, Elsevier, Amsterdam, 1983.
16 A. Chrambach, P. Doerr, G. R. Finlayson, L. E. M. Miles, R. Sherins and D. Rodbard, *Ann. NY Acad. Sci.*, 209 (1973) 44.
17 W. Thormann, N. B. Egen, R. A. Mosher and M. Bier, *J. Biochem. Biophys. Methods*, 11 (1985) 287.
18 P. J. Svendsen and C. Schafer-Nielsen, in D. Stathakos (Editor), *Electrophoresis '83*, de Gruyter, Berlin, 1983, p. 91.

Journal of Chromatography, 351 (1986) 39–46
Elsevier Science Publishers B.V., Amsterdam — Printed in The Netherlands

CHROM. 18 144

HIGH-PERFORMANCE LIQUID CHROMATOGRAPHIC MOLECULAR WEIGHT DETERMINATION OF ALLERGEN EXTRACTS

EXAMINATION OF THE INFLUENCE OF THE COLUMN MATERIAL ON ALLERGENIC ACTIVITY AND ALLERGEN PATTERNS

R. WAHL*, H. J. MAASCH and W. GEISSLER
Allergopharma, Research and Development Laboratories for Allergen Preparations, D-2057 Reinbek (F.R.G.)
(Received August 27th, 1985)

SUMMARY

To investigate whether the column material employed in size-exclusion high-performance liquid chromatography (HPLC) influences the allergenic activity and antigen/allergen patterns of allergen extracts, the molecular weights of a mite and a birch pollen allergen extract were determined using a Bio-Sil TSK 250 column with a guard column. The allergenic acitivities were measured by RAST inhibition and the antigen/allergen patterns were determined by crossed (radio)immunoelectrophoresis. The original extracts and the corresponding eluates after HPLC runs showed the same allergenic activity and the same number of antigen/allergen precipitation lines. Only slight differences in the peak heights of some precipitates were observed.

INTRODUCTION

The active components in allergen extracts are proteins and glycoproteins with different molecular weights, so the determination of their molecular weights is an important analytical criterion, especially for in-process control of production. Traditionally, molecular weight determinations of allergen extracts were carried out by gel filtration[1] or sodium dodecyl sulphate (SDS)–polyacrylamide gel electrophoresis[2]. However, both of these methods are time consuming. Moreover, using the SDS method only subunits of the proteins are analysed. For these reasons, a rapid and precise method for the determination of the molecular weights of the native proteins would be useful. Florvaag *et al.*[3] and Maasch *et al.*[4] used size-exclusion high-performance liquid chromatography (HPLC) for molecular weight determinations in native and modified allergen preparations, and reduced the time necessary for the analysis from *ca.* 10 h using gel filtration to 35 min.

The application of HPLC to the preparative separation of fractions from allergen extracts was reported recently by Calam *et al.*[5] and Haavik *et al.*[6]. The successful application of HPLC to analytical and preparative work in allergen extract

0021-9673/86/$03.50

research requires an inert separation material in the column, ensuring complete recovery of the allergenic activity in the eluate.

In this work we investigated whether the column material used for size-exclusion HPLC influences the allergenic activity and the antigen/allergen patterns of dialysed birch pollen and mite allergen extracts. Finally, we tested the reproducibility of HPLC for the molecular weight determination of allergen extracts by twelve independent runs of the same allergen preparations.

EXPERIMENTAL

Allergen extract preparations

We prepared allergen extracts from pollens of birch (*Betula verrucosa*) (Allergon, Engelholm, Sweden) and purified mite bodies of *Dermatophagoides pteronyssinus* (Commonwealth Serum Laboratories, Melbourne, Australia). Extractions were carried out at 4°C with Coca's solution without phenol overnight. Subsequently, the extracts were dialysed[7] and lyophilized.

Prior to separation, the lyophilized allergen extracts were reconstituted to a protein concentration of 7.5 mg/ml[8]. For each run, 20 μl of these solutions were injected. Eluates from five injections were collected and blended (*ca.* 150 ml). In parallel, an equal amount of protein of the original lyophilized allergen extracts was dissolved in 150 ml of 0.5 *M* ammonium acetate buffer (pH 6.5). For further specific investigations, these two samples were desalted using Visking dialysis tubing (Serva, Heidelberg, F.R.G.) with a cut-off of 8000–15 000 daltons. Subsequently, the extracts were lyophilized and dissolved in equal volumes of doubly distilled water.

HPLC system

The HPLC system employed consisted of a 300 × 7.5 mm I.D. Bio-Sil TSK 250 column (separation range 1000–300 000 D) with a guard column (Bio-Rad Labs., Munich, F.R.G.), a constametric pump, a Rheodyne 7125 injection valve, a Model D UV monitor (254 nm) and a type 301 integrator (Milton Roy, Hasselroth, F.R.G.). As the solvent, 0.5 *M* ammonium acetate buffer (pH 6.5) (Merck, Darmstadt, F.R.G.) was used at a flow-rate of 0.9 ml/min. The system was calibrated with a Bio-Rad Labs. calibration kit, containing a mixture of proteins of 1350–670 000 daltons.

Measurement of allergenic activity using RAST inhibition

To establish whether the allergenic activity of the extracts is influenced by the column material used for HPLC, the allergenic activity of the desalted original extracts and of the corresponding eluates were determined by RAST inhibition[9]. Briefly, different dilutions of allergen extracts were incubated in test-tubes (55 × 12 mm) with dilutions of pooled sera from patients allergic to birch pollen or mites. These mixtures were incubated overnight at room temperature with allergen-coupled paper disks[10]. After washing steps, rabbit ^{125}I-labelled anti-human IgE (Fc specific) (Pharmacia, Freiburg, F.R.G.) was added as tracer for IgE. After a second overnight incubation, the allergen disks were washed carefully and counted for bound radioactivity in a gamma counter. The allergenic activity of an extract was determined by its capacity to induce 50% inhibition of uptake of allergen-specific IgE by the allergen disks in comparison with an uninhibited sample.

Measurement of antigens and allergens by crossed (radio)immunoelectrophoresis (CIE/CRIE)

The patterns of antigens and allergens of the desalted original extracts and the corresponding eluates were determined by CIE/CRIE. CIE was performed as described by Løwenstein[11], employing 28 µl of each sample. Volumes of 50 µl of the rabbit antisera (ALK, Copenhagen, Denmark) per millilitre of separation gel were used, *i.e.*, anti-*Dermatophagoides pteronyssinus* and anti-*Betula verrucosa.*

Separation in the first dimension was carried out for 30 min at 10 V/cm and 15°C and in the second dimension for 17 h at 2 V/cm. CIE plates were washed with 0.1 *M* sodium chloride solution and in distilled water and finally dried in a stream of cold air. For CRIE, the method of Weeke and Løwenstein[12] was used with the following modifications: each CIE plate was incubated with 12 ml of a diluted serum pool (1:24) collected from patients with known sensitivity to birch or mites. As a tracer for bound IgE we used *ca.* 400 nCi of ^{125}I-labelled anti-IgE (Pharmacia) in 12 ml of buffer. Each incubation was carried out overnight with gentle horizontal shaking. From each CRIE plate three autoradiographs were produced by exposing Kodak X-Omat AR films at −20°C for 3, 7 and 14 days. The CIE plates were finally stained with Coomassie Brillant Blue R 250.

Measurement of reproducibility of HPLC

To assess the reproducibility of size-exclusion analysis by HPLC, dialysed birch pollen and mite allergen extracts were analysed in twelve independent runs. The retention times and percentage areas of the prominent peaks in each measurement were compared.

RESULTS

HPLC of allergen extracts and assessment of reproducibility

Fig. 1 shows the HPLC traces of the dialysed birch pollen and mite allergen extracts. The mean retention times and the mean percentage areas of the prominent

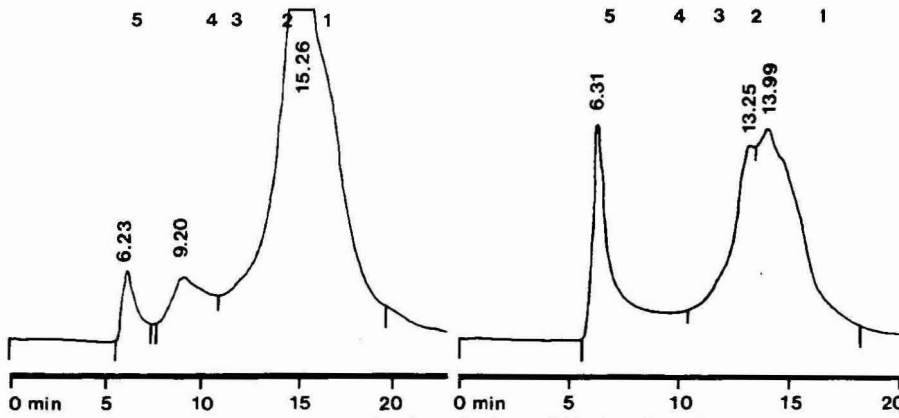

Fig. 1. HPLC molecular weight determination of mite and birch pollen allergen extracts with a Bio-Sil TSK 250 column with guard column. Solvent: 0.5 *M* ammonium acetate (pH 6.5), flow-rate 0.9 ml/min. Left, chromatogram of the dialysed mite allergen extract; right, chromatogram of the dialysed birch pollen allergen extract. 1–5 indicate RTs of the calibration substances: (1) vitamin B_{12} (1350 daltons); (2) myoglobin (horse) (17 000 daltons); (3) ovalbumin (chicken) (44 000 daltons); (4) gamma-globulin (bovine) (158 000 daltons); (5) thyroglobulin (bovine) (670 000 daltons).

TABLE I

MEAN RETENTION TIMES AND PERCENTAGE AREAS OF THE PROMINENT PEAKS OF DIALYSED BIRCH POLLEN AND MITE ALLERGEN EXTRACT (n = 12) AND RESULTS OF MOLECULAR WEIGHT DETERMINATIONS

Allergen extract	*t_R (min)*	*C.V. (%)*	*MW (D)*	*Peak (%)*	*C.V. (%)*
Birch pollen	6.31	0.25	>670 000	27.64	2.40
Birch pollen	13.23	0.30	14 125	26.35	5.17
Birch Pollen	13.95	0.19	7940	45.91	2.65
Mite	6.28	0.58	>670 000	2.27	15.00
Mite	9.21	0.33	281 000	6.34	2.16
Mite	15.28	0.14	5011	90.33	1.29

peaks are shown in Table I. The molecular weights were determined by using the regression line of a calibration graph (Fig. 2) obtained with a calibration kit. The coefficients of variation (C.V.) of retention times calculated from twelve independent runs of the dialysed birch pollen and mite allergen extracts were in the range 0.14–0.58% and for the percentage peak areas in the range 1.29–15.0%, indicating good reproducibility of the analysis.

Measurement of allergenic activity using RAST inhibition

The allergenic activities of the samples were determined by RAST inhibition. The regression lines of the RAST inhibition curves for the original samples and those of the corresponding eluates were nearly congruent (Fig. 3). Using a statistical programme[13] we were unable to find significant differences in the 50% inhibition values and slopes of the curves. The relative potency (P_{rel}), calculated from the quotient of the 50% inhibition values of reference (original sample) and sample (corresponding eluates), was 1.08 for birch pollen allergen extracts and 0.97 for mite allergen extracts.

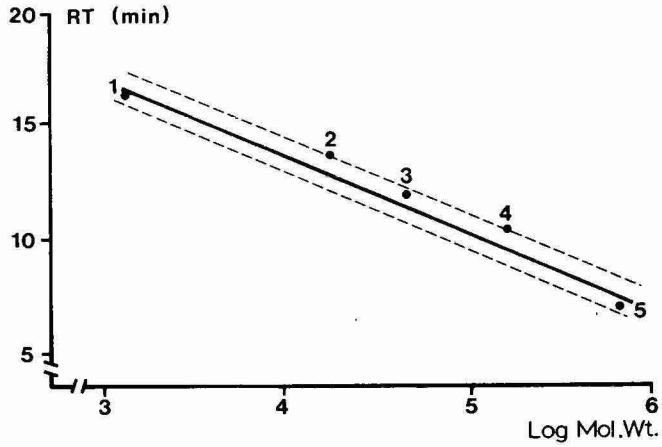

Fig. 2. Regression line of the calibration graph of a mixture of proteins: (1) 1350 daltons; (2) 17 000 daltons; (3) 44 000 daltons; (4) 158 000 daltons; (5) 670 000 daltons; $p < 0.01$. ----, Confidence limit.

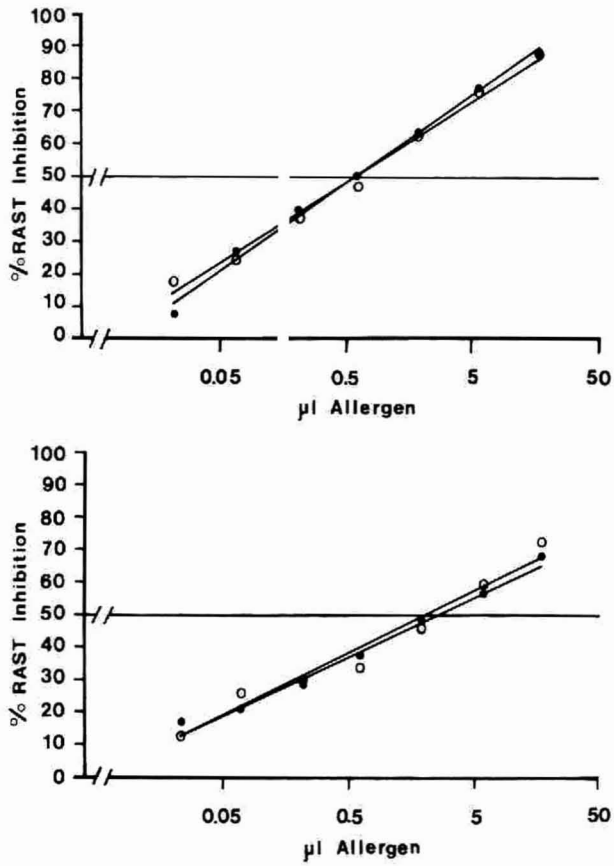

Fig. 3. Regression lines of the RAST inhibition of the original samples and corresponding eluates of mite and birch pollen allergen extracts. Top, RAST inhibition of the mite allergen extracts; bottom, RAST inhibition of the birch pollen allergen extracts. ●, Original samples; ○, corresponding eluates.

This indicates equal allergenic activities and compositions of the allergenic determinants of the samples before and after separation by HPLC.

Determination of the number of antigens and allergens by CIE/CRIE

The antigen/allergen patterns of the samples were determined by CIE/CRIE. As shown in Fig. 4 and Table II, birch pollen and mite allergen extracts showed nearly the same CIE/CRIE patterns and the same number of antigens (precipitation lines) and allergens (allergen bands) in the original samples and the corresponding eluates when analysed on an equal-volume basis.

DISCUSSION

Molecular weight determination is often used as a descriptive analytical method for allergen extracts. Especially for modified allergen preparations, molecular weight determination is part of the final quality control[4]. The method most commonly employed for this purpose is gel filtration[1]. However, this method is very time

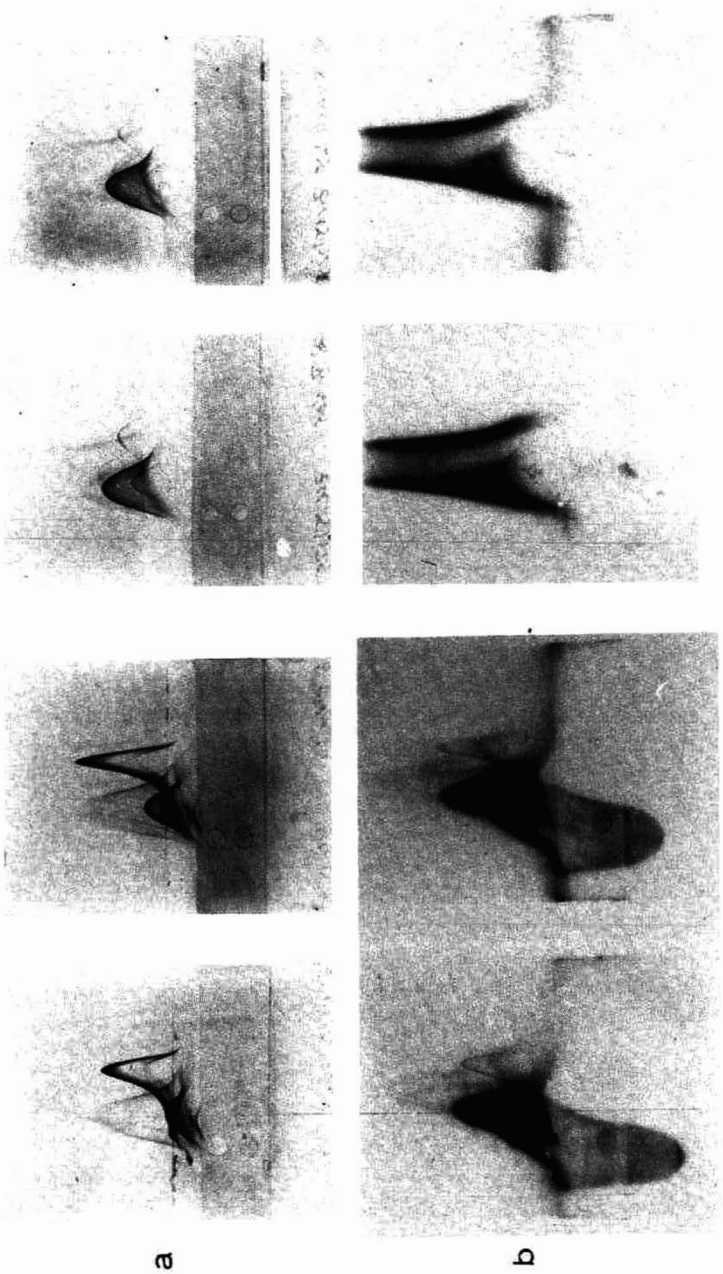

Fig. 4. CIE/CRIE of the desalted allergen extracts. (a) CIE; (b) CRIE. Left-hand pairs, original sample of mite allergen extract (M_1) and corresponding eluate (M_2); right-hand pairs, original sample of birch pollen allergen extract (B_1) and corresponding eluate (B_2).

TABLE II

NUMBER OF ANTIGENS [PRECIPITATION LINES (PL)] AND ALLERGENS [ALLERGEN BANDS (AB)] OF THE ORIGINAL SAMPLES OF MITE AND BIRCH POLLEN ALLERGEN EXTRACTS AND OF THE CORRESPONDING ELUATES DETERMINED BY CIE/CRIE

Allergen extract	*PL*	*AB*
Mite, original sample	8	7
Mite, corresponding eluate	8	7
Birch pollen, original sample	8	4
Birch pollen, corresponding eluate	8	4

consuming and particularly when molecular weight determinations of allergen extracts need to be carried out routinely, *e.g.*, for in-process control of production, an extended analysis time causes problems. The application of HPLC for this purpose were reported recently[3,4], and the time necessary for molecular weight determination could be reduced by a factor of almost 1:20, *i.e.*, from *ca.* 10 h by gel filtration to 35 min. Hence molecular weight determinations of allergen extracts by HPLC seems suitable for the purposes of in-process control, the testing of the consistency of different batches of allergen extracts and the analysis of chemically modified allergen extracts.

When using HPLC for molecular weight determinations of allergen extracts, it is essential that the activity of the samples is not retained or influenced by the column material employed, especially if HPLC is to be used in preparative work.

By RAST inhibition measurements on the original samples and the corresponding eluates we were able to show that the allergenic activity of the extracts was not influenced by the column material. The original extracts and the corresponding eluates were of the same allergenic activity. This was confirmed by CIE/CRIE. The original samples and the corresponding eluates showed the same number of antigen/allergen bands and nearly the same antigen/allergen patterns. The slight differences in the peak heights of the antigen/allergen precipitates in CIE/CRIE of the original mite allergen extracts in comparison with that of the corresponding eluates must be attributed to the variability of the method.

If HPLC is to be applied as an analytical tool for in-process control and monitoring the consistency for different production batches of allergen extracts, high reproducibility of the method is essential. As can be seen in Table I, HPLC molecular weight determinations of allergen extracts showed good reproducibility. In twelve independent measurements of birch pollen and mite allergen extracts, the coefficients of variation of the retention times of the prominent peaks of the birch pollen and mite allergen extracts were in the range 0.14–0.58% and for the percentage peak areas in the range 1.29–15.0%.

According to the recommendations of the manufacturer (Bio-Rad Labs.), the molecular weight range of the Bio-Sil TSK 250 column is 1000–300 000 daltons. The regression line of the calibration graph (protein mixture of 1350–670 000 daltons) (Fig. 2) showed a highly significant correlation between molecular weight and retention time ($p < 0.01$), *i.e.*, molecular weight determinations with the TSK 250 column can be carried out in the range 1350–670 000 daltons.

The column material employed was extremely stable. By using clear solutions, a well degassed solvent and a guard column, the lifetime of the Bio-Sil TSK 250 column could be maintained over a long period. Only after 1500 injections did the guard column show the first signs of damage. We were able to continue to work with the same Bio-Sil TSK 250 column after changing the guard column.

In conclusion, these studies show that the column material used for HPLC does not influence the allergenic activity and the antigen/allergen patterns of the extracts. Hence it is possible to isolate components of allergen extracts by HPLC prior to further investigation by more specific biochemical and immunological methods.

ACKNOWLEDGEMENTS

The authors are grateful to Mrs. M. Marquass and Mrs. A. Zieren for their skillful technical assistance. They thank Mrs. L. Bozzardi for typing the manuscript.

REFERENCES

1 D. G. Marsh, P. S. Norman, M. Roebber and L. M. Lichtenstein, *J. Allergy Clin. Immunol.*, 68 (1981) 449.
2 M. D. Chapman and T. A. E. Platts-Mills, *J. Immunol.*, 125 (1980) 587.
3 E. Florvaag, S. Elsayed and J. Apold, *Int. Arch. Allergy Appl. Immunol.*, 67 (1982) 49.
4 H. J. Maasch, W. Geissler, R. Wahl, G. Winter and J. Maass, *Allergologie*, 3 (1982) 83.
5 D. H. Calam, J. Davidson and A. W. Ford, *J. Chromatogr.*, 288 (1984) 137.
6 S. Haavik, B. S. Paulsen and J. K. Wold, *J. Chromatogr.*, 321 (1985) 199.
7 R. Wahl, H. J. Maasch and W. Geissler, *J. Chromatogr.*, 329 (1985) 153.
8 A. Bensadoun and D. Weinstein,*Anal. Biochem.*, 70 (1976) 241.
9 R. Wahl, H. J. Maasch and W. Geissler, *Anal. Biochem.*, 134 (1983) 189.
10 M. Ceska, R. Eriksson and J. M. Varga, *Allergy Clin. Immunol.*, 49 (1972) 1.
11 H. Løwenstein, *Prog. Allergy*, 25 (1978) 1.
12 B. Weeke and H. Løwenstein, *Scand. J. Immunol.*, 2, Suppl. 2 (1973) 149.
13 M. C. Anderson and H. Baer, *RAST-Inhibition Procedure, Technical Report*, Bureau of Biologics, Food and Drug Administration, Bethesda, MD, 1981.

Journal of Chromatography, 351 (1986) 47–56
Elsevier Science Publishers B.V., Amsterdam — Printed in The Netherlands

CHROM. 18 170

2-CYANOETHYLDIMETHYL(DIETHYL)AMINOSILANE, A SILYLATING REAGENT FOR SELECTIVE GAS CHROMATOGRAPHIC ANALYSIS USING A NITROGEN–PHOSPHORUS DETECTOR

M. J. BERTRAND*, S. STEFANIDIS and B. SARRASIN
Department of Chemistry, University of Montreal, P.O. Box 6210, STN A, Montreal, Québec H3C 3V1 (Canada)
(First received July 15th, 1985; revised manuscript received September 9th, 1985)

SUMMARY

The synthesis of 2-cyanoethyldimethyl(diethyl)aminosilane (CEDMSDEA) as a reagent to form silyl derivatives detectable using nitrogen–phosphorus detection (NPD) in gas chromatographic (GC) analysis, is described. This new reagent was reacted with carboxyl, phenolic and secondary hydroxyl groups from fatty acids, phenols and cholesterol, respectively. The corresponding 2-cyanoethyldimethylsilyl (CEDMS) derivatives were analyzed by GC using NPD and their retention and detection characteristics compared with trimethylsilyl equivalents, analyzed by flame ionization detection. Results indicate that these new derivatives have chromatographic properties which are similar to other silyl derivatives with longer retention times then trimethylsilyl analogues. This new silylating reagent can thus be used selectively to analyze non-nitrogen containing compounds with high sensitivity using NPD. The mass spectral fragmentation of the CEDMS derivatives is briefly discussed with reference to their detection by selected ion monitoring GC–mass spectrometry.

INTRODUCTION

In the last two decades, considerable attention has been given to derivatization techniques and their use is widespread in the fields of chemical synthesis and chemical analysis[1,2]. Derivatives are used to protect reactive groups in synthesis and to enhance volatility and stability in instrumental techniques such as gas chromatography (GC) and mass spectrometry (MS). In the early developments in derivatization, the search was oriented towards universal reagents that would produce a one-step reaction with most functional groups. This led to a series of techniques of which acylation and silylation reactions are successful examples. As detection limits were lowered and the mixtures to be analyzed became more complex, chemically selective reactions were developed to discriminate against the background.

Numerous derivatization reagents presently exist and their applications have been presented in several reviews[1,3,4]. Within the existing reagents, silylating agents have received wide acceptability and are extensively used in the fields of chromato-

0021-9673/86/$03.50

graphy and MS because they offer excellent properties for chemical analysis, are easy to use and have universal applicability. The silylating reagents can be classified as universal or selective depending on the detection properties of the formed derivatives. For example, trialkylsilyl groups possess universal properties and their derivatives are generally analyzed using flame ionization detection (FID) and MS[5]. In order to make use of the advantages of selective detectors while retaining the basic chromatographic properties of alkylsilyl derivatives, halogenated silylating reagents have been introduced to form derivatives detectable by electron-capture detection (ECD)[6–8]. These derivatives have been used to analyze trace levels of biological materials and subnanogram detection limits have been reported[8].

In order to expand the applications of selective silylating reagents, which so far have been limited to the use of ECD, we have sought a reagent that would allow the use of an alternate selective detection method in situations where the use of ECD is not desirable. Such examples are the analysis of mixtures of halogenated compounds having a wide range of response factors for ECD or analysis of matrices that can seriously contaminate the electron-capture detector or cause strong interferences. A detection method that offers analytical potential for selective detection of organic compounds at trace levels is nitrogen–phosphorus detection (NPD). The nitrogen–phosphorus detector, of the Kolb type[9], has good sensitivity to nitrogen (10^{-13}g N), selectivity (10^4), a wide dynamic range (10^5), stability, is easy to operate and fairly resistant to contamination[10]. Because of this analytical potential, we have searched for a selective silylating reagent forming derivatives that would be detectable by NPD and also have mass spectral fragmentation suitable for detection by selected ion monitoring in GC–MS.

EXPERIMENTAL

Chemicals

2-Cyanoethyldimethyl(diethyl)aminosilane (CEDMSDEA) was prepared by the addition of 66 mmol dimethylchlorosilane (Pierce, silylation grade) to 65 mmol acrylonitrile (Aldrich) in the presence 65 μmol tris(triphenylphosphine)rhodium chloride (Aldrich) according to an existing proceddure[11]. The reactants were sealed in a test tube under an atmosphere of argon and heated to 50°C until the reaction mixture became dark (60–70 min). The reaction mixture was distilled under reduced pressure (5 Torr) and 2-cyanoethyldimethylchlorosilane (CEDMCS), a colorless liquid, was collected at 62°C. The chlorine radical was further displaced by diethylamine in tetrahydrofuran (THF)[12]. In 100 ml of THF containing 68 mmol of CEDMCS, 145 mmol of diethylamine were added over a period of 2 h. The mixture maintained under an atmosphere of argon was filtered and the desired compound isolated by distillation (80°C, 2 Torr). The reagent was treated with a 0.5% (w/v) solution of 3,4,5-trimethoxybenzoic acid (Aldrich) in THF to remove reactive side products. CEDMSDEA was kept and used as a 10% (v/v) solution in ethyl acetate. This solution may be kept for several months without degradation.

Derivatization reactions were carried in Reacti-Vials using ethyl acetate as a solvent. To a solution of ethyl acetate containing the compound of interest ($\approx$ 1 m*M*) CEDMSDEA was added in excess (80:1). The reaction time and temperature are given with the kinetic data.

All chemicals and solvents used in this study were purified by usual procedures prior to their use. Fatty acids (C_8–C_{18}) were obtained from Polyscience (IL, U.S.A.), cholesterol from Dr. J. C. Roy, Ste Justine Hospital (Montreal, Canada) and chlorophenols from Aldrich. In all cases, chlorophenols were purified by vacuum sublimation prior to their use.

Instrumentation

Mass spectral data were obtained on a Kratos MS-50TA mass spectrometer. The electron energy was 70 eV, the source temperature 220°C and the transfer line was kept at 260°C. The IR spectra were obtained on Digilab FT-15C/E Fourier Transform Michelson interferometer, the ^{1}H NMR spectra on a Bruker WH-90 spectrometer. All GC data were obtained on a Perkin Elmer (Norwalk, CT, U.S.A.) sigma 2B gas chromatograph equipped with a nitrogen–phosphorus detector and a flame ionization detector. The capillary column was 15 m × 0.23 mm I.D. coated with polydimethylsiloxane DB-1 (Chromatographic Specialties, Brockville, Ontario, Canada). The oven temperature was programmed from 120 to 280°C at 12°C/min for the analysis of fatty acids and chlorophenols derivatives. The derivative of cholesterol was analyzed at 280°C. The split injector ratio was 32:1 and injector and detector temperature was 300°C. Helium was used as carrier gas and in all cases aliquots (1 μl) of the reaction mixture were injected without prior separations of the products from the reactants. The nitrogen–phosphorus detector was operated with 30 ml/min of helium as make up gas and tuned for maximum selectivity according to a procedure use in this laboratory[13,14]. The hydrogen and air flow-rates at the detector were 2.6 and 100 ml/min, respectively. The bead current was kept below the optimum sensitivity (routine operation) to increase the lifetime of the bead.

RESULTS AND DISCUSSION

Only a few derivatization techniques have been introduced to permit the selective analysis of non-nitrogen or non-phosphorus containing compounds using NPD. A reaction using dimethylthiophosphinic chloride to form esters has been reported[15]. This procedure introduces phosphorus in the derivatives, as the NPD selective element. Another approach made use of the silylating reagent N,N-diethylaminodimethylsilane[16] to form nitrogen-containing derivatives. The latter had limited application because of the chemical reactivity of the formed derivatives[16]. Following the example of chloromethyldimethylsilyl derivatives where the trialkyl group was modified to insert an ECD compatible group, we have synthetized CEDMSDEA in which a cyano group (NPD reactive) is attached to the dimethyl silicone moiety.

The general structure of silylating reagents incorporates two parts that gives them specific properties. These are the silicone moiety and the leaving group L (see structures 1–3). The silicone moiety caracterizes the formed derivatives and the leaving group determines the reactivity of the reagent. Since the objective of this study was to develop a reagent for selective detection, attention was given to the silicone moiety. However, since the electronic effects of the cyano group on the silicon were not known, diethylamine was chosen as the leaving group because its reactivity is intermediate both in the trialkylsilyl and flophemesyl reagents[8].

In order to modify the character of the silicone moiety so that the derivatives

could be detected by NPD while retaining the basic properties of trimethylsilyl (TMS) derivatives (structure 1), a cyano group was introduced on one of the alkyl groups substituting the silicone atom. A cyano group was chosen because it is easily detected by NPD and it is believed to play an important role in the detection mecanism of NDP[17]. The cyano radical is used as a chemical tag in a fashion similar to the halogen in the chloromethyldimethylsilyl radical (structure 2) for ECD. Since the cyano radical could not be introduced directly on the silicone atom because silico-cyanides readily isomerize to their isocyanide form[18], it was introduced on the silicone moiety using the ethyl group as a carrier (structure 3).

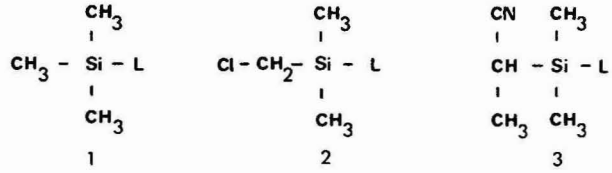

The use of the ethyl group instead of the methyl, confers additional chemical stability to the methine proton which can be acidic in the cyanomethyl group. Furthermore, the presence of the cyanoethyl group, while keeping the mass of the added

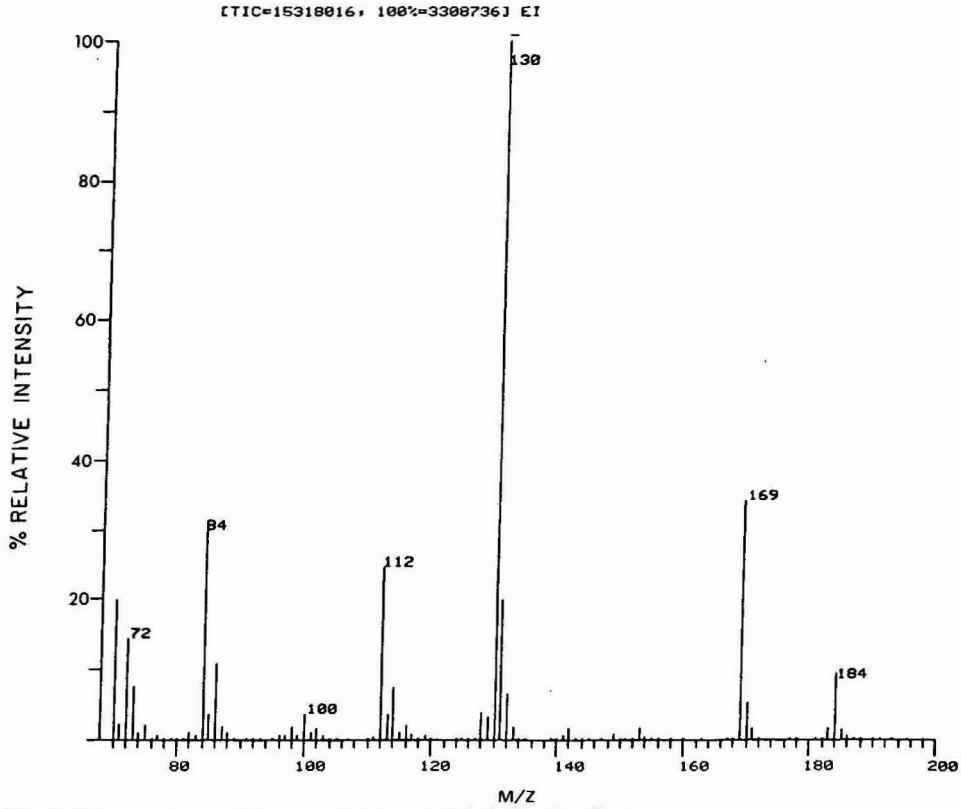

Fig. 1. Mass spectrum of 2-cyanoethyldimethyl(diethyl)aminosilane.

radical to a minimum, should favor the elimination of the cyanoethyl radical under electron impact providing an intense and specific ion at [M − 54].

The identity of CEDMSDEA has been ascertained by IR, ^{1}H NMR and MS. The IR spectrum shows an intense absorption band at 2220 cm^{-1} (C≡N). The ^{1}H NMR signals at 0.25 ppm (CH_3–S_i) (s), 1.01 ppm (CH_3–CH_2) (t), 1.26 ppm (CH_3–CH) (d), 1.74 ppm (CH) (q) and 2.86 ppm (CH_2–CH_3) (q) are supportive of the structure. The mass spectrum (Fig. 1) shows an M^+ ion at *m/z* 184 and a base peak at *m/z* 130 due to the loss of the cyanoethyl radical. Peaks at *m/z* 169 and 112 are explained by the elimination of the CH_3 and $N(C_2H_5)_2$ radicals.

Model compounds were selected to study the reactivity of the reagent and the analytical characteristics of the formed derivatives. The general reactivity was studied using carboxyl, phenolic and secondary hydroxyl groups from fatty acids, chlorophenols and cholesterol, respectively. Fatty acids (C_8–C_{18}) are of biological interest and represent a good system to study, in the same series, the reactivity of the carboxylic group and retention properties of the derivatives. Mono- and pentachlorophenols permit the study of two halogenated phenolic compounds with different pK_a values (9.2 and 4.8) and different halogen content. Cholesterol, which is often used as a reference compound, was chosen to examine the application of these derivatives to steroid analysis both in chromatography and mass spectrometry.

The carboxyl group of fatty acids reacts readily with CEDMSDEA in ethyl acetate. Fig. 2A shows kinetic data for the C_8 and the C_{18} homologues and it can be seen that quantitative reaction is achieved within a few minutes in ethyl acetate at room temperature. The use of higher temperatures does not affect the overall yield and the derivatives are stable in the reaction mixture for hours indicating that no secondary reactions or thermal degradation are occurring. Fig. 2B shows the kinetic

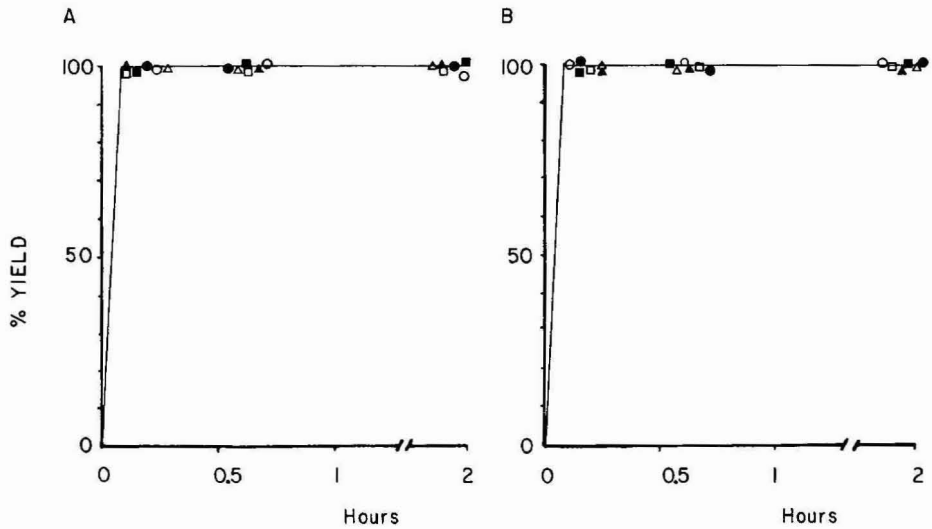

Fig. 2. (A) Reaction kinetics of octanoic (C_8) and octadecanoic (C_{18}) acids with CEDMSDEA in ethyl acetate at different temperatures. C_8: (●) 25°C, (■) 55°C and (▲) 75°C. C_{18}: (○) 25°C, (□) 55°C and (△) 75°C. (B) Reaction kinetics of mono- and pentachlorophenols with CEDMSDEA in ethyl acetate at different temperatures. 2-Chlorophenol: (●) 25°C, (■) 55°C and (▲) 75°C. Pentachlorophenol: (○) 25°C, (□) 55°C and (△) 75°C.

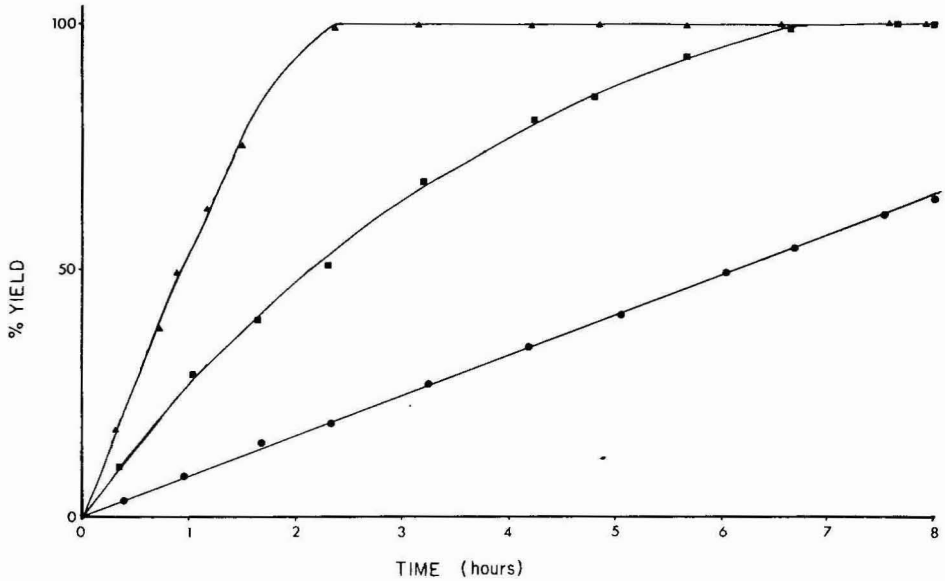

Fig. 3. Reaction of cholesterol with CEDMSDEA in ethyl acetate at (●) 25°C, (■) 55°C and (▲) 75°C.

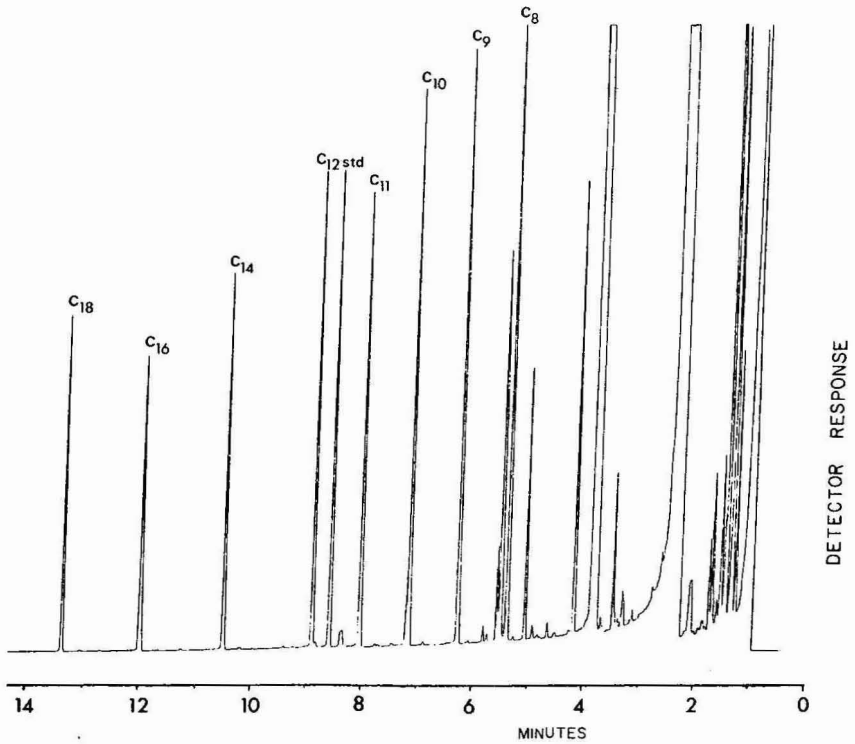

Fig. 4. Chromatogram of a mixture containing CEDMS derivatives of C_8–C_{18} fatty acids 70 ng analyzed with NPD. STD = triphenylamine (external standard).

data obtained for the two phenolic compounds studied and again the reaction is very rapid. Results indicate that the acidity of the hydroxyl group has no noticeable effect on the reaction rate and the reaction is complete in minutes at room temperature in ethyl acetate. The overall reaction yield does not vary when the temperature is raised to 55 or 75°C and the products are stable in the reaction mixture. The results obtained for the silylation of the secondary hydroxyl group of cholesterol are presented in Fig. 3. For this compound it can be seen that the reaction proceeds at a much slower rate taking 17 h to be completed at room temperature. In this case, quantitative reaction can be achieved in about 2 h if the reaction temperature is raised to 75°C.

The 2-cyanoethyldimethylsilyl (CEDMS) derivatives of the model compounds were analyzed on a polydimethylsiloxane stationary phase using NPD in order to study their retention and detection characteristics. Fig. 4 shows a typical chromatogram obtained from a mixture containing the C_8–C_{18} fatty acids after reaction with CEDMSDEA. As can be seen from the figure, the elution profile of the peaks is symmetrical and no tailing can be seen. The GC behavior of the CEDMS derivatives is similar to other silyl derivatives. Under our experimental conditions the retention times of the CEDMS derivatives are 1.4–2 times longer than the corresponding TMS

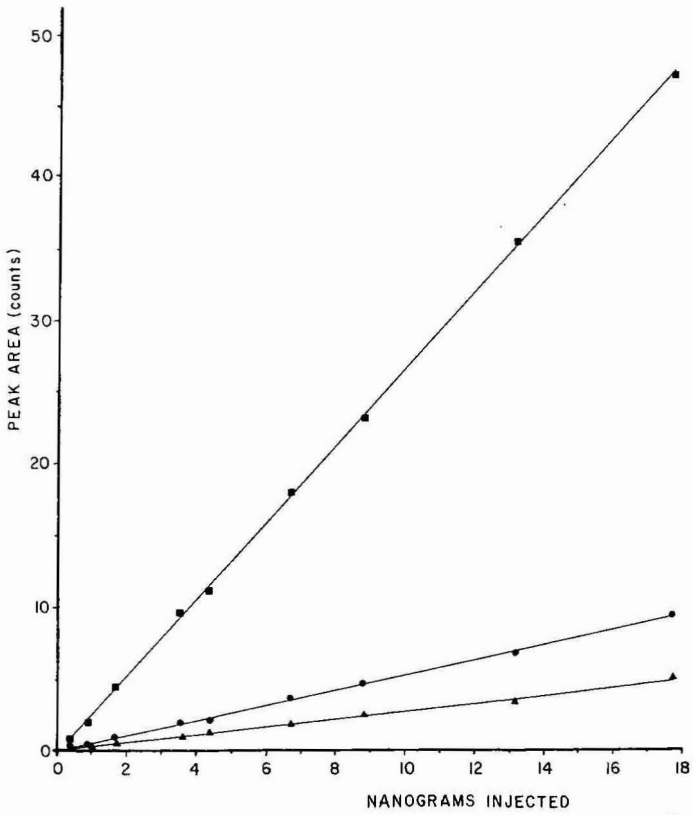

Fig. 5. Concentration–response plots of CEDMS and TMS derivatives of octadecanoic acid: (■) CEDMS derivatives with NPD, (●) TMS derivatives with FID and (▲) CEDMS derivatives with FID.

derivatives. Furthermore, Fig. 4 clearly demonstrates that these derivatives can be detected by NPD. Since the contribution of the discrimination effect on the signal-to-noise (S/N) ratio of the detector depends on the matrix to be analyzed, the increase in the sensibility obtained using this procedure was studied by comparison with FID. In these experiments, concentration–response plots were obtained by analyzing CEDMS and TMS derivatives of the fatty acids using FID and compared with the plots obtained for CEDMS derivatives when analyzed by NPD. The resulsts are shown on Fig. 5 and the response is linear with concentration in all cases. However,

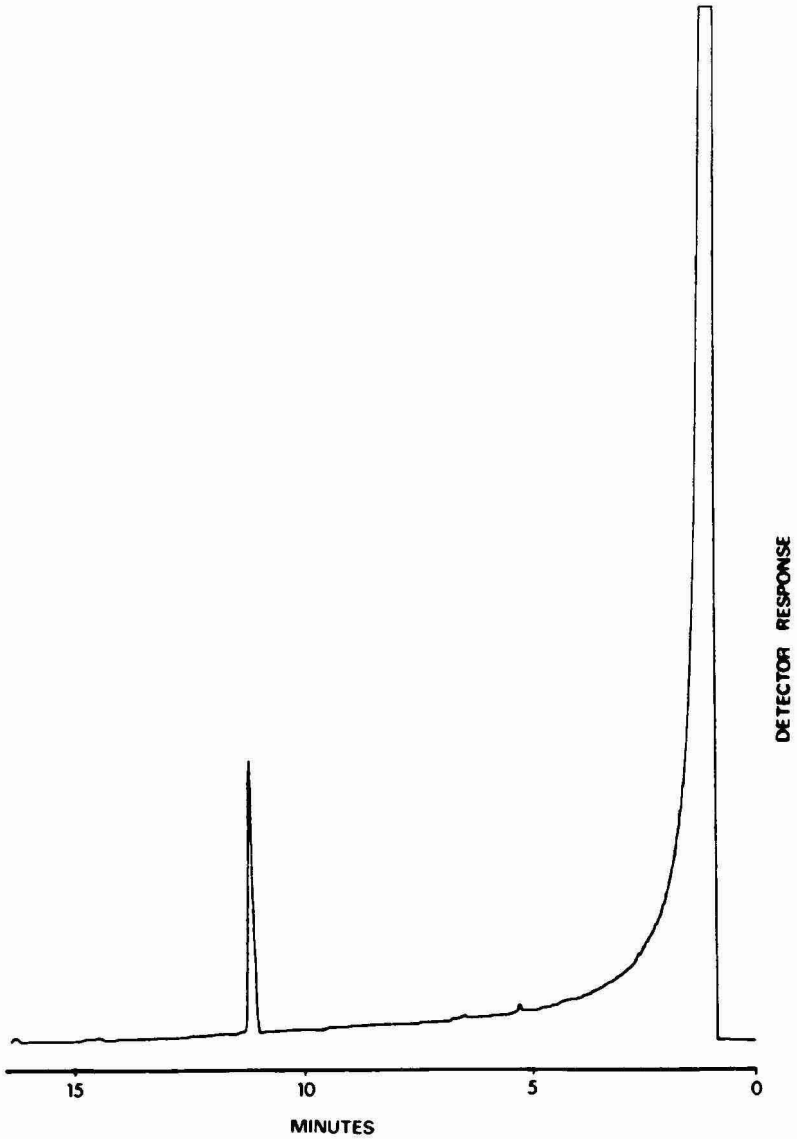

Fig. 6. Chromatogram of a reaction mixture containing cholesterol (65 ng). Column, DB1; isothermal at 300°C.

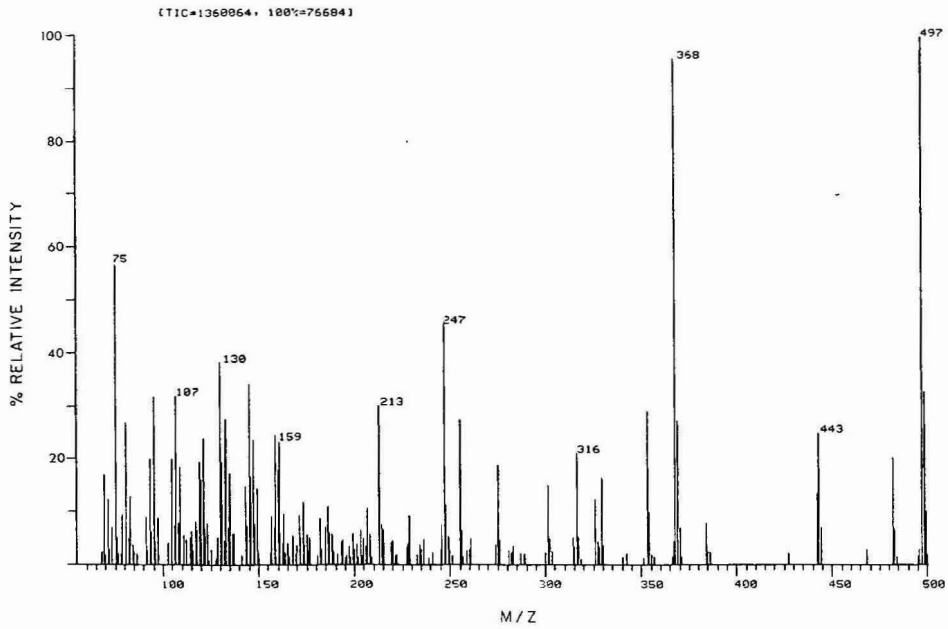

Fig. 7. Mass spectrum of the CEDMS derivative of cholesterol.

when the sensitivities obtained with both detectors are compared (slope ratio) it is found that the gain in sensitivity is at least fivefold when NPD is used. The combination of the increase in sensitivity and the selectivity is reflected in the detection limit for these compounds which was found to be $1 \cdot 10^{-13}$–$3 \cdot 10^{-13}$ g N (S/N = 3) under our experimental conditions. Similar results have been obtained for the derivatives of cholesterol and the two chlorophenols studied. The chromatogram of the derivative of cholesterol is shown on Fig. 6 and it can be seen that under our experimental condition the peak is unique and free from interferences from the reaction mixture. The chromatographic behaviour of chlorophenols is adequate for their analysis and this is reported elsewhere[21].

Since selected ion monitoring MS is often used as a specific detection method in conjunction with GC the behavior of the CEDMS derivatives under electron impact was briefly studied. The presence of specific ions at high mass is of particular interest since these ions are often used for quantitation or confirmation in selected ion monitoring GC–MS. For fatty acids derivatives the moleccular ions are present but their relative intensities are below 5% as in *tert.*-butyldimethyl derivatives[19]. However, the mass spectra are characterized by the presence of intense ions at m/z 75 and 129, [M − 54] and [M − 15] which are characteristic of the particular acid. The [M − 15] and [M − 54] ions are due to the losses of the CH_3 and C_2H_4CN radicals, the latter being more intense and occuring at an odd mass since the "nitrogen rule" is applicable. The mass spectrum of the cholesterol CEDMS derivative is shown on Fig. 7. The general features of the spectrum are like those of the equivalent TMS derivative[20] but some additional features can be seen. The molecular ion at m/z 497 is of odd mass and also the base peak in the spectrum. Other intense high mass peaks are seen at [M − 15], [M − 54] and [M − 129] corresponding to the losses of CH_3,

C_2H_4CN and the silanol. Again these four peaks are highly characteristic of the structure and may be used for selected ion monitoring detection. These preliminary results indicate that CEDMS may have fragmentation features under electron impact which are of analytical interest.

CONCLUSION

The results presented in this study indicate that CEDMSDEA is a silylating reagent that can be used to form derivatives for specific detection. The CEDMS derivatives have the general chromatographic properties of other silyl derivatives and offer new features that can be of analytical interest. They can be used in conjunction with NPD and as such can expand the field of application of silylating reagent. Furthermore, it appears from the mass spectra of the compounds studied that they offer mass spectral features which are complementary to existing TMS and *tert.*-butyldimethylsilyl derivatives for MS identification or analysis by selected ion monitoring GC–MS.

ACKNOWLEDGEMENTS

We wish to thank the National Science and Engineering Research Council of Canada (NSERC) and the Fonds FCAC, Government of Quebec for financial assistance in this study.

REFERENCES

1 G. S. King and K. Blau, in K. Blau and G. S. King (Editors) *Handbook of Derivatives in Chromatography*, Heyden & Son, London, 1978, pp. 1–37.
2 A. E. Pierce, *Silylation of Organic Compounds*, Pierce Chemical, Rockford, 1982, p. 446.
3 C. F. Poole, in K. Blau and G. S. King (Editors), *Handbook of Derivatives in Chromatography*, Heyden & Son, London, 1978, p. 152.
4 C. F. Poole and A. Zlatkis, *J. Chromatogr.*, 184 (1980) 99.
5 A. E. Pierce, *Silylation of Organic Compounds*, Pierce Chemical, Rockford, 1982, p. 33.
6 W. J. A. Vandenheuvel, *J. Chromatogr.*, 27 (1967) 85.
7 E. D. Morgan and C. F. Poole, *J. Chromatogr.*, 89 (1974) 225.
8 E. D. Morgan and C. F. Poole, *J. Chromatogr.*, 104 (1975) 351.
9 B. Kolb and J. Bischiooff, *J. Chromatogr. Sci.*, 12 (1974) 625.
10 S. O. Farwell, D. R. Gage and R. A. Kagel, *J. Chromatogr. Sci.*, 19 (1981) 358.
11 I. Okima, K. Kumagai and Y. Nagai, *J. Organomet. Chem.*, 111 (1976) 43.
12 R. A. Pike and R. L. Schank, *J. Org. Chem.*, 27 (1960) 2190.
13 R. Dugal, R. Masse, G. Sanchez and M. J. Bertrand, *J. Anal. Toxicol.*, 4 (1980) 1.
14 S. Stefanidis, *MSc Thesis*, University of Montreal, 1984.
15 K. Jacob and W. Vogt, *J. Chromatogr.*, 150 (1978) 339.
16 R. Massé, R. Dugal and M. J. Bertrand, in A. Frigerio and M. McCamish (Editors), *Recent Developments in Chromatography and Electrophoresis, 10*, Elsevier, Amsterdam, 1980, p. 169.
17 B. Kolb, M. Auer and P. Pospisil, *J. Chromatogr. Sci.*, 15 (1977) 53.
18 D. A. Evans, L. K. Truesdale and G. L. Carroll, *J. Chem. Comm.*, (1973) 55.
19 A. P. J. M. de Jong, J. Elema and B. J. T. van de Berg, *Biomed. Mass Spectrom.*, 7 (1980) 361.
20 C. J. W. Brooks, W. Henderson and G. Steel, *Biochim. Biophys. Acta*, 296 (1973) 43.
21 M. J. Bertrand, S. Stefanidis, A. Donais and B. Sarrasin, *J. Chromatogr.*, in press.

Journal of Chromatography, 351 (1986) 57–64
Elsevier Science Publishers B.V., Amsterdam — Printed in The Netherlands

CHROM. 18 154

GAS CHROMATOGRAPHY OF ECDYSTEROIDS AS THEIR TRIMETHYLSILYL ETHERS

C. R. BIELBY and E. D. MORGAN*
Department of Chemistry, University of Keele, Keele, Staffordshire (U.K.)
and
I.D. WILSON
Department of Drug Metabolism, Hoechst Pharmaceutical Research Laboratories, Walton Manor, Walton, Milton Keynes, Bucks MK7 7AJ (U.K.)
(Received August 21st, 1985)

SUMMARY

Conditions for the preparation of some 60 silyl ethers of ecdysteroids using trimethylsilylimidazole are reported. The thin-layer and gas–liquid chromatographic properties of the resulting derivatives, together with information on mass spectrometry as an aid to structure identification, are described.

INTRODUCTION

The ecdysteroids, a family of polyhydroxylated steroids structurally related to ecdysone (Fig. 1), are important as the moulting hormones of insects and crustaceans as well as other arthropods. These compounds are also encountered in certain species of plants particularly conifers and ferns[1]. To date over 100 different structures have been reported.

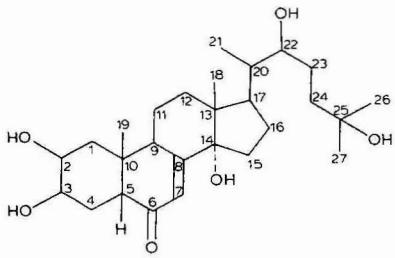

Fig. 1. The structure of ecdysone showing the numbering.

A variety of methods have been developed for the analysis of ecdysteroids including thin-layer chromatography (TLC)[2,3], high-performance liquid chromatography (HPLC)[4,5], gas–liquid chromatography (GLC)[6,7] and radioimmunoassay (RIA)[8] or a combination of more than one of these methods (*e.g.* HPLC–RIA).

0021-9673/86/$03.50

GLC, when combined with electron-capture detection (ECD) or mass spectrometry (MS) (using single ion monitoring, SIM), provides a method of great sensitivity and specificity for the analysis of these compounds. However, the ecdysteroids are involatile and thermally unstable and require conversion to their trimethylsilyl (TMS) ethers for GLC. The derivatisation procedure requires careful control because of the different rates of reaction of the various hydroxyls present.

Though fast atom bombardment MS has established itself as the best method for determining the molecular mass of the ecdysteroids, the electron impact mass spectra (EI) of their silyl ethers remains one of the best sources of structural information.

We present here the conditions required for making some 60 silyl ethers of ecdysteroids, together with their relative retention data in GC.

MATERIALS AND METHODS

The ecdysteroids used in this study were gifts from a number of sources.

Silylation

A sample of ecdysteroid (0.2–1.0 mg) was dissolved in acetone and methanol to give a concentration of 500 μg ml^{-1}. A 50-μl aliquot (approx. 25 μg) of this solution was evaporated to dryness under nitrogen in a 1-cm^3 ReactiVial (Pierce and Warriner, Chester, U.K.). This sample was redissolved in a mixture of pyridine (65 μl) and trimethylsilylimidazole (TMSI, 35 μl) and the vial sealed. The mixture was allowed to react at either room temperature (30 min), 120°C (5 h) or 140°C (60 h) depending on the degree of silylation required. After reaction, an aliquot (usually 10 μl) was diluted with purified "ECD"-grade toluene (see ref. 6) to give a concentration of 1–10 ng ml^{-1}. Samples of this solution (1 μl) were taken for GLC–ECD as described below.

The remainder of the reaction mixture was either stored at 0–4°C, at which temperature the silyl ethers are stable for several weeks, or purified by TLC.

Purification of ecdysteroid TMS ethers by TLC

The TMS ethers were purified using preparative TLC on 0.6 mm thick 20 cm × 20 cm plates coated with methanol-washed silica gel 60 P F_{254} (E. Merck, Darmstadt, F.R.G.). The volume of the reaction mixture was first reduced by evaporation of some of the pyridine under a stream of nitrogen. The concentrated solution was applied to the origin of the plate which was developed in toluene–ethyl acetate (7:3, v/v) for 15 cm. The tetrakis-TMS ether of ecdysone was also spotted onto a portion of the plate for comparison. The derivatives were located on the plate by visualisation at 254 nm when present in sufficient quantity. They were recovered from the plate by removing the appropriate zone of silica gel and eluting with diethyl ether. After evaporation of the ether the samples were redissolved in ECD-grade toluene for analysis by GLC. Recoveries of ecdysteroid TMS ethers were generally 80–90% of the material applied to the plate. The R_F values for these derivatives are given in Table I.

GC of ecdysteroid TMS ethers

GC was performed using a Pye Unicam Series 104 gas chromatograph, fitted with a ^{63}Ni electron capture detector, on silanised glass columns (0.9 m or 1.5 m × 4 mm I.D.) containing 1.5% (w/w) OV 101 silicone phase (Magnus Scientific, Aylesbury, U.K.) on Chromosorb W. The chromatographic conditions were a column temperature of 285°C, detector temperature 300°C, and a carrier gas (oxygen free nitrogen) flow-rate of 50–60 ml min^{-1}. Samples (1–2 μl) were injected directly onto the top of the column using a 5-μl syringe fitted with an 11-cm needle.

RESULTS AND DISCUSSION

The hydroxyl groups present on the ecdysteroid possess a range of reactivities towards TMSI, due to their different steric environments. Previous work with model compounds[6] together with ecdysone and 20-hydroxyecdysone has established the following order of reactivity of the hydroxyl groups. 2β, 3β, 22R, 25 > 20S ⩾ 14α. The reaction conditions employed in this study exploit these differences to allow the formation of a number of different derivatives. Thus the reaction of 20-hydroxyec-

TABLE I

R_F VALUES OF THE TMS ETHERS OF ECDYSTEROIDS ON SILICA

Parent compound	*R_F value of the derivative formed after silylation for:*		
	30 min at room temperature	*5 h at 120°C*	*60 h at 140°C*
Ecdysone	0.72	0.72	0.82
20-Hydroxyecdysone	0.65	0.69	0.75
Ajugasterone C	0.63	0.8	0.8
Calonysterone	0.7	0.76	0.76
Carpesterol	0.7	0.7	0.7
Cyasterone	–	–	0.72
Dacrysterone	0.54	077	0.81
2-Deoxyecdysone	0.74	0.74	0.78
2-Deoxy-3-epiecdysone	0.74	0.74	0.77
2-Deoxy-20-hydroxyecdysone	0.74	0.68	–
20-Hydroxyecdysone 2-cinnemate	0.64	0.81	0.75
Inokosterone	0.65	0.72	0.8
22-Isoecdysone	–*	0.77	0.79
Kaladasterone	0.7	0.73	0.75
Makisterone A	0.67	0.72	0.78
Muristerone	–*	0.47*	0.59
Polypodine B	0.65	0.74	0.76
Polypodine B 2-cinnamate	0.4	0.76	0.83
Ponasterone A	0.67	0.78	0.71
Ponasterone C	0.34	0.71	–
Ponasterone C 2-cinnamate	0.38	0.75	0.78
Poststerone**	0.6–0.8	0.6–0.8	0.6–0.8
Pterosterone	0.71	0.71*	0.73

* Silylation of these ecdysteroids under these conditions formed mixed derivatives.

** Too small a sample to be viewed under UV illumination.

TABLE II

PROPOSED DERIVATIVES OF SOME ECDYSTEROID TMS ETHERS

Parent compound	*Conditions of silylation*					
	30 min, room temperature		*5 h, 120°C*		*60 h, 140°C*	
	No. of silyl groups	*Position of hydroxyl groups silylated*	*No. of silyl groups*	*Position of hydroxyl groups silylated*	*No. of silyl groups*	*Position of hydroxyl groups silylated*
Ecdysone	4	2,3,22,25	4	2,3,22,25	5	2,3,14,22,25
20-Hydroxyecdysone	4	2,3,22,25	5	2,3,20,22,25	6	2,3,14,20,22,25
2-Deoxyecdysone	3	3,22,25	3	3,22,25	4	3,14,22,25
2-Deoxy-3-epiecdysone	3	3epi,22,25	3	3epi,22,25	4	3epi,14,22,25
2-Deoxy-20-hydroxyecdysone	3	3,22,25	4	3,20,22,25	5	3,14,20,22,25
Inokosterone	4	2,3,22,26	5	2,3,20,22,26	6	2,3,14,20,22,26
Makisterone A	4	2,3,22,25	5	2,3,20,22,25	6	2,3,14,20,22,25
Ponasterone A	3	2,3,22	4	2,3,20,22	5	2,3,14,20,22
Poststerone	2	2,3	2	2,3	3	2,3,14
Pterosterone	4	2,3,22,24	4	2,3,20,22,24	6	2,3,14,20,22,24

dysone with TMSI, at room temperature for 30 min (or longer) produces the 2,3,22,25-tetrakis-TMS ether, 5 h at 120°C the 2,3,20,22,25-pentakis-TMS ether, and 60 h at 140°C the fully derivatised 2,3,14,20,22,25-hexakis-TMS ether.

Thus our knowledge of the rate of silylation of hydroxyl groups located on these carbons allows us to identify tentatively the derivatives formed from ecdysteroids that possess hydroxyl groups on C-2, C-3, C-14, C-20, C-22 and C-25. Ecdysteroids containing only hydroxyl groups on these carbons and their proposed derivatives are shown in Table II. This table also includes inokosterone and pterosterone which have an hydroxyl group on C-26 and C-24 respectively, both of which are in unhindered positions and are very likely to be readily silylated. These proposed derivatives have yet to be confirmed by MS. GC retention time data are given in Table III.

The remaining ecdysteroids either possess an additional chemical moiety or a hydroxyl group in such a position that it would be unwise to predict its rate of silylation without confirmation of the structure of the derivatives by MS. In cyasterone a lactone ring occurs on the side chain on C-24 which increases the molecular weight and the polarity of the silyl ether in comparison with other ecdysteroids. This causes the derivative to have a longer retention time, and poor peak shape at the temperature used for other ecdysteroid derivatives (Table III).

A group of plant ecdysteroids were also studied that have an additional chemical group, a cinnamate ester, present on the C-2 hydroxyl. These ecdysteroids, originally isolated from the bark of *Dacrydium intermedium* by Russell *et al.*[9], are 20-hydroxyecdysone-2-cinnamate, polypodine B-2-cinnamate and ponasterone C-2-cinnamate. These compounds also exhibited poor GC characteristics with broad peak shape and multiple product formation (which may have arisen from partial hydrolysis of the ecdysteroid derivative and formation of a silyl ether of the parent compound and cinnamic acid on silylation).

Four of the ecysteroids studied possess a C-5 β-hydroxyl group. These were dacrysterone (5β-hydroxymakisterone A) kaladasterone (2β,3β,5β,14α,20,22-hexahydroxycholest-7-en-6-one), muristerone (11α-hydroxykaladasterone) and polypodine B (2β,3β,5β,14α,20,22,25-heptahydroxycholest-7-en-6-one). A mass spectrum of the derivative formed after silylation of polypodine B at 120°C for 5 h is shown in Fig. 2. This indicates that six of the seven hydroxyl groups have been silylated to form the hexakis TMS ether. Given that the 14α-hydroxyl group is not silylated in ecdysone and 20-hydroxyecdysone under these conditions we deduced that the 5β-hydroxyl group had been derivatised. As yet we do not know whether this hydroxyl group is silylated readily at room temperature. Extrapolating this result to other ecdysteroids with a 5β-hydroxyl group it is likely that the hexakis TMS ether of dacrysterone and the pentakis TMS ether of kaladasterone are formed at 5 h, whilst 60 h at 140°C, probably results in complete silylation (heptakis and hexakis TMS ethers respectively).

In ajugasterone C (11α-hydroxyponasterone A) and muristerone A an extra hydroxyl group is present on the C ring at C-11α. Only small quantities of these two ecdysteroids were available and mass spectra were not obtained, it is therefore not possible to propose the rate of silylation for this group. Additionally; with muristerone A, multiple peaks were obtained on GC suggesting that, either the compound was impure (also indicated by HPLC) or that some of the hydroxyl groups were only partially silylated under the conditions employed.

TABLE III

GAS CHROMATOGRAPHIC PROPERTIES OF ECDYSTEROID TMS ETHERS

GC conditions: 0.9 m × 4 mm I.D. column, 1.5% OV-101 silicone phase, gas flow-rate 50–60 ml min^{-1}, temperature 285°C, detector temperature 300°C.

Ecdysteroid	*Conditions of silylation*					
	39 min, room temperature		*5 h, 120°C*		*60 h, 140°C*	
	t_R	t_R *relative to ecdysone*	t_R	t_R *relative to ecdysone*	t_R	t_R *relative to ecdysone*
Ecdysone	6.9	1	6.9	1	5.85	1
20-Hydroxyecdysone	7.95	1.15	9.45	1.37	7.55	1.3
Ajugasterone C	6.55	0.95	7.8	1.13	6.15	1.05
Calonysterone	9.25	1.34	10.5	1.52	10.5	1.79
Carpesterol	–		27.5*	4	–	
Cyasterone	–		19.8**	2.78	19.5	3.3
Dacrysterone	12.7*	1.84	9.85	1.43	–	
2-Deoxyecdysone	5.9	0.85	5.9	0.85	5.3	0.9
2-Deoxy-3-epiecdysone	5.5	0.8	5.5	0.8	5.3	0.9
2-Deoxy-20-hydroxyecdysone	7.1	1.03	8.5	1.23	–	
20-Hydroxyecdysone 2-cinnamate	11.6	1.68	>30	–	8.6	
Inokosterone	9.9	1.43	10.8	1.57	8.0	
22-Isoecdysone	7.5 → 6.5***	1.09	6.5	0.94	6.4	
Kaladasterone	6.8	0.98	6.3	0.91	4.1	
Makisterone A	10.0	1.45	11.4	1.65	9.15	
Muristerone	**	–	9.25**	1.34	5.1**	
Polypodine B	9.1	1.32	10.7	1.55	7.5	
Polypodine B 2-cinnamate	11.0*	1.59	≈10.6*	–	**	
Ponasterone A	5.9	0.85	6.2	0.9	4.4	
Ponasterone C	11.0	5.9	9.0	1.3	–	
Ponasterone C 2-cinnamate	**	–	≈10.0	–	–	
Poststerone	1.65	0.24	1.65	0.24	1.3	
Pterosterone	8.7	1.26	9.1	1.32	8.5	

* Very broad peak.
** Mixed derivatives.
*** If left longer than 30 min at room temperature.

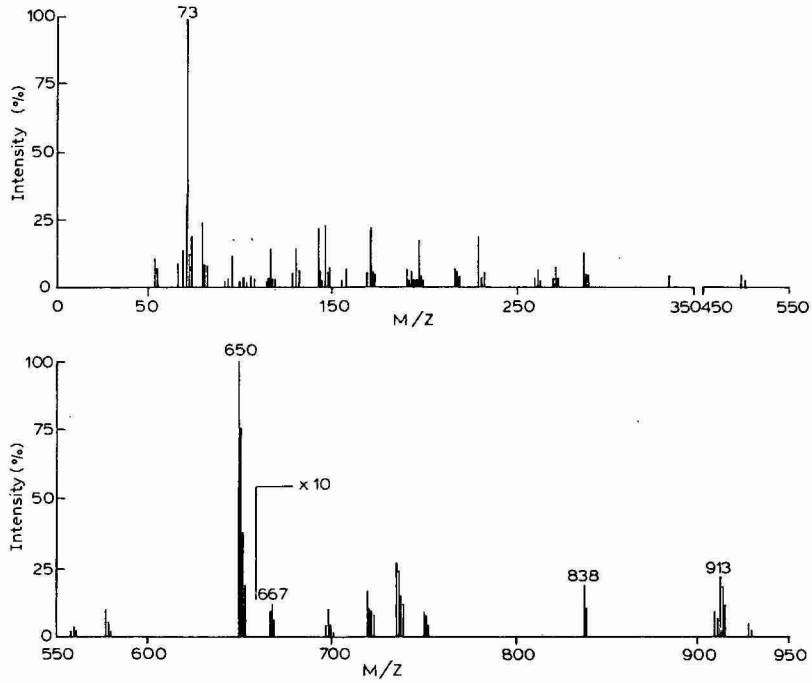

Fig. 2. The EI mass spectrum of the hexakis-TMS ether of polypodine B. The strong ion at *m/z* 650 arises from cleavage between C-20 and C-22 this is characteristic of ecdysteroids with hydroxyl groups at both of these positions. The ion at *m/z* 261 results from the side chain fragment of the same cleavage.

Calonysterone [2β,3β,6,20,22,25-hexahydroxycholesta-5,8(9),14-trien-7-one] is an unusually modified ecdysteroid[10], lacking a 14α-hydroxyl, with a ketone on C-7 (as opposed to C-6), an hydroxyl group on the C-6 position and a higher degree of unsaturation than "normal". This compound yielded two products, one after derivatisation for 30 min at room temperature and the other after 5 h at 120°C. No further derivatisation occurred by increasing the silylation time or temperature and it was concluded that after 5 h the ecdysteroid was fully derivatised as the hexakis TMS ether. The derivative formed by silylation at room temperature was assumed to be the pentakis TMS ether where all but the hydroxyl group on C-20 had been derivatised.

The final ecdysteroid investigated was a synthetic analogue, 22-isoecdysone differing from ecdysone (which has a 22*R* configuration) only in being its optical antipode at C-22. If this difference has no effect on the rate of silylation compared to ecdysone we would expect two derivatives to be formed (tetra and pentakis TMS). In fact three derivatives were observed. After a 30 min silylation at room temperature a single derivative was detected with a retention time of 7.5 min. Further silylation at room temperature resulted in a second peak gradually developing with a shorter retention time (6.5). This derivative was obtained as a single peak by silylation for 5 h at 120°C. Silylation at 140°C for 60 h then resulted in the formation of a third derivative with a retention time of 6.4 min. From these results we speculate that the C-22 hydroxyl group on 22-isoecdysone does not silylate as readily as the C-22 hy-

droxyl of ecdysone. Hence the first derivative was the tris-TMS ether where the C-2, C-3 and C-25 hydroxyl groups were silylated and the derivative formed after 5 h at 120°C was the tetrakis TMS ether where the C-22 group had also been fully derivatised.

CONCLUSION

GC with ECD (or GC with SIM) provides a specific and highly sensitive method for the qualitative and quantitative analysis and identification of most of the ecdysteroids which we have been able to investigate. The ability to form a number of different derivatives for each compound by varying the reaction conditions is useful in the identification of these compounds by GC–MS and as derivatives in the same way that acetates and acetonides are used in TLC and HPLC.

REFERENCES

1 C. Hetru and D. H. S. Horn, in J. A. Hoffmann (Editor), *Progress in Ecdysone Research*, Elsevier/North-Holland Biomedical Press, Amsterdam, 1980, p. 13.
2 E. D. Morgan and C. F. Poole, in J. E. Treherne, M. J. Berridge and V. B. Wigglesworth (Editors), *Advances in Insect Physiology 12*, Academic Press, London, New York, 1976, p. 17.
3 I. D. Wilson, *J. Chromatogr.*, 318 (1985) 373.
4 R. Lafont, G. Somme-Martin, B. Mauchamp, B. F. Maume and J.-P. Delbeque, in J. A. Hoffmann (Editor), *Progress in Ecdysone Research*, Elsevier/North-Holland Biomedical Press, Amsterdam, 1980, p. 45.
5 I. D. Wilson, C. R. Bielby and E. D. Morgan, *J. Chromatogr.*, 238 (1982) 97.
6 C. F. Poole and E. D. Morgan, *J. Chromatogr.*, 115 (1975) 587.
7 C. R. Bielby, A. R. Gande, E. D. Morgan and I. D. Wilson, *J. Chromatogr.*, 194 (1980) 43.
8 J. D. O'Connor and D. W. Borst, *Science*, 178 (1972) 418.
9 G. B. Russell, D. G. Fenemore, D. H. S. Horn and E. J. Middleton, *Aust. J. Chem.*, 25 (1972) 1935.
10 L. Canonica, B. Danieli, G. Ferrari, J. Krepinsky and G. Rainoldi, *Chem. Commun.*, (1973) 737.

Journal of Chromatography, 351 (1986) 65–75
Elsevier Science Publishers B.V., Amsterdam — Printed in The Netherlands

CHROM. 18 169

IDENTIFICATION OF VOLATILES IN THE HEAD SPACE OF ACID-TREATED PHOSPHATE ROCK BY GAS CHROMATOGRAPHY–MASS SPECTROMETRY

H. VAN LANGENHOVE* and N. SCHAMP
Laboratory of Organic Chemistry, Faculty of Agricultural Sciences, State University of Gent, Coupure links 653, B-9000 Gent (Belgium)
(Received August 16th, 1985)

SUMMARY

Phosphate rock samples were treated with sulphuric and hydrochloric acid. Compounds volatilized during this treatment were sampled on Tenax GC and analysed by gas chromatography–mass spectrometry. The identification revealed the presence of a few organosilicon fluorides, as well as numerous hydrocarbons and organosulphur compounds. A mercaptan, acyclic and cyclic sulphides, disulphides and alkylthiophenes were fully or partially identified. Since the human olfactory system is about 1000 times more sensitive for sulphur compounds than for hydrocarbons, it was concluded that the sulphur compounds were responsible for the typical pungent odour of the headspace mixture.

INTRODUCTION

The current annual consumption of phosphate rock, as the raw material for phosphorus chemicals and fertilizers is about 130 million tonnes. The major part of this commercial phosphate rock is mined from ores of marine sediments, in which phosphate occurs as carbonate-apatite[1].

About 90% of all phosphate rock is processed by the "wet process", which essentially is a treatment of the rock with a mineral acid. Sulphuric acid is generally used, but depending on the desired end-products, phosphoric, hydrochloric or nitric acid are used as well. In order to minimize the environmental impact of the wet process, some control measures have to be taken. When sulphuric acid is used, *ca.* 5–6 tons of phosphogypsum are produced per ton of phosphorus pentoxide. Since this gypsum is impure, it is not competitive with mined gypsum for the building industry and therefore it has to be disposed of. Besides, phosphate rock contains between 2.5 and 4.5% of fluorine. Much of this fluorine is volatilized as hydrogen fluoride and silicon tetrafluoride during acid treatment. To prevent the release of these compounds into the environment gases are scrubbed with water.

Another problem is the characteristic sour odour which is observed in the neighbourhood of phosphate plants, and which may sometimes constitute a public

0021-9673/86/$03.50

nuisance. The compounds responsible for the odour have yet not been identified. Therefore phosphate rock samples were treated in the laboratory with mineral acids; head-space volatiles were concentrated by adsorption on Tenax GC and the volatiles present in the head-space samples were identified by gas chromatography–mass spectrometry (GC–MS).

EXPERIMENTAL

Adsorption sampling

Before adsorption tubes were packed with Tenax GC, the adsorbent was extracted for 24 h with acetone, in a Soxhlet apparatus, and dried by evaporating the solvent under reduced pressure. Glass tubes (15 × 0.8 cm I.D.) were filled with 0.75 g of adsorbent, which was positioned between two glasswool plugs. Before use, packed tubes were conditioned by heating (220°C) overnight under a helium flow.

Fig. 1 illustrates the sampling apparatus. Samples were placed in a three-necked flask, which was mounted in a waterbath to keep the temperature at 60°C. Acid was added through a separatory funnel, and a helium supply was connected. In the initial stage of acid treatment, gas evolved spontaneously from the phosphate rock. After that a helium flow of 0.2 l/min was started in order to transfer head-space volatiles to the adsorption tube. Gas volumes were measured with a wet-gas meter.

The phosphate rock used in these investigations originated from Morocco. It consisted mainly of small pellets of marine origin. In the experiments 20 g of phosphate rock were treated with 100 ml of acid and 5 l of gas were sampled.

GC–MS analyses

A laboratory-made thermal desorption system[2] was used to concentrate adsorbed volatiles before GC–MS analyses. The GC–MS apparatus consisted of a Varian 2700 gas chromatograph fitted with a flame ionization detector, and a MAT 112 mass spectrometer.

A glass column (100 m × 0.5 mm I.D.) statically coated with SE52 (2 mg/ml) was used. Temperature programmes were varied from one analysis to another. The usual detector sensitivity was 80 pA/mV. Mass spectrometer conditions were as follows: source pressure, 10^{-6} Torr; electron energy, 70 eV; emission current, 0.7 mA; scan range, 0–250 *m/e*; scan speed, 100 mass units/s. Mass spectrometer scans were performed according to the signal from the flame ionization detector.

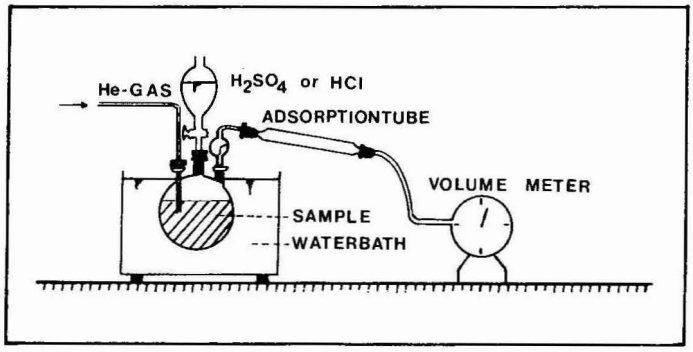

Fig. 1. Schematic drawing of the sampling apparatus.

Synthesis of reference compounds

In order to confirm results of the interpretation of mass spectra, some reference compounds were synthesized. To synthesize 2-methyl thiacyclohexane, 2-methylpiperidine was benzoylated and the N-benzoylpiperidine was treated with phosphorus pentabromide to obtain 2,6-dibromohexane. The substitution and cyclization with sodium sulphide was carried out according to the procedure of Whitehead *et al.*[3]. The purity of the compound was checked with GC and flame photometric detection (FPD) and it was necessary to perform preparative GC (Carbowax 20M 10% on Chromosorb W/AW, 3 m × 3 mm I.D.) with catharometer detection, to obtain the pure compound.

Disulphides were prepared by oxidation of mercaptans with iodine, according to McAllen *et al.*[4]. This reaction was carried out with methanethiol–ethanethiol; methanethiol–1-propanethiol and methanethiol–2-propanethiol. Since these compounds were used for the determination of Kovats indices and reference mass spectra by GC–MS, no effort was made to separate the three different disulphides present in each reaction mixture.

Asymmetric sulphides were prepared by nucleophilic substitution of a halogenide with a mercaptide[5]. This reaction was carried out with ethanethiol–iodomethane, methanethiol–2-bromopropane and propanethiol–iodomethane.

GC–FPD analyses

GC–FPD analyses were performed on a Tracor 560 instrument with a glass capillary column (50 m × 0.5 mm I.D.) statically coated with SE52 (2 mg/ml). This system was equipped with the same thermodesorption system as the GC–MS apparatus.

RESULTS

Blank analyses

It has been established that artefacts may be formed during adsorption sampling on porous polymers such as Tenax GC or XAD-2[6,7]. In order to check the sampling procedure, the sampling flask was flushed with helium (0.5 l/min, 10 min). A conditioned adsorption tube was then connected, and 5 l of helium gas were sampled through the system. As can be seen from Fig. 2 no artefacts were detected under these conditions. This does not conflict with literature results because artefact formation occurs primarily during sampling at elevated temperatures (more than 100°C) and in oxidizing atmospheres. Besides, according to Hanson *et al.*[6] the major degradation product of Tenax GC is 2,6-diphenylquinone, a high-boiling compound (M.W. 260) that will probably not desorb from Tenax GC under the conditions used in the present study (maximum desorption temperature 220°C).

Identification of volatiles in raw materials

In a first series of experiments, the volatiles present in the head space of raw materials were identified. These raw materials included: distilled water (100 ml); phosphate rock (20 g) and distilled water (100 ml); hydrochloric acid (50 ml, 36 *N*) and distilled water (100 ml). In each case 5 l of helium were used as transfer gas. Results of the GC–MS analyses of these samples are presented in Table I, and a typical

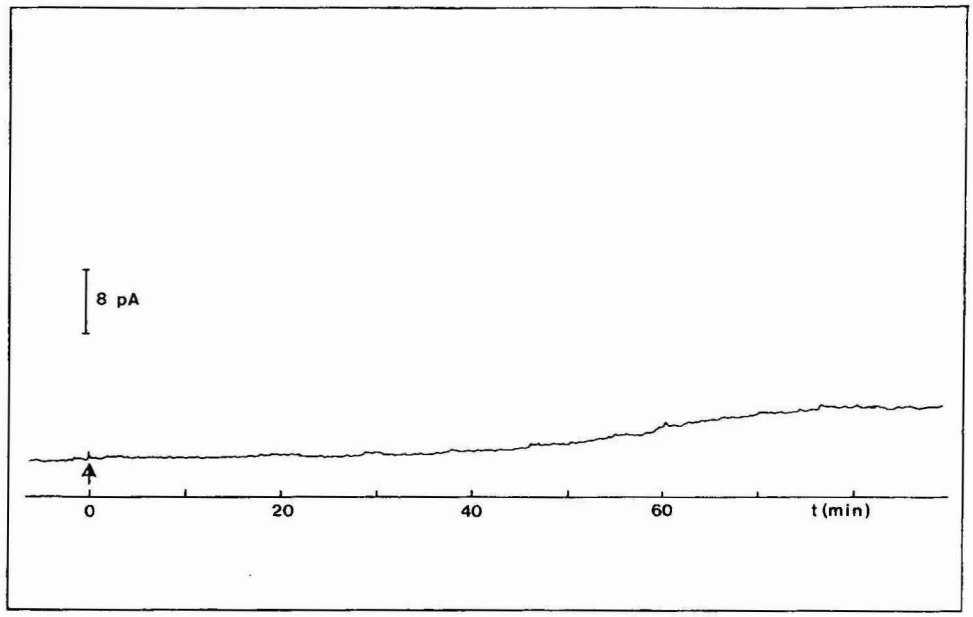

Fig. 2. Chromatogram of the blank GC–MS analysis. Temperature programme, linear from 20°C at 4°C/min.

chromatogram is shown in Fig. 3. As can be seen, minor amounts of some frequently occurring organics were detected. Based on the experimentally determined flame ionization detector response for benzene (1 pA for 2.4 ng of benzene), it was calculated that head-space concentrations of individual organics evolved from the raw materials were less than 5 ppb (v/v).

TABLE I

RESULTS OF THE GC–MS IDENTIFICATION OF VOLATILES IN THE HEAD SPACE OF THE RAW MATERIALS

Compound	*Distilled water*	*Phosphate rock*	*Water plus HCl*	*Water plus H_2SO_4*
1 Acetone	×	×	×	×
2 Pentene				×
3 Dichloromethane	×			×
4 2-Methylpentane				×
5 3-Methylpentane				×
6 Chloroform	×			×
7 Benzene	×	×	×	×
8 Heptane				×
9 Toluene	×	×	×	×
10 Tetrachloroethene	×			
11 Ethylbenzene	×			×
12 *m,p*-Xylene	×			×
13 *o*-Xylene	×			×

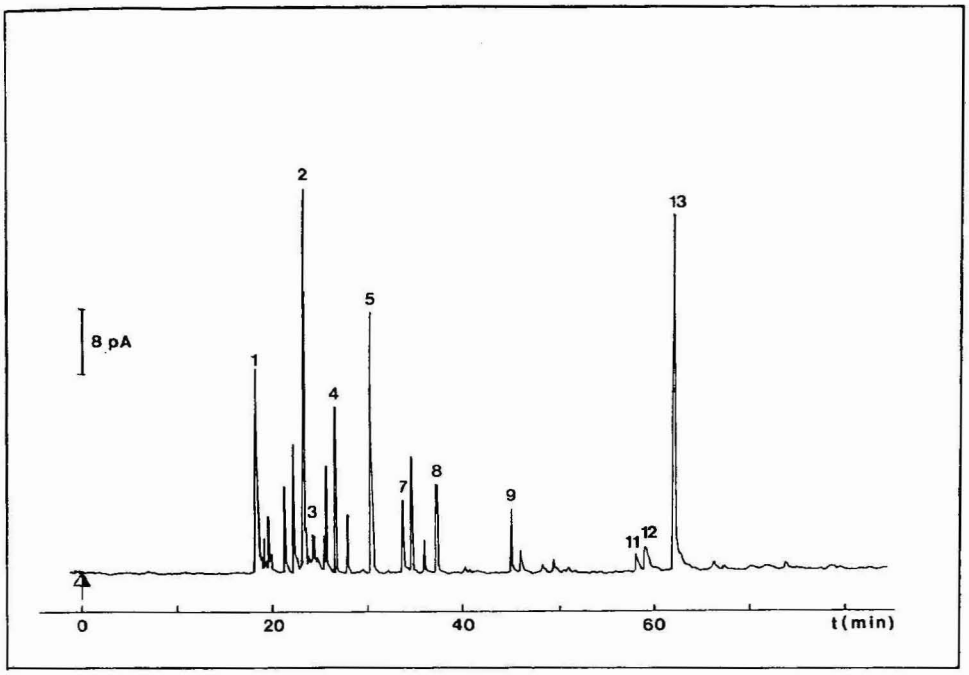

Fig. 3. Chromatogram of the GC–MS analysis of one of the raw materials (sulphuric acid–distilled water). Peak numbers refer to Table I.

Identification of volatiles in acid–treated phosphate rock

A typical chromatogram of the GC–MS analysis of the volatiles liberated during acid treatment of phosphate rock sample is given in Fig. 4. Results of the identification are given in detail in Tables II and III. In order to have a good picture of

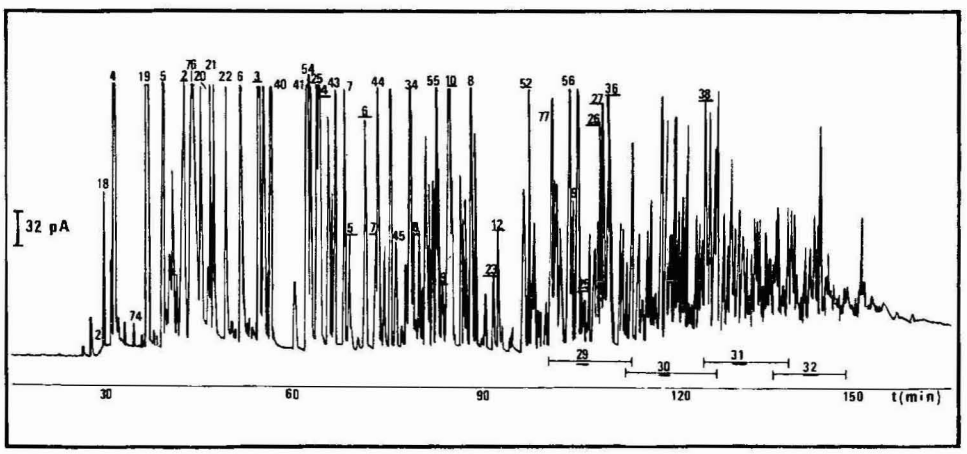

Fig. 4. Chromatogram of the identification of volatiles liberated during treatment of phosphate rock with hydrochloric acid. Temperature programme, linear from 20°C at 2°C/min to 220°C. Normal digits refer to Table II, underlined digits refer to Table III.

TABLE II

NON-ORGANO SULPHUR COMPOUNDS IDENTIFIED BY GC–MS IN THE HEAD SPACE OF ACID-TREATED PHOSPHATE ROCK

Ip = Kovats retention index. In column 1, symbols have the following meaning: S, peak height less than 32 pA; M, peak height between 32 and 320 pA; L, peak height greater than 320 pA. In column 2, × means that the retention index was confirmed by the injection of an authentic sample; n.d. not determined.

Compound	*Ip*	*Phosphate rock treated with*		*1*	*2*
		H_2SO_4	*HCl*		
(I) Silicon compounds					
(1) Silicon tetrafluoride	<400	×	×	S	
(2) Dimethyl silicon difluoride	<400	×	×	S	
(3) Trimethyl silicon fluoride	416	×	×	S	
(II) Hydrocarbons					
(A) Linear aliphatic					
(4) Butane	400	×	×	L	×
(5) Pentane	500	×	×	L	×
(6) Hexane	600	×	×	L	×
(7) Heptane	700	×	×	L	×
(8) Octane	800	×	×	M	×
(9) Nonane	900	×	×	M	×
(10) Decane	1000	×	×	M	×
(11) Undecane	1100	×	×	M	×
(12) Dodecane	1200	×	×	M	×
(13) Tridecane	1300	×	×	M	×
(14) Tetradecane	1400	×	×	M	×
(15) Pentadecane	1500	×	×	S	×
(16) Hexadecane	1600	×	×	S	×
(17) Heptadecane	1700	×	×	S	×
(B) Branched aliphatic					
(18) 2-Methylpropane	<400		×	M	
(19) 2-Methylbutane	467	×	×	M	×
(20) 2,3-Dimethylbutane	560	×	×	L	×
(21) 2-Methylpentane	566	×	×	L	×
(22) 3-Methylpentane	580	×	×	L	×
(23) 2,2,3-Trimethylbutane	627	×		M	×
(24) 2,4-Dimethylpentane	667	×	×	M	×
(25) 3-Methylhexane	672	×	×	L	×
(26) 2,5-Dimethylhexane	728	×		M	×
(27) 2,3-Dimethylhexane	760		×	M	×
(28) 3-Methylheptane	766	×	×	M	×
(29) 3,4-Dimethylhexane	770	×	×	M	×
(30) 2-Ethylhexane	775		×	M	×
(C) Aliphatic unsaturated					
(31) 1-Butene	<400		×	S	×
(32) 2-Methylpropene	409		×	S	×
(33) 2-Butene (*trans*)	421		×	S	
(34) 3-Butene (*cis*)	456		×	S	
(35) 1-Pentene	485	×		L	×
(36) 2-Methyl-1-pentene	590	×		M	
(37) Methylcyclopentene	650	×		S	
(38) 1-Propylcyclohexene	n.d.	×		S	

TABLE II *(continued)*

Compound	*Ip*	*Phosphate rock treated with*		*1*	*2*
		H_2SO_4	*HCl*		
(D) Aliphatic cyclic					
(39) Cyclopentane	572	×		M	×
(40) Methylcyclopentane	628	×	×	L	×
(41) Cyclohexane	666	×	×	L	×
(42) 1,3-Dimethylcyclopentane (*cis*)	686	×	×	M	×
(43) 1,3-Dimethylcyclopentane (*trans*)	690	×	×	L	×
(44) Methylcyclohexane	725	×		L	
(45) Ethylcyclopentane	734	×	×	L	
(46) 1,2,3-Trimethylcyclopentane	740	×	×	M	
(47) 1,2,3-Trimethylcyclopentane	747	×	×	S/M	
(48) 1,2-Dimethylcyclohexane	785	×	×	S	
(49) 1,2-Methylethylcyclopentane	792	×	×	M	
(50) 1,2-Methylethylcyclopentane	794	×	×	M	
(51) Isopropylcyclopentane	810	×		M	
(52) Ethylcyclohexane	840	×	×	L	
(53) Isopropylcyclohexane	908	×		L	
(E) Aromatic					
(54) Benzene	666	×	×	L	×
(55) Toluene	771	×	×	L	×
(56) Ethylbenzene	870	×	×	L	×
(57) *m,p*-Xylene	876	×	×	L	×
(58) *o*-Xylene	900	×	×	L	×
(59) Isopropylbenzene	933	×		M	×
(60) Propylbenzene	964	×	×	L	×
(61) 1-Ethyl-3-methylbenzene	969	×		M	×
(62) 1-Ethyl-4-methylbenzene	970	×	×	M	×
(63) 1,3,5-Trimethylbenzene	976	×	×	M	×
(64) 1-Ethyl-2-methylbenzene	988	×		M	×
(65) 1,2,4-Trimethylbenzene	1001	×	×	M	×
(66) 1,2,3-Trimethylbenzene	1033	×		M	×
(67) Benzene-C_4	n.d.	4 isomers	3 isomers		
(68) Indane	n.d.	×		S	
(69) Ethylindane	1210	×		M	
(70) Benzene-C_6	1238	×		S	
(71) Benzene-C_5	1302	×		S	
(72) 2-Methylnaphthalene	1327	×		S	
(73) 1-Methylnaphthalene	1345	×		S	

the composition of the mixture of volatiles, compounds were classified according to their chemical nature and then in order of elution from the GC column. It is indicated in the tables whether or not the identification was based on MS alone or on the combination of mass spectra and retention data, obtained either from the literature or by analysing authentic samples. No quantitative determinations were performed but, based on peak heights, an indication of the amount of compounds is given.

Since, in the industrial process, phosphate rock is usually treated with sulphuric acid, this acid was also used in the first experiments. GC–MS analyses of the head-space volatiles revealed the presence of a few silicon fluorides as well as numerous hydrocarbons and organic sulphur compounds. Since it was not clear whether the

TABLE III

ORGANOSULPHUR COMPOUNDS IDENTIFIED IN THE HEAD SPACE OF ACID-TREATED PHOSPHATE ROCK

For the meaning of the symbols see Table II.

Compound	*Ip*	*Phosphate rock treated with*		*1*	*2*
		H_2SO_4	*HCl*		
(I) Mercaptans					
(1) Methanethiol	n.d.	(×)		L	
(II) Sulphides					
(A) Acyclic					
(2) Dimethyl sulphide	527	×	×	L	×
(3) Ethyl methyl sulphide	617	×	×	L	×
(4) Isopropyl methyl sulphide	676	×	×	L	×
(5) Diethyl sulphide	704	×	×	M	×
(6) Methyl propyl sulphide	717	×	×	M	×
(7) Methyl *tert.*-butyl sulphide	725		×	S	
(8) Ethyl isopropyl sulphide	754	×	×	S	
(9) Methyl isobutyl sulphide	776		×	S	
(10) Ethyl propyl sulphide	782	×	×	L	
(11) Methyl *sec.*-butyl sulphide	805	×		S	
(12) Methyl butyl sulphide	820	×	×	M	
C-6 sulphides					
(13) Isomer a	845	×	×	S/M	
(14) Isomer b	849		×	S	
(15) Isomer c	857	×	×	S/M	
(16) Isomer d	876	×	×	S/M	
(17) Dipropyl sulphide	877	×	×	S/M	×
(18) Isomer f	886		×	M	
C-7 sulphides					
(19) Isomer a	n.d.	×		S	
(20) Isomer b	n.d.	×	×	S/M	
(21) C-8 sulphide	n.d.	×		S	
(22) C-10 sulphide	1296	×		S	
(B) Cyclic					
(23) Thiacyclopentane	815	×	×	S	×
(24) Thiacyclohexane	860	×	×	M	×
(25) 2-Methylthiacyclopentane	879	×	×	S	
(26) 2,5-Dimethylthiacyclopentane	890	×	×	M	
(27) 2,5-Dimethylthiacyclopentane	895	×	×	M	
(28) 2-Methylthiacyclohexane	910	×	×	M	×
(29) Cyclic isomers with structure $C_6H_{12}S$	890–1000	×	×	M-S	
(30) Cyclic isomers with structure $C_7H_{14}S$	950–1050	×	×	M-S	
(31) Cyclic isomers with formula $C_8H_{16}S$	1000–1100	×	×	M-S	
(32) Cyclic isomers with formula $C_9H_{18}S$	1050–1250	×	×	M-S	
(33) Cyclic isomers with formula $C_{10}H_{20}S$	1200–1350	×	×	M-S	
(III) Disulphides					
(34) Dimethyl disulphide	752	×	×	L	×
(35) Ethyl methyl disulphide	872	×		M	×
(36) Isopropyl methyl disulphide	899	×	×	M	
(37) Diethyl disulphide	903	×	×	M	×

TABLE III *(continued)*

Compound	*Ip*	*Phosphate rock treated with*		*1*	*2*
		H_2SO_4	*HCl*		
(IV) Thiophenes					
(38) Trimethylthiophene	n.d.	×		S	
(39) Thiophene-C_4	n.d.	3 isomers	1 isomer	S	
(40) Thiophene-C_5	1209	×		S	
(41) Thiophene-C_6	1279	×	×	S	

nature of the mineral acid was determining the identity of the head-space volatiles, a number of treatments with hydrochloric acid were also performed; as can be seen from Tables II and III, only minor changes in the composition of the head space were observed. So it was concluded that the nature of the mineral acid was not influencing the identity of the head-space volatiles.

Three silicon compounds were identified in the head space of acid-treated phosphate rock. Silicon tetrafluoride was easily recognized by the presence of an intense fragment at *m/e* 85 and isotopic peaks at *m/e* 86 and *m/e* 87. Dimethyl silicon difluoride and trimethyl silicon fluoride showed characteristic peaks at *m/e* 81 and *m/e* 77, respectively. Silicon tetrafluoride and hydrogen fluoride are well-known by-products of phosphate treatment. To prevent the emission of these compounds, industrial gases are usually scrubbed with water, which yields a diluted orthosilicic acid solution. Hydrogen fluoride was not detected during the GC–MS analyses, probably because of its low molecular weight.

Assuming the same detector response for all volatiles, 75% of the mixture consisted of hydrocarbons. Linear, branched, unsaturated, and cyclic aliphatic and aromatic hydrocarbons with boiling points ranging from 0 to 300°C were detected. The identification of these compounds by their mass spectra was generally straightforward, although for isomeric structures retention data were used to confirm the interpretation of the spectra.

All other volatiles in the mixture were organosulphur compounds, belonging to different classes: a mercaptan, acyclic and cyclic sulphides, disulphides and alkyl thiophenes. Methylmercaptan was detected in two of the nine samples of phosphate rock treated with sulphuric acid and not in samples treated with hydrochloric acid. Therefore this compound seems to be present rather sporadically.

Acyclic sulphides up to diethyl sulphide were identified by MS alone. Owing to the rapidly increasing number of possible isomeric structures, the combination of mass spectra and retention data was necessary to identify higher sulphides. Cyclic sulphides showed rather prominent molecular ions in the series with *m/e* 88 + 14N. Alkyl-substituted thiacycloalkanes often produce base peaks by splitting of the alkyl branch: thus thiacyclopentanes produce a base peak at *m/e* 87 and thiacyclohexanes at *m/e* 101. The elimination of an alkene fragment from the ring structure was also observed, and resulted in a typical fragment at *m/e* 74 ($C_3H_6S^+$). Throughout the chromatograms cyclic structures with formulae from C_4H_8S to $C_{10}H_{20}S$ were detected. In most cases it was not possible to indicate the exact isomer because of the

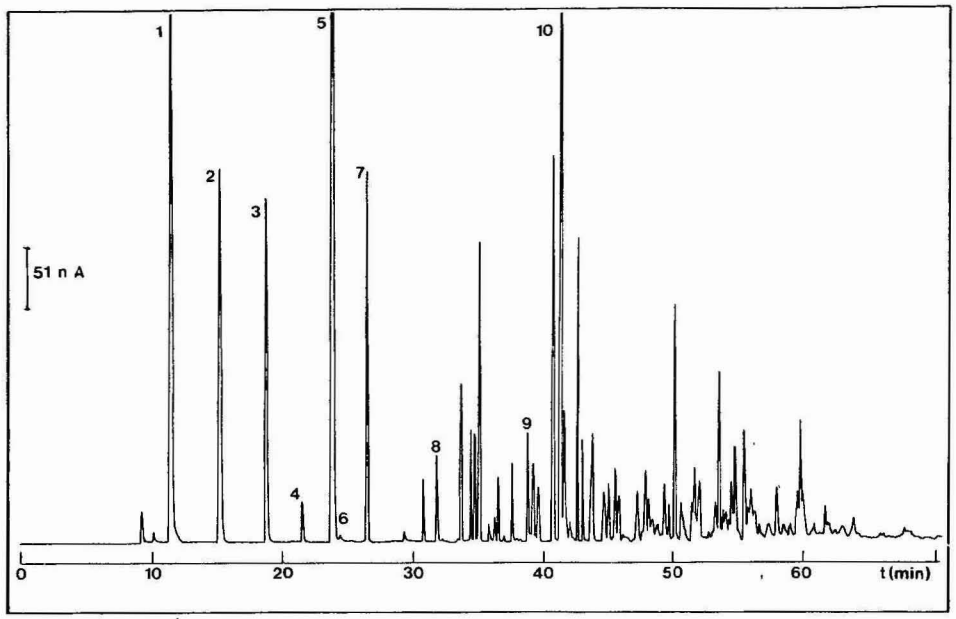

Fig. 5. Chromatogram of the GC–FPD analysis of volatiles in the head space of acid-treated phosphate rock. Temperature programme: linear from 20°C at 2°C/min. Peaks: 1 = dimethyl sulphide; 2 = ethyl methyl sulphide; 3 = isopropyl methyl sulphide; 4 = diethyl sulphide; 5 = dimethyl disulphide; 6 = isopropyl ethyl sulphide; 7 = ethyl propyl sulphide; 8 = thiacyclopentane; 9 = thiacyclohexane; 10 = isopropyl methyl disulphide.

great numbers of possible isomers (*e.g.* a cyclic sulphide with formula $C_7H_{14}S$ and with at least a five ring gives 59 isomers) and because of the lack of reference compounds.

Four disulphides and some alkyl thiophenes were identified in the head space of phosphate rock treated with sulphuric acid or hydrochloric acid.

In order to confirm GC–MS results, 2-methylthiacyclohexane, three disulphides and three asymmetric sulphides were synthesized. The mass spectra of the synthesized compounds were in good agreement with the spectra of the compounds in the samples. The following retention indices were calculated for the synthesized compounds: ethyl methyl sulphide, 617; isopropyl methyl sulphide, 676; methyl propyl sulphide, 717; 2-methylthiacyclohexane, 910; ethyl methyl disulphide, 872; isopropyl methyl disulphide, 899; methyl propyl disulfide, 912.

Finally, to obtain a chromatogram in which the interference of hydrocarbons and organic sulphur compounds would be at a minimum, five samples were analysed by GC–FPD; a typical chromatogram is given in Fig. 5. The GC–FPD apparatus was not coupled with the mass spectrometer. Therefore dimethyl sulphide, dimethyl disulphide and isopropyl methyl disulphide, which were the most abundant organosulphur compound peaks in the GC–MS analyses, were used to calculate the retention indices of other organosulphur compounds in the GC–FPD chromatograms. These chromatograms confirmed that numerous sulphur compounds are present in the head space of acid-treated phosphate rock and that, within this class of com-

pounds, dimethyl sulphide, dimethyl disulphide, isopropyl methyl disulphide, ethyl methyl sulphide and ethyl propyl sulphide are the most abundant compounds. As far as the abundance of the different classes of organosulphur compounds is concerned, the following figures were measured (as a percentage of the total FID-integrated signal): acyclic sulphides, 15%; cyclic sulphides, 6.7%; disulphides, 2.7%; and thiophenes, 0.5%.

CONCLUSION

GC–MS identification of volatiles in the head space of acid-treated phosphate rock revealed the presence of some organosilicon compounds and numerous hydrocarbons and organosulphur compounds. A mercaptan, acyclic and cyclic sulphides, disulphides and alkylthiophenes were identified. The presence of organic compounds in phosphate rock is in accordance with the generally accepted theory that phosphogenic events are associated with a high organic productivity[8].

Since the human olfactory system is about 1000 times more sensitive for sulphur compounds than for hydrocarbons, the sulphur compounds identified are probably responsible for the odour problems caused by acid treatment of phosphate rock.

REFERENCES

1 J. M. McLellan, in J. A. Kent (Editor), *Riegel's Handbook of Industrial Chemistry*, Van Nostrand Reinhold, New York, Cincinnati, Toronto, London, Melbourne, 8th ed., 1983, Ch. 7, p. 236.
2 H. R. Van Langenhove, F. A. Van Wassenhove, J. K. Coppin, M. R. Van Acker and N. M. Schamp, *Environ. Sci. Technol.*, 16 (1982) 883.
3 E. V. Whitehead, R. A. Dean and F. A. Fidler, *J. Am. Chem. Soc.*, 73 (1951) 3632.
4 D. T. McAllen, T. V. Cullum, R. A. Dean and F. A. Fidler, *J. Am. Chem. Soc.*, 73 (1951) 3627.
5 A. I. Vogel, *A Textbook of Practical Organic Chemistry*, Longmans, London, 3rd ed., 1961, p. 496.
6 R. L. Hanson, C. R. Clark, R. L. Carpenter and C. H. Hobbs, *Environ. Sci. Technol.*, 15 (1981) 701.
7 R. L. Hanson, C. R. Clark, R. L. Carpenter and C. H. Hobbs, in L. H. Keith (Editor), *Identification and Analysis of Organic Pollutants in Air*, Butterworth, Boston, London, Sydney, Wellington, Durban, Toronto, 1984, p. 79.
8 P. J. Cook and J. H. Shergold, *Nature (London)*, 308 (1984) 231.

Journal of Chromatography, 351 (1986) 77–89
Elsevier Science Publishers B.V., Amsterdam — Printed in The Netherlands

CHROM. 18 166

PROCEDURES FOR TWO-DIMENSIONAL ELECTROPHORETIC ANALYSIS OF NUCLEAR PROTEINS

THIERRY RABILLOUD*, MICHELLE HUBERT and PHILIPPE TARROUX
Laboratoire de Zoologie, Ecole Normale Supérieure, Paris (France)
(First received July 22nd, 1985; revised manuscript received September 6th, 1985)

SUMMARY

A series of methods designed for electrophoresis of nuclear proteins is described. They deal with the low solubility of many nuclear proteins and with the presence of large amounts of nucleic acids. These were eliminated by enzymatic digestion, centrifugation, partition or precipitation. A combination of RNAse digestion and centrifugation is the method of choice when proteolysis is low. In the opposite case, precipitation or partition methods are preferred, at the expense of precipitation of some proteins. When the nuclear RNA content is low, centrifugation in an Airfuge is the simplest and the most efficient method, superseding the widely used S1 nuclease method.

INTRODUCTION

Nuclear proteins have been studied extensively because of their relevance to genetic regulation. One-dimensional electrophoretic techniques were first used in numerous studies on the variations of these proteins related to different genetic expression schemes[1,2]. An increase in resolution seemed necessary and two-dimensional separations were introduced by Busch and co-workers[3]. These systems used electrophoresis under two sets of conditions, but the separation criteria were linked, so that the proteins were displayed principally on the diagonal, providing therefore a small increase in resolution. Systems using two independent separation criteria (p*I* and molecular mass) were introduced by Barret and Gould[4], and their use became widespread after the pioneering work of O'Farrell[5]. The first application of this system to nuclear protein was reported by Peterson and Mc Conkey[6], and numerous other studies have followed[7–10]. However, good quality and reproducible gels have been obtained in only a few cases[6,10], most of the gels published exhibiting a marked background and considerable streaking[8]. Moreover, reproducibility is generally poor[11]. These phenomena are caused by the low solubility of most nuclear proteins and by high levels of nucleic acids, which induce numerous artefacts in two-dimensional electrophoresis[12].

Our aim in this work is to describe techniques giving a significant increase in resolution and in the reproducibility of the patterns obtained.

0021-9673/86/$03.50

MATERIALS AND METHODS

Cell culture

This work was carried out on *Drosophila* Kc cells[13]. A diploid subclone, 8-9K, was kindly provided by G. Echalier and M. Bestbelpomme, and was used throughout this study. The cells were grown on Echalier's D22 medium and plated every 5 days. The lag phase lasts approximately 1 day and the growth phase 3 days. Cells remain wholly viable for over a week after the plating (*ca.* 12 days). The radiolabelling of cells was carried out as described[14] or by labelling for 48 h in complete medium with 100 μCi/ml [^{35}S]methionine (> 800 Ci/mmol, Amersham).

Cell fractionation

The nuclei were prepared by a modification of previously described methods[15]. Briefly, cells were disrupted in hypotonic medium (0.1 *M* sucrose; 25 m*M* 4-(2-hydroxyethyl)-1-piperazineethanesulphonic acid (HEPES)–sodium hydroxide; 10 m*M* $MgCl_2$) containing 0.5% Nonidet P-40. The homogenate was centrifuged for 25 min at 30 000 *g* over a 2-ml cushion of 1.8 *M* sucrose in the same buffer. The resulting pellet of nuclei contained almost no cytoplasmic tags when examined by phase-contrast microscopy.

Protein radiolabelling

The proteins were labelled either *in vivo* by [^{35}S]methionine incorporation or *in vitro* by reductive methylation using formaldehyde and tritiated sodium tetrahydroborate as described for example by Kuhn and Wilt[16]. In some experiments reductive methylation was performed as described by Jentoft and Dearborn[17] but using cold formaldehyde and tritiated sodium cyanoborohydride (30–150 Ci/g, Amersham).

Sample preparation

The samples were freed from nucleic acids and prepared for two-dimensional electrophoresis by different methods, which can be classified into four types.

Enzymatic methods. These methods use either S1 nuclease, as described by Zechel and Weber[18], or a cocktail of DNAse and RNAse. For maximum enzymatic activity, digestion was performed at 25°C for 30 min in a non-denaturing medium. This medium contains 2 *M* sodium chloride for dissociating the chromatin, 2 m*M* magnesium chloride and 25 m*M* HEPES buffer pH 7.5. DNAse and RNAse are each added at 5 μg per 100 μg DNA. In some experiments, RNAse alone was used, DNA being eliminated by another method. The digestion buffer comprised 25 m*M* HEPES buffer, 5 m*M* EDTA and 0.35 *M* sodium chloride. In all the cases, 1 m*M* phenylmethanesulphonyl fluoride (PMSF) was used as a protease inhibitor. The digestion was stopped and the proteins separated by precipitation with trichloroacetic acid (TCA). The sample was resuspended in 100 μl of modified O'Farrell lysis buffer and loaded onto the first dimension gel.

Centrifugation methods. In these methods, the nuclear pellet was resuspended in modified O'Farrell buffer containing 3-(3-cholamidopropyl)dimethylammonio-1-propanesulphonate (CHAPS), lysolecithin or lecithin as detergent. The solution was centrifuged to yield pellet particles with a sedimentation coefficient greater than 7S. The supernatant was carefully collected and loaded onto the first dimension gel.

Partition methods. T is method is an adaptation of LeStourgeon's method[19] for two-dimensional electi ophoresis. Briefly, the nuclear pellet was dissolved in HEPES buffer (100 m*M* p I 7.5) containing 35 m*M* EDTA, 2.5% sodium dodecyl sulphate (SDS) and 5% m rcaptoethanol. The viscosity was reduced by pipetting and the solution heated at 00°C for 2 min. The insoluble material was then pelleted at 10 000 *g* for 10 min. T e supernatant was collected and one volume of water-saturated phenol was adde . The extraction was carried out at room temperature for 15 min and the phases wer separated by centrifugation (10 000 *g* for 10 min). The phenol phase was collecte and ten volumes of SDS-extracting solution, acetone–tributylamine–acetic acid– vater (89:5:5:1, v/v/v/v), were added[20]. After 1 h at −20°C, the protein precip tate was collected by centrifugation, washed once with diethyl ether and thoroug ly dried. The pellet was resuspended in lysis buffer and used in two-dimensional el ctrophoresis.

Precipitation metho . The nuclear pellet was redissolved in 9.5 *M* urea containing 2% Nonidet P-40, 0 m*M* Tris–HCl pH 7.8 and 5% mercaptoethanol. A 0.1 volume of 0.2 *M* lanthanu n trichloride in water was added, and the solution left at room temperature for 1 h. It was then centrifuged at 10 000 *g* for 30 min. The supernatant was collected and 0.1 volume of ampholines was added. This mixture was used for two-dimensional electrophoresis.

In another method, the nuclear pellet was dissolved in 100 µl of HUC buffer (25 m*M* HEPES buffer pH 7.5, 8 *M* urea, 1 *M* calcium chloride). The mixture was centrifuged for 1 h at 30 p.s.i. in an Airfuge ultracentrifuge. The supernatant was collected, diluted with water to 0.7 *M* urea concentration and the proteins were precipitated by 20% TCA. The precipitate was collected by centrifugation, rinsed with diethyl ether and redissolved in modified O'Farrell lysis buffer for loading.

Two-dimensional electrophoresis

Two-dimensional electrophoresis was performed essentially as described by O'Farrell, with the following alterations. For isoelectric focusing, the electrolyte molarity was raised to 50 m*M* and the voltage applied to 9500 V h, as described by Duncan and Hershey[21]. The sample was always applied at the basic end, except in a few control experiments. In some experiments, Nonidet P-40 was replaced by CHAPS in the lysis buffer and in the gel mixture, as suggested by Perdew *et al.*[22]. The second dimension gel was a linear 7–14% acrylamide gradient gel. As the proteins were radiolabelled, detection was performed by fluorography[23] using a dimethyl sulphoxide–2,5-diphenyloxazole (DMSO–PPO) procedure[23]. The impregnated gels were generally exposed for 4 days at −80°C on Kodak X-Omat S film.

RESULTS AND DISCUSSION

Two-dimensional electrophoretic analysis of nuclear proteins is very difficult. The poor solubility of many of these proteins leads to precipitation artefacts as shown in Fig. 1. Moreover, the great amount of material precipitated at the sample application point precludes all quantitative analysis of the gels. To solve this problem, we tried to increase the solubilizing power of the medium and to lower the amount of material necessary to obtain a good pattern, *i.e.*, to use a detection method with the highest sensitivity. Silver staining was not sensitive enough and detected the nucleic

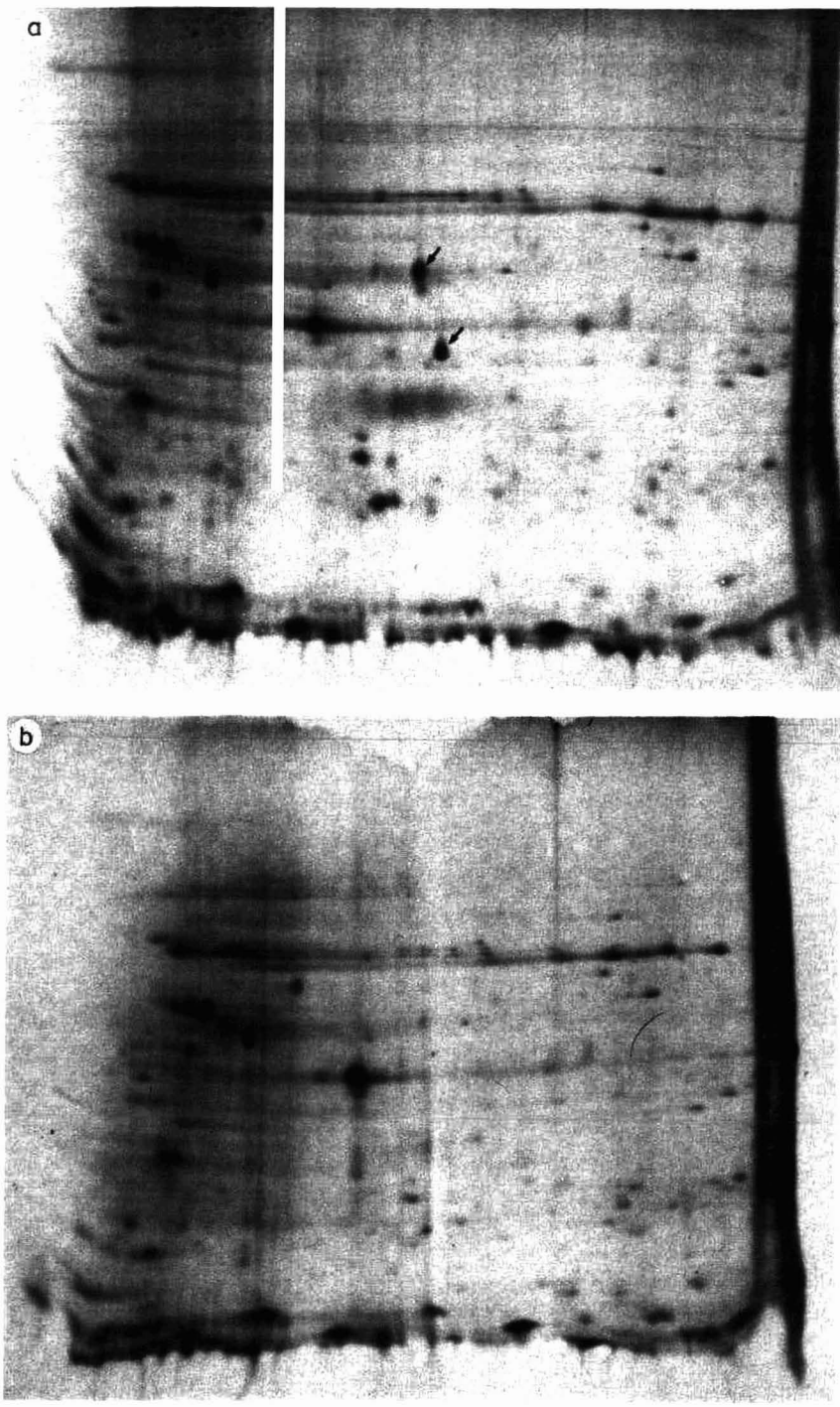

Fig. 1. Two-dimensional electrophoresis of nuclear proteins. After *in vivo* labelling with radioactive methionine, the nuclear proteins were freed from DNA and RNA by lanthanum precipitation. 150 (a) and 300 μg (b) of proteins were loaded onto the first dimension gel. The proteins which have precipitated in the most heavily loaded gel are indicated by arrows. All the gels are displayed with the acidic end on the left, and the high molecular weights at the top.

acids, causing an increase background (data not shown). We therefore chose to radiolabel the proteins. Ra iolabelling by incorporation of a radioactive amino acid was not convenient for sev ral reasons. First, labelling with a single amino acid such as [^{35}S]methionine does n t allow the detection of all the proteins. Secondly, high efficiency labelling method require depletion of the culture medium in the labelling amino acid. This may cau metabolic perturbation to the cells and therefore artefactual changes of the nuc ar protein patterns. Thirdly, the incorporated radioactivity may cause irradiatio damage to the cells, and changes in the protein patterns have already been observe [24]. This is especially true of long-term labelling, which is required for maximum spe ific activity[25].

We therefore chose n *in vitro* labelling method. Only a few methods can be applied to two-dimensio l electrophoretic analysis. Among them, we chose the method described by Kuh and Wilt[16], but we used a tritiated borohydride with a higher specific activity (80 nstead of 20 Ci/mmol). Specific activities as high as 10^6 cpm per μg protein can be reached. This allows the detection of over 1000 protein spots with a 4-days exposu e and a 25-μg protein load (see Fig. 4a for an example). An additional advantage of this method lies in its general use even when radioactive amino acid incorporation cannot be used, as with whole organs.

We then searched for a dissociating medium which would allow maximum solubilization of the nuclear proteins. A variety of detergents and chaotropics were tested, since O'Farrell's medium (Nonidet P-40 and urea) is known to be insufficient for hydrophobic[22] and nuclear proteins[26]. As detergents, we tried lecithins, lysolecithins[26] and sulphobetaines[27], but their low solubility in urea forced us to use Nonidet P-40 as additional detergent, which decreased the solubilization power. On the other hand, the use of CHAPS, which is a peculiar sulphobetaine, led to considerable improvement in the solubilization step[22]. In some non-equilibrium pH gradient gel electrophoresis (NEPHGE) experiments (Fig. 2), histones are clearly shown as streaks at the basic end of the gels (as in ref. 26) and no precipitate can be seen at the sample application point on the acidic side of the gel, indicating a total solubilization of the proteins. However, the chromatin is not fully dissociated under these conditions, and some proteins are eliminated with the nucleic acids. It is our feeling that additional research in the field of zwitterionic detergents will lead to media having a still higher solubilizing power, leading to full chromatin dissociation.

We also tested chaotropics other than urea. Preliminary experiments showed that tetramethylurea was a quite promising agent, and the dissociating power of a mixture of sulphobetaines (3-N-tetradecyl-N,N-dimethylammonio-1-propanesulphonate, SB 3-14) and tetramethylurea is comparable to that of boiling SDS (Table I). However, tetramethylurea is not compatible with acrylamide polymerization. While this work was in progress, the synthesis of modified acrylic derivatives compatible with organic solvents was reported[28]. This also should lead to new isoelectric focusing media with much higher performances than the current ones.

The other major problem in nuclear protein analysis lies in the high level of nucleic acids which strongly interfere with the isoelectric focusing dimension. Their level must thus be reduced, but the strong affinity of many nuclear proteins for the nucleic acids makes this reduction difficult if minimum losses in protein are expected. The first method used for the elimination of nucleic acids was devised by Peterson and Mc Conkey[6] and used digestion by S1 nuclease in the presence of SDS and urea.

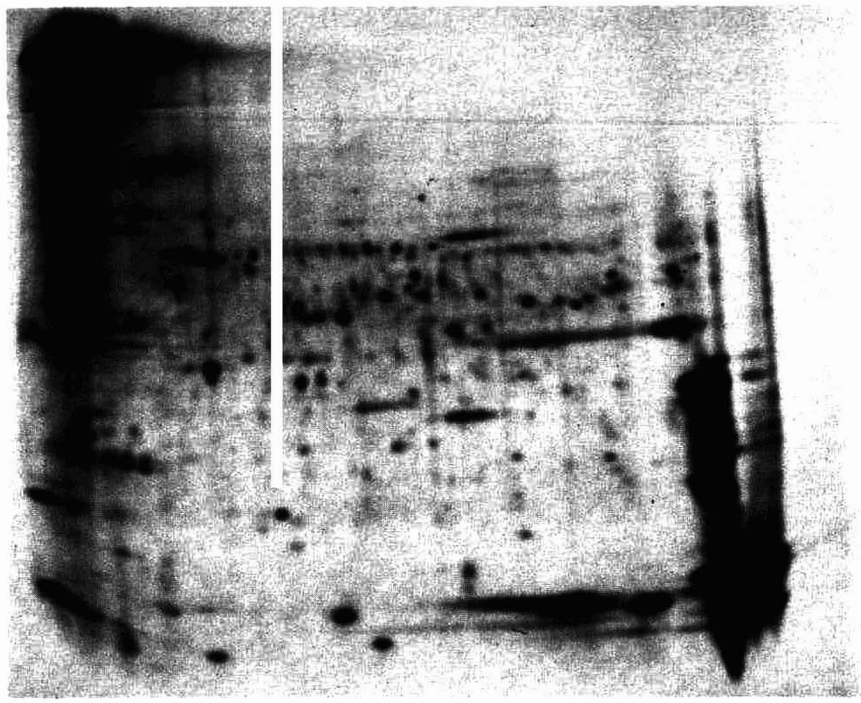

Fig. 2. NEPHGE analysis of nuclear proteins labelled *in vitro* by reductive methylation, 6000 V h were used for the electrofocusing. Histones migrate as streaks at the basic end of the gel.

TABLE I

COMPARISON OF THE EFFICIENCIES OF DIFFERENT AGENTS AS DISSOCIATING MEDIA FOR CHROMATIN

After radioactive labelling as described under Materials and methods, the nuclei were suspended at a DNA concentration of 0.5 mg/ml in the different media. The suspension was centrifuged to pellet all the molecules having a sedimentation coefficient higher than 7S. The supernatant was carefully decanted and the percentage of cpm recovered in the supernatant was taken as the yield. 2-ME = 2-Mercaptoethanol.

Solubilization medium	*Recovery of protein (%)*
2.5% SDS, 5% 2-ME, 100°C, 3 min	>97
9.5 *M* Urea, 2% Nonidet P-40, 2% ampholines	50
9.5 *M* Urea, 2% CHAPS, 2% ampholines	80
2.5% SB 3-14, 5% 2-ME, 100°C, 3 min	25
50% (v/v) Tetramethylurea, 5% 2-ME, 2% ampholines	50
2% SB 3-14, 50% (v/v) tetramethylurea, 5% 2-ME, 2% ampholines	95

However, nuclear RNA is)adly eliminated by this method[18]. Moreover, the digestion is performed at high t :mperature, and the risk of carbamylation is greatly increased[7]. These drawbacks ead to variable results which are principally linked to the nuclear RNA content. In 'act, little emphasis has previously been placed on the importance of RNA in th streaking and background problems encountered when dealing with nuclear protei s. Our *Drosophila* cells have a high nuclear RNA content and were therefore an idea tool for such an investigation. We observed (Fig. 3) that RNA induces severe strea ing and background, comparable with those previously obtained with low mobilit group (LMG) protein preparations[8], which are devoid of DNA, but not of RNA. We therefore investigated several methods which can deal with large amounts of nu lear RNA and which are not subject to carbamylation artefacts. We first tried to get rid of both types of nucleic acids by ultracentrifugation[26]. This method comp etely eliminates DNA, but cannot reduce the RNA level to a reasonable extent (Fi . 4a, b). When using the urea–CHAPS medium already described, the yields are fai (*ca.* 80%) as shown in Table II. The fact that some RNA remains in the supernatan with the proteins may be correlated with the presence of small RNAs (snRNA) and with the presence of products of degradation of larger RNAs by the endogenous RNAses which remain active during the isolation of the

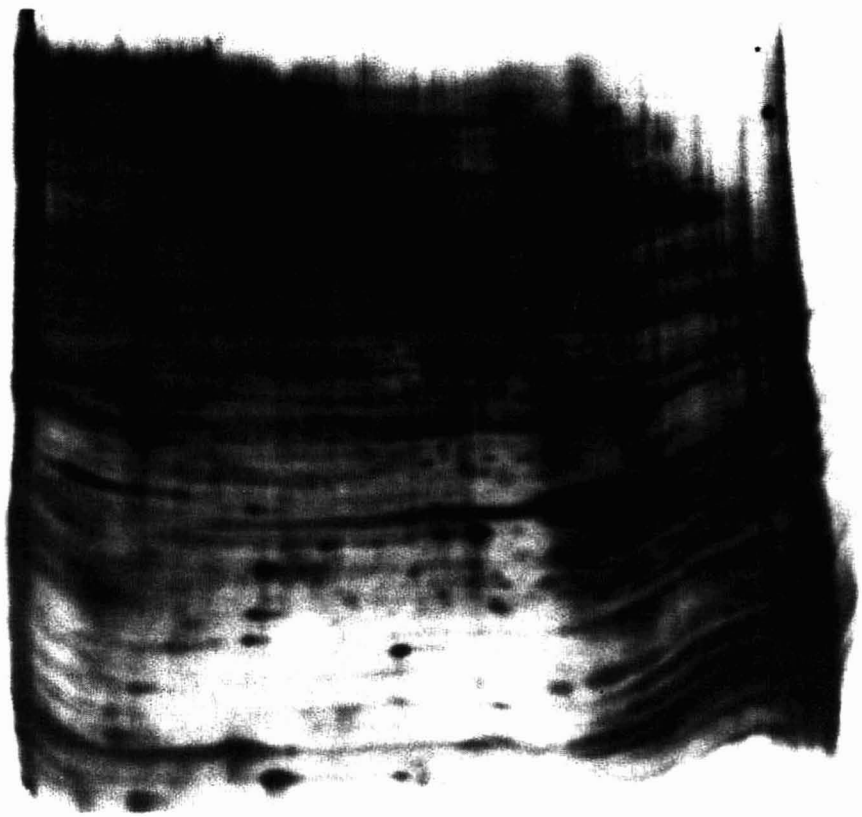

Fig. 3. Background induced by RNA in two-dimensional electrophoresis.

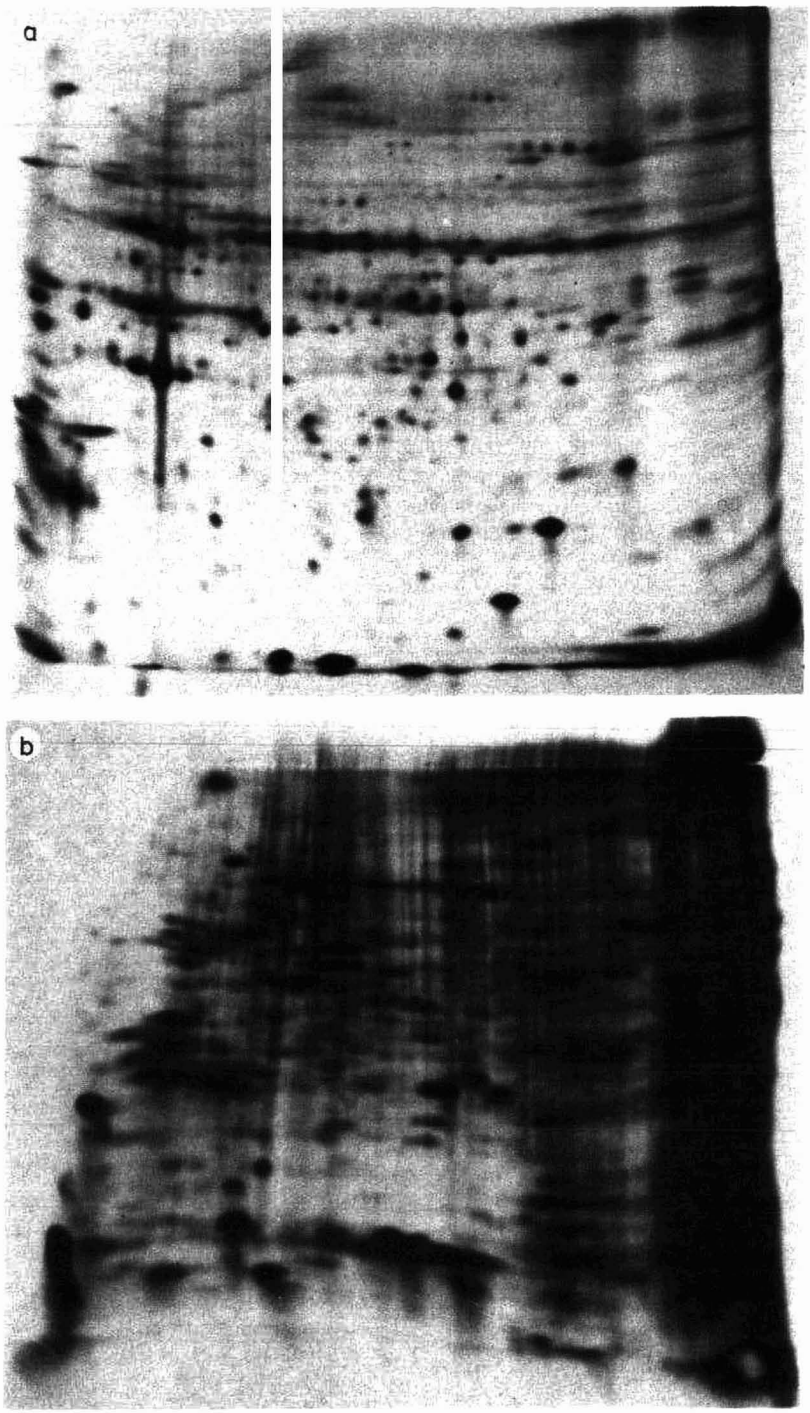

Fig. 4. Two-dimensional electrophoresis of nuclear proteins labelled *in vitro* by reductive methylation and freed from nucleic acids by centrifugation. (a) Pattern obtained from cells having a low RNA content; (b) pattern obtained from exponentially growing cells (high RNA content).

TABLE II

MAIN FEATURES OF THE DIFF :RENT METHODS OF ELIMINATION OF NUCLEIC ACIDS

The yield was determined as the pe :entage of cpm remaining just before the gel loading compared to the cpm obtained just after labelling. The qual y index was subjective and determined on exponentially growing cultures (high RNA) and confluent ones (low RNA . The RNA levels were determined as described[29].

Method	*Sensitiv ty to RN.*	*Sensitivity to proteolysis*	*Precipitation of protein*	*Protein recovery (%)*	*Overall quality*
SI nuclease	+	–	–	80	Variable
DNAse–RNAse	–	+	–	80	Poor
Centrifugation	+	–	–	85	Variable
RNAse centrifugation	–	±	–	85	Good
Phenol extraction	±	–	±	70	Variable
Lanthanum precipitation	–	–	+ +	30–75	Good
Calcium precipitation	–	–	±	50–70	Rather good

nuclei. We therefore decided to digest the RNA with RNAse. The first attempt at digestion in multimolar urea was completely unsuccessful, but digestion in non-denaturing media proved far more efficient. We determined that maximum efficiency was reached when sodium chloride and EDTA were included in the digestion medium in order to dissociate the RNA–protein complexes. Elimination of the RNA by diges-

Fig. 5. Two-dimensional electrophoresis of *in vitro* labelled nuclear proteins freed from RNA by RNAse digestion and from DNA by centrifugation.

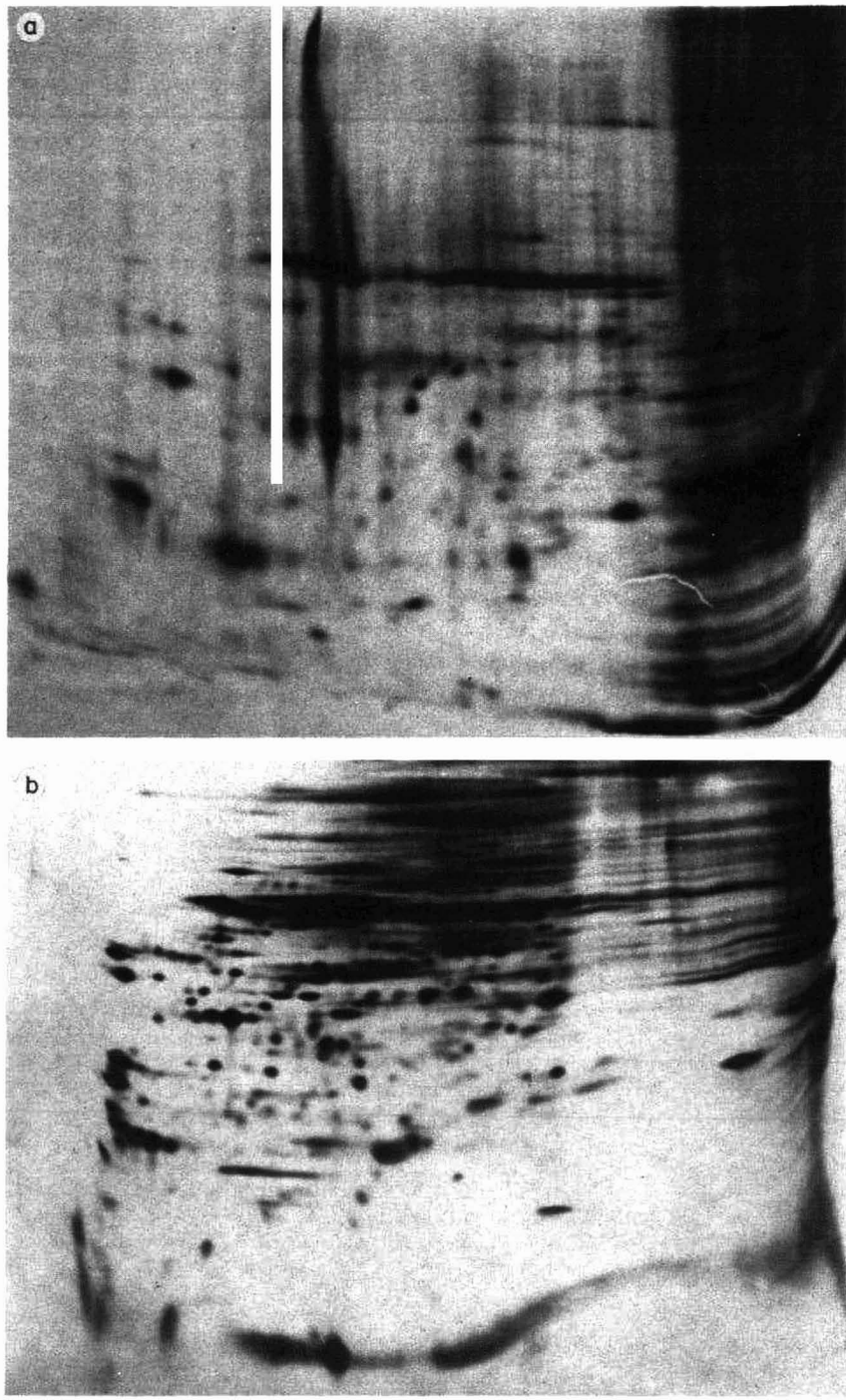

Fig. 6. Two-dimensional electrophoretic patterns of nuclear proteins freed from nucleic acids by phenol partition. (a) Without removal of SDS before the electrofocusing; (b) partition at 65°C and SDS removed by ion-pair extraction.

tion, followed by TCA pre ipitation to eliminate the oligonucleotides and the salts, then radioactive labelling nd finally elimination of the DNA by centrifugation proved to be the method o choice in our system, leading to high quality gels (Fig. 5). On the other hand, the use of a DNAse–RNAse cocktail failed to digest DNA even in the presence of 2 M sodium chloride to dissociate the histones.

The major drawback of this method is its sensitivity to endogenous proteases, RNAse being heat-treated o inactivate contaminating proteases[29]. *Drosophila* cells have a low protease conte nt, but many types of cells have high levels of nuclear proteases[30], which are not always completely inactivated by protease inhibitors. We therefore developed anothe set of methods in which the sample is always in highly denaturing conditions.

One method is the p enol–SDS method in which chromatin is dissociated by boiling in SDS and the pro eins are partitioned into phenol, nucleic acids being excluded in the aqueous pha e[19]. Some points must be kept in mind when using such a method. First, the SDS must be carefully eliminated, because CHAPS is far less efficient than Nonidet P-40 n removing SDS from proteins. Otherwise, precipitation and streaking occur at the sample application point, as shown in Fig. 6a. Secondly, the temperature of phenol extraction is of great importance. At low temperature, DNA is eliminated very well, but a lot of RNA, especially poly A + RNA, is trapped

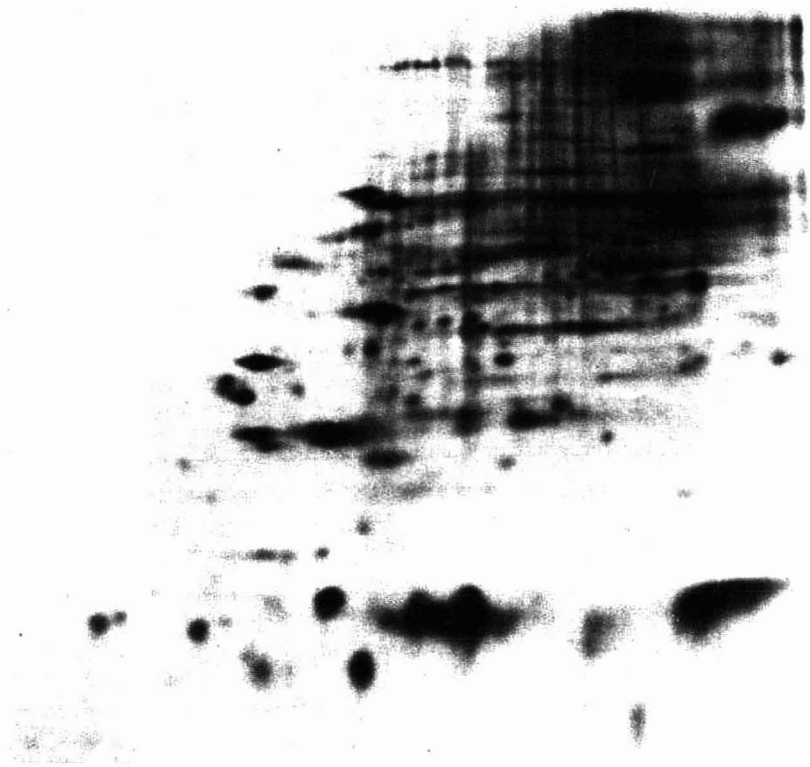

Fig. 7. Two-dimensional electrophoresis of nuclear proteins freed from nucleic acids by calcium precipitation.

with the proteins, blurrir g the patterns. At elevated temperature, much more RNA is eliminated, but DNA i pelleted in the phase separation, and a clean separation of the phenol phase is ther fore difficult. However, good quality patterns can be obtained by this method (F ig. 6b). Moreover, this method can be applied with great success to the analysis of whole cells having both a high protease activity and a high level of RNA (data not s own).

However, this meth od cannot be used with cell lines which have a high nuclear poly A + RNA content. For this case of cells having both a high protease activity and a high poly A + R NA content, we developed precipitation methods. Among many precipitants tested such as spermine, protamine, laurylamine acetate, manganese, calcium and lantl anum, only the last two gave satisfactory results. The lanthanum method is efficie t but very difficult to control, and the proteins frequently precipitate along with the nucleic acids, leading to very variable yields (Table II) and considerable pattern vari ition from one experiment to another. Note that, for the experiment described in ig. 1, the sample applied on both gels arose from a single precipitation. The calciu m method is far safer and gives high quality patterns (Fig. 7), but the protein yield is rather low (*ca.* 60%) and selective precipitation of proteins may occur.

CONCLUSIONS

In conclusion, the main features of the methods tested have been summarized in Table II. It appears that four methods are applicable, the choice of which depending on factors linked to the biological material. If the sample has a low RNA content, a simple ultracentrifugation in urea–CHAPS medium is sufficient and leads to very high quality patterns. When the sample has a high RNA content but a low protease level, prior digestion of RNA by pancreatic RNAse in the presence of EDTA and sodium chloride followed by ultracentrifugation to pellet the DNA gives the best results. When both the RNA content and the proteolytic activity are high, this method cannot be used. In most of these cases, a phenol partition in the presence of SDS, followed by elimination of the latter, gives the best patterns. In rare cases where all these methods are inefficient, precipitation by calcium chloride gives good results, but precipitation of proteins is likely to occur. Progress in protein detection methods (more efficient labelling methods) and in dissociation media are currently under investigation in our laboratory, and should soon yield a simplification of the methods required for analysis of nuclear proteins by two-dimensional electrophoresis.

REFERENCES

1 S. C. R. Elgin and J. Bonner, *Biochemistry*, 11 (1972) 772.
2 G. Cognetti, D. Settineri and G. Spinelli, *Exp. Cell Res.*, 71 (1972) 465.
3 L. Orrick, M. Olson and H. Busch, *Proc. Natl. Acad. Sci. U.S.A.*, 70 (1973) 1316.
4 T. Barret and H. J. Gould, *Biochim. Biophys. Acta*, 294 (1973) 165.
5 P. H. O'Farrell, *J. Biol. Chem.*, 250 (1975) 4007.
6 J. L. Peterson and E. H. Mc Conkey, *J. Biol. Chem.*, 251 (1976) 544.
7 C. C. Howe and D. Solter, *Dev. Biol.*, 74 (1980) 351.
8 C. W. Heizmann, E. M. Arnold and C. C. Kuenzle, *J. Biol. Chem.*, 255 (1980) 11 504.
9 G. Unterreger, K. D. Zang and O. G. Issinger, *Electrophoresis*, 4 (1983) 303.
10 K. E. Peters and D. E. Comings, *J. Cell Biol.*, 86 (1980) 135.

11 J. L. Couderc, personal communication.
12 P. H. O'Farrell and P. Z. O'Farrell, *Methods Cell Biol.*, 16 (1977) 407.
13 G. Echalier and A. Ohanessian, *C.R. Acad. Sci. Paris*, 268 (1968) 1771.
14 P. Cherbas, L. Cherbas, C. Savakis and M. D. Koehler, *Am. Zool.*, 21 (1981) 743.
15 C. Wu, P. M. Bingam, K. J. Livak, R. Holmgren and S. C. R. Elgin, *Cell*, 16 (1979) 797.
16 O. Kuhn and F. H. Wilt, *Anal. Biochem.*, 105 (1980) 274.
17 N. Jentoft and D. C. Dearborn, *J. Biol. Chem.*, 254 (1979) 4359.
18 K. Zechel and K. Weber, *Eur. J. Biochem.*, 77 (1977) 133.
19 W. M. LeStourgeon and A. L. Beyer, *Methods Cell Biol.*, 16 (1977) 387.
20 L. E. Henderson, S. Oroszlan and W. Konigsberg, *Anal. Biochem.*, 93 (1979) 153.
21 R. Duncan and J. W. B. Hershey, *Anal. Biochem.*, 138 (1984) 144.
22 G. H. Perdew, H. W. Schaup and D. P. Selivonchick, *Anal. Biochem.*, 135 (1983) 453.
23 W. M. Bonner and R. A. Laskey, *Eur. J. Biochem.*, 46 (1974) 83.
24 E. Zeindl and J. Klose, *Electrophoresis*, 5 (1984) 303.
25 R. Bravo and J. E. Celis, *J. Cell Biol.*, 84 (1980) 795.
26 K. E. Willard, C. S. Giometti, N. L. Anderson, T. E. O'Connor and N. G. Anderson, *Anal. Biochem.*, 100 (1979) 289.
27 D. Satta, G. Schapira, P. Chafey, P. G. Righetti and J. P. Wahrmann, *J. Chromatogr.*, 299 (1984) 57.
28 G. Artoni, E. Gianazza, M. Zanoni, C. Gelfi, M. C. Tanzi, C. Barozzi, P. Ferruti and P. G. Righetti, *Anal. Biochem.*, 137 (1984) 420.
29 T. Maniatis, E. F. Fritsch and J. Sambrook, *Molecular Cloning*, Cold Spring Harbor Laboratory, 1982, p. 451.
30 B. D. Carter and C. B. Chae, *Biochemistry*, 15 (1976) 180.

Journal of Chromatography, 351 (1986) 91–102
Elsevier Science Publishers B.V., Amsterdam — Printed in The Netherlands

CHROM. 18 181

SIMULTANEOUS DETERMINATION OF N-ACETYLGLUCOSAMINE, N-ACETYLGALACTOSAMINE, N-ACETYLGLUCOSAMINITOL AND N-ACETYLGALACTOSAMINITOL BY GAS–LIQUID CHROMATOGRAPHY

THOMAS P. MAWHINNEY
Departments of Child Health and Biochemistry, University of Missouri – Columbia, 322-A Chemistry Building, Columbia, MO 65211 (U.S.A.)
(First received June 17th, 1985, revised manuscript received September 9th, 1985)

SUMMARY

A gas–liquid chromatographic procedure is described which will concomitantly separate and quantitate N-acetylglucosamine, N-acetylgalactosamine, N-acetylglucosaminitol and N-acetylgalactosaminitol in a single analytical run. The hexosamines, as their O-methyloximes, and the hexosaminitols can be separated as either their per-O-acetylated or per-O-trimethylsilylated derivatives. This method is particularly useful with samples that possess both N-acetylhexosaminitols and N-acetylhexosamines as are seen with N-linked oligosaccharides that are cleaved from glycoproteins by alkaline borohydride treatment. This procedure demonstrates a range of acceptable linearity of 1–1000 nmoles for each type of amino sugar.

INTRODUCTION

Both N-acetylglucosamine (GlcNAc) and N-acetylgalactosamine (GalNAc) have been identified as being involved in the linkage region of side-chain oligosaccharides to the protein core of many glycoproteins[1]. Typically, GlcNAc is bound to asparagine (GlcNAc–Asp) in the formation of N-linked oligosaccharides, commonly found on plasma glycoproteins, and GalNAc is covalently bound to serine and threonine (GalNAc–Ser/Thr) forming the O-linked oligosaccharides, generally found on epithelial mucins[2]. In the analysis of glycoprotein side-chain oligosaccharides the GalNAc–Ser/Thr glycosidic linkage is usually cleaved under mild alkaline conditions in the presence of sodium borohydride[3,4]. The GlcNAc–Asp linkage is cleaved under stronger alkaline conditions in the presence of sodium borohydride[3,5]. In both cases the oligosaccharide side-chains are released from the protein core and the aldehyde of the hexosamine originally involved in the protein–oligosaccharide linkage is concomitantly reduced to the corresponding N-acetylglucosaminitol (GlcNAc-ol) or N-acetylgalactosaminitol (GalNAc-ol) sugar alcohol.

For monosaccharide analysis the released side-chained oligosaccharides are then subjected to acid hydrolysis and the resulting sugar monomers are generally reduced to their respective sugar alcohols with sodium borohydride. Following ace-

0021-9673/86/$03.50

tylation, the hexosaminitols and the neutral sugar alcohols are then concomitantly quantified by capillary[6,7] or packed-column[8] gas–liquid chromatography (GLC). Via this method all oligosaccharide N-hexosamine residues, *i.e.*, those involved in the protein–oligosaccharide linkage and those within the oligosaccharide structure, form the same respective hexosaminitol derivative and thus provide no structural information.

A sensitive and quantitative GLC–mass spectrometry (MS) method has been reported that is able to differentiate between the GalNAc involved in the N-glycosidic linkage of an oligosaccharide to the protein core and other GalNAc residues that are not involved in this linkage but are present within the oligosaccharide structure[9]. By this procedure a glycoprotein possessing an oligosaccharide with GalNAc as a linkage sugar is treated with alkaline sodium borohydride which effectively cleaves the oligosaccharide from the protein core and reduces the GalNAc linkage sugar to GalNAc-ol. The sample is then hydrolyzed and the resulting sugars are reduced with sodium borodeuteride and then acetylated. By substituting sodium borodeuteride in the latter reduction step all but the previously reduced linkage sugar (*i.e.*, GalNAc-ol) form derivatives that possess deuterium on carbon-1. GLC–MS is then used to determine the ratio of deuterium-labeled and hydrogen-labeled carbon-1 containing ion pairs which gives the ratio of GalNAc to GalNAc-ol.

An alternative to this method employs the amino acid analyzer to separate the hydrochloride salts of the hexosaminitols and hexosamines that are produced as the result of acid hydrolysis of alkaline borohydride released oligosaccharides[10]. Though this method provides excellent results, it requires a two-buffer system, modification of the ninhydrin reaction coil and approximately 2 h per run-time analysis.

To date, no capillary or packed-column GLC procedure is available which allows for the simultaneous separation and quantitation of GlcNAc, GalNAc, GlcNAc-ol and GalNAc-ol. The present investigation reports a GLC method that enables in a single analysis the separation and quantification of both the individual hexosamines involved and not involved in the oligosaccharide linkage region. Following the cleavage and reduction of the glycoprotein oligosaccharide side-chains and subsequent hydrolysis and re-N-acetylation of the hexosamines, the non-reduced hexosamines are derivatized to their respective O-methyloxime acetates and the existing hexosaminitols, which do not react to form the oxime, form their respective hexosaminitol acetates. Each of these acetylated derivatives is then separated on a polar GLC column. Alternatively, the resulting O-methyloxime and hexosaminitol mixture can be trimethylsilylated and then quantitated by GLC. Because of this flexibility in the choice of hexosamine derivative and of GLC column it is possible, in many cases, to perform the concomitant analysis of neutral carbohydrates as well.

MATERIALS AND METHODS

Instrumentation

Gas chromatography was performed using a Perkin-Elmer (Norwalk, CT, U.S.A.) Sigma 3 instrument equipped with dual flame ionization detectors. Chromatographic columns were 6 ft. × 1/8 in. O.D. (1.8 mm I.D.), glass columns packed with either 3.0% diethylene glycol adipate (DEGA), stabilized (Foxboro/Analabs, North Haven, CT, U.S.A.), on Chromosorb W HP, 100–120 mesh, with 3% SP-2250

(Supelco, Bellefonte, PA, U.S.A.) on Supelcoport, 100–120 mesh or with 3% SP-2340 on Supelcoport, 100–120 mesh. Peak areas were measured using a Shimadzu (Rockville, MD, U.S.A.) C-R3A Chromatopac integrator.

Materials

All carbohydrate standards were obtained from Pfanstiehl Laboratories (Waukegan, IL, U.S.A.). Pyridine, methanol, 1-dimethylamino-2-propanol, acetic anhydride, hydroxylamine hydrochloride and sodium borohydride were purchased from Aldrich (Milwaukee, WI, U.S.A.). All solvents were redistilled prior to use. Sodium borodeuteride was obtained from Alfa (Danvers, MA, U.S.A.). O-Methylhydroxylamine hydrochloride was obtained from Pierce (Rockford, IL, U.S.A.).

Isolation of glycoproteins

All glycoproteins and glycopeptides were purified as described in the literature cited below. For consistency in the isolation methods, the oligosaccharides from each glycoconjugate were cleaved from the protein core via the appropriate alkaline-borohydride procedure described below. Subsequent purification of the isolated oligosaccharides was performed as described in each respective study. Oligosaccharide IV and an acidic pentasaccharide from porcine submaxillary mucin were isolated by the procedure of Carlson[11] and by Aminoff *et al.*[12], respectively. The glycopeptide I oligosaccharide from human serum thyroxine-binding globulin was prepared as described by Zinn *et al.*[13] and the desialated oligosaccharide from bovine prothrombin was isolated by the procedure of Mizuochi *et al.*[14]. Tracheobronchial mucus glycoprotein (TBG) from sputum from a patient with cystic fibrosis was prepared as outlined by Boat *et al.*[15] without carboxymethylation of cysteine residues. Isolation of the 3a(1) neutral pentasaccharide from TBG was performed as described by Van Hanlbeek *et al.*[16].

Reductive cleavage of the oligosaccharide–protein linkage

Mild alkaline-borohydride cleavage of the base labile GalNAc–Ser/Thr linkages via beta elimination was performed by treating each glycoprotein or glycopeptide (50–500 μg) with 0.05 *M* sodium hydroxide–1.0 *M* sodium borohydride (1.0 ml/mg sample) at 45°C for 15 h. Cleavage of the base resistant GlcNAc–Asp linkage via alkaline hydrolysis was accomplished by dissolving the glycoprotein or glycopeptide (50–500 μg) in 1.0 *M* sodium hydroxide–1.0 *M* sodium borohydride (1.0 ml/mg sample) and heating it at 100°C for 6 h. D-Glucoheptitol was added as internal standard. At the end of the respective incubation period dilute acetic acid was added to acidify each solution which was then passed through a 3 cm × 0.8 cm I.D. column of Dowex 50W-X8 (hydrogen form, 50–100 mesh). Each sample was then dried to a syrup *in vacuo* and the boric acid removed by the sequential addition and evaporation of 5 × 1.0 ml dry methanol.

Hydrolysis of oligosaccharides

Oligosaccharides and methyl glycoside standards were each subjected to acid hydrolysis in 0.2 ml 4.0 *M* hydrochloric acid at 100°C for 4 h under nitrogen atmosphere. Samples were then dried *in vacuo* at 30°C using a rotary evaporator, redissolved in 0.25 ml of 95% ethanol to which was then added 2.0 ml benzene, and were again dried. This latter step was repeated twice.

Derivatization of carbohydrates

Hydrolyzed samples to be oximated and trimethylsilylated, or to be reduced with sodium borohydride or sodium borodeuteride to the alditols and acetylated, were first treated with pyridine and acetic anhydride in dry methanol by the procedure of Kozulic *et al.*[17] to re-N-acetylate the hexosamines. The per-O-acetyl O-methyloxime, the per-O-trimethylsilyl O-methyloxime and the per-O-trimethylsilyl O-trimethylsilyloxime derivatives of the hexosamines and neutral sugars, and the aldononitrile acetates of the neutral sugars were prepared as previously described[18].

Samples to be O-methyloximated and acetylated were treated in two ways. In the first way, a sample was divided into two equal fractions with one being O-methyloximated and acetylated for hexosamine analysis and the other analyzed for their content of neutral sugars as their alditol acetates[6–8] or aldononitrile acetates[18]. Alternatively, the hexosamines and hexosaminitols in a sample were separated from the neutral sugars and isolated with the use of cation-exchange resins by the procedure of Boas[19]. The hexosamines and hexosaminitols were then subjected to O-methyloximation and acetylation and the neutral sugars analyzed as alditol acetates or aldononitrile acetates.

For comparison to other analytical methods each oligosaccharide was also analyzed for amino sugars by GLC–MS and by analysis on an amino acid analyzer as described by Weber and Carlson[9] and Cheng and Boat[10], respectively.

RESULTS AND DISCUSSION

GLC separations

The GLC separation of both the per-O-acetylated O-methyloxime and per-O-acetylated alditol derivatives of N-acetylglucosamine and N-acetylgalactosamine on a 3% DEGA, stabilized, column is presented in Fig. 1. As shown, each amino sugar derivative displayed a single symmetrical chromatographic peak and exhibited no significant peak tailing. Though it has been shown that when a sugar is oximated, two isomeric products are produced, representing the *syn* and *anti* forms of the O-methyloxime function[20], these were unresolved for the per-O-acetylated O-methyloximated N-acetylhexosamines on the DEGA column[18].

It should be noted that the per-O-acetylated O-methyloxime derivatives of neutral pentoses and hexoses emerge from the GC column well before the hexosamines and do not interfere with their analysis. Though this is of little use for the analysis of the neutral sugars as these derivatives on the DEGA column, since they exhibit overlapping *syn* and *anti* peaks, it does allow for the analysis of the amino sugars even when neutral sugars are present in the sample. Because of this, a sample containing both amino and neutral sugars can simply be divided into two aliquots of which one is analyzed for amino sugars, as described above. The per-O-acetylated O-methyloximes of the neutral sugars that are present in this aliquot elute early from the column and are not assayed. The neutral sugars in the second aliquot can then be separately quantitated as their aldononitrile acetates[18], alditol acetates[6–8] or by another method. In this way, the same internal standard (*e.g.*, myo-inositol, D-glucoheptitol, etc.) can be utilized in both analyses. Alternatively, especially for samples with low carbohydrate content, the amino sugars can be separated from the neutral sugars by ion-exchange chromatography[19] and then each can be analyzed separately.

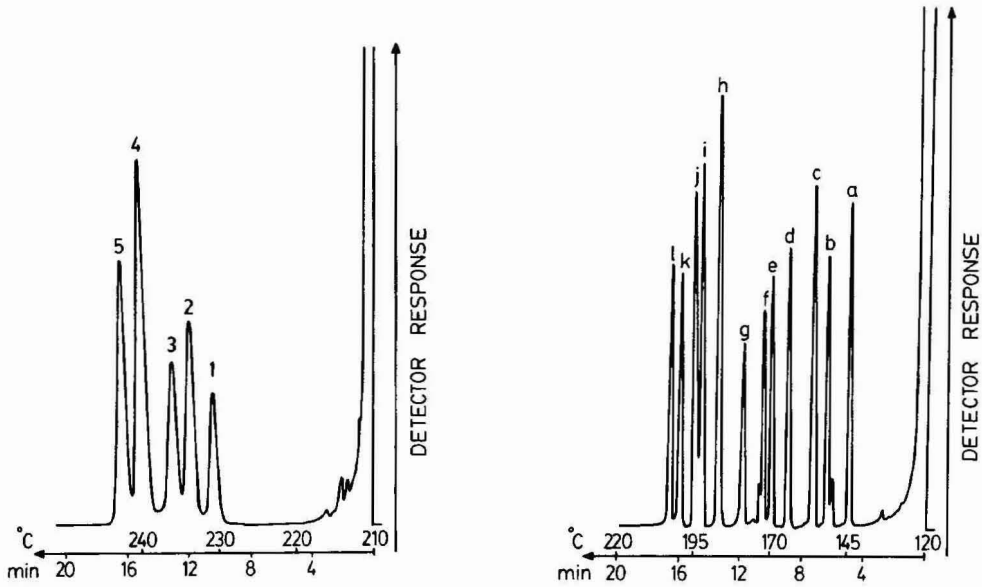

Fig. 1. Gas–liquid chromatogram of the per-O-acetylated derivatives of (1), D-glucoheptitol = internal standard; (2), (1-O-methyloxime)-N-acetylglucosamine; (3), (1-O-methyloxime)-N-acetylgalactosamine; (4), N-acetylglucosaminitol and (5), N-acetylgalactosaminitol. Injected sample contained 0.5 μg of each oximated amino sugar and internal standard and 1 μg of each hexosaminitol. Sample was separated on a 3.0% DEGA (stabilized) on Chromosorb W HP, 100–120 mesh, GC column. Program: temperature was increased from 210°C to 240°C at a rate of 2°C/min. Nitrogen was used as the carrier gas at a flow-rate of 20 ml/min.

Fig. 2. Gas–liquid chromatogram of the per-O-trimethylsilyl derivatives of (a), (1-O-methyloxime)-2-deoxy-D-ribose; (b), (1-O-methyloxime)-D-ribose; (c), (1-O-methyloxime)-L-fucose; (d), (1-O-methyloxime)-2-deoxy-D-glucose; (e), (2-O-methylketoxime)-D-fructose; (f), (1-O-methyloxime)-D-glucose; (g), (1-O-methyloxime)-D-glucuronic acid; (h), myo-inositol = internal standard; (i), N-acetylglucosaminitol; (j), N-acetylgalactosaminitol; (k), (1-O-methyloxime)-N-acetylglucosamine and (l), (1-O-methyloxime)-N-acetylgalactosamine. Unlabeled small peaks at the base of (b) D-ribose and (f) D-glucose represent the resolved *syn* or *anti* isomer of that respective sugar. Injected sample contained 1 μg of each oximated amino sugar, internal standard and hexosaminitol. Sample was separated on a 3.0% SP-2250 Supelcoport, 100–120 mesh, GC column. Program: temperature was increased from 120°C to 220°C at a rate of 5°C/min. Nitrogen was used as the carrier gas at a flow-rate of 18 ml/min.

Fig. 2 shows the separation of the trimethylsilyl derivatives of GlcNAc-ol and GalNAc-ol and of the per-O-trimethylsilyl O-methyloximes of GlcNAc, GalNAc and several neutral sugars on a 3% SP-2250 GLC column. Although the major peaks in this chromatogram may be easily integrated, baseline separation of the N-acetylated hexosaminitols is not achieved as it is for the O-methyloximated amino sugars. The *syn* and *anti* forms of the O-methyloxime function[18] were unresolved for the amino sugars and most neutral sugars[20] as is evident by their single symmetrical GC peaks. Ribose and glucose, on the other hand, each demonstrate a large peak with a small side peak which is indicative of resolved *syn* and *anti* isomers[20]. For glycoproteins containing N-linked oligosaccharides which possess only one type of hexose, though, this method is particularly useful since the reducible hexosamines and neutral sugars in the sample are both derivatized to their respective O-methyloximes and thus do

TABLE I

GAS CHROMATOGRAPHIC RETENTION DATA FOR ACETYLATED AND FOR TRIMETHYLSILYLATED DERIVATIVES OF 2-ACETAMIDO-2-DEOXY-HEXOSAMINES

Retention times given in min. Retention times presented in parentheses indicate the presence of a second peak due to separation of *syn* and *anti* isomers of the oxime.

	*DEGA**	*DEGA***	*SP-2340****	*SP-2250*§
O-methyloxime acetates				
N-Acetylglucosamine	11.95	8.40	8.85 (8.91)	–
N-Acetylgalactosamine	13.02	9.52	10.80 (10.93)	–
N-Acetylmannosamine	13.56	9.68	10.85	–
Alditol acetates				
N-Acetylglucosaminitol	15.15	11.90	17.12	–
N-Acetylgalactosaminitol	16.25	12.60	19.83	–
N-Acetylmannosaminitol	16.32	12.71	19.87	–
O-Methyloxime trimethylsilyl ethers				
N-Acetylglucosamine	–	–	–	16.20
N-Acetylgalactosamine	–	–	–	16.75
N-Acetylmannosamine	–	–	–	16.79
Alditol trimethylsilyl ethers				
N-Acetylglucosaminitol	–	–	–	14.60
N-Acetylgalactosaminitol	–	–	–	15.25
N-Acetylmannosaminitol	–	–	–	15.28

* 3% DEGA, stabilized, on Chromosorb W HP, 100–120 mesh. Column: glass, 6 ft. × 1/8 in. O.D. (1.8 mm I.D.). Program: temperature was increased from 210°C to 240°C at a rate of 2°C per/min. Nitrogen was used as the carrier gas at a flow-rate of 20 ml/min.

** 3% DEGA, stabilized, on Chromosorb W HP, 100–120 mesh. Column: glass, 6 ft. × 1/8 in. O.D. (1.8 mm I.D.). Program: isothermal at 230°C. Nitrogen was used as the carrier gas at a flow-rate of 20 ml/min.

*** 3% SP-2340 on Supelcoport, 100–120 mesh. Column: glass, 6 ft. × 1/8 in. O.D. (1.8 mm I.D.). Program: isothermal at 240°C. Nitrogen was used as the carrier gas at a flow-rate of 30 ml/min.

§ 3% SP-2250 on Supelcoport, 100–120 mesh. Column: glass, 6 ft. × 1/8 in. O.D. (1.8 mm I.D.). Program: temperature was increased from 120°C to 260°C at a rate of 5°C per/min. Nitrogen was used as the carrier gas at a flow-rate of 18 ml/min.

not require prior separation of hexosamines from the neutral sugars before derivatization. In contrast to the per-O-trimethylsilyl O-methyloximes of GlcNAc and GalNAc (Fig. 2), no separation of GlcNAc and GalNAc could be achieved as their per-O-trimethylsilyl O-trimethylsilyloximes (not shown) and, in addition, the per-O-trimethylsilyl O-trimethylsilyloximes of any hexoses that may be in a sample interfere with the trimethylsilylated hexosaminitol peaks. Lastly, it should be noted that trimethylsilylation of oximated hexosamines in their hydrochloride salt or free base form produced derivatives that were both degraded readily on the GLC column and are not useful in resolving GlcNAc from GalNAc and GlcNAc-ol from GalNAc-ol. Re-N-acetylation of the free amines prior to trimethylsilylation[17] prevented their degradation on the GLC column and resulted in the separation of the different hexosamine derivatives, as described above.

Retention data

Retention data for each acetylated derivative on 3% DEGA and 3% SP-2340 and each trimethylsilyl derivative on 3% SP-2250 are given in Table I. On the polar DEGA and the very polar SP-2340 columns the hexosaminitol acetates elute from the column after the O-methyloxime acetates. This elution order is reversed when the trimethylsilyl derivatives of these amino sugars are separated on an intermediate polar 3% SP-2250 GC column. As indicated above, no separation of *syn* and *anti* isomers of the O-methyloximes of the N-acetylhexosamines was observed on the DEGA column but was evident as closely related peaks on SP-2340. Under the same chromatographic conditions, retention times for all hexosamine derivatives were typically shorter on the DEGA column than on the SP-2340 column. Notably, the SP-2340 packed column demonstrated significant column bleed at the higher operating temperatures required to separate the amino sugars. Lastly, isothermal separation of the hexosamine derivatives can also be performed on the 3% DEGA column which readily permits sample injections every 20 min. This run time can be reduced further by utilizing a 1.5% DEGA column (not shown).

Quantitative aspects

Employing N-acetylhexosamine and N-acetylhexosaminitol standards a linear response curve in the range of 1 to 1000 nmoles was obtained for each sugar using flame ionization as the GLC detector. In general practice, though, for the analysis of hydrolyzed biological samples a working range of 2 to 100 nmoles for amino sugars was typically employed.

Analysis of purified oligosaccharides

Since excellent separation of the amino sugar alcohols and the O-methyloximated amino sugars is achieved as their per-O-acetylated derivatives on a 3% DEGA column (Fig. 1) this procedure is readily applicable to samples possessing both types of amino sugars, such as hydrolyzed N-linked oligosaccharides that were liberated from glycoproteins via alkaline borohydride treatment. In the latter case, the amino sugar involved in the N-linkage to the protein core would have been reduced to its respective N-acetylhexosaminitol upon cleavage and, following acid hydrolysis of the liberated oligosaccharide, the amino sugars that were present within the oligosaccharide structure would be reducible and would form O-methyloximes whereas the N-acetylhexosaminitol would not. Table II presents the results of the N-acetylhexosamine analysis of representative oligosaccharides that were cleaved from different glycoproteins by alkaline borohydride treatment. The neutral sugars in these samples were assayed as their aldononitrile acetates[18]. Five separate samples (10 μg each) of each alkaline borohydride released oligosaccharide were subjected to acid hydrolysis. Following the O-methyloximation of the reducible amino sugars with O-methylhydroxylamine the O-methyloximated amino sugars and the hexosaminitols in each sample were analyzed as their per-O-acetylated derivatives on a 3% DEGA column, as described above. Three of the oligosaccharides were reported to have GalNAc involved in the original protein–oligosaccharide linkage and the other two involved GlcNAc in the linkage. In addition, these specific oligosaccharides were chosen because they also possess amino sugars other than the linkage hexosamine within their structure. As shown in Table II, analysis of the amino sugars, via this method (GLC),

TABLE II

N-ACETYLHEXOSAMINE ANALYSIS OF SOME KNOWN ALKALINE BOROHYDRIDE RELEASED GLYCOPROTEIN OLIGOSACCHARIDES

Data expressed as the mean weight (in μg) with the standard deviation in parentheses of five separate analyses and the mole ratio in brackets of each carbohydrate relative to the identified N-acetylhexosaminitol (involved in the protein–oligosaccharide linkage) found in each sample. In the GLC method, amino sugars were assayed as described in Fig. 1 and their neutral sugars were determined as their aldononitrile acetates[18]. For comparison the same oligosaccharides were assayed for amino sugars by a GLC–MS method[9] in which GlcNAc-ol and GalNAc-ol (protein-linked amino sugar), and GlcNAc and GalNAc (non-protein-linked amino sugars) were determined by the mass ratio of hydrogen-labeled and deuterium-labeled C-1 fragments, respectively. The neutral sugars in these samples were assayed as their alditol acetates[8]. Abbreviations: GlcNAc, N-acetylglucosamine; GalNAc, N-acetylgalactosamine; GlcNAc-ol, N-acetylglucosaminitol; GalNAc-ol, N-acetylgalactosaminitol; Fuc, D-fucose; Man, D-mannose; Gal, D-galactose.

Oligosaccharide	*Reference*	*Method*
Fuc–Gal–GalNAc-ol | GalNAc	11	GLC GLC–MS
NeuNGl–GalNAc-ol | GalNAc–Gal | Fuc	12	GLC GLC–MS
NeuNAc–Gal–GlcNAc–Man \ Man–GlcNAc–GlcNAc-ol / NeuNAc–Gal–GlcNAc–Man	13	GLC GLC–MS
Gal–GlcNAc–Man–Man–GlcNAc–GlcNAc-ol | Gal–GlcNAc–Man	14	GLC GLC–MS
Gal–GlcNAc–Gal–GalNAc-ol | Fuc	15, 16	GLC GLC–MS

concomitantly quantified both the amino sugar involved and not involved in the linkage to the protein core for each oligosaccharide structure. The small standard deviation observed for each series of amino sugar determinations clearly shows the excellent precision of analysis for this method. In all cases the results of the present method were in agreement with published structural data. Furthermore, the results were comparable with those amino sugar data acquired from the analysis of each of the above oligosaccharides by an alternate method (GLC–MS). This procedure is similar to the above method in that the oligosaccharides are cleaved from the protein core of the glycoproteins with alkaline borohydride but differs in that the reducible amino sugars (*i.e.*, those not involved in the protein linkage) that are formed following hydrolysis of the oligosaccharides are reduced to their corresponding hexosaminitols with sodium borodeuteride in lieu of oximation. GLC is then used to separate the per-O-acetylated hexosaminitol derivatives of N-acetylglucosamine and N-acetylgalactosamine. Analysis of each hexosaminitol GLC peak by MS provides

GlcNAc	*GalNAc*	*GlcNAc-ol*	*GalNAc-ol*	*Fuc*	*Man*	*Gal*
–	4.21(0.02) [1.04]	–	4.08(0.04) [1.00]	2.88(0.13) [0.96]	–	3.06(0.12) [0.93]
–	3.66(0.13) [0.90]	–	4.11(0.12) [1.00]	2.84(0.04) [1.02]	–	3.11(0.03) [1.02]
–	3.31(0.02) [0.97]	–	3.44(0.04) [1.00]	2.63(0.13) [1.04]	–	2.80(0.12) [1.01]
–	2.98(0.15) [0.89]	–	3.38(0.16) [1.00]	2.38(0.05) [0.96]	–	2.67(0.03) [0.98]
3.66(0.03) [2.93]	–	1.26(0.02) [1.00]	–	–	3.16(0.11) [3.11]	1.99(0.10) [1.96]
3.48(0.16) [2.85]	–	1.20(0.13) [1.00]	–	–	2.92(0.04) [3.02]	1.99(0.03) [1.99]
5.08(0.01) [3.05]	–	1.68(0.02) [1.00]	–	–	4.15(0.12) [3.06]	2.67(0.11) [1.97]
5.01(0.16) [2.89]	–	1.75(0.11) [1.00]	–	–	4.15(0.04) [2.94]	2.79(0.05) [1.98]
3.14(0.03) [0.97]	–	–	3.27(0.03) [1.00]	2.26(0.12) [0.94]	–	5.58(0.12) [1.98]
2.88(0.12) [0.93]	–	–	3.10(0.14) [1.00]	2.19(0.04) [0.96]	–	5.02(0.05) [2.01]

the ratio of amino sugar reduced with sodium borohydride and reduced with sodium borodeuteride by measuring the ratio of hydrogen-labeled and deuterium-labeled C-1 containing fragment ion pairs, representing the protein-linked and non-protein-linked amino sugars, respectively. The neutral sugars in these samples were assayed as their alditol acetates[8].

Fig. 3 illustrates the GC separation of the amino sugars found in the porcine blood group H substance oligosaccharide fraction 14.5[21] employing D-glucoheptitol as the internal standard. As shown, excellent separation of the amino sugars N-acetylglucosamine and N-acetylgalactosaminitol is achieved on the 3% DEGA, stabilized, GLC column. Also shown in Fig. 3 is the concomitant separation of the oligosaccharide's neutral sugars as their aldononitrile acetates with β-methyl-D-glucopyranoside as the internal standard. This was accomplished by separating the amino sugars from the neutral sugars after hydrolysis of the oligosaccharide. Following the addition of the respective internal standard the amino sugar fraction was

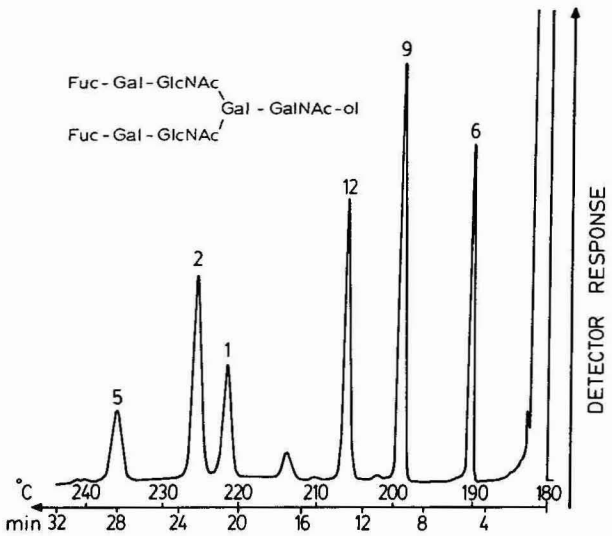

Fig. 3. GC separation of the amino sugars and neutral sugars (aldononitrile acetates) of the porcine blood group H substance oligosaccharide fraction 14.5[18] on a 3% DEGA GLC column. Following hydrolysis of the oligosaccharide (8.2 μg), the sample's hexosamines were separated from the neutral sugars. After the addition of the respective internal standards and subsequent derivatizations the sugars were then recombined for GLC analysis. (1) D-glucoheptitol = internal standard for amino sugars; (2) (1-O-methyloxime)-N-acetylglucosamine; (5) N-acetylgalactosaminitol; (9) β-methyl-D-glucopyranoside = internal standard for neutral sugars, and the aldononitrile acetates of (6) L-fucose and (12) D-galactose. The unassigned peak at approximately 17 min is a side-product cyclic oxime produced during the derivatization of L-fucose to its aldononitrile acetate. Sample was separated on a 3.0% DEGA (stabilized) on Chromosorb W HP, 100–120 mesh, GC column. Program: temperature was increased from 180°C to 240°C at a rate of 2°C/min. Nitrogen was used as the carrier gas at a flow-rate of 20 ml/min.

O-methyloximated and acetylated and the neutral sugars were derivatized to their aldononitrile acetates[18]. Both derivatized samples were recombined prior to GLC injection. The separated amino sugars and neutral sugars were then quantitated against their own respective internal standard, thus eliminating errors in mixing. The

TABLE III

N-ACETYLHEXOSAMINE ANALYSIS OF THE PORCINE BLOOD GROUP H SUBSTANCE OLIGOSACCHARIDE FRACTION 14.5

Data expressed as the mean weight (in μg) with the standard deviation in parentheses of five separate analyses and the mole ratio in brackets of each carbohydrate relative to N-acetylgalactosaminitol in the sample. Amino sugars were assayed as described in Fig. 1 and their neutral sugars were determined as their aldononitrile acetates[15]

Oligosaccharide	*Reference*	*GlcNAc*	*GalNAc-ol*	*Fuc*	*Gal*
Fuc–Gal–GlcNAc \ Gal–GalNAc-ol / Fuc–Gal–GlcNAc	15	3.66(0.03) [2.93]	1.26(0.04) [1.00]	3.16(0.11) [3.11]	1.99(0.10) [1.96]

results of the analyses are presented in Table III. The unassigned peak at approximately 17 min (Fig. 3) is a by-product cyclic oxime of L-fucose[22]. Though shown being separated as their per-O-acetylated O-methyloxime and hexosaminitol derivatives for the amino sugars and as the aldononitrile acetates for the neutral sugars, and because of the few types of carbohydrates involved in this oligosaccharide, analysis could also have been performed as the per-O-trimethylsilyl O-methyloxime derivatives of both amino and neutral sugars, as mentioned above as being useful for oligosaccharides which possess amino sugars and only one type of hexose. Since the sample's reducible hexosamines and neutral sugars are both derivatized to, and analyzed as, their respective per O-trimethylsilyl O-methyloxime derivatives, no prior separation of hexosamines from the neutral sugars before derivatization is needed.

CONCLUSION

Two GLC methods are described which permit the simultaneous determination of GlcNAc, GalNAc, GlcNAc-ol and GalNAc-ol. Both procedures are based upon the O-methyloximation of GlcNAc and GalNAc but differ in that the resulting O-methyloximated N-acetylhexosamines along with the N-acetylhexosaminitols are then per-O-acetylated or per-O-trimethylsilylated. These methods are particularly useful with samples that possess both N-acetylhexosaminitols and N-acetylhexosamines as are seen with N-linked oligosaccharides cleaved from glycoproteins by alkaline borohydride treatment. Though the examples given were focused on purified oligosaccharides which possessed only one type of N-acetylhexosaminitol (*i.e.*, the protein-linked amino sugar), these methods are readily applicable to alkaline borohydride cleaved mixtures of oligosaccharides which may contain both GlcNAc-ol and GalNAc-ol. This would provide valuable quantitative information on the number and types of N-linked oligosaccharides present in the sample. Furthermore, since these methods concomitantly measure GlcNAc and GalNAc they would also simultaneously provide quantitative data on the N-acetylhexosamines that are present within the oligosaccharides and not involved in the N-linkage to the protein core of the glycoprotein.

Lastly, with regards to the analysis of the neutral sugars in these samples, there is considerable flexibility with the application of the above amino sugar methods. With small samples, analysis of the amino sugars via their per-O-acetylated O-methyloxime and per-O-acetylated alditol derivatives on a 3% DEGA GLC column (Fig. 1) is best accomplished by the separation of the amino sugars from the neutral sugars before derivatization with the latter being analyzed separately as their aldononitrile acetates, alditol acetates or by another method. Provided there is no interference from the by-product cyclic oximes of the neutral sugar aldononitrile acetates (as seen with xylose and arabinose) it is possible to recombine these derivatives with the derivatized amino sugars and analyze them together on the 3% DEGA GLC column, quantitating them against their own respective internal standard. With larger samples, and employing the same per-O-acetylated derivatives, it is not necessary to separate the amino sugars from the neutral samples for quantitation but rather the sample can be simply divided into two aliquots with one being assayed directly for amino sugars (as their O-methyloximes) and the other for neutral sugars (by another GLC method), as described above. Alternatively, the reducing carbohydrates in a

single sample can be O-methyloximated and then all the sugars per O-trimethylsilylated. GlcNAc, GalNAc, GlcNAc-ol, GalNAc-ol and the neutral sugars are then analyzed on a 3% SP-2250 GLC column with a single injection. As noted above, if more than one hexose is present an aliquot of the sample should be analyzed separately for neutral sugars by another method. Notably, since trimethylsilylated sugars are subject to eventual hydrolysis the samples should be analyzed shortly after derivatization.

ACKNOWLEDGEMENT

This research was supported by grant HL-32026 from the National Heart, Blood and Lung Institute, National Institutes of Health.

REFERENCES

1 M. I. Horowitz and W. Pigman (Editors), *The Glycoconjugates*, Vol. 1, Academic Press, New York, 1977, p. 69.
2 W. J. Lennarz (Editor), *The Biochemistry of Glycoproteins and Proteoglycans*, Plenum Press, New York, 1980, p. 1.
3 P. A. Denny and P. C. Denny, *Carbohydr. Res.*, 110 (1982) 305.
4 F. Downs and W. Pigman, *Methods Carbohydr. Chem.*, 7 (1976) 200.
5 R. D. Marshall and A. Neuberger, *Methods Carbohydr. Chem.*, 7 (1976) 212.
6 C. Green, V. M. Doctor, G. Holzer and J. Oró, *J. Chromatogr.*, 207 (1981) 268.
7 A. Fox, S. L. Morgan, J. R. Hudson, Z. T. Zhu and P. Y. Lau, *J. Chromatogr.*, 256 (1983) 429.
8 T. Anastassiades, R. Puzic and O. Puzic, *J. Chromatogr.*, 225 (1981) 309.
9 P. L. Weber and D. M. Carlson, *Anal. Biochem.*, 121 (1982) 140.
10 A. P. Cheng and T. F. Boat, *Anal. Biochem.*, 85 (1978) 276.
11 D. M. Carlson, *J. Biol. Chem.*, 243 (1968) 616.
12 D. Aminoff, W. D. Gathmann and M. Baig, *J. Biol. Chem.*, 254 (1979) 8909.
13 B. Zinn, J. S. Marshall and D. M. Carlson, *J. Biol. Chem.*, 253 (1978) 6768.
14 T. Mizuochi, K. Yamashita, K. Fujikawa, W. Kisiel and A. Kobata, *J. Biol. Chem.*, 254 (1979) 6419.
15 T. F. Boat, P. W. Cheng, R. N. Iyer, D. M. Carlson and I. Polony, *Arch. Biochem. Biophys.*, 177 (1976) 95.
16 H. Van Hanlbeek, L. Dorland, J. F. G. Vliegenthart, W. E. Hull, G. Lamblin, M. Lhermitte, A. Boersma and P. Roussel, *Eur. J. Biochem.*, 127 (1982) 7.
17 B. Kozulic, B. Ries and P. Mildner, *Anal. Biochem.*, 94 (1979) 36.
18 T. P. Mawhinney, M. S. Feather, G. J. Barbero and J. R. Martinez, *Anal. Biochem.*, 101 (1980) 112.
19 N. F. Boas, *J. Biol. Chem.*, 204 (1953) 553.
20 R. A. Laine and C. C. Sweeley, *Carbohydr. Res.*, 27 (1973) 199.
21 H. Van Hanlbeek, L. Dorland, J. F. G. Vliegenthart, N. K. Kochetkov, N. P. Arbatsky and V. A. Derevitskaya, *Eur. J. Biochem.*, 127 (1982) 21.
22 R. H. Furneaux, *Carbohydr. Res.*, 113 (1983) 241.

Journal of Chromatography, 351 (1986) 103–110
Elsevier Science Publishers B.V., Amsterdam — Printed in The Netherlands

CHROM. 18 182

HIGH-PERFORMANCE LIQUID CHROMATOGRAPHIC SEPARATION OF LENS CRYSTALLINS AND THEIR SUBUNITS*

R. E. PERRY and E. C. ABRAHAM*
Department of Cell and Molecular Biology, Medical College of Georgia, Augusta, GA 30912 (U.S.A.)
(First received August 19th, 1985; revised manuscript received September 12th, 1985)

SUMMARY

A high-performance liquid chromatography (HPLC) method for the separation of lens crystallins has been developed which utilizes molecular sieve HPLC. Also described is a rapid one-step separation of the lens crystallin subunits using a reversed-phase C_4 column.

INTRODUCTION

The lens crystallins have been the subject of investigations involving structure and aging[1]. organ development[2], evolutionary changes[3], and cataract formation[1,4]. In such studies it is often necessary to examine the crystallin distribution and subunit composition of many samples using individual lenses. Techniques using gel filtration[5], DEAE-cellulose[6], and even chromatofocusing[7] have been described for separation of the intact crystallins and subunits. These methodologies do not allow for quantitative measurement involving individual lenses. In this paper we describe a rapid and sensitive molecular sieve high-performance liquid chromatographic technique which easily resolves the α-, β_{high}-, β_{low}-, and γ-crystalline. A second reversed-phase methodology using a large pore C_4 column is described which allows one-step separation of the individual crystallin subunits from either isolated crystallins or the total water-soluble fraction.

MATERIALS AND METHODS

Lens crystallin preparation

Lens protein was obtained from 6-week-old and 2-year-old Sprague-Dawley rats. Animals were sacrificed and lenses removed. The lenses from each individual animal were homogenized in 50 m*M* sodium phosphate buffer pH 6.8. The resulting homogenate was centrifuged at 5000 *g* for 30 min. The supernatant is the crystallin containing water-soluble fraction.

* Contribution number 0930.

0021-9673/86/$03.50

High-performance liquid chromatography (HPLC) techniques

Equipment. The instrument consists of a Beckman dual 110A pump gradient system with a 421 controller, Model 160 detector and a Hewlett-Packard 3390A recording integrator.

Molecular sieve HPLC. The molecular sieve columns used were Altex TSK 3000 SW, 600 × 7.5 mm, particle size 10 μm, coupled in series with an Altex TSK 4000 SW, 300 × 7.5 mm, particle size 10 μm. The sample size was 100–200 μg in 20 μl for analytical runs, while for semipreparative runs the sample size was 20 mg in 200 μl. All chromatograms were performed at ambient temperature. The mobile phase was 50 m*M* sodium phosphate, 50 m*M* sodium chloride, pH 6.8 with an isocratic flow-rate of 1.0 ml/min. Pressure remained at 45 bar. Absorbance was monitored at 280 nm.

Reversed-phase HPLC separation of crystallin subunits. The column used for the reversed-phase system was the Vydac-large pore (300 Å) C_4 column manufactured by The Separation Group, Hesperia, CA, U.S.A. The developers consisted of (A) 1% trifluoroacetic acid (TFA) in water and (B) 100% acetonitrile. All developers were HPLC grade, filtered and degassed under vacuum. The gradient system was as follows: 20 min equilibration with 20% B followed by a linear gradient 20% B to 50% B in 50 min. Isocratic 50% B for 10 min then 50% to 70% B in 1 min and isocratic for 10 min at 70% B. The column is then purged for 10 min at 100% B. The flow-rate was 1.5 ml/min and the pressure maintained at 165 bar. The sample size was 100–200 μg with chromatogram run at ambient temperature.

Amino acid analysis of crystallins and subunits

The crystallins and crystallin subunits were hydrolyzed in 6 *M* hydrochloric acid under vacuum at 100°C for 24 h. The amino acid composition was then determined with a Beckman 121M amino acid analyzer.

Calibration of molecular sieve HPLC columns

An amount of 200 μg of a molecular weight standard mixture consisting of thyroglobulin (mol.wt. 670 000) γ-globulin (mol.wt. 157 000), ovalbumin (mol.wt. 44 000), myoglobin (mol.wt. 17 000), and cyanocobalamine (mol.wt. 1250) was injected onto the molecular sieve HPLC system described previously. The results were plotted as log molecular weight *vs.* K_{av} [$K_{av} = (V_e - V_0)/(V_i - V_0)$ where V_e = elution volume of peak, V_i = column volume, and V_0 = void volume].

RESULTS

Molecular sieve HPLC separation of lens crystallins

The lens crystallins have been routinely separated in the past by Sephadex G-200 gel filtration into four classes; α-, β_{high}, β_{low}, and γ-crystallins[4]. The elution profiles obtained for soluble lens crystallins are shown in Fig. 1. Crystallin preparations from 6-week-old (Fig. 1A) and 2-year-old (Fig. 1B) rats were used for this study. By comparison to the calibration curve the resulting peaks are identified as a high-molecular-weight aggregate (HMW) (mol.wt. $1.5 \cdot 10^6$), α-crystallin (mol.wt. $8.0 \cdot 10^5$), β_{high} (mol.wt. $1.6 \cdot 10^5$, β_{low} (mol.wt. $4.2 \cdot 10^4$), and γ-crystallin (mol.wt. $2.0 \cdot 10^4$), eluted in that order. The results show excellent separation of each peak as

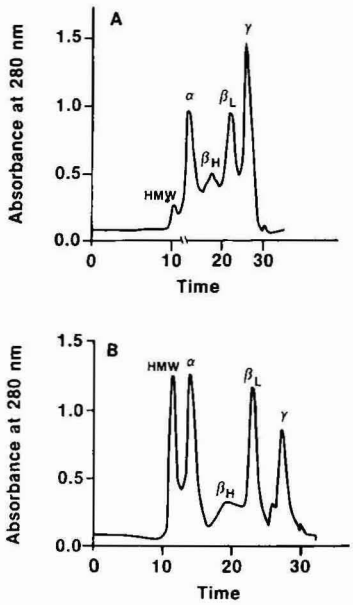

Fig. 1. Molecular sieve HPLC separation of lens crystallins from 6-week-old rat lens (A) and 2-year-old rat lens (B). Time is in minutes.

well as correlation with the established molecular weights of each protein[5].

Each peak was subsequently collected, dialyzed against water and lyophilized. The lyophilized protein was then subjected to amino acid analysis. The results shown in Table I confirm that the peaks correspond to α, β_{high}, β_{low}, and γ-crystallin.

Molecular sieve separations of lens crystallins from old and young rat lenses

Molecular sieve HPLC techniques provide a remarkable opportunity for micro-analytical experiments. An example of this capability is shown in Fig. 1 where lenses from individual animals were homogenized and 100 μg of the water-soluble fraction was injected onto HPLC. The resulting chromatogram depicts the different crystallin distribution that exists between 6-week-old rats *vs.* 2-year-old rats. The results show a dramatic decrease in the γ-crystallin fraction from 32% in the young animal to 16% in the older animal. Also shown is the increase in the high molecular weight fraction from 3% in the young rat to 18% in the older animals. Table II gives the summary of the results obtained for seven 6-week-old rats and seven 2-year-old rats. Similar changes have been reported previously where separations of crystallins was achieved by Sephadex G-200[1].

Reversed-phase separation of crystallin subunits

The α- and β-crystallins are composed of several individual subunits which have been isolated previously with CM-cellulose–urea chromatography[8], urea chromatofocusing[7], and urea isoelectric focusing[9]. Using the reversed-phase HPLC system it was possible to separate the major polypeptide subunits of the α- and β-crystallins in one step. Fig. 2 depicts the separation of the lens crystallin subunits using

TABLE I

AMINO ACID COMPOSITION OF LENS CRYSTALLINS OBTAINED FROM MOLECULAR SIEVE HPLC

Values in parentheses are expected values (ref. 1).

Amino acid	*Peak*			
	α	β_{high}	β_{low}	γ
Asp	75 (73)	71 (73)	88 (85)	165 (166)
Thr	34 (35)	24 (29)	30 (30)	29 (30)
Ser	106 (105)	79 (79)	79 (81)	77 (76)
Glu	112 (107)	150 (146)	148 (146)	126 (127)
Pro	78 (82)	58 (60)	56 (59)	48 (48)
Gly	65 (61)	96 (93)	93 (91)	55 (57)
Ala	42 (45)	54 (54)	49 (49)	31 (29)
Cys	– –	12 (17)	5 (9)	– –
Val	61 (59)	60 (61)	64 (63)	50 (50)
Met	13 (12)	17 (18)	9 (10)	31 (30)
Ile	48 (48)	31 (33)	37 (35)	36 (36)
Leu	86 (88)	53 (53)	64 (62)	70 (70)
Tyr	– (32)	30 (41)	– (41)	76 (83)
Phe	82 (77)	45 (48)	44 (43)	57 (57)
Trp	– –	42 (45)	41 (38)	– –
Lys	50 (49)	43 (43)	58 (54)	24 (25)
His	40 (39)	39 (41)	42 (44)	35 (35)
Arg	76 (74)	65 (67)	60 (61)	115 (111)

200 μg of the water-soluble fraction. With the use of volatile solvents in this system, identification of each peak by amino acid analysis becomes a simple procedure. Table III gives the results of the amino analysis identification of the subunits obtained by reversed-phase HPLC. The slight variation between expected values and our results reflect species differences. However, there were no gross differences which would indicate a noncrystallin subunit.

The results show both separation and quantitation of the αA and αB subunits from α-crystallin. Using the area under each peak to quantitate the individual subunits a ratio of αA:αB = 3.4:1 is found which correlates to the approximate 3:1 ratio reported previously[10]. Similarly, the β-crystallins separate well into the major Bp

TABLE II

LEVELS OF THE VARIOUS LENS CRYSTALLINS AS DETERMINED BY MOLECULAR SIEVE HPLC IN 6-WEEK-OLD RATS (n = 7) AND 2-YEARS-OLD RATS (n = 7)

	Lens crystallin			
	HMW (%)	*α (%)*	*β (%)*	*γ (%)*
Young	3.8 ± 1.2*	26.7 ± 3.1	36.9 ± 4.2	32.6 ± 3.9
Old	18.9 ± 5.8	28.4 ± 4.4	30.8 ± 5.2	21.9 ± 4.7

* Mean ± S.D.

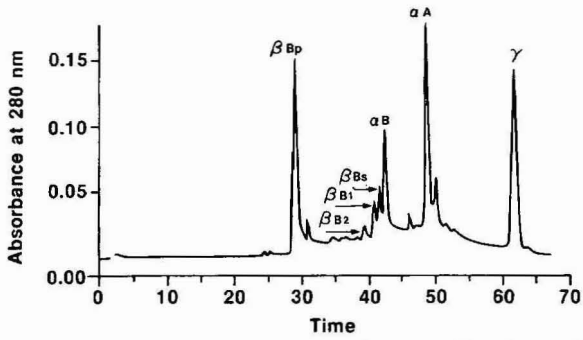

Fig. 2. Reversed-phase HPLC separation on a C_4 column of lens crystallin subunits from total soluble fraction. Time is in minutes.

subunit and the minor components B1, B2, and βs. Quantitation of the β-crystallin subunits indicate that the major subunit Bp comprises approximately 65% of the intact β-crystallin. The γ-crystallin consists of a single polypeptide and therefore elutes as a single peak.

Comparison between molecular sieve vs. reversed-phase HPLC system

Peaks were isolated from the molecular sieve HPLC and 100 μg of each α, β, and γ-crystallin was injected individually onto the reversed-phase HPLC system. The results depicted in Fig. 3 show that the polypeptide subunits of α-, β-, and γ-crystallins

TABLE III

AMINO ACID COMPOSITION OF CRYSTALLIN SUBUNITS OBTAINED BY REVERSED-PHASE HPLC

Values in parentheses represent expected values (ref. 1). Peak 1–6 are from bovine, peak 7 is from rat.

Amino acid	*Peak 1 βBp*	*Peak 2 βBs*	*Peak 3 βB2*	*Peak 4 βB1*	*Peak 5 αB*	*Peak 6 αA*	*Peak 7 γ*
Asp	85 (83)	78 (80)	82 (80)	90 (89)	80 (75)	93 (97)	165 (166)
Thr	27 (34)	30 (28)	37 (35)	25 (28)	42 (44)	30 (37)	29 (30)
Ser	86 (84)	77 (75)	88 (85)	61 (61)	92 (96)	125 (126)	77 (76)
Glu	155 (158)	142 (148)	152 (158)	120 (126)	110 (100)	99 (95)	130 (127)
Pro	68 (68)	72 (76)	51 (49)	37 (37)	86 (94)	65 (67)	50 (48)
Gly	91 (93)	78 (80)	99 (106)	83 (87)	58 (56)	63 (60)	55 (57)
Ala	40 (42)	54 (58)	49 (53)	52 (57)	49 (53)	36 (35)	30 (29)
Cys	10 (09)	— —	14 (13)	30 (37)	00 (00)	05 (06)	— —
Val	72 (75)	58 (59)	68 (67)	47 (49)	52 (55)	54 (55)	50 (50)
Met	11 (09)	21 (18)	07 (09)	27 (33)	19 (13)	13 (12)	28 (30)
Ile	25 (31)	33 (32)	30 (26)	37 (41)	38 (47)	45 (50)	32 (36)
Leu	48 (50)	45 (47)	62 (59)	57 (57)	84 (84)	82 (84)	70 (70)
Tyr	47 (44)	45 (43)	50 (47)	59 (65)	17 (14)	29 (33)	70 (83)
Phe	42 (40)	52 (50)	60 (55)	57 (57)	73 (70)	77 (78)	60 (57)
His	44 (41)	39 (37)	46 (47)	43 (41)	50 (47)	38 (41)	37 (35)
Lys	59 (60)	59 (60)	50 (52)	47 (49)	54 (58)	38 (41)	24 (25)
Arg	52 (50)	87 (90)	68 (62)	74 (73)	82 (78)	80 (73)	110 (111)

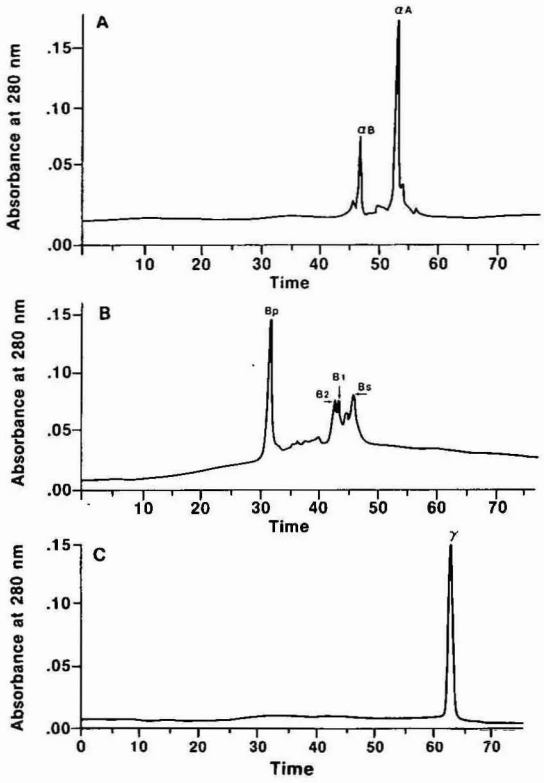

Fig. 3. Reversed-phase HPLC separations on a C_4 column of the subunits of α-crystallin (A), β-crystallin (B), and γ-crystallin (C). Time is in minutes.

elute in the exact position expected from the amino acid analysis data. This helps to demonstrate both the identity of the peaks obtained by reversed-phase HPLC as well as the relative purity of the lens crystallins obtained from the molecular sieve HPLC system.

DISCUSSION

The lens crystallins have been routinely separated by gel filtration or DEAE-cellulose into four classes: α-, β_{high}-, β_{low}-, and γ-crystallins. Each method, however, has its own inherent problems. To separate such large molecular weight proteins as the lens crystallins, molecular sieve gels such as Sephadex G-200 or Bio-Gel A5M must be used. These large pore gels are very fragile requiring a great deal of care in packing and slow flow-rates. DEAE-cellulose requires extensive equilibration of the column as well as sample equilibration. With the advent of HPLC molecular sieve columns the separation of proteins has become simplified. We have demonstrated excellent separations of the lens crystallins and their subunits using molecular sieve HPLC and reversed-phase HPLC. Molecular sieve HPLC only recently became available through the use of macroporous silica based supports. Bindels *et al.*[11,12] originally used these TSK columns to separate the bovine lens crystallins. Their system

employed a guard column, one TSK 4000 SW column, and two TSK 3000 SW columns connected in series with a low-angle laser light scattering detection system. Their results showed separation of all the lens crystallins and resolved the β-crystallins into up to eight discernable fractions. However, they were not able to resolve adequately the high-molecular-weight aggregate (HM-crystallin) from the α-crystallin and the α-crystallin showed excessive tailing. In our earlier experience with the TSK columns we were not able to ressolve the HM-crystallin from the α-crystallin when a guard column was included in the system. Presumably the HM-crystallin is too large to pass through the guard column and the loose packing possibly results in a dead volume which would cause the peak tailing.

Ample evidence has now accumulated that the new HPLC molecular sieve columns are weakly anionic and slightly hydrophobic. It is often overlooked that this deviation from the ideal behavior of a size exclusion column may be manipulated to the point where great selectivity between select molecular species is obtained. Kopaciewicz and Regnier[13] demonstrated that by varying the pH and the ionic strength of the mobile phase, the retention behavior of myoglobin and ovalbumin may be adjusted for optimum separations. Similar results may be obtained with the lens crystallins. By varying the pH from 6.0 to 7.0 and the ionic strength from 0.25 to 0.1 we were able to achieve a variety of separations of the lens crystallins. Since our current research involves the HM-crystallins we chose the conditions described here for our experimental separations. However, ideal separation based solely on molecular weight may be obtained by merely maintaining an ionic strength above 0.2. Our experience has been that after over 300 runs the separations are still excellent with no tailing of peaks or changes in elution patterns. Sample size has been varied from 100 μg to 20 mg with no effect on results. The only limitation is that the ionic strength be high enough to obviate any ionic or absorption effects (50 mM salts are sufficient) and a pH between 2 and 8. Manufacturers claim that sample sizes of up to 60 mg may be applied without overloading the column. This capacity allows for semipreparative operations with extremely short turn-around time.

In the past the subunits of α- and β-crystallins have been separated by CM-cellulose urea chromatography, urea chromatofocusing or urea isoelectric focusing[7–9]. The largest drawback to these procedures is the extensive sample preparation before and after. Desalting, removal of urea and ampholines, requires long term dialysis or gel filtration both of which involve time and sample losses. The Vydac C_4 column has a large pore size and short hydrocarbon reactive side chains which practically eliminate the irreversible binding found in conventional C_{18} columns. Described here is a one-step separation of the polypeptide subunits of the lens crystallins. The TFA–water–acetonitrile gradient has the advantage not only of simplicity but also of volatility so that subsequent operations such as amino acid analysis, sequencing, etc. may be done after evaporation of the solvent. Additionally, with only slight modifications of the buffers and gradient it is possible to achieve separation of the post-translationally modified crystallins such as the deaminated αA_2 and αB_2 polypeptides from the αA_1 and αB_1 counterparts. These simple and rapid techniques provide methods for effective and sensitive examination of progressive changes which occur within the lens during aging, differentiation, and disease states.

ACKNOWLEDGEMENTS

Supported in part by a grant from American Diabetes Association, Inc. We thank Dr. Brooke Webber for his assistance in the amino acid analysis.

REFERENCES

1 J. J. Harding and K. J. Dilley, *Exp. Eye Res.*, 22 (1976) 1.
2 H. Bloemendal, *Science*, 197 (1977) 127.
3 W. W. de Jong, in H. Bloemendal (Editor), *Molecular and Cellular Biology of the Eye Lens*, Wiley, New York, 1981, p. 221.
4 A. Spector and D. Roy, *Proc. Natl. Acad. Sci. U.S.A.*, 75 (1978) 3244.
5 F. A. M. Asselberys, M. Koopmans, W. J. van Venrooij and H. Bloemendal, *Exp. Eye Res.*, 28 (1979) 223.
6 A. Spector, L. K. Li, R. C. Augusteyn, A. Schneider and T. Freund, *Biochem. J.*, 124 (1971) 337.
7 H. Bloemdal and G. Groenewood, *Anal. Biochem.*, 117 (1981) 327.
8 R. C. Augusteyn and A. Spector, *Biochem. J.*, 124 (1971) 345.
9 P. Herbrink and H. Bloemendal, *Biochim. Biopohys. Acta*, 336 (1974) 370.
10 J. Delcour and J. Papaconstantinou, *Biochem. Biophys. Res. Commun.*, 57 (1974) 134.
11 J. G. Bindels, B. M. De Man and H. J. Hoenders, *J. Chromatogr.*, 252 (1982) 255.
12 J. G. Bindels and H. J. Hoenders, *J. Chromatogr.*, 261 (1983) 381.
13 B. Kopaciewicz and F. E. Regnier, in M. T. W. Hearn, F. E. Regnier and C. T. Wehr (Editors), *High Performance Liquid Chromatography of Proteins and Peptides*, Academic Press, New York, 1983, p. 150.

Journal of Chromatography, 351 (1986) 111–121
Elsevier Science Publishers B.V., Amsterdam — Printed in The Netherlands

CHROM. 18 190

Note

Use of Kováts retention indices for characterization of solutes in linear temperature-programmed capillary gas–liquid chromatography

J. KRUPČÍK
Department of Analytical Chemistry, Chemical Faculty, Slovak Technical University, Janska 1, 812 37 Bratislava (Czechoslovakia)
P. CELLAR
Analytical Laboratory, VVZ, Slovnaft, 824 12 Bratislava (Czechoslovakia)
D. REPKA and J. GARAJ
Department of Analytical Chemistry, Chemical Faculty, Slovak Technical University, Janska 1, 812 37 Bratislava (Czechoslovakia)
and
GEORGES GUIOCHON*
Department of Chemistry, Georgetown University, 37 and O Streets N.W., Washington, DC 20057 (U.S.A.)
(Received September 17th, 1985)

Kováts retention indices[1] are generally considered to be the most practical parameter to characterize the retention of compounds in gas chromatography[2]. These indices are defined after the isothermal retention time of the compounds of interest and of the *n*-alkanes eluted immediately before and after them:

$$I = 100z + 100\frac{\log(t'_{R,i}/t'_{R,z})}{\log(t'_{R,z+1}/t'_{R,z})} \quad (1)$$

In linear temperature-programmed gas chromatography (LTPGC) the retention time of *n*-alkanes increases linearly with the number of carbon atoms, so Van den Dool and Kratz[3] proposed to calculate the retention indices by a linear interpolation:

$$I_{\text{prog}} = 100z + 100\frac{T_{R,i} - T_{R,z}}{T_{R,z+1} - T_{R,z}} \quad (2)$$

where $T_{R,i}$ is the retention temperature of compound *i*. Since the isothermal retention indices do vary, albeit slowly, with temperature, there has been much attention devoted to the derivation of a reliable relationship between the programmed retention indices and the isothermal indices measured at some "equivalent temperature".

Van den Dool and Kratz[3] found a good agreement between programmed indices and the isothermal indices measured at the retention temperature (equivalent temperature equal to retention temperature). Guiochon[4] has shown that there is a better agreement if the equivalent temperature is taken as T_R minus 20°C. Giddings[5] suggested that the equivalent temperature is equal to $0.92T_R$. Lee and Taylor[6] found

that the equivalent temperature is better approximated by the harmonic mean between the retention temperature and the initial temperature of the programmed run: $T = 2T_R \cdot T_0/(T_R + T_0)$.

Golovnya and Uraletz[7] preferred to calculate the programmed indices as the arithmetic average between the isothermal indices at the retention temperature and at the initial temperature of the run. Other authors[8,9] have used polynomial dependence between retention temperature in LTPGC and the number of carbon atoms of the *n*-alkanes involved.

Kratzsch[10] and Anders *et al.*[11] have used iterative processes to recalculate retention times and decrease the differences found between isothermal and temperature programmed retention indices. They have not taken the thermal variation of the isothermal indices into account, however.

Unfortunately none of these approaches has been entirely successful and it is generally considered that the agreement between retention indices measured in LTPGC and those derived from isothermal data is not satisfactory for identification purposes[12].The aim of this work is to present an alternative approach to the use of isothermal retention indices for the identification of compounds separated by LTPGC.

THEORETICAL

We shall make the following, simplifying asumptions:

(i) Linear temperature programming begins when the sample is injected. There is no isothermal period at the beginning of the run.

(ii) All compounds considered are eluted in LTPGC conditions. This precludes applicability of the method to early eluting compounds, with retention temperature below $1.09T_0$ (ref. 5).

(iii) The isothermal retention indices vary linearly with temperature ($\mathrm{d}I/\mathrm{d}T$ = constant).

(iv) The experimental conditions, and especially the initial temperature and carrier gas flow-rate, are kept constant.

Under these conditions it is observed that the retention indices of *n*-alkanes (which are, by definition, equal to one hundred times the number of their carbon atoms) are not linearly related to their retention temperatures in LTPGC (*cf.* Fig. 1). The slope of each segment on this figure depends both on the program rate ($a = \mathrm{d}T/\mathrm{d}t$) and on the number of carbon atoms of the alkane considered. It must be observed, however, that for a starting temperature of 40°C, only the compounds which are eluted at a temperature above $(273 + 40)/0.92 = 340$ K or 67°C can be considered as eluted in actual temperature programming conditions[5,13]. This is not the case of *n*-heptane in most of the experiments reported in Fig. 1 (except for $a =$ 0.8 and 1°C/min), nor even of *n*-octane in the two first runs ($a = 0.1$ and 0.2°C/min). This explains in part the non-linear behavior of the plots on Fig. 1[13].

If the asumption of Van den Dool and Kratz[3] is correct and the programmed temperature index is equal to the isothermal index at the elution temperature, $T_{R,i}$, we can relate that temperature to the known value of the index at some reference temperature and the coefficient of thermal variation of the index. As a first approximation, it has been shown that the index of most compounds increases linearly with temperature:

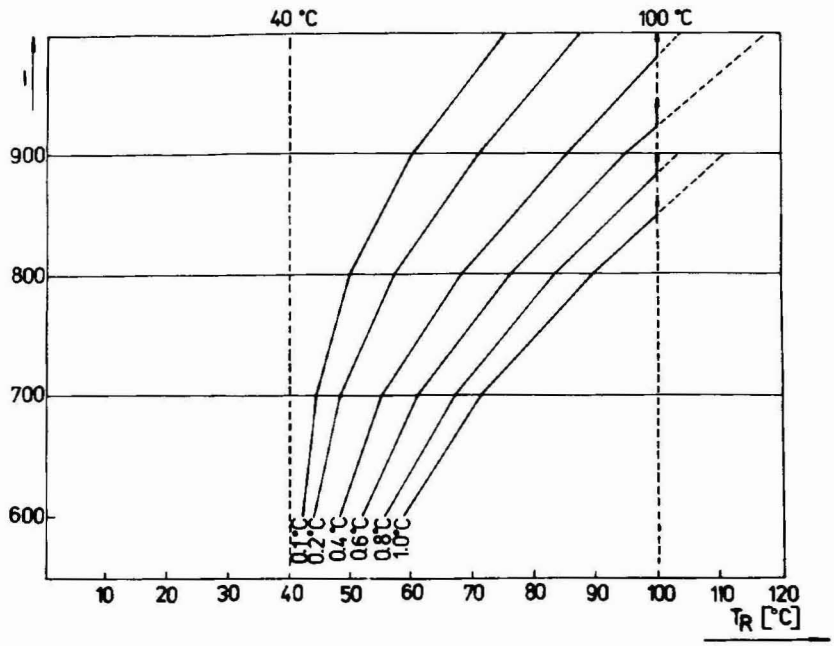

Fig. 1. Plot of retention indices of *n*-alkanes *versus* their elution temperature. Column B, squalane. The temperature gradient is indicated on each line.

$$I(T_{R,i}) = I(T_1) + (T_{R,i} - T_1)i \tag{3}$$

with:

$$i = \frac{dI}{dT} \tag{4}$$

For most branched, cyclic and aromatic hydrocarbons dI/dT is between 0 and 0.3 unit/°C (*cf.* data below).

If now we equal eqns. 2 and 3 and solve for $T_{R,i}$, we obtain:

$$T_{R,i} = \frac{[I(T_1) - 100 \cdot z - i \cdot T_1](T_{R,z+1} - T_{R,z}) + 100 \cdot T_{R,z}}{100 - i(T_{R,z+1} - T_{R,z})} \tag{5}$$

Deviations between experimental values of $T_{R,i}$ and those calculated from eqn. 5 are easy to determine. They are a measure of the validity of the asumptions that (i) the elution actually takes place in programmed-temperature conditions and that (ii) the programmed-temperature index is closely approximated by the isothermal index at the retention temperature. Other asumptions such as the one suggested by Giddings[5] can be checked by replacing $100 - i(T_{R,z+1} - T_{R,z})$ in the denominator of the right-hand side of eqn. 5 by $100 - 0.92 \cdot i(T_{R,z+1} - T_{R,z})$.

The difference between our approach and the one taken originally by Van den Dool and Kratz[3] is illustrated in Fig. 2. In the first case[3], one can derive the retention

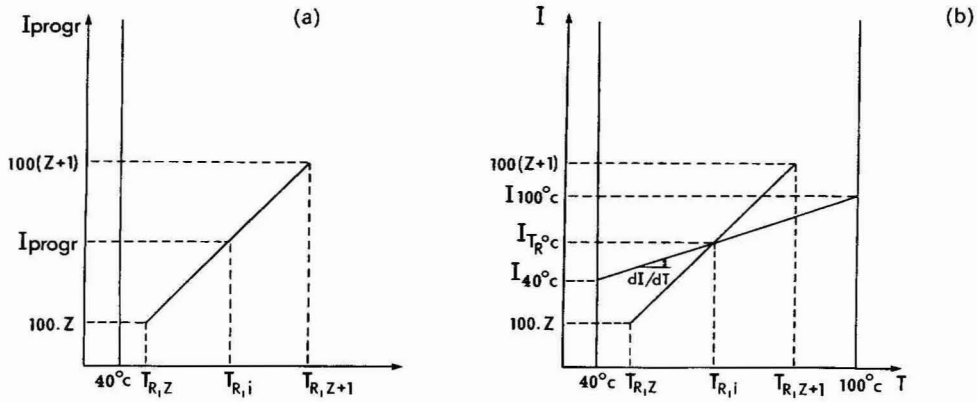

Fig. 2. Comparison between the methods described by Van den Dool and Kratz[3] (a) and by this work (b) for the determination of the retention temperature. This diagram illustrates how the temperature dependence of the isothermal retention indices is taken into account for the determination of the retention temperature.

TABLE I

LIST OF COMPOUNDS IN THE MODEL MIXTURE

Name	*Abbreviation*
1,1,3-Trimethylcyclopentane	1,1,3-Tri-MeCyPe
1-*trans*-2-*cis*-4-Trimethylcyclopentane	1-Tr-2-Cis-4-TriMeCyPe
1-*trans*-2-*cis*-3-Trimethylcyclopentane	1-Tr-2-Cis-3-TriMeCyPe
1,1,2-Trimethylcyclopentane	1,1,2-TriMeCyPe
1-*cis*-2-*trans*-4-Trimethylcyclopentane	1-Cis-2-Tr-4-TriMeCyPe
1-*cis*-2-*cis*-4-Trimethylcyclopentane	1-Cis-2-Cis-4-TriMeCyPe
1-*cis*-2-*trans*-3-Trimethylcyclopentane	1-Cis-2-Tr-3-TriMeCyPe
1-Methyl-*cis*-3-ethylcyclopentane	1-MeCis-3-EtCyPe
1-Methyl-*trans*-3-ethylcyclopentane	1-MeTr-3-EtCyPe
1-Methyl-*trans*-2-ethylcyclopentane	1-MeTr-2-EtCyPe
1-Methyl-1-ethylcyclopentane	1-Me-1-EtCyPe
Isopropylcyclopentane	iso-ProCyPe
1-Methyl-*cis*-2-ethylcyclopentane	1-MeCis-2-EtCyPe
Propylcyclopentane	n-ProCyPe
1-*cis*-2-*cis*-3-Trimethylcyclopentane	1-Cis-2-Cis-3-TriMeCyPe
1-*trans*-4-Dimethylcyclohexane	1-Tr-4-DiMeCyHex
1,1-Dimethylcyclohexane	1,1-DiMeCyHex
1-*cis*-3-Dimethylcyclohexane	1-Cis-3-DiMeCyHex
1-*trans*-2-Dimethylcyclohexane	1-Tr-2-DiMeCyHex
1-*trans*-3-Dimethylcyclohexane	1-Tr-3-DiMeCyHex
1-*cis*-4-Dimethylcyclohexane	1-Cis-4-DiMeCyGHex
1-*cis*-2-Dimethylcyclohexane	1-Cis-2-DiMeCyHex
Ethylcyclohexane	EtCyHex
Ethylbenzene	EtBe
1,4-Dimethylbenzene	*p*-Xylene
1,3-Dimethylbenzene	*m*-Xylene
1,2-Dimethylbenzene	*o*-Xylene

index from the retention temperature, as indicated in Fig. 2a. To relate the programmed-temperature and the isothermal indices, one has to assume that the isothermal index does not depend on the temperature, which is only approximative. As shown in Fig. 2b, we take directly the temperature dependence of the isothermal retention index into account. Then the difference between the predicted and the measured retention temperatures derives mainly from the effect of experimental errors, such as the reproducibility of the oven temperature, the temperature gradient inside the oven, the influence of a secondary retention mechanism due to solid–gas or liquid–gas adsorption.

The validity of this approach has been studied in the simple case of complex hydrocarbon mixtures analyzed on squalane.

EXPERIMENTAL

A model mixture containing mostly C_8 cyclopentanes, cyclohexanes and aromatic hydrocarbons was prepared by catalytic hydrogenation of a C_8 aromatic hy-

TABLE II

KOVÁTS INDICES OF COMPOUNDS EXPERIMENTALLY FOUND (I_F) AND PUBLISHED[14] (I_P) AT 50°C ON SQUALANE AS WELL AS EXPERIMENTALLY FOUND TEMPERATURE INCREMENTS OF KOVÁTS INDICES ($\Delta I/10°C$)

Compound No.	*Abbreviation*	I_F	I_P	$\Delta I/10°C$
8	1,1,3-TriMeCyPe	723.7	723.6	1.91
13	1-Tr-2-Cis-4-TriMeCyPe	741.0	741.1	1.69
15	1-Tr-2-Cis-3-TriMeCyPe	747.8	747.8	1.65
17	1,1,2-TriMeCyPe	763.4	763.2	2.32
20	1-Cis-2-Tr-4-TriMeCyPe	773.0	773.1	2.18
21	1-Cis-2-Cis-4-TriMeCyPe	774.8	774.6	2.19
22	1-Cis-2-Tr-3-TriMeCyPe	778.8	778.6	2.21
23	1-Cis-3-DiMeCyHex	785.1	784.7	2.42
24	1-Tr-4-DiMeCyHex	785.6	784.9	2.20
25	1,1-DiMeCyHex	787.1	787.0	2.91
26	1-MeTr-3-EtCyPe	787.7	787.6	1.99
27	1-MeCis-3-EtCyPe	790.3	790.3	1.92
28	1-MeTr-2-EtCyPe	791.2	790.8	1.90
29	1-Me-1-EtCyPe	794.0	793.6	2.0
31a	1-Cis-2-Cis-3-TriMeCyPe	802.3	802.2	–
31	1-Tr-2-DiMeCyHex	801.8	801.8	2.75
32	1-Cis-4-DiMeCyHex	805.0	805.2	2.61
33	1-Tr-3-DiMeCyHex	805.4	805.6	2.67
34	iso-ProCyPe	812.0	812.1	2.47
35	1-MeCis-2-EtCyPe	820.7	821.0	2.33
36	1-Cis-2-DiMeCyHex	829.0	829.3	3.07
37	*n*-ProCyPe	829.9	830.3	1.84
38	EtBe	833.3	834.6	2.62
39	EtCyHex	834.3	834.3	2.69
41	*p*-Xylene	848.0	848.3	2.47
42	*m*-Xylene	850.2	850.3	2.20
43	*o*-Xylene	968.4	968.8	2.85

drocarbon sample[14]. The qualitative composition of the sample is given in Table I.

This mixture was analyzed in isothermal conditions on a 180 m × 0.25 mm I.D. open-tubular glass column coated with squalane (column A), at 40, 50, 60, 69 and 82°C. Analysis of this mixture with addition of *n*-heptane, *n*-octane and *n*-nonane allowed the determination of the retention indices and their thermal coefficient (*cf.* Table II). Another squalane column, made with a 100 m × 0.25 mm I.D. stainless-steel tube (column B), was used to carry out isothermal analysis at 40, 70 and 100°C, as well as LTPGC analysis with program rates of 0.1, 0.2, 0.4, 0.6, 0.8 and 1.0°C/min.

Details about the preparation of the column are given elsewhere[14].

Column A was used with a Fractovap 2350 gas chromatograph (Carlo Erba, Milan, Italy) and column B with an HP 5880A (Hewlett-Packard, Avondale, PA, U.S.A.), both equipped with flame ionization detectors and using nitrogen as carrier gas. Elution temperatures were derived from the elution time measured with a digital integrator and the known temperature program rate. Because of the relatively high vapor pressure of squalane, temperature-programmed runs had to be stopped at 100°C in order not to lose stationary phase.

Fig. 3 shows four of the chromatograms obtained with the model mixture on column A. Fig. 4 shows five chromatograms obtained with column B, in gradient elution at different program rates. It is seen that even with a mixture of hydrocarbons of relatively low polarity the elution order of some component pairs changes with temperature. Accordingly, this order changes also with program rate in LTPGC.

Also in Table II are reported values of the retention indices found in the lit-

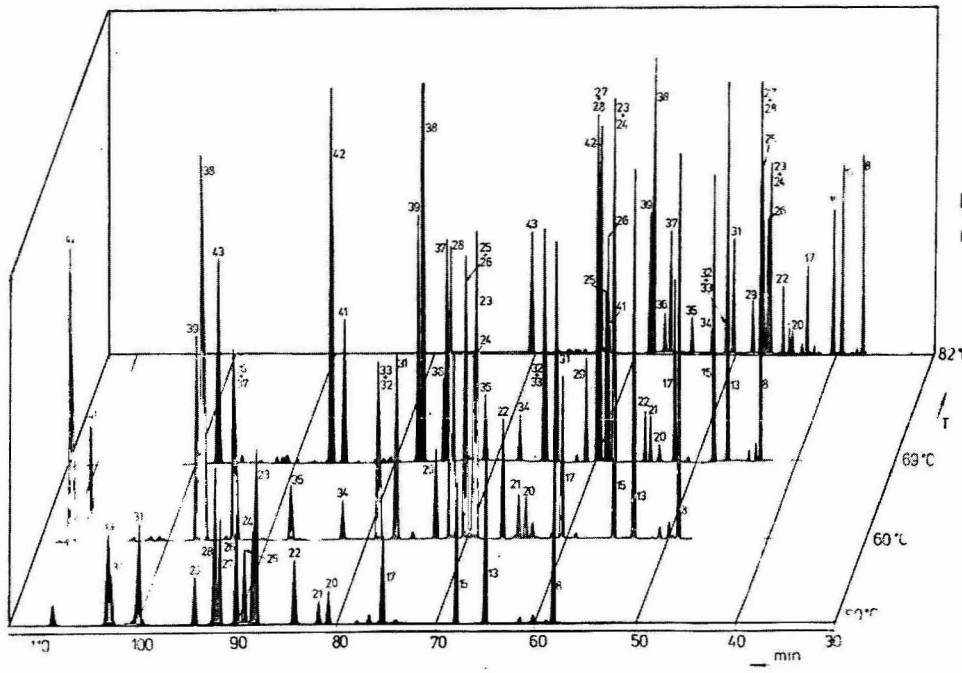

Fig. 3. Chromatograms obtained in isothermal conditions at different temperatures for a hydrocarbon mixture (*cf.* Table I). Column A, squalane. For peak identification, see compound Nos. in Table II.

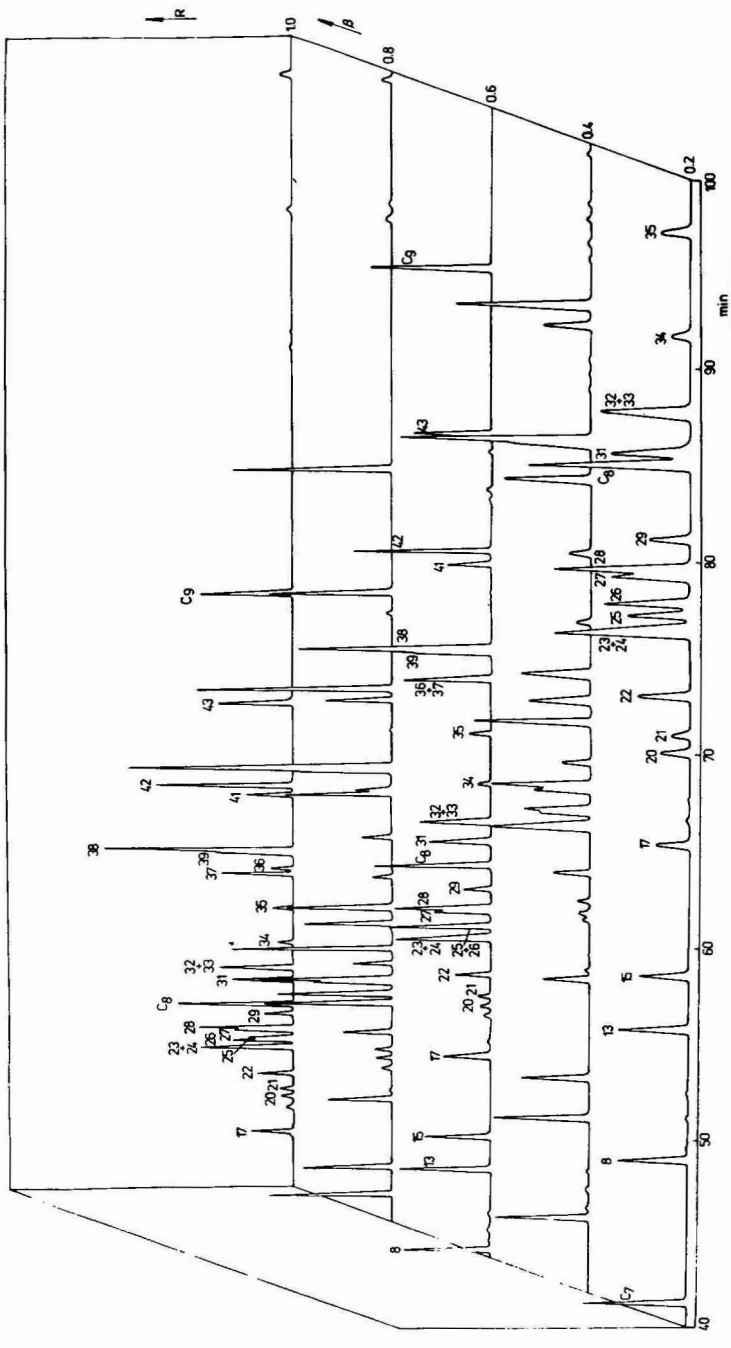

Fig. 4. Chromatograms obtained in LTPGC for a hydrocarbon mixture (*cf.*, Table II and Fig. 3). Column B, squalane. Different temperature program rates, as indicated on the right-hand-side axis. For peak identification, see compound Nos. in Table II.

erature[14] for the component of our model mixture. The agreement is excellent. The average difference between the two sets of experimental data is 0.03 index unit, while the standard deviation of the differences is 0.4 unit.

RESULTS AND DISCUSSION

Eqn. 5 permits the prediction of the retention temperature in LTPGC from the retention index and its thermal coefficient (*cf.*, Table II), and from the retention temperatures of two *n*-alkanes.

An alternative graphic procedure can be used. Fig. 5 shows a plot of the retention index of 27 of the model mixture components *versus* column temperature (in isothermal conditions). Straight lines are obtained. Their slopes are equal to $i = dI/dT$ (*cf.* eqn. 4). Fig. 5 also shows the straight lines (program lines) joining the points I, $T_{R,z}$ for *n*-heptane, *n*-octane and *n*-nonane at various program rates (column B). If the asumption that the programmed temperature index is equal to the isothermal index at the retention temperature is valid, the retention temperature is given by the abscissa of the point at which the plot of isothermal index *versus* temperature cuts the corresponding program line. This procedure is illustrated in Fig. 6 for 1,1,2-trimethylcyclopentane. This procedure is simpler than the use of eqn. 5 (unless a modern programmable pocket calculator is available), and turns out to be as pre-

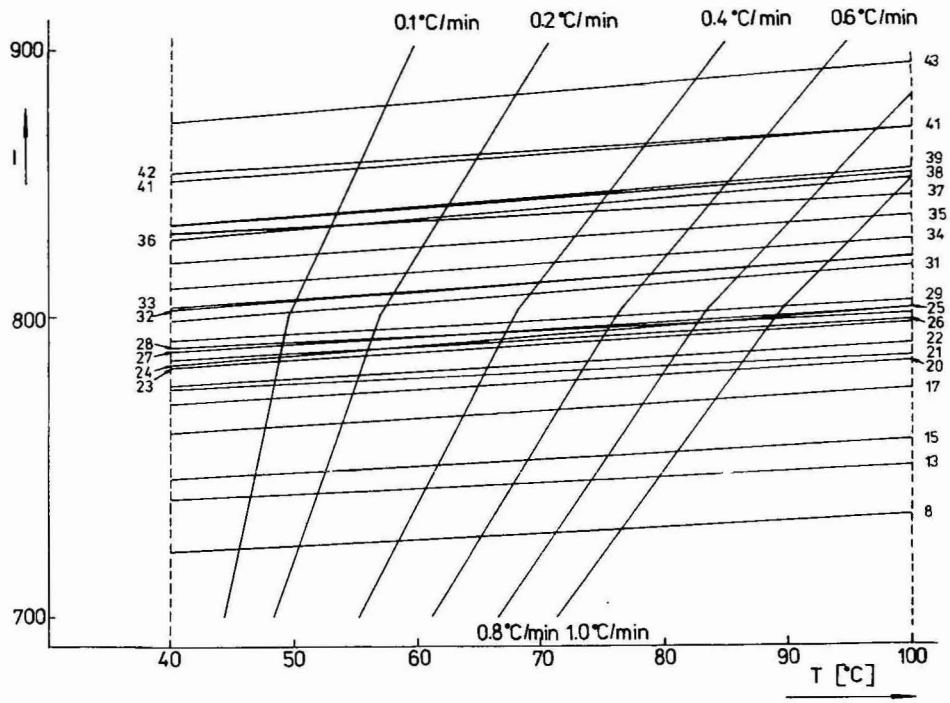

Fig. 5. Plot of isothermal retention index of hydrocarbons (*cf.* Table I) *versus* temperature and program lines of *n*-alkanes for different program rates, as indicated on these lines (*cf.* text). For compound Nos., see Table II.

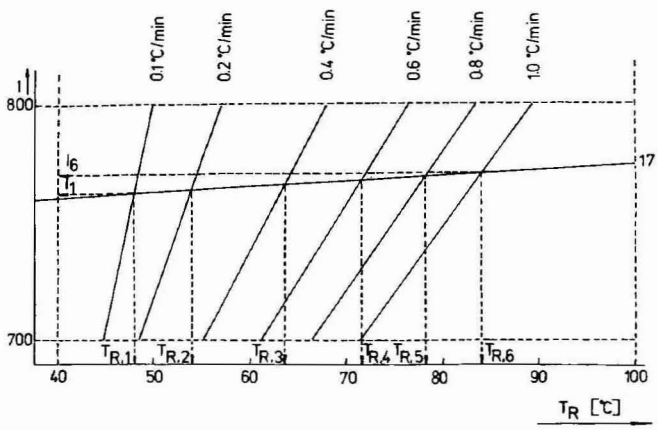

Fig. 6. Graphical procedure for the determination of the retention temperature of 1,1,2-trimethylcyclopentane (compound No. 17) at different temperature program rates.

TABLE III

KOVÁTS INDICES OF CYCLIC AND AROMATIC HYDROCARBONS AT EXPERIMENTALLY FOUND (I_F) AND PREDICTED (I_{Pr}) ELUTION TEMPERATURES IN LTPGC USING DIFFERENT TEMPERATURE PROGRAM RATES

Compound No.	*0.1°C/min*		*0.2°C/min*		*0.4°C/min*		*0.6°C/min*		*0.8°C/min*		*1.0°C/min*	
	I_F	I_{Pr}	I_F	I_{Pr}	I_F	I_{Pr}	I_F	I_{Pr}	I_F	I_{Pr}	I_F	I_{Pr}
8	722.7	722.7	723.6	723.7	725.1	725.2	726.3	726.5	727.4	727.6	728.4	728.7
13	740.4	740.5	741.3	741.4	742.7	742.9	743.9	744.1	745.0	745.2	745.9	746.1
15	747.2	747.3	748.1	748.2	749.5	749.7	750.7	750.9	751.6	752.0	752.7	752.9
17	762.6	762.7	763.9	764.1	766.1	766.4	767.9	768.2	769.4	769.7	770.8	771.1
21	–	774.3	775.5	775.7	777.7	778.0	779.5	779.7	781.0	781.3	782.2	782.6
22	778.2	778.3	779.6	779.8	781.9	782.0	783.7	783.9	785.2	785.4	786.5	786.8
23	784.4	784.4	786.0	786.1	788.5	788.7	790.5	790.7	792.2	792.4	793.7	793.9
24	784.6	784.7	786.1	786.2	788.4	788.6	790.2	790.4	791.7	791.9	793.1	793.3
25	786.6	786.7	788.6	788.8	791.7	791.9	794.1	794.4	796.1	796.5	797.9	798.4
26	787.4	787.4	788.7	788.8	790.8	791.0	792.5	792.6	793.8	794.0	795.0	795.2
27	790.1	790.1	791.4	791.5	793.5	793.6	795.1	795.2	796.4	796.6	797.6	797.8
28	790.6	790.6	791.9	792.0	794.0	794.0	795.6	795.7	796.9	797.0	798.0	798.2
29	793.4	793.5	794.9	794.9	797.0	797.1	798.7	798.8	800.1	800.3	801.4	801.6
31	–	801.7	803.8	803.9	806.8	807.1	809.2	809.6	811.2	811.6	813.0	813.5
32	805.2	805.3	807.2	807.3	810.1	810.4	812.4	812.7	814.3	814.8	816.0	816.5
33	805.6	805.7	807.6	807.8	810.6	810.9	813.0	813.3	814.9	815.4	816.6	817.2
34	812.2	812.3	814.2	814.3	817.0	817.3	819.2	819.6	821.0	821.5	822.6	823.2
35	821.3	821.5	823.2	823.4	826.0	828.7	828.1	828.5	829.8	830.3	831.3	831.9
36	829.9	830.3	832.5	833.0	836.3	836.9	839.1	839.9	841.5	842.5	843.5	844.6
37	830.7	830.9	832.3	832.5	834.5	834.8	836.2	836.5	837.6	838.0	838.8	839.2
38	835.3	835.5	837.6	837.9	840.8	841.3	843.3	843.8	845.3	846.0	847.0	–
39	835.0	835.8	837.9	838.4	841.4	842.0	844.0	844.6	846.2	847.0	–	–
41	849.3	849.6	851.5	852.0	854.7	855.3	857.1	857.7	859.1	859.9	–	–
42	851.2	851.5	853.2	853.6	856.1	856.6	858.2	858.7	860.0	860.7	–	–
43	970.5	970.9	973.4	974.0	977.3	978.1	980.1	981.0	982.5	–		

cise. The error is about 0.2°C, corresponding to a precision in the determination of the retention index of 0.1 unit, which is better than the reproducibility of the retention index measurement on the columns used.

A comparison between retention indices measured in LTPGC and derived by the graphic procedure is given in Table III. The largest deviation is 3.3°C, and is obtained for the compound which has the larger thermal coefficient *i*. Not surprisingly, there is a good correlation between the magnitude of the difference between calculated and observed temperature and the value of the thermal coefficient (*cf.* Table III).

Finally, in Table IV we compare the retention temperatures measured in LTPGC to those derived from eqn. 5. The largest difference is 1.1 unit, which is not large compared to the precision of the determination, if we take into account that in the case of this compound (No. 36), which is the one with the larger thermal coefficient (*ca.* 1.5), there are also larger sources of error in the determination of its

TABLE IV

ELUTION TEMPERATURES OF CYCLIC AND AROMATIC HYDROCARBONS AND C_7–C_9 *n*-ALKANES ON SQUALANE FOUND EXPERIMENTALLY ON COLUMN A (*F*) AND PREDICTED FROM EQN. 5 ON COLUMN B (*P*) IN LTPGC USING DIFFERENT TEMPERATURE PROGRAM RATES

Compound No.	*0.1°C/min*		*0.2°C/min*		*0.4°C/min*		*0.6°C/min*		*0.8°C/min*		*1.0°C/min*	
	F	*P*	*F*	*P*	*F*	*P*	*F*	*P*	*F*	*P*	*F*	*P*
8	45.3	45.5	49.8	50.3	57.6	58.3	64.3	65.1	70.1	71.0	75.3	76.5
13	46.1	46.5	51.2	52.0	59.7	60.5	66.8	67.7	73.0	74.0	78.4	79.5
15	46.4	46.8	51.8	52.5	60.5	61.6	67.8	69.0	73.1	75.4	79.6	80.9
17	47.2	47.8	53.1	53.9	62.6	63.8	70.3	71.5	76.9	78.2	82.7	84.1
21	–	48.5	54.3	55.1	64.2	65.4	72.2	73.2	79.0	80.4	84.9	86.4
22	48.2	48.5	54.7	55.4	64.8	65.6	72.9	73.8	79.7	80.8	85.7	87.0
23	48.6	48.8	55.3	55.8	65.7	66.5	74.0	74.9	81.0	82.0	87.1	88.1
24	48.6	48.9	55.3	55.9	65.7	66.6	74.0	74.9	81.0	82.0	87.1	88.1
25	48.7	49.0	55.5	56.1	66.1	66.9	74.4	75.4	81.4	82.8	87.6	89.0
26	48.8	49.0	55.6	56.1	66.1	66.9	74.4	75.2	81.4	82.3	87.4	88.4
27	49.0	49.1	55.9	56.2	66.5	67.0	74.9	75.6	81.9	82.7	88.0	88.9
28	49.1	49.2	56.0	56.3	66.6	67.1	75.0	75.6	82.0	82.7	88.1	88.9
29	49.2	49.3	56.3	56.6	67.1	67.6	75.5	76.1	82.7	83.3	88.8	89.8
31	–	49.8	57.2	57.5	68.3	69.2	77.0	78.2	84.3	85.8	90.6	92.6
32	50.1	50.2	57.6	58.1	68.9	69.8	77.7	78.9	85.0	86.6	91.3	93.4
33	50.1	50.3	57.6	58.2	68.9	69.8	77.7	78.9	85.0	86.6	91.3	93.4
34	50.6	51.0	58.4	59.1	70.0	71.2	78.8	80.3	86.2	88.1	92.6	94.8
35	51.4	52.0	59.5	60.5	71.4	82.9	80.4	82.1	87.9	89.9	94.4	96.9
36	52.1	53.1	60.5	62.0	72.9	74.9	82.0	84.5	89.9	92.9	96.4	99.7
37	52.2	53.1	60.7	61.8	72.9	74.4	82.0	83.6	89.7	91.9	96.2	98.6
38	52.6	53.5	61.3	62.5	73.8	75.5	83.1	85.1	90.9	93.4	97.4	–
39	52.6	53.5	61.3	62.6	73.8	75.6	83.1	85.3	90.9	93.8	97.4	–
41	53.9	55.2	63.1	64.9	76.1	78.4	85.6	88.1	93.6	97.1	–	–
42	54.2	55.5	63.4	65.1	76.5	78.6	86.1	88.4	94.1	97.2	–	–
43	56.1	57.5	66.1	68.1	79.8	82.6	89.8	92.9	98.0	–	–	–
C_7	44.1	–	48.3	–	55.2	–	61.1	–	66.5	–	71.3	–
C_8	49.8	–	57.1	–	67.9	–	76.3	–	83.3	–	89.3	–
C_9	59.9	–	70.7		85.0		94.9	–	–	–	–	–

retention time or temperature as it is difficult to separate it from its neighbours (Nos. 37 and 38) as can be seen in Figs. 2–4.

CONCLUSION

Provided the retention indices and their thermal coefficients can be measured in the temperature range in which the compounds studied are eluted in LTPGC, it is possible to predict with an acceptable precision the retention temperatures of hydrocarbons. The deviation remains of the order of the precision of the determination of the indices using efficient open tubular columns. Further work is necessary to assess the importance of the deviation with more polar compounds which have a larger thermal coefficient.

REFERENCES

1 E. sz. Kováts, *Adv. Chromatogr.*, 1 (1964) 1.
2 M. V. Budahegyi, E. R. Lombosi, T. S. Lombosi, S. Y. Mészáros, Sz. Nyiredy, G. Tarján, I. Timár and J. M. Takács, *J. Chromatogr.*, 271 (1981) 213.
3 M. van den Dool and P. D. Kratz, *J. Chromatogr.*, 11 (1963) 463.
4 G. Guiochon, *Anal. Chem.*, 36 (1964) 661.
5 J. C. Giddings, in N. Brenner and M. D. Weiss (Editors), *Gas Chromatography*, Academic Press, New York, 1963, p. 57.
6 J. Lee and R. D. Taylor, *Chromatographia*, 16 (1982) 286.
7 R. V. Golovnya and V. P. Uraletz, *J. Chromatogr.*, 36 (1968) 276.
8 W. A. Halang, R. Langlais, E. Kugler, *Anal. Chem.*, 50 (1978) 1829.
9 R. E. Kaiser and A. J. Rackstraw, *Computer Chromatography*, Vol. 1, Hüthig, Heidelberg, 1983, p. 123.
10 T. Kratzsch, *Diplomarbeit*, Karl Marx Universität, Leizig, 1978.
11 G. Anders, M. Scheller, C. Schuhler and H. G. Struppe, *Chromatographia*, 15 (1982) 43.
12 N. G. Johansen, L. S. Ettre and R. L. Miller, *J. Chromatogr.*, 256 (1983) 393.
13 J. Merle d'Aubigne and G. Guiochon, in H. G. Struppe (Editor), *5. Symposium über Gas Chromatographie, Berlin, 1965*, Akademie Verlag, Berlin, 1966, p. H435.
14 J. Krupčík, P. Cellar, A. Kocan, T. Pietryga and P. Hudec, *Ropa a Uhlie*, in press.

Journal of Chromatography, 351 (1986) 122–127
Elsevier Science Publishers B.V., Amsterdam — Printed in The Netherlands

CHROM. 18 197

Note

Influence of stationary phase modifications on lipophilicity measurements of benzophenones using reversed-phase thin-layer chromatography

GREETJE J. BIJLOO* and ROELOF F. REKKER
Department of Pharmacochemistry, Vrije Universiteit, De Boelelaan 1083, 1081 HV Amsterdam (The Netherlands)
(Received September 19th, 1985)

In a previous publication on reversed-phase thin-layer chromatography (RPTLC), Kakoulidou and Rekker[1] reported data obtained from a series of benzophenones. The experiments were performed on silica gel plates impregnated with paraffin oil and elution was done with acetone–water, preferably a 65:35 (v/v) mixture. The R_M values could be perfectly correlated in the following equation:

$$\Sigma f = 4.247\ (\pm 0.116)R_M - 0.312\ (\pm 0.027)kn + 4.482\ (\pm 0.034) \quad (1)$$
$$n = 17,\ r = 0.998,\ s = 0.077,\ F = 2052$$

where Σf is the sum of the hydrophobic fragmental values[2] of the constituent parts of the benzophenone, including one c_M factor (= 0.289) to account for cross-conjugation in molecules that are not too hindered sterically (occupation of both *ortho*-positions in one of the two phenyl moieties by methyl groups will fully prevent cross-conjugation).

Parameter kn in eqn. 1 is the coefficient of the constant c_M factor (= 0.289). It has a corrective role in the final fit and is connected with resonance, steric and systemic peculiarities of the structure under consideration[3]. Although the relationship between the three indicated factors is not yet completely understood, they are useful in improving relationships such as eqn. 1 to a statistical level comparable to that attained for alkyl benzenes[4].

The results obtained so far have encouraged further study. The present investigations are mainly concerned with a comparison of a number of reversed-phase thin-layer conditions, which seem to influence the moving pattern of the benzophenones over the thin-layer plate. We take into account:

(a) replacement of silica gel by a silica gel–Kieselguhr mixture; (b) application of methanol–water instead of acetone–water elution. (Grünbauer *et al.*[5], in their RPTLC study on *n*-alkylphenyl ketones, observed a distinct non-linearity between R_M and the acetone–water ratio of high acetone concentrations. These deviations can be ascribed to acetone-induced perturbations of the stationary phase and are not observed in the corresponding methanol–water elutions.); (c) replacement of paraffin

0021-9673/86/$03.50

oil by silicone oil, *i.e.*, modification of experimental conditions as frequently applied by Biagi *et al.*[6].

Some of the benzophenones investigated are identical to the Kakoulidou–Rekker series, but others have not been considered in RPTLC experiments before.

MATERIALS AND METHODS

The benzophenones investigated were of several origins, from laboratory stock. They were all of sufficient purity.

Experiments were performed on DC Fertigplatten Kieselgel 60 F254 (Merck) and on DC Fertigplatten Kieselgel 60–Kieselguhr F254 (Merck) impregnated with liquid paraffin oil (Baker) or with silicone oil (Merck). Impregnation was carried out by a standard method as described by Grünbauer *et al.*[5]. The plates were eluted with methanol–water [65:35 (v/v), Baker, double-distilled water] in closed tanks at 21°C. The plates were dried at 75°C and the spots were located under UV light.

The R_F values given are the averages of at least ten determinations. The R_M values were calculated from R_F values using the following equation:

$$R_M = \log (1/R_F - 1)$$

Only R_M values derived from R_F values of between 0.2 and 0.8 were used in the calculations.

Part of the investigation was carried out by nine students during a short QSAR laboratory course.

RESULTS AND DISCUSSION

Tables I, II and III summarize both R_F and R_M values and include the calculated standard deviations.

TABLE I

RPTLC DATA [METHANOL–WATER (65:35)] FOR BENZOPHENONES USING SILICA GEL PLATES COATED WITH PARAFFIN OIL

Substituent	R_F	R_M	Σf^*	*kn*	Σf_{est}
None	0.522 (±0.017)	−0.039 (±0.030)	3.193	0	3.217
2-Methyl	0.402 (±0.030)	0.172 (±0.055)	3.712	0	3.782
4-Methyl	0.430 (±0.019)	0.123 (±0.034)	3.712	0	3.648
2-Ethyl	0.328 (±0.026)	0.312 (±0.052)	4.231	0	4.159
4-Trichloromethyl	0.184 (±0.011)	0.647 (±0.031)	5.071	0	5.074
4-Methoxy	0.514 (±0.022)	−0.024 (±0.038)	3.273	0	3.271
4-Fluoro	0.507 (±0.030)	−0.012 (±0.053)	3.402	0	3.298
4-Chloro	0.361 (±0.028)	0.248 (±0.052)	3.935	0	3.998
4-Bromo	0.336 (±0.020)	0.295 (±0.038)	4.127	0	4.132
4-Nitro	0.507 (±0.029)	−0.012 (±0.051)	2.958	1	3.020
2-Trifluoromethyl	0.517 (±0.033)	−0.029 (±0.058)	4.339	−4	4.355

* Including one *kn* to account for cross-conjugation.

TABLE II

RPTLC DATA [METHANOL–WATER 65:35)] FOR BENZOPHENONES USING SILICA GEL–KIESELGUHR PLATES COATED WITH PARAFFIN OIL

Substituent	R_F	R_M	Σf^*	*kn*	Σf_{est}
None	0.583 (±0.018)	−0.146 (±0.033)	3.193	0	3.276
2-Methyl	0.447 (±0.023)	0.093 (±0.040)	3.712	0	3.814
4-Methyl	0.490 (±0.029)	0.017 (±0.050)	3.712	0	3.657
2-Ethyl	0.360 (±0.017)	0.250 (±0.032)	4.231	0	4.172
4-Trichloromethyl	0.193 (±0.010)	0.621 (±0.027)	5.071	0	5.001
4-Methoxy	0.598 (±0.023)	−0.173 (±0.042)	3.273	0	3.231
4-Fluoro	0.577 (±0.029)	−0.135 (±0.052)	3.402	0	3.298
4-Chloro	0.390 (± 0.007)	0.194 (±0.013)	3.935	0	4.038
4-Bromo	0.359 (±0.024)	0.252 (±0.046)	4.127	0	4.194
4-Nitro	0.603 (±0.036)	−0.183 (±0.065)	2.958	1	2.939
2-Trifluoromethyl	0.591 (±0.031)	−0.160 (±0.055)	4.339	−4	4.334

* Including one *kn* for cross-conjugation.

TABLE III

RPTLC DATA [METHANOL–WATER (65:35)] FOR BENZOPHENONES USING SILICA GEL–KIESELGUHR PLATES COATED WITH SILICONE OIL

Substituent	R_F	R_M	Σf^*	*kn*	Σf_{est}
None	0.685 (±0.035)	−0.339 (±0.071)	3.193	0	3.284
2-Methyl	0.544 (±0.030)	−0.077 (±0.052)	3.712	1	3.741
4-Methyl	0.606 (±0.045)	−0.188 (±0.083)	3.712	0	3.713
2-Ethyl	0.474 (±0.050)	0.046 (±0.087)	4.231	1	4.112
4-Trichloromethyl	0.323 (±0.018)	0.322 (±0.036)	5.071	0	5.170
4-Methoxy	0.699 (±0.026)	−0.367 (±0.052)	3.273	0	3.198
4-Fluoro	0.649 (±0.039)	−0.269 (±0.075)	3.402	0	3.484
4-Chloro	0.563 (±0.051)	−0.111 (±0.090)	3.935	0	3.941
4-Bromo	0.553 (±0.052)	−0.093 (±0.092)	4.127	0	3.998
4-Nitro	0.687 (±0.021)	−0.341 (±0.042)	2.958	1	2.998
2-Trifluoromethyl	0.600 (±0.050)	−0.178 (±0.091)	4.339	−2	4.314

* Including one *kn* for cross-conjugation.

The three sets of experiments are coded as follows: gelpar, elutions on silica gel plates coated with paraffin oil; gelgurpar, elutions on silica gel–kieselguhr plates coated with paraffin oil; gelgursil, elutions on silica gel–kieselguhr plates coated with silicone oil. The DC Fertigplatten Kieselgel 60 F254 coated with silicone oil could not be eluted with a methanol–water mixture.

Eqns. 2, 3 and 4 allow a first comparison of the three modes of separation

$$R_{M(\text{gelpar})} = 0.835\ (\pm 0.054) R_{M(\text{gelgurpar})} + 0.106\ (\pm 0.014) \quad (2)$$
$$n = 11,\ r = 0.996,\ s = 0.020,\ F = 1180$$

$$R_{M(\text{gelpar})} = 1.133\ (\pm 0.302) R_{M(\text{gelgursil})} + 0.325\ (\pm 0.069) \quad (3)$$
$$n = 11,\ r = 0.941,\ s = 0.076,\ F = 69.8$$

$$R_{M(\text{gelgurpar})} = 1.362\ (\pm 0.338) R_{M(\text{gelsursil})} + 0.263\ (\pm 0.079) \quad (4)$$
$$n = 11,\ r = 0.948,\ s = 0.085,\ F = 80.6$$

The discriminative power of gelgurpar (the spread that is effected in the eluted spots) is slightly better than that of gelpar and gelgursil. The mutual ratios can be expressed as *ca.* 1.4:1.1:1.0, in the order gelgurpar > gelpar > gelgursil. The decreased statistical quality of eqns. 3 and 4 is mainly due to the behaviour of 2-trifluoromethylbenzophenone. This compound has too high a lipophilicity (R_F value too low) in the gelgursil system.

The R_M values from Table I, II and III were correlated with Σf values. These Σf values were composed from the constituent fragments of the structure, applying one c_M factor to account for cross-conjugations.

$$\Sigma f = 2.345\ (\pm 1.215) R_{M(\text{gelpar})} + 3.454\ (\pm 0.310) \quad (5)$$
$$n = 11,\ r = 0.820,\ s = 0.369,\ F = 18.5$$

$$\Sigma f = 1.978\ (\pm 1.005) R_{M(\text{gelgurpar})} + 3.701\ (\pm 0.251) \quad (6)$$
$$n = 11,\ r = 0.826,\ s = 0.364,\ F = 19.2$$

$$\Sigma f = 2.763\ (\pm 0.920) R_{M(\text{gelgursil})} + 4.216\ (\pm 0.222) \quad (7)$$
$$n = 11,\ r = 0.913,\ s = 0.264,\ F = 44.8$$

Eqns. 5–7 are all of unacceptable quality, especially eqns. 5 and 6. Notorious outliers in all three equations are 4-nitrobenzophenone and 2-trifluoromethylbenzophenone:

	4-NO_2	2-CF_3
eqn. 5	$\Delta = -0.47$	0.96
eqn. 6	$\Delta = -0.39$	0.95
eqn. 7	$\Delta = -0.32$	0.62

Optimal fits of the compounds, including both 4-NO_2 and 2-CF_3 derivatives, could be achieved by assigning a proper *kn* parametrization:

$$\Sigma f = 2.691\ (\pm 0.222) R_{M(\text{gelpar})} - 0.278\ (\pm 0.037) kn + 3.325\ (\pm 0.058) \quad (8)$$
$$n = 11,\ r = 0.995,\ s = 0.069,\ F = 440$$

$$\Sigma f = 2.240\ (\pm 0.240) R_{M(\text{gelgurpar})} - 0.270\ (\pm 0.048) kn + 3.612\ (\pm\ 0.061) \quad (9)$$
$$n = 11,\ r = 0.992,\ s = 0.089,\ F = 261$$

$$\Sigma f = 2.858\ (\pm 0.318) R_{M(\text{gelgursil})} - 0.286\ (\pm 0.077) kn + 4.256\ (\pm 0.077) \quad (10)$$
$$n = 11,\ r = 0.990,\ s = 0.694,\ F = 230$$

The observed regressor values of *kn* are well within the range of the expected value of 0.289. The *kn* parameterizations used in the three equations (see Tables I–III) emphasize the similarities between gelpar and gelgurpar experiments, as evident from eqn. 2. They also confirm the unusual behaviour of gelgursil found in eqns. 3 and 4. Table IV gives five representative items.

TABLE IV

COMPARISON OF ESTIMATED LIPOPHILICITIES OF FIVE REPRESENTATIVE BENZOPHENONES

Substituent	Σf_{est}*			$\Sigma f_{(est.av.)}$	$\Sigma f_{(calc.)}$
	gelpar	*gelgurpar*	*gelgursil*		
None	3.22	3.28	3.29	3.26	3.19
2-Methyl	3.78	3.81	$4.04-1c_M$	3.78	3.71
2-Ethyl	4.16	4.17	$4.39-1c_M$	4.15	4.23
4-NO_2	$3.29-1c_M$	$3.21-1c_M$	$3.28-1c_M$	2.98	2.96
2-CF_3	$3.24+4c_M$	$3.25+4c_M$	$3.74+2c_M$	4.34	4.34

* $c_{M(av.)} = 0.278$.

The 2-methyl- and 2-ethyl-benzophenones on the paraffin-oil-coated plates fully agree with previous experiments by Kakoulidou and Rekker[1]. The steric effects of both methyl and ethyl groups can be neglected. On a gelgursil plate, however, the steric effect has to be considered in order to obtain an acceptable fit (*i.e.*, a correlation coefficient of at least 0.99 as attained in previous studies[1,4]. Assuming a comparable steric effect for the 2-CF_3 in our gelgursil experiments, this would mean that the *kn* parameter, given as -2 for the 2-CF_3 group, is actually the sum of two terms -3 and $+1$, respectively. We believe that the value of -3 (as well as the values of -4 in Tables I and II) is connected with systemic factors. The comparison between an octanol–water partition system and an RPTLC system with a less soluble organic phase needs a down-correction for halogen lipophilicity[3]. The value of $+1$ is connected with steric effects.

The 4-NO_2 group with $kn=1$, independent of the applied plate-type, has to be considered a resonance-decreasing group. Its negative mesomeric effect counteracts the similar negative mesomeric effect of C=O, resulting in decreased lipophilicity.

Not all factors that govern the transport of benzophenones over a thin-layer plate are understood as yet. We intend to perform more experiments with some structures that have not been investigated before.

The modifications of the stationary phase envisaged in the present study show that the replacement of paraffin oil by silicone oil may cause significant changes in retention behaviour of particular functional groups. However, these changes might make it difficult to explain the investigated structures in terms of lipophilicity. The addition of kieselguhr to the silica gel coating of the thin-layer plate seems to be important for silicone-oil-coated plates but does not influence the paraffin-oil-coated plates.

ACKNOWLEDGEMENTS

The authors wish to thank S. P. A. Boom, E. E. J. Haaksma, L. M. Huberts, R. Leurs, M. M. Mennen, D. Pappie, J. P. M. Plug, F. B. Pruijn and M. Ursem for valuable practical assistance.

REFERENCES

1 A. Kakoulidou and R. F. Rekker, *J. Chromatogr.*, 295 (1984) 341.
2 R. F. Rekker and H. M. de Kort, *Eur. J. Med. Chem.*, 14 (1979) 479.
3 R. F. Rekker, in M. Tichy (Editor), *QSAR in Toxicology and Xenobiochemistry*, Elsevier, Amsterdam, Oxford, New York, Tokyo, 1985, p. 3.
4 R. E. Koopmans and R. F. Rekker, *J. Chromatogr.*, 285 (1984) 267.
5 H. J. M. Grünbauer, G. J. Bijloo and T. Bultsma, *J. Chromatogr.*, 270 (1983) 87.
6 G. L. Biagi, O. Gandolfi, M. C. Guerra, A. M. Barbaro and G. Cantili-Forti, *J. Med. Chem.*, 18 (1975) 868.

Journal of Chromatography, 351 (1986) 128–135
Elsevier Science Publishers B.V., Amsterdam — Printed in The Netherlands

CHROM. 18 201

Note

α-, β- and γ-cyclodextrins as mobile phase additives in the high-performance liquid chromatographic separation of enantiomeric compounds

I. Separation of optical isomers of D,L-norgestrel

M. GAZDAG*, G. SZEPESI and L. HUSZÁR
Chemical Works of Gedeon Richter Ltd., P.O. Box 27, H-1475 Budapest (Hungary)
(Received September 20th, 1985)

The separation or resolution of enantiomeric compounds is of great importance in pharmaceutical analysis. The demand for an efficient, accurate technique for the determination of the optical purity of biologically active compounds has resulted in a great amount of chromatographic research in this area. One of the methods in this field is the use of cyclodextrins to form inclusion complexes between the solute to be tested and cyclodextrin molecule. Based on the selective interaction of α-, β- and γ-cyclodextrins with molecules, the methods can be divided into two groups.

In the first group the cyclodextrins are chemically bonded to the stationary phase surface, resulting in stable, fully derivatized, high-performance packings[1–8]. In most of these experiments β-cyclodextrin and its derivatives have been bonded to silica[3,5–7] because of the poorer resolution for the same components obtained on α-cyclodextrin-coated stationary phases[8].

The second group involves the use of cyclodextrins as mobile phase additives, a technique first introduced in thin-layer chromatography[9–11]. In high-performance liquid chromatography (HPLC) the extensive work of Debowski and Sybilska[12–16] can be mentioned: they used β-cyclodextrin as a chiral agent in the eluent.

The first successful application of this method was reported by Japanese workers[17] for the separation of prostaglandin isomers.

Generally it has to be noted that no data in the literature can be found for the use of γ-cyclodextrin as mobile phase additive in HPLC.

The main aim of our work was to clarify the role of different cyclodextrins in the HPLC separation of steroid optical isomers, which has not been studied before. The two isomers (D and L) of norgestrel seemed to be an excellent model, because the optical purity of D-norgestrel can be checked merely by measuring its optical rotation. D,L-Norgestrel is official in the *United States Pharmacopoeia*, D-norgestrel in the *United States Pharmacopoeia* and *British Pharmacopoeia* as Levonorgestrel[18–20].

The two isomers differ only in the stereochemistry on the C-13 ethyl group. To improve the selectivity and efficiency of the separation, the dependence of the resolution on the concentration of γ-cyclodextrin in the mobile phase, as well as on the nature and concentration of organic solvents in the eluent, has also been studied.

0021-9673/86/$03.50

EXPERIMENTAL

A Liquochrom 2010 high-pressure liquid chromatograph (Labor MIM, Esztergom-Budapest, Hungary) equipped with a variable-wavelength UV detector, a loop injector and a recorder (Labor MIM) was used. The separations were performed on prepacked LiChrosorb RP-18 (10 μm and 5 μm) (Chrompack, Middelburg, The Netherlands), Nucleosil 5 C_{18} (Chrompack), Hypersil ODS (5 μm) (Chrompack), and Ultrasphere ODS (5 μm) (Beckmann, Wien, Austria) columns. The size of the columns was 250 × 4.6 mm I.D. The eluents were prepared with HPLC-grade solvents and were degassed prior to use.

Cyclodextrins (α, β and γ) were obtained from Chinoin (Budapest, Hungary) and were used without further purification. The steroids to be tested were prepared at Chemical Works of Gedeon Richter (Budapest, Hungary): they were of pharmacopoeial quality.

RESULTS AND DISCUSSION

Dependence of capacity ratios on the γ-cyclodextrin concentration

The separation system was optimized by investigating the effect of the concentration of γ-cyclodextrin (γ-CYD) in the eluent on the capacity ratios of various steroids (Fig. 1). As it can be seen, the retentions of the compounds are considerably diminished with increasing γ-CYD concentration, indicating strong formation of more polar inclusion complexes. It is also apparent that the separation of D- and L-isomers of norgestrel can be carried out in the concentration range from $5 \cdot 10^{-3}$ to 10^{-2} mol/l γ-CYD.

These experiments were performed on the 10-μm LiChrosorb RP-18 column; however, for further optimization of chiral separation of norgestrel isomers, the 5-μm Hypersil ODS column and a methanol–water eluent were used.

Fig. 2 shows the dependence of the most important chromatographic parameters (k', α, H and R_s) on the concentration of γ-CYD. It can be concluded that the best separation can be achieved by using γ-CYD in a concentration of 10^{-2} mol/l: the resolution somewhat poorer, but the separation can be carried out within a reasonable time.

To elucidate the retention mechanism, the possible adsorption of γ-CYD on the stationary phase was studied by means of breakthrough curves, as well as by the effect of the presence and absence of γ-CYD in the eluent on the capacity ratios. Table I shows the retention behaviour of norgestrel isomers in the presence and absence of γ-CYD in the eluent when the stationary phase is loaded and unloaded with γ-CYD. From these results we deduce that liquid–liquid partition of the inclusion complexes formed in the mobile phase should be an acceptable model for the retention mechanism, because a significant increase of the measured capacity ratios is observed when a γ-CYD-loaded column and an eluent without γ-CYD were used.

Effect of the nature and concentration of organic solvents on the selectivity and efficiency of the separation

Fig. 3 shows the dependence of the capacity ratios on concentration of the organic solvent in the eluent, with methanol, ethanol, 2-propanol, acetonitrile or tetrahydrofuran as the organic solvent. Fig. 4 shows the changes in selectivity factor, resolution and column efficiency using the same solvent systems.

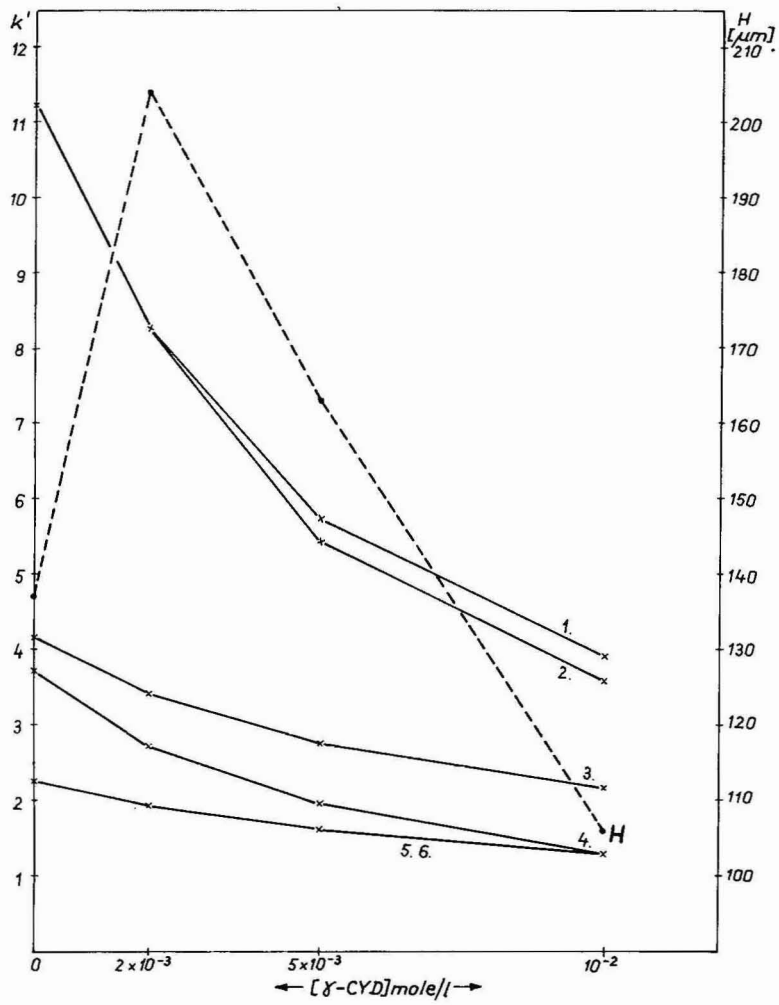

Fig. 1. Dependence of chromatographic parameters on γ-CYD concentration. Column, LiChrosorb RP-18, 10 μm (250 × 4.6 mm I.D.); eluent, water–methanol (3:4); flow-rates, 1 cm³/min; detection at 240 nm. Compounds: 1, L-norgestrel; 2, D-norgestrel; 3, hydrocortisone acetate; 4, triamcinolone acetonide; 5, prednisolone; 6, hydrocortisone.

From the data illustrated in Figs. 3 and 4 the following general conclusions can be drawn:

(1) When different organic solvents were used the elution order was unchanged, and the selectivity was not been significantly affected (the D-isomer is eluted first).

(2) The resolution of the two isomers is considerably influenced by the column efficiency, which is highly dependent on the nature of organic modifier in the eluent. The organic solvent tends to compete with the solutes for the preferred location in the hydrophobic cavity, resulting in various degrees of interaction of the compounds to be tested with γ-CYD.

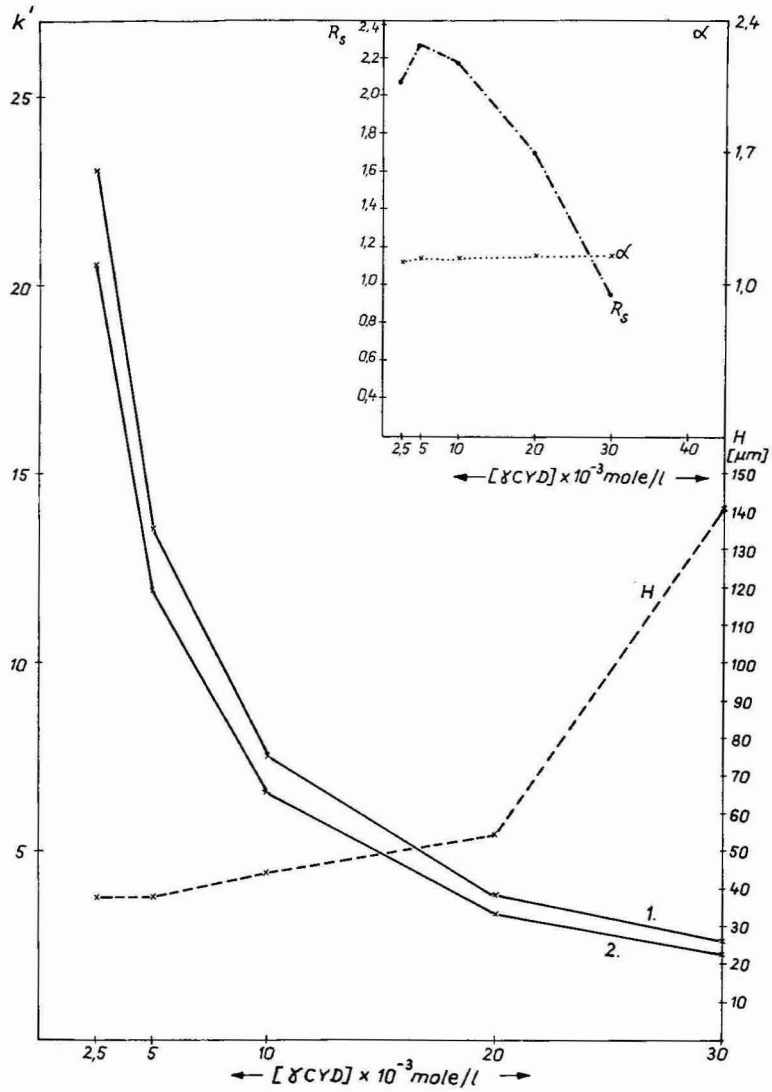

Fig. 2. Effect of γ-CYD concentration on the capacity ratios of D,L-norgestrel. Column, Hypersil ODS, 5 μm; eluent, water–methanol (6:4); other conditions as in Fig. 1.

(3) As the concentration of the organic solvent in the eluent increases, the capacity factors are significantly diminished because of the decreased interaction between the inclusion complexes and the stationary phase.

The most efficient separation can be obtained with an alcohol as the organic solvents compared to acetonitrile and tetrahydrofuran. Maximum resolution is achieved in a water–methanol mixture.

Effect of the size of the cavity in the CYD-ring on the selectivity of the separation

As the formation of inclusion complexes of steroids with cyclodextrins should

TABLE I

EFFECT OF THE PRESENCE OF γ-CYD IN THE ELUENT ON THE CAPACITY RATIO

Column, Hypersil ODS, 5 μm (250 × 4.6 mm I.D.); flow-rates, 1 cm³/min; detection at 240 nm. A = unloaded column; eluent, water–methanol (1:1); B = loaded column; eluent, water–methanol (1:1) containing 10^{-2} mol/l γ-CYD; C = loaded column; eluent, water–methanol (1:1).

Compound	*Capacity ratio**		
	A	*B*	*C*
D-Norgestrel	19.6	4.04	19.6
L-Norgestrel	19.6	4.54	19.6

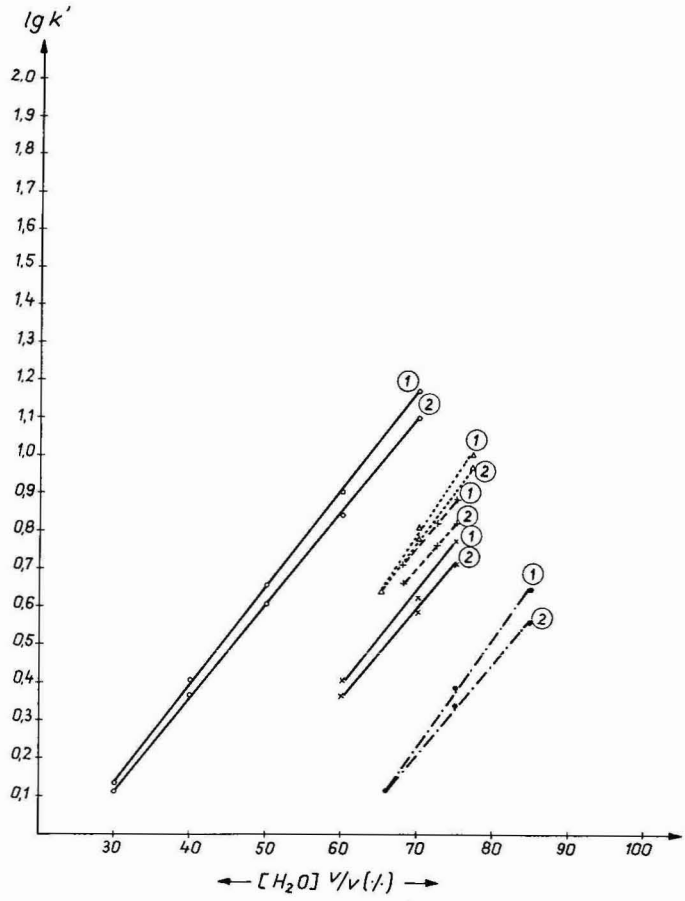

Fig. 3. Dependence of capacity ratios on the nature and concentration of organic modifier used in the eluent. γ-CYD concentration, 10^{-2} mol/l; other conditions as in Fig. 2. 1 = (−)-L; 2 = (+)-D. ○, Methanol; ×, ethanol; ●, isopropanol; +, acetonitrile; △, tetrahydrofuran.

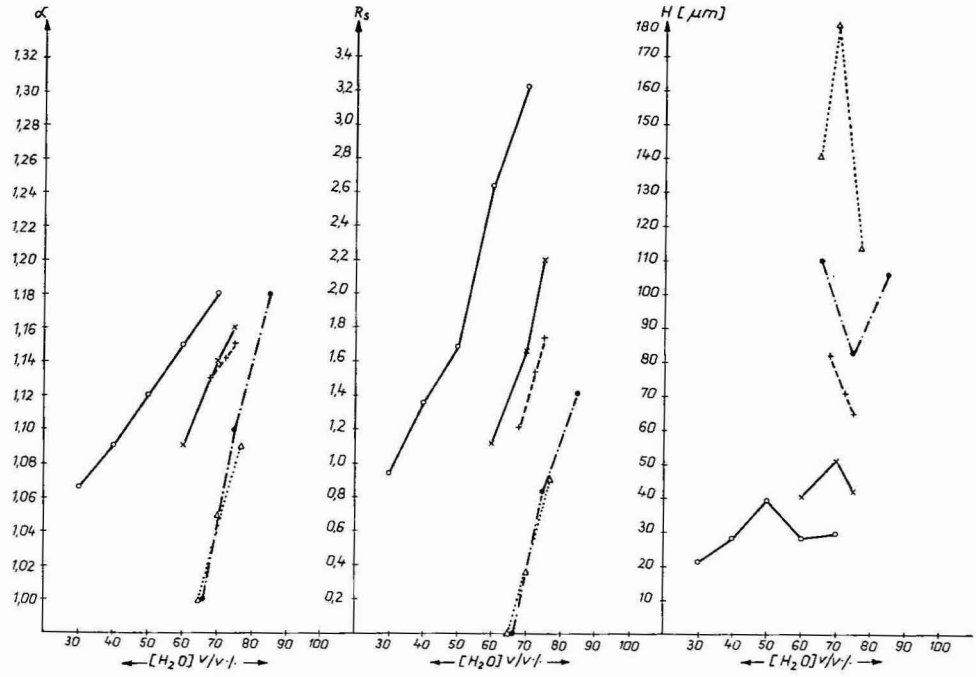

Fig. 4. Dependence of selectivity and efficiency on the nature and concentration of organic modifier used in the eluent. Conditions and key as in Fig. 3.

be influenced by the size of cavity of the CYD-ring, the use of α-, β- and γ-CYD in the eluent for the separation of D,L-norgestrel has been investigated. The results (Table II) show that no inclusion complexes are formed in the presence of α-CYD, and the retention time is the same as when no CYD is used in the eluent. In the presence of β-CYD inclusion complexes can be formed but no chiral recognition for D- and L-norgestrel occurs. When γ-CYD is applied a perfect resolution of enantiomeric compounds can be obtained. This can be explained by the intimate contact of a solute with the chiral CYD-cavity depending on the size and structure of the mol-

TABLE II

DEPENDENCE OF THE CAPACITY RATIOS ON THE SIZE OF CYD MOLECULES

Column, Ultrasphere ODS, 5 μm; flow-rate, 1 cm³/min; detection at 240 nm.

Eluent	*Capacity ratio*		*L:D*
	D-Norgestrel	*L-Norgestrel*	
Water–methanol (1:1)	26.3	26.3	–
Water–methanol (1:1) + 10^{-2} α-CYD	26.3	26.3	–
Water–methanol (1:1) + $5 \cdot 10^{-3}$ mol β-CYD*	24.2	24.2	–
Water–methanol (1:1) + 10^{-2} mol γ-CYD	4.10	4.60	1.12

* No more β-CYD can be dissolved in the eluent.

ecule investigated. In the case of steroids the size of γ-CYD cavity is appropriate for the separation, whereas the α-CYD cavity is too small.

Effect of type of octadecyl silica packing on the separation

To investigate the general applicability of our method, the norgestrel isomers were separated on four different C_{18} columns with the same eluent composition. Fig. 5 shows that all four have the same resolving power, but the compounds are more

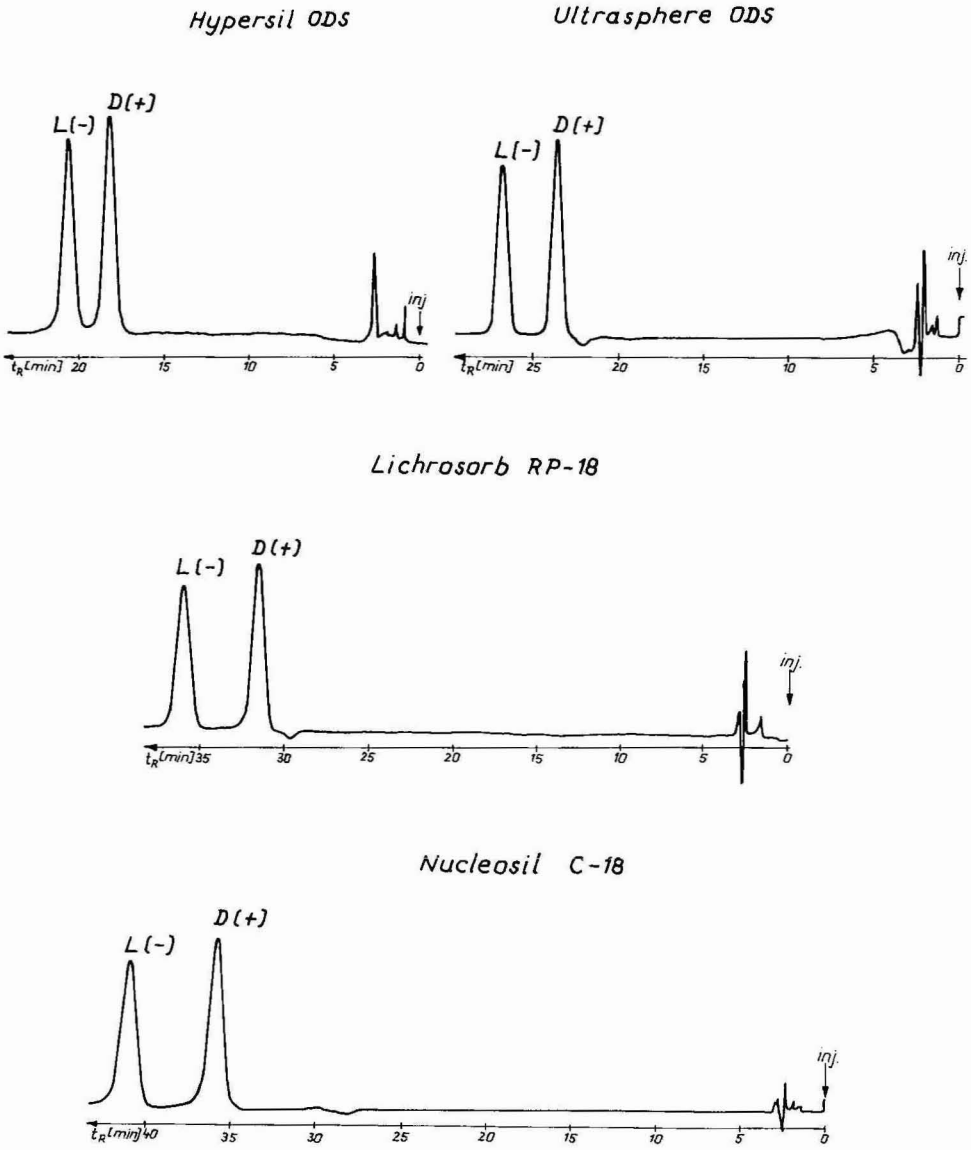

Fig. 5. Separation of D,L-norgestrel on different packing materials. Conditions as in Figs. 3 and 4.

retarded on LiChrosorb RP-18 and Nucleosil C_{18}, probably because of the higher carbon content in these two materials.

CONCLUSION

Our experiments show that γ-CYD forms strong inclusion complexes with D- and L-norgestrel, and baseline separation can be achieved. We think that the use of γ-CYD as a mobile phase additive shows promise presents for the effective separation chiral compounds of the size of steroids.

REFERENCES

1 Y. Mizobuchi, M. Tanaka and T. Shono, *J. Chromatogr.*, 208 (1981) 35.
2 M. Tanaka, Y. Kawaguchi, M. Nakae, Y. Mizobuchi and T. Shono, *J. Chromatogr.*, 246 (1982) 207.
3 M. Tanaka, Y. Kawaguchi and T. Shono, *J. Chromatogr.*, 267 (1983) 285.
4 B. Zsadon, L. Décsei, M. Szilasi, F. Tüdös and J. Szeitl, *J. Chromatogr.*, 270 (1983) 127.
5 K. Fujimura, T. Uedas and T. Ando, *Anal. Chem.*, 55 (1983) 446.
6 D. W. Armstrong and W. DeMond, *J. Chromatogr. Sci.*, 22 (1984) 411.
7 K. G. Feitsma, B. F. H. Dienth and R. A. de Zeeuw, *J. High Resolut. Chromatogr. Chromatogr. Commun.*, (1984) 147.
8 M. Tanaka, Y. Kawaguchi, M. Nakae, Y. Mizobuchi and T. Shano, *J. Chromatogr.*, 299 (1984) 341.
9 D. W. Armstrong, *J. Liq. Chromatogr.*, 3 (1980) 895.
10 W. L. Hinze and D. W. Armstrong, *Anal. Lett.*, 13 (1980) 1093.
11 W. G. Bulkert, C. N. Owensky and W. L. Hinze, *J. Liq. Chromatogr.*, 4 (1981) 1065.
12 J. Debowski, D. Sybilska and J. Jurczak, *Chromatographia*, 16 (1982) 198.
13 D. Sybilska, J. Lipkowski and J. Wóycikowski, *J. Chromatogr.*, 253 (1982) 95.
14 J. Dębowski, D. Sybilska and J. Jurczak, *J. Chromatogr.*, 237 (1982) 303.
15 J. Dębowski, J. Jurczak and D. Sybilska, *J. Chromatogr.*, 282 (1983) 83.
16 J. Dębowski, J. Jurczak, D. Sybilska and J. Zukowski, *J. Chromatogr.*, 329 (1985) 206.
17 K. Uekama, F. Hirayama and K. Ikeda, *J. Pharm. Sci.*, 66 (1977) 706.
18 *USP XXI*, USP Convention Inc., Rockville, MD, 1985, p. 746.
19 *USP XXI*, USP Convention Inc., Rockville, MD, Suppl. 1, 1985, p. 1738.
20 *British Pharmacopoeia 1980 Addendum 83*, HMSO, London, 1984, p. 240.

Journal of Chromatography, 351 (1986) 136–139
Elsevier Science Publishers B.V., Amsterdam — Printed in The Netherlands

CHROM. 18 199

Note

Column lifetime of Superose 6 at 37°C and basic pH

BO-LENNART JOHANSSON* and LARS ÅHSBERG
Pharmacia AB, Biotechnology, Department of Quality Control, S-751 82 Uppsala (Sweden)
(Received September 20th, 1985)

We are currently involved in a large-scale study of the lifetime of liquid chromatography columns for the separation of biomolecules. A recent study has shown that the lifetime of cation- and anion-exchange columns (Mono Q and Mono S) for fast protein liquid chromatography (FPLC) is well over 1000 repetitive injections[1]. Furthermore, it has been shown that the agarose-based high-performance gel filtration columns (Superose® 12) are unaffected by 1000 repetitive serum injections at basic pH[2].

Yet another newly launched agarose-based gel filtration column, Superose 6 (ref. 3), has been investigated in this work. This agarose matrix is cross-linked to a lesser extent than Superose 12, and is therefore a gel designed for larger biomolecules[3]. The lifetime of a Superose 6 column has been investigated under physiological conditions, *i.e.*, with a column temperature of 37°C and a mobile phase of basic pH (8.4).

EXPERIMENTAL

Chemicals and apparatus

All inorganic reagents were of p.a. quality. The serum sample was prepared daily from aliquots of frozen, normal, human serum. The serum was diluted (1:8) with mobile phase buffer and filtered through a 0.22-μm bacteriological filter prior to injection. The mobile phase buffer was 0.05 *M* Tris (pH 8.4) with addition of 0.15 *M* sodium chloride and 0.02% sodium azide. The eluent was filtered through a 0.45-μm filter.

The Pharmacia-prepacked Superose 6 HR 10/30 column was tested on a Pharmacia FPLC system comprising an LCC-500 control unit, a P-500 high-precision pump, a UV-1 UV monitor (280 nm, HR 10 cell), an MV-7 sample injector with a 100-μl loop, and an REC-481 recorder. To control the temperature at 37°C (±0.1°C), the column was water-jacketed.

Procedure

The serum was injected every 44 min, at a flow-rate of 0.6 ml/min, until 1000 injections had been completed.

0021-9673/86/$03.50

RESULTS AND DISCUSSION

The lifetime of a Superose 6 HR 10/30 column was investigated by making 1000 repetitive injections. The choice of eluent (phosphate buffer, pH 8.4) and column temperature (37°C) was done to make it possible to draw conclusions about the stability of Superose 6 under physiological conditions. In addition, the use of a serum sample makes the test more realistic.

The chromatograms from the 1st and the 1000th serum injections (Fig. 1) show that the Superose 6 column can withstand 1000 repetitive injections. In addition, the retention volume (V_R) stability was excellent for the three main peaks, as shown in Fig. 1. The relative standard deviation (R.S.D.) was lower than 0.2% (Table I).

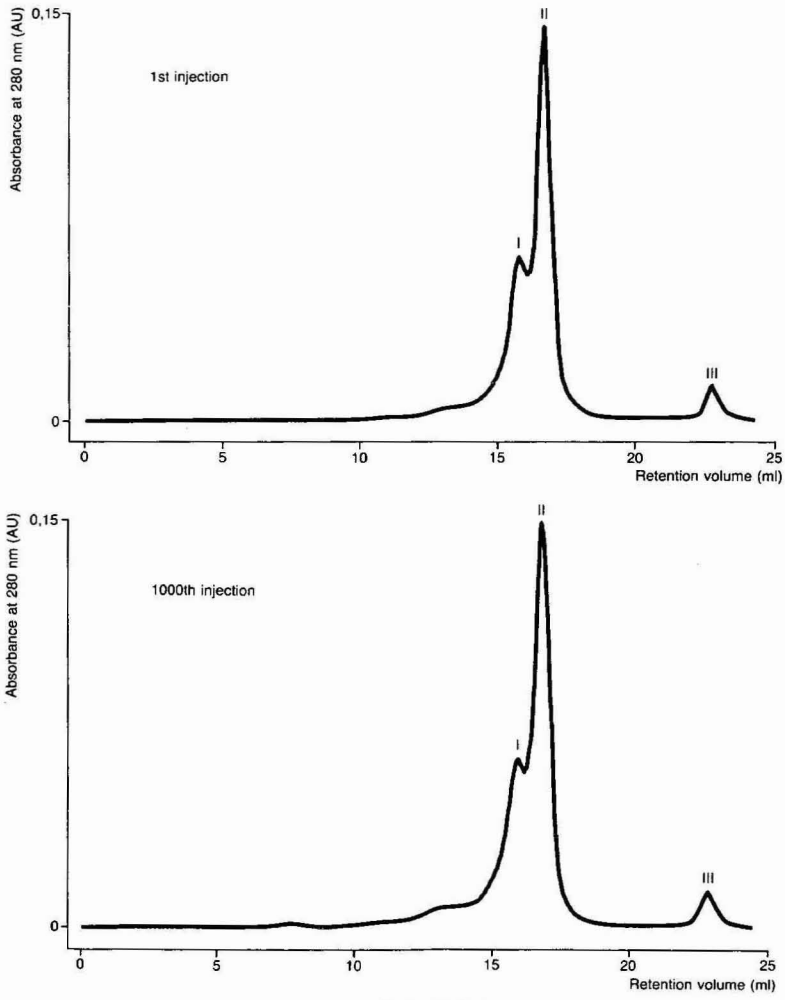

Fig. 1. Chromatograms from the 1st and the 1000th separation of normal human serum on Superose 6 HR 10/30. Chromatographic conditions: sample volume, 100 μl; eluent, 0.05 M Tris in 0.15 M sodium chloride adjusted to pH 8.4; flow-rate, 0.6 ml/min; column temperature, 37°C.

TABLE I

VARIATION OF RETENTION VOLUME (V_R) AND PEAK HEIGHT (h') OF THE THREE MAIN PEAKS AND THE TOTAL ACCUMULATED AREA DURING 1000 INJECTIONS OF NORMAL HUMAN SERUM ON A SUPEROSE 6 HR 10/30 COLUMN AT pH 8.4 AND COLUMN TEMPERATURE 37°C

Injection number	*Peak 1*		*Peak 2*		*Peak 3*		*Total accumulated area above 0.006 AU (ml AU)*
	V_R *(ml)*	h' *(AU)*	V_R *(ml)*	h' *(AU)*	V_R *(ml)*	h' *(AU)*	
1	16.07	0.060	16.97	0.146	22.91	0.014	0.208
50	16.03	0.060	16.95	0.147	22.92	0.013	0.205
100	16.04	0.061	16.94	0.149	23.00	0.014	0.207
150	16.03	0.063	16.94	0.150	22.98	0.013	0.208
200	16.07	0.062	16.95	0.149	23.01	0.014	0.206
250	16.08	0.062	16.96	0.151	23.01	0.014	0.203
300	16.04	0.061	16.93	0.148	22.94	0.013	0.209
350	16.07	0.062	16.98	0.151	22.99	0.014	0.213
400	16.04	0.063	16.94	0.152	22.96	0.013	0.209
450	16.04	0.060	16.91	0.148	23.00	0.014	0.207
500	16.06	0.059	16.95	0.147	22.96	0.014	0.207
550	16.05	0.059	16.96	0.148	22.97	0.013	0.206
600	16.09	0.059	16.94	0.148	22.98	0.013	0.206
650	16.07	0.059	16.95	0.148	23.00	0.013	0.208
700	16.04	0.058	16.93	0.146	22.97	0.013	0.203
750	16.03	0.059	16.94	0.147	23.01	0.013	0.214
800	16.09	0.058	16.95	0.150	22.97	0.012	0.205
850	16.01	0.058	16.93	0.148	22.94	0.013	0.210
900	16.07	0.058	16.94	0.148	22.96	0.013	0.210
950	16.07	0.058	16.95	0.144	22.99	0.012	0.203
1000	16.02	0.062	16.92	0.149	22.91	0.014	0.205
Mean	16.05	0.060	16.94	0.148	22.97	0.013	0.207
R.S.D. (%)	0.14	2.9	0.09	1.26	0.14	4.8	1.43

Furthermore, the maximum spread, calculated from the highest and lowest V_R obtained during the test, was less than 150 μl for all three peaks. The detector response (peak height, h') of the three main peaks was constant throughout the test (Table I). Furthermore, no significant baseline drift was observed and the total accumulated area showed no trends during the test (Table I). These results indicate that the sample did not accumulate in the gel matrix. However, the back-pressure rose from 0.6 MPa to 0.8 MPa during the test. This is probably caused by clogging of the column top filter, which was also observed by Johansson and Ellström[2].

CONCLUSION

It has been demonstrated that a Superose 6 column can manage 1000 repetitive injections of a serum sample under physiological conditions, with no significant degradation in column performance. The high precision of the retention data (Table I) shows that Superose 6 columns are well suited for accurate molecular-weight determinations during long-term use.

REFERENCES

1 B.-L. Johansson and N. Stafström, *J. Chromatogr.*, 314 (1984) 396.
2 B.-L. Johansson and C. Ellström, *J. Chromatogr.*, 330 (1985) 360.
3 T. Andersson, M. Carlsson, L. Hagel, J.-C. Janson and P.-Å. Pernemalm, *J. Chromatogr.*, 326 (1985) 33.

Journal of Chromatography, 351 (1986) 140–143
Elsevier Science Publishers B.V., Amsterdam — Printed in The Netherlands

CHROM. 18 195

Note

Comparison of high-performance thin-layer chromatography–densitometry and gas–liquid chromatography for the determination of conessine in *Holarrhena floribunda* stem bark

P. DUEZ* and S. CHAMART
Laboratoire de Chimie Analytique, Chimie Pharmaceutique Inorganique et Toxicologie, CP 205/1, Université Libre de Bruxelles, Campus Plaine, 1050 Bruxelles (Belgium)
M. VANHAELEN and R. VANHAELEN-FASTRÉ
Laboratoire de Pharmacognosie, CP 205/4, Université Libre de Bruxelles, Campus Plaine, 1050 Bruxelles (Belgium)
and
M. HANOCQ and L. MOLLE
Laboratoire de Chimie Analytique, Chimie Pharmaceutique Inorganique et Toxicologie, CP 205/1, Université Libre de Bruxelles, Campus Plaine, 1050 Bruxelles (Belgium)
(Received September 18th, 1985)

Conessine, the main alkaloid from the stem and root bark of Seoulou (*Holarrhena floribunda* Wall.) and Kurchi (*H. antidyssenterica* (G. Don.), Dur. & Schinz.), which are Apocynaceae from West-Africa and India, respectively, is known for its amoebicide, antidysenteric and febrifuge properties[1]. Unquestionable toxic effects, such as restlessness, tremors, insomnia, vertigo or even severe neuropsychopathic effects, have led to the withdrawal of this substance from modern pharmacopoeia[2].

However, *H. floribunda* bark is still in use in Africa either for its antiblennorragic or its supposed diuretic activity[3]. In order to study the possible local use of the amoebicide properties of this plant, it was decided to standardize the total alkaloidal[4] content of the drug, and particularly conessine.

Two analytical procedures were developed for the assay of conessine: gas–liquid chromatography (GLC) on a 3% SE-30 column, and high-performance thin-layer chromatography (HPTLC)–densitometry with Dragendorff and iodo-platinate as chromogenic reagents. The use of high-performance liquid chromatography was also investigated.

EXPERIMENTAL

A Packard-Becker Model 421 gas chromatograph with a flame ionization detector (Delft, The Netherlands) was equipped with a packed column (1 m × 2 mm I.D.) of 3% SE-30 Chromosorb W-AW (100–120 mesh) DMCS. The flow-rate of the helium carrier gas was 30 ml/min, the oven temperature was 230°C, and the detector and injector temperatures were 245°C. The chromatograph was interfaced with a Shimadzu integrator model CR-3A. The internal standard was codeine (Merck, Darmstadt, F.R.G.).

0021-9673/86/$03.50

HPTLC precoated plates of silica gel 60F 254 (10 × 20 cm) were obtained from Merck. The solutions (1 μl, standards or crude extracts) were applied 15 mm from the lower edge of the plates and then developed with ethyl acetate–hexane–diethylamine (75:24:6); this mobile phase was allowed to travel, in a saturated tank, a distance of 100 mm. After development and drying at 105°C for 2 h, the plates were sprayed with 30 ml of a Dragendorff reagent [1.7% bismuth subnitrate in acetic acid–water (1:4)–40% potassium iodide aqueous solution–acetic acid–ethyl acetate (5:5:20:ad 100)] and then with an iodoplatinate reagent (0.03% potassium hexaiodoplatinate aqueous solution) until dis-colouration of plate background. Plates were covered with a glass plate during measurement of the orange spots with a Shimadzu high speed TLC scanner CS-920, at the following settings: λ_{abs}, 500 nm; zig-zag stroke width, 9 mm; beam size, 1.2 × 1.2 mm; linearizer 1, AZS off. The mean values were calculated from integration of nine spots corresponding to three different standard concentrations, each being analysed twice, and three spots of the solution of unknown concentration.

H. floribunda stem bark powder (100 mg, 315 μm) was weighed into 10-ml glass-stoppered centrifuging tubes, mixed with 10 mg of calcium hydroxide, 0.2 ml of water and 5 ml of methanol; this suspension was shaken for 15 min and centrifuged at 2000 *g*, these last steps being repeated thrice with 5 ml of methanol. Supernatants were combined and evaporated to dryness under reduced pressure; the residue was dissolved in 1 ml of a methanolic codeine solution (0.06%) and filtered through a Millipore HV-4 filter.

Standard solutions were 2:10 to 8:10 dilutions in the same methanolic codeine solution of a stock solution prepared by dissolving 25 mg of conessine (Pfaltz & Bauer, U.S.A.) in 25 ml of methanol containing the same concentration of internal standard.

RESULTS AND DISCUSSION

HPLC

HPLC with UV detection was found to be unsuitable for the determination of conessine. On chemically modified phases, no conditions allowed sufficient separation and resolution of the peaks in plant extracts, even after a specific alkaloid extraction, with either ionic or non-ionic mobile phases. Furthermore, the shape of the conessine peak was irregular and extremely dependent on small variations in the organic content of the mobile phase. With straight phases, the cut-offs of the usable organic solvents were found to be inconsistent with the conessine detection wavelength (205 nm).

GLC

Conessine was easily separated (Fig. 1) without derivatization or temperature programming. No interference appeared in the chromatograms even after the injection of a large number of extracts. This shows that the high temperature required for conessine elution does not limit the separation of this compound from the other constituents of crude extracts; hence preliminary purification of these methanolic plant extracts was not required. The detection limit was 20 ng; codeine was used as an internal standard.

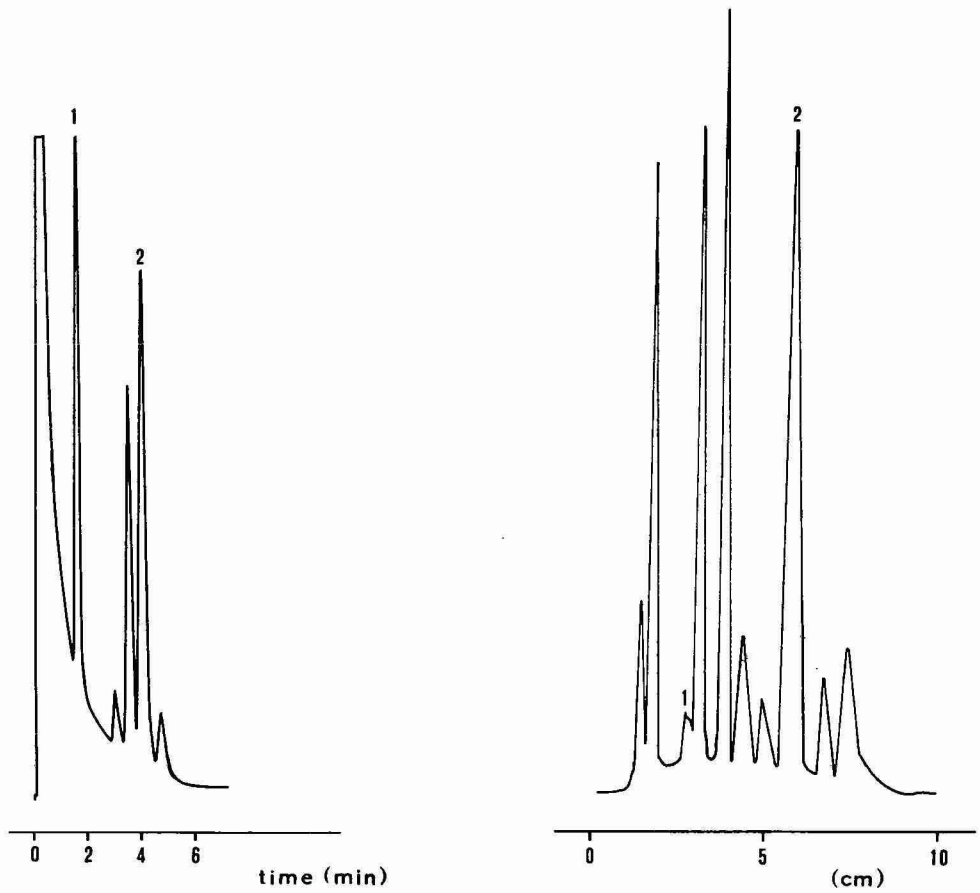

Fig. 1. GLC chromatogram of a *Holarrhena* stem bark extract. Column, 3% SE-30 Chromosorb W AW DMCS (100–120 mesh); carrier gas, helium; flow-rate, 30 ml/min; oven temperature, 230°C; detector and injector temperatures, 245°C. Peaks: 1 = codeine; 2 = conessine.

Fig. 2. TLC scanning profile of a *Holarrhena* stem bark extract. Adsorbent, HPTLC silica gel 60 F254; mobile phase, ethyl acetate–hexane–diethylamine (75:24:6); absorption wavelength, 500 nm. Peaks as in Fig. 1.

HPTLC–densitometry

The TLC system was derived as described previously[5], and led to efficient separation of conessine from other compounds in crude extracts (Fig. 2). None of the previously described colorimetric reactions of conessine[6] showed an acceptable sensitivity, either for detection or for HPTLC–densitometric assays. The combination of the alkaloid reagents Dragendorff and iodoplatinate significantly enhanced the detection limits and reproducibility, with orange derivatives well contrasted against a nearly colourless background. It was found necessary to cover the chromatoplate with a glass plate immediately after spraying of the second reagent and during measurement, in order to avoid recolouration of background as well as the evaporation of acetic acid, which could damage the densitometer. Codeine (internal standard for

TABLE I

DETERMINATION OF CONESSINE IN STEM BARK EXTRACTS; COMPARISON OF THE DENSITOMETRIC AND GLC RESULTS

Sample	*HPTLC results*			*GLC results*		
	Mean conessine (%) (dried powder)	*Standard deviation*		*Mean conessine (%) (dried powder)*	*Standard deviation*	
		Absolute	*Relative*		*Absolute*	*Relative*
1	0.11	0.01	10	0.15	0.01	5
2	0.36	0.02	6	0.37	0.02	4
3	0.07	0.01	15	0.09	0.01	10
4	0.42	0.02	4	0.41	0.01	3
5	0.79	0.01	2	0.76	0.02	3

GLC) reacted poorly with the chromogenic reagents, so it could not be used as an internal standard in TLC; it was completely separated from conessine and did not interfere in measurements. Concentrations of 0.1–0.9 μg of alkaloid base per microlitre spotted afforded a linear calibration graph with r values (correlation coefficient) typically greater than 0.990; the detection limit was *ca.* 40 ng.

Extraction procedure and comparison between HPTLC–densitometry and GLC results

A four-step extraction procedure guaranteed that at least 99% of the total conessine was extracted. The proposed densitometric HPTLC method was applied to conessine determination on stem bark of *H. floribunda* from Burkina-Faso (Africa); data were compared with those obtained by GLC (Table I) and show little difference in mean values or in coefficients of variation. Therefore these two assay methods should both prove to be of use in the rapid determination of conessine in plant material.

ACKNOWLEDGEMENTS

We thank Mr. A. Livaditis for his very skilful technical assistance, and the Administration Générale de Coopération au Développement of Ministère des Affaires Etrangères de Belgique and UNIDO (Vienna) for financial support.

REFERENCES

1 A. Bouquet and M. Debay, *Plantes médicinales de la Côte d'Ivoire*, Travaux et documents de l'Orstom, 32, Orstom, Paris, 1974, pp. 25–27.
2 W. Martindale, *The Extra Pharmacopoeia*, 25th ed., The Pharmaceutical Press, London, 1967, pp. 579–583.
3 R. R. Paris and H. Moyse, *Précis de Matière Medicale*, Vol. III, Masson and Cie, Paris, 1971, pp. 57–64.
4 *British Pharmaceutical Codex*, 5th ed., The Pharmaceutical Press, London, 1949.
5 A. B. Svendsen and R. Verpoorte, *Chromatography of Alkaloids, Part A*, Elsevier, Amsterdam, 1983, p. 27.
6 A. Schmit, *Travaux Lab. Mat. Med. Paris*, 35 (1950) 37.

Journal of Chromatography, 351 (1986) 144–149
Elsevier Science Publishers B.V., Amsterdam — Printed in The Netherlands

CHROM. 18 204

Note

Dosage d'alcaloïdes dihydrofuro[2,3-*b*]quinoleinium dans des tissus végétaux *in vitro* par chromatographie sur couche mince de gel de silice et fluorodensitométrie

M. MONTAGU* et P. LEVILLAIN
Laboratoire de Chimie Analytique, Faculté de Pharmacie, B.P. 3213, 37032 Tours Cedex (France)
et
J. C. CHENIEUX et M. RIDEAU
Laboratoire de Biologie Végétale, Faculté de Pharmacie, B.P. 3213, 37032 Tours Cedex (France)
(Reçu le 8 août 1985; manuscrit modifié reçu le 17 septembre 1985)

Les études sur la production de métabolites secondaires par des cellules végétales *in vitro* ont fait des progrès considérables ces dernières années[1]. La stratégie classiquement adoptée repose à la fois sur la sélection de souches à haute production et sur l'optimisation des conditions de culture. Au cours de ces deux étapes, la nécessité de doser les métabolites produits dans des quantités très faibles de tissus exige l'utilisation de techniques sensibles, simples et très rapides[2–6].

Les métabolites que nous étudions sont des alcaloïdes quaternaires dihydrofuro[2,3-*b*]quinoleinium synthétisés en culture *in vitro* à partir de tissus de diverses Rutacées[7] et présentant des propriétés cytotoxiques[8]. L'absence de méthodes analytiques pour ces composés nous a conduits antérieurement à proposer deux techniques mises au point sur des échantillons de cultures de *Choisya ternata*.

Fluorimétrie[9]

La technique nécessite une purification des extraits végétaux suivie d'une chromatographie sur couche mince de gel de silice et d'une élution à partir de ce support, ce qui entraîne une perte de sensibilité par dilution.

Chromatographie liquide haute performance[10]

Très fiable, beaucoup plus simple que la précédente méthode, cette technique demeure encore longue et onéreuse principalement quand on l'utilise pour de grandes séries expérimentales.

Les contraintes imposées par ces deux techniques nous ont conduits à rechercher un dosage par fluorodensitométrie, utilisable en routine.

MATÉRIEL ET MÉTHODES

Alcaloïdes étalons

Le platydesminium perchlorate et le balfourodinium chlorure ont été précédemment isolés à partir de feuilles de *Choisya ternata* H.B.K. (Rutacées) et analysés par résonance magnétique nucléaire et spectrographie de masse[8].

0021-9673/86/$03.50

Matériel végétal

Quatre souches de *Choisya ternata* sont cultivées *in vitro* selon les techniques précédemment décrites[11]. Elles diffèrent par leur aspect, leur physiologie et leur teneur en alcaloïdes.

Extraction, purification et chromatographie des alcaloïdes

Après culture, les tissus végétaux lyophilisés et pulvérisés sont extraits par du méthanol (10 mg/ml; macération sous agitation, 2 h; centrifugation).

Les extraits méthanoliques sont utilisés selon trois procédés: (1) sans purification; (2) après agitation (2 h) en présence de 50 mg/ml d'alumine (Prolabo 21013); (3) après complexation des alcaloïdes avec le bleu de bromothymol[9]. Le résidu d'évaporation de 2 ml d'extrait est repris par 2 ml d'une solution de colorant (10^{-4} *M*, en tampon phosphate pH 6). Les paires d'ions sont extraites par le dichlorométhane (3 × 1 ml). Après évaporation de la phase organique, le résidu est solubilisé dans 0,5 ml de méthanol. Des volumes de 1 μl d'extraits (correspondant respectivement à 10 μg, 10 μg, 40 μg de matériel végétal sec pour les procédés 1, 2, 3 précédents) sont chromatographiés sur gel de silice 60 (Merck 5553) dans les conditions suivantes: cuve sandwich (Camag); mélange éluant eau–acide formique–acétate d'éthyle (1:1:10); durée 15 min; dépôts réalisés avec une micro-seringue (Hamilton) ou avec un déposeur automatique (Camag). Les plaques chromatographiques sont séchées 2 h à l'air libre avant la lecture fluorodensitométrique.

Mesures de fluorescence

Les mesures de fluorescence ont été réalisées avec un fluorodensitomètre Shimadzu CS 920, équipé d'une lampe à vapeur de mercure, d'un monochromateur à l'excitation et offrant un choix de quatre filtres d'arrêt pour l'émission. Les caractéristiques de cet appareil ont été récemment étudiées par Huf[12].

RÉSULTATS

Fluorodensitométrie du platydesminium et du balfourodinium

La Fig. 1 montre les spectres d'excitation et d'émission des deux alcaloïdes en solution aqueuse[13]. Avec un fluorodensitomètre à filtres (Shimadzu) ne disposant à l'excitation que des raies du mercure, les meilleures conditions de lecture sont les suivantes: platydesminium $\lambda_{exc.}$ = 313 nm, balfourodinium $\lambda_{exc.}$ = 254 nm. Même dans ces dernières conditions qui ne sont pas optimales, les limites de détection sont voisines de 3 pmoles pour le platydesminium et de 0,1 pmole pour le balfourodinium. Comme l'indique le Tableau I, le coefficient de variation, calculé pour huit échantillons déposés sur huit plaques distinctes, est de 5–8% et les relations entre quantités d'alcaloïdes et signal lu après migration chromatographique sont linéaires (dans la limite de 60 pmoles pour le platydesminium). Selon Shellard[14], ces relations peuvent servir de base de calcul pour des dosages ultérieurs.

Fluorodensitométrie d'extraits de culture in vitro

La possibilité de doser les alcaloïdes dans des cultures *in vitro* a été étudiée avec des extraits provenant de souches chlorophylliennes ou non et accumulant des teneurs variables en alcaloïdes.

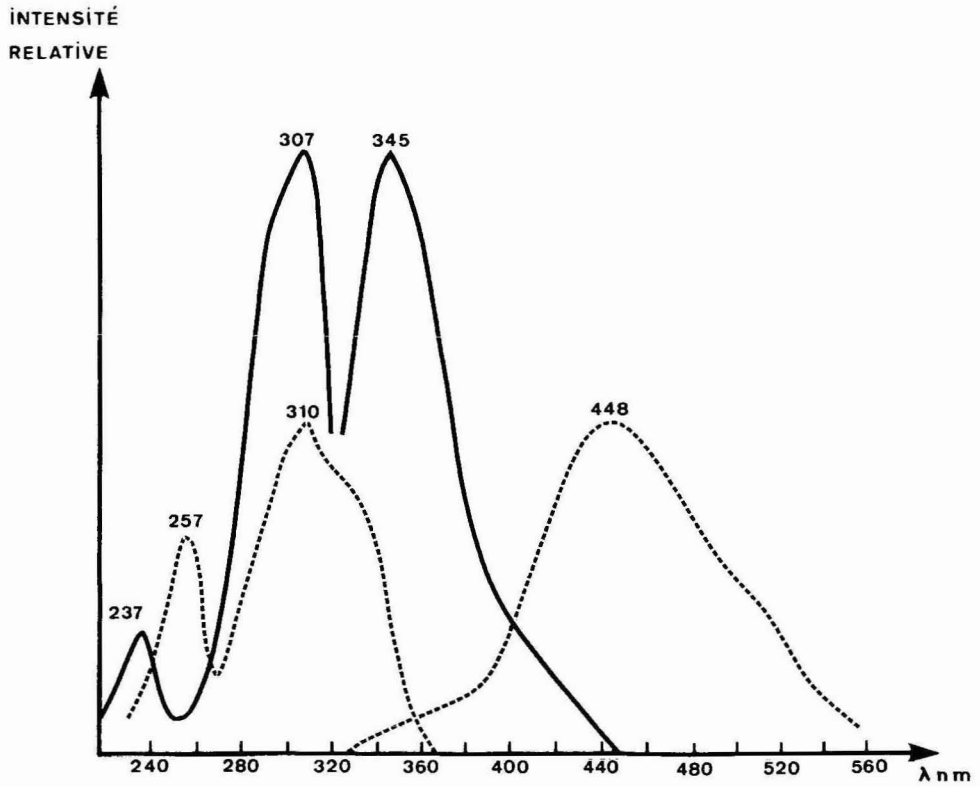

Fig. 1. Spectres d'excitation et d'émission des alcaloïdes en solution aqueuse. (——) Platydesminium; (– – –) balfourodinium.

TABLEAU I

LINÉARITÉ ET REPRODUCTIBILITÉ POUR LE DOSAGE DES DEUX ALCALOÏDES

$\bar{x}$ est la moyenne de 8 mesures (en unités arbitraires) effectuées sur 8 plaques de chromatographie. Les relations entre quantités d'alcaloïdes en picomoles (Q) et valeurs lues (V) sont pour le platydesminium: $Q = 2{,}99 \cdot 10^{-2} V + 2{,}73 \cdot 10^{-1}$ et pour le balfourodinium: $Q = 3{,}0 \cdot 10^{-3} V - 9{,}7 \cdot 10^{-3}$.

Alcaloïdes	*Quantité déposée (pmoles)*	*Valeurs lues ($\bar{x}$ ± écart-type)*	*Coefficient de variation (%)*
Platydesminium	1,2	35 ± 23	65
	6	191 ± 9	5
	12	388 ± 19	5
	60	1988 ± 120	6
	120	3316 ± 232	7
Balfourodinium	0,65	209 ± 16	8
	3,25	1094 ± 87	8
	6,50	2180 ± 130	6

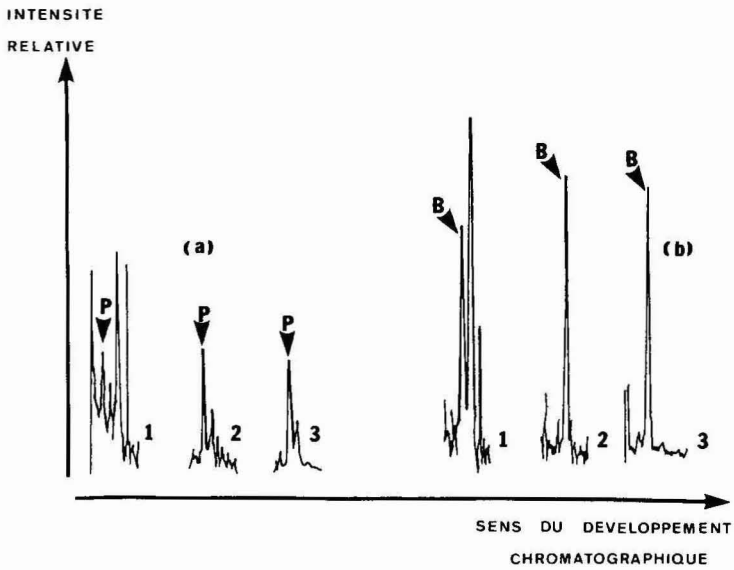

Fig. 2. Chromatogrammes obtenus pour la souche 2. (a) Lecture du platydesminium (P) ($\lambda_{exc.}$: 313 nm). (b) Lecture du balfourodinium (B) ($\lambda_{exc.}$: 254 nm). Filtre d'arrêt No. 1 à l'émission. Les extraits méthanoliques sont chromatographiés: 1, sans purification; 2, après purification par l'alumine; 3, après purification par extraction de paires d'ions.

La Fig. 2 présente les tracés chromatographiques obtenus pour l'une de ces souches, les autres donnant des tracés similaires. Elle met en évidence la complexité du tracé chromatographique d'extraits non purifiés (Fig. 2a1 et b1) dont la ligne de base est mal définie. Ceci explique que, principalement pour le platydesminium, les teneurs déterminées dans ces souches sont bien supérieures à celles obtenues après purification. Il est donc nécessaire de purifier les extraits méthanoliques.

Une étude antérieure du comportement chromatographique des alcaloïdes sur divers supports a mis en évidence la sélectivité d'une purification par l'alumine[10]. Une simple agitation des extraits avec cet adsorbant suffit à améliorer considérablement les tracés chromatographiques (Fig. 2a2 et b2) qui deviennent alors similaires à ceux obtenus en purifiant les alcaloïdes par extraction de paires d'ions formées avec le bleu de bromothymol (Fig. 2a3 et b3 et Tableau II), compte tenu du rendement de l'étape d'élution de ce dernier procédé qui est de 93 ± 2%[9]. Le coefficient de corrélation entre ces deux procédés, de 0,9944 pour le platydesminium et de 0,9998 pour le balfourodinium, montre l'exactitude de la méthode proposée.

CONCLUSION

Comparée aux techniques décrites antérieurement: chromatographie liquide haute performance et fluorimétrie après élution, la méthode décrite ici pour le dosage des alcaloïdes dihydrofuro[2,3-*b*]quinoléinium dans des tissus de Rutacées, utilisant la fluorodensitométrie, présente divers avantages:

(1) la souplesse d'exécution: compte tenu de la complexité du matériel végétal,

TABLEAU II

DOSAGES DES ALCALOÏDES POUR QUATRE SOUCHES DE *CHOISYA TERNATA* APRÈS CHROMATOGRAPHIE D'EXTRAITS DIVERSEMENT PURIFIÉS

Les résultats sont exprimés en micromoles d'alcaloïdes par gramme de matériel végétal sec.

Extraits méthanoliques	*Souches*	*Teneurs en alcaloïdes*			
		Platydesminium		*Balfourodinium*	
		Moyenne ± écart-type	*Coefficient de variation (%)*	*Moyenne ± écart-type*	*Coefficient de variation (%)*
Non purifiés	1	0,178 ± 0,092	50	non détecté	
	2	1,340 ± 0,071	5	0,211 ± 0,008	3
	3	2,674 ± 0,044	2	0,240 ± 0,008	3
	4	4,542 ± 0,360	8	0,522 ± 0,016	3
Purifiés par l'alumine	1	0,113 ± 0,060	50	non détecté	
	2	0,684 ± 0,027	4	0,166 ± 0,015	9
	3	1,800 ± 0,110	6	0,182 ± 0,012	7
	4	3,050 ± 0,150	5	0,488 ± 0,026	5
Purifiés par extraction de paires d'ions	1	0,140 ± 0,070	50	0,015 ± 0,004	30
	2	0,589 ± 0,055	9	0,156 ± 0,022	14
	3	1,439 ± 0,074	5	0,164 ± 0,015	9
	4	2,872 ± 0,192	7	0,455 ± 0,012	3

les étapes de purification, de chromatographie et de lecture sont très rapides (environ 30 min de manipulation pour 10 dosages).

(2) la sensibilité: les quantités d'alcaloïdes déposées sur la couche mince de gel de silice correspondent à 0,01 mg de matériel végétal. Elles sont 2500 fois plus faibles que celles déposées en utilisant la méthode fluorimétrique proposée antérieurement[9] et 25 fois plus faibles que celles injectées en chromatographie liquide haute performance[10]. Les limites de détection obtenues sont de 3 pmoles pour le platydesminium et de 0,1 pmole pour le balfourodinium alors qu'elles sont respectivement de 10 et de 100 pmoles lorsqu'on utilise la chromatographie liquide haute performance[10] ou la méthode fluorimétrique[9].

(3) le coût peu élevé: les quantités de solvants utilisées sont en effet très réduites.

Nous appliquons maintenant cette technique en routine dans notre laboratoire, non seulement pour les alcaloïdes des souches de *Choisya ternata* mais aussi pour d'autres souches de Rutacées: *Ruta graveolens* (15) et *Ptelea trifoliata* synthétisant d'autres alcaloïdes dihydrofuro[2,3-*b*]quinoléinium.

BIBLIOGRAPHIE

1 A. Fujiwara, *Plant Tissue Culture*, JAPTC, Tokyo, 1982, 839 pp.
2 R. Verpoorte, T. Mulder-Krieger, R. Wijnsma, J. M. Verzijl et A. Baerheim Svendsen, *Z. Naturforsch. C*, 39 (1984) 680.
3 F. Sasse, J. Hammer et J. Berlin, *J. Chromatogr.*, 194 (1980) 234.

4 E. W. Weiler, dans W. Barz, E. Reinhard et M. H. Zenk (Rédacteurs), *Plant Tissue Culture and its Biological Application*, Springer, New York, 1977, p. 266.
5 F. Sasse, U. Heckenberg et J. Berlin, *Plant Physiol.*, 69 (1982) 400.
6 B. D. Neumann et M. H. Zenk, *Planta Med.*, 162 (1984) 250.
7 P. G. Waterman, *Biochem. Systematics Ecol.*, 3 (1975) 149.
8 M. Rideau, C. Verchere, P. Hibon, J. C. Chenieux, P. Maupas et C. Viel, *Phytochemistry*, 18 (1979) 155.
9 M. Montagu-Bourin, M. Rideau, P. Levillain et J. C. Chenieux, *Planta Med.*, 38 (1980) 50.
10 M. Montagu, P. Levillain, J. C. Chenieux et M. Rideau, *J. Chromatogr.*, 331 (1985) 437.
11 M. Gras, J. Creche, J. C. Chenieux et M. Rideau, *Planta Med.*, 46 (1982) 231.
12 F. A. Huf, *Pharm. Weekbl. Sci.*, 6 (1984) 7.
13 M. Montagu, P. Levillain, M. Rideau et J. C. Chenieux, *Talanta*, 28 (1981) 709.
14 E. J. Shellard, *Quantitative Paper and Thin-layer Chromatography*, Academic Press, Londres, 1968, 140 pp.
15 K. G. Ramawatt, M. Rideau et J. C. Chenieux, *Phytochemistry*, 24 (1985) 441.

Journal of Chromatography, 351 (1986) 150–154
Elsevier Science Publishers B.V., Amsterdam — Printed in The Netherlands

CHROM. 18 139

Note

Comparative study of isotachophoretic and liquid chromatographic analysis of 2-(5-cyanotetrazolato)pentaamminecobalt(III) perchlorate

R. J. SCHUMACHER* and J. P. McCARTHY
Monsanto Research Corporation, Mound, Miamisburg, OH 45342 (U.S.A.)*
(Received August 26th, 1985)

A perchlorate salt of a transition metal complex which has dependable explosive characteristics has been developed in recent years. The attractive explosive properties shown by 2-(5-cyanotetrazolato(pentaamminecobalt(III) perchlorate (CP) have resulted in its use in low-voltage detonators[1–3]. Potentional byproducts from the manufacture of CP are 2-(5-carboxamidetetrazolato)pentaamminecobalt(III) perchlorate (amide) and 1-(5-amidinotetrazolato)pentaamminecobalt(III) perchlorate (amidine) (Fig. 1).

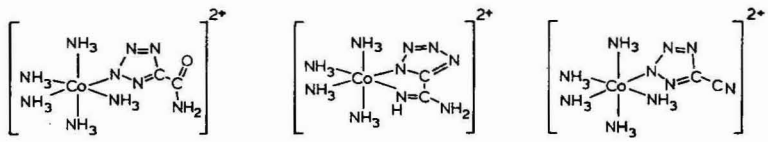

Fig. 1. Structures of the compounds investigated (shown without perchlorate anion).

Various methods have been reported for the analysis of these impurities in CP[4,5]. These methods involve cumbersome chemical pretreatment and/or do not provide desirable sensitivity or selectivity. One or more methods were sought which would provide accurate and precise results for routine analysis of a large number of CP samples. It is desirable to have two confirmatory methods due to the nature of the analyte in water. CP has not been obtained free of the amide impurity, since the amide is a hydrolysis product of CP and the only reasonable solvent for CP is water. It is soluble in dimethyl sulfoxide but decomposes to the amidine[6]. Other solvents dissolve only negligible amounts of CP[7].

A liquid chromatographic analysis was developed[8]. In addition, the isotachophoretic separation of Lavoie and Back[4] was refined to provide accurate quantitative data. These two methods are described, compared, and applied in this work.

---

* Mound is operated by Monsanto Research Corporation for the U.S. Department of Energy. This manuscript has been authored by a contractor of the U.S. Government under Contract No. DE-AC04-76-DP00053.

0021-9673/86/$03.50

EXPERIMENTAL

A Spectra-Physics SP 8000B liquid chromatograph with a pneumatically operated injector was used with a loop-filling autosampler. A Kratos 757 UV detector was set at 210 nm and 0.02 a.u.f.s. The sorbent, MN polyamide 6 is manufactured by Macherey Nagel & Co. (F.R.G.) and obtained from Brinkmann Instruments (Westbury, NY, U.S.A.). The 15 cm × 4 mm columns were packed by Applied Science Labs. (State College, PA, U.S.A.) from an aqueous slurry at 1000 p.s.i. Flow-rate for the 0.1 *M* $NaClO_4$ mobile phase was 5 ml/min. This compressible sorbent eventually collapses at this high rate, plugging the column. A better rate for column longevity is 2 ml/min. Injection of 10 μl contained about 10 μg of CP. Quantitation was by electronic integration of the peaks.

Isotachophoresis was carried out on an LKB 2127 with UV detection at 254 nm using 50 cm of PTFE capillary of 0.8 mm I.D. The cations were separated using a leading electrolyte of 0.012 *M* KH_2PO_4 in 20% methanol adjusted to pH 2.4 with phosphoric acid, and a terminating electrolyte of 0.00625 *M* Tris. Both electrolytes contained 500 ppm of Triton X-100. Injections of 4.5 μl were made consisting of 2.5 μl of aqueous CP solution (3.67 μg/8.4 n*M*) and 2 μl of ampholyte solution sequentially drawn into the 10-μl syringe. Ampholine ampholyte solution, pH 3.5–10, was obtained from LKB. The separation requires 20 min at 500 μA.

RESULTS AND DISCUSSION

The low solubility of CP in organic solvents precluded most liquid chromatographic systems. Ion-exchange chromatography on the available columns was not promising. However, thin-layer chromatography on a commercial polyamide sorbent gave a separation of CP from the amide. This sorbent is an unlikely one for high-performance liquid chromatography (HPLC). Electron photomicrographs show the particle size range to be 10–140 μm. The surface area is only 21.7 m^2/g (BET), with no pore structure. A column packed with this sorbent resulted in baseline resolution of the important materials (Fig. 2).

The capacity factor (k') for the amide is 3.0, while that for CP is 13.8, giving in α of 4.6. The response for amide is linear up to 2 μg with a detection limit of 0.08 μg. The practicality of using an autosampler was examined by reinjecting a CP sample hourly over a 12-h period. The standard deviation of these measurements is 0.09% amide with no upward trend discernable in the data, indicating no hydrolysis. Spiking of a CP sample with a known amount of amide gave a 97.5% recovery.

Isotachophoresis is uniquely applicable to this analysis. The amidine, CP, and the amide are separated, migrating in that order. However, a problem arises in quantitation. If a substance is present in sufficient quantity to provide a zone long enough to fill the UV cell window, the length of the resulting zone on the graph is proportional to the amount of the substance present. If insufficient material is present to fill the detector window, zone height may be brought into the calculation[9]. This is the situation which arises when the analyte is a minor constituent as in the present analysis. The zones are convoluted such that the zone height due to amide cannot be unambiguously measured, as in Fig. 3A. If a spacer ion can be found of intermediate ionic mobility, these zones can be deconvoluted. A mixture of ions (ampholytes),

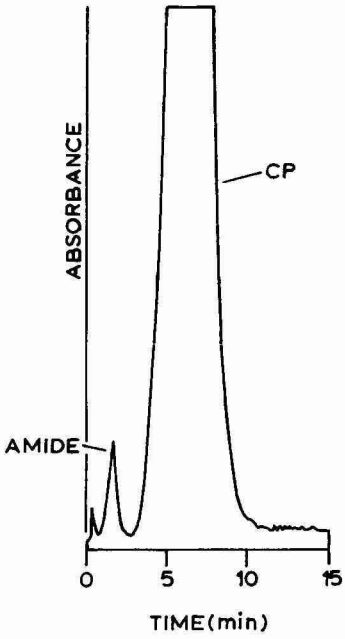

Fig. 2. Typical chromatogram.

available from LKB, was used with success (Fig. 3B). Zone height for the amide can easily be measured and assigned in this isotachopherogram.

Amide analysis by isotachophoresis is linear up to 10 μg amide with a detection limit of 0.4 μg. Repetitive injections of a CP sample gives a standard deviation of 0.14%. Analysis of a sample spiked with a known amount of amide gave 92.7% recovery.

No spacer ion has been found to deconvolute the amidine zone. However, spiking experiments have shown a detection limit of 0.1% amidine. Of the numerous samples of CP analyzed in this work, none was found which contains that much amidine.

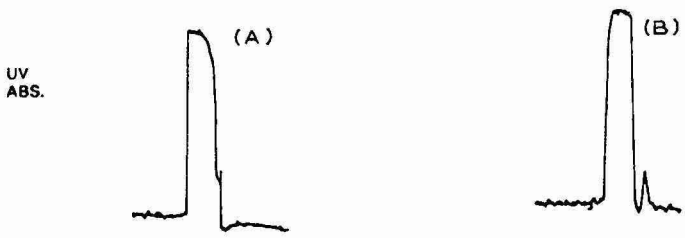

Fig. 3. Separation of analytes for UV quantification by spacer ion technique. (A) CP amide separation; (B) CP amide separation with ampholyte spacer ions.

APPLICATION TO THERMALLY REACTED CP SAMPLES

Supplied samples, in which CP had been degraded by thermal reaction for various periods of time, were used to directly compare these two analytical methods. A single solution of each sample was prepared and part of it directly injected into each instrument, eliminating any variation in sample preparation. The results demonstrate good agreement between the methods (Table I). Samples C and, especially, D were the most thermally reacted samples. Decomposition was advanced enough to produce samples partially insoluble in water. Solutions were filtered from insolubles before analysis. Two sample preparations were carried out for Sample D, giving remarkable agreement between the two methods for each solution, but a great difference from the first sample preparation to the second indicating lack of sample homogeneity.

TABLE I

AMIDE ANALYSES

Sample	*Liquid chromatography*	*Isotachophoresis*
A	2.07 ± 0.01%*	2.03 ± 0.06%**
B	2.11 ± 0.01%	2.24 ± 0.03%
C	3.79 ± 0.20%	3.14 ± 0.08%
D	1.76%, 3.95%	1.56%, 3.73%
E	9.62 ± 0.28%	9.33 ± 0.06%
F	1.71 ± 0.01%	1.59 ± 0.09%
G	2.87 ± 0.10%	3.03 ± 0.14%

* Average deviation of three measurements.
** Range of two measurements.

CONCLUSIONS

Two methods of amide analysis have been developed and shown to give good agreement. Isotachophoresis has the particular strength that it is able to detect the amidine, whereas the HPLC method can not. However, since isotachophoretic analysis of multiple samples have shown the amidine concentration to be less than 0.1%, the HPLC method is the one of choice due to the readiness with which it is automated.

REFERENCES

1 W. B. Leslie, R. W. Dietzel and J. Q. Searcy, *Sixth Symposium (International) on Detonation, San Diego, CA, August 1976*, U.S. Government Printing Office, Washington, DC, document ACR-221, pp. 455–459.
2 M. L. Lieberman, F. J. Villa, D. L. Marchi, A.L. Lause, D. Yates and J. W. Fronabarger, *Proceedings of the Eleventh Symposium on Explosives and Pyrotechnics, Philadelphia, PA, September 1981*, Franklin Institute Research Labs., Philadelphia, PA, pp. 37-1–37-13.
3 M. L. Lieberman, *Ind. Eng. Chem. Prod. Res. Dev.*, in press.
4 J. M. Lavoie and P. S. Back, *J. Chromatogr.*, 264 (1983) 329–335.
5 V. M. Loyola and J. Womelsduff, *Sandia Laboratories Report, SAND80-2390*, U.S. Department of Energy, Albuquerque, NM, February 1981.

6 E. M. Pitre and A. Attalla, *Nuclear Magnetic Resonance Study of the Rearrangement of 2-(5-Cyanotetrazolato)pentamminecobalt(III) Perchlorate*, U.S. Department of Energy Report MLM-3226, March 1985, 13 pp.
7 J. P. McCarthy, personal communication.
8 R. J. Schumacher and K. Bullock, *Determination of Amide Content in 2-(5-Cyanotetrazolato)pentaamminecobalt(III) Perchlorate by High Performance Liquid Chromatography on Polyamide*, U.S. Department of Energy Report MLM-3121, November 1983, 6 pp.
9 M. Svoboda and J. Vacík, *J. Chromatogr.*, 119 (1976) 539–547.

PUBLICATION SCHEDULE FOR 1986

Journal of Chromatography (incorporating *Chromatographic Reviews*) and *Journal of Chromatography, Biomedical Applications*

MONTH	O 1985	N 1985	D 1985	J	F	
Journal of Chromatography	346 347/1	347/2 347/3 348/1	348/2 349/1 349/2 350/1 350/2	351/1 351/2 351/3	352 353 354	The publication schedule for further issues will be published later
Chromatographic Reviews						
Bibliography Section					372/1	
Biomedical Applications				374/1 374/2	375/1	

INFORMATION FOR AUTHORS

(Detailed *Instructions to Authors* were published in Vol. 329, No. 3, pp. 449–452. A free reprint can be obtained by application to the publisher.)

Types of Contributions. The following types of papers are published in the *Journal of Chromatography* and the section on *Biomedical Applications:* Regular research papers (Full-length papers), Short communications and Notes. Short communications are preliminary announcements of important new developments and will, whenever possible, be published with maximum speed. Notes are usually descriptions of short investigations and reflect the same quality of research as Full-length papers, but should preferably not exceed four printed pages. For review articles, see page 2 of cover under Submission of Papers.

Submission. Every paper must be accompanied by a letter from the senior author, stating that he is submitting the paper for publication in the *Journal of Chromatography.* Please do not send a letter signed by the director of the institute or the professor unless he is one of the authors.

Manuscripts. Manuscripts should be typed in double spacing on consecutively numbered pages of uniform size. The manuscript should be preceded by a sheet of manuscript paper carrying the title of the paper and the name and full postal address of the person to whom the proofs are to be sent. Authors of papers in French or German are requested to supply an English translation of the title of the paper. As a rule, papers should be divided into sections, headed by a caption (*e.g.,* Summary, Introduction, Experimental, Results, Discussion, etc.). All illustrations, photographs, tables, etc., should be on separate sheets.

Introduction. Every paper must have a concise introduction mentioning what has been done before on the topic described, and stating clearly what is new in the paper now submitted.

Summary. Full-length papers and Review articles should have a summary of 50–100 words which clearly and briefly indicates what is new, different and significant. In the case of French or German articles an additional summary in English, headed by an English translation of the title, should also be provided. (Short communications and Notes are published without a summary.)

Illustrations. The figures should be submitted in a form suitable for reproduction, drawn in Indian ink on drawing or tracing paper. Each illustration should have a legend, all the *legends* being typed (with double spacing) together on a *separate sheet.* If structures are given in the text, the original drawings should be supplied. Coloured illustrations are reproduced at the author's expense, the cost being determined by the number of pages and by the number of colours needed. The written permission of the author and publisher must be obtained for the use of any figure already published. Its source must be indicated in the legend.

References. References should be numbered in the order in which they are cited in the text, and listed in numerical sequence on a separate sheet at the end of the article. Please check a recent issue for the layout of the reference list. Abbreviations for the titles of journals should follow the system used by *Chemical Abstracts.* Articles not yet published should be given as "in press", "submitted for publication", "in preparation" or "personal communication".

Dispatch. Before sending the manuscript to the Editor please check that the envelope contains three copies of the paper complete with references, legends and figures. One of the sets of figures must be the originals suitable for direct reproduction. Please also ensure that permission to publish has been obtained from your institute.

Proofs. One set of proofs will be sent to the author to be carefully checked for printer's errors. Corrections must be restricted to instances in which the proof is at variance with the manuscript. "Extra corrections" will be inserted at the author's expense.

Reprints. Fifty reprints of Full-length papers, Short communications and Notes will be supplied free of charge. Additional reprints can be ordered by the authors. An order form containing price quotations will be sent to the authors together with the proofs of their article.

Advertisements. Advertisement rates are available from the publisher on request. The Editors of the journal accept no responsibility for the contents of the advertisements.

ANNOUNCING A NEW JOURNAL

CHEMOMETRICS AND INTELLIGENT LABORATORY SYSTEMS

An International Journal

Editor-in-Chief: D.L. Massart, Brussels, Belgium

This international journal publishes articles about new developments on laboratory techniques in chemistry and related disciplines, which are characterized by the application of statistical and computer methods.

Special attention is given to emerging new technologies and techniques for the building of intelligent laboratory systems i.e. artificial intelligence and robotics.

One of the main aims of the journal is to be an interdisciplinary journal; more particularly it intends to build bridges between chemists, statisticians, and designers of laboratory systems. The journal deals with the following topics:

* **chemometrics:** the chemical discipline that uses mathematical and statistical methods

– to design or select optimal procedures and experiments
– to provide maximum chemical information by analyzing chemical data

* **computerized acquisition, processing and evaluation of data**
* **developments in statistical theory destined to be used in chemistry**
* **intelligent laboratory systems including self-optimizing instruments and the application of expert systems and robotics in the laboratory**
* **techniques for the modelling of chemical processes such as environmental models and industrial processes including quality control**
* **new software to implement the methods described above**

The journal will be of interest to chemists, as well as pharmacists, statisticians and information specialists working in the different fields of chemistry such as analytical chemistry, organic chemistry, environmental chemistry, food chemistry and pharmaceutical chemistry.

There will be no page charges; fifty reprints of each article will be supplied free of charge.

Instructions for the preparation of manuscripts can be obtained from the publisher.

Volume 1 – four issues – will cover 1986/1987. The subscription price is 242 Dutch guilders or US $ 83.50.

Requests for further information and orders may be sent to the publishers.

7343

ELSEVIER SCIENCE PUBLISHERS

P.O. Box 1663, Grand Central Station, New York, NY 10163, USA P.O. Box 330, 1000 AH Amsterdam, The Netherlands